UNIVERSIDAD DE EXTREMADURA

TESIS DOCTORAL

CONTROL HORMONAL Y TRANSCRIPCIONAL DEL DESARROLLO DEL FRUTO DE OLIVO

MARÍA DEL CARMEN CAMARERO GARCÍA

PROGRAMA DE DOCTORADO
BIOLOGÍA MOLECULAR Y CELULAR, BIOMEDICINA Y BIOTECNOLOGÍA

Conformidad de directora y codirectoras:
Dr. María del Carmen Gómez Jiménez (directora)
Dr. Juana Labrador Moreno (codirectora)
Dr. Mercedes Gallardo Medina (codirectora)

Esta tesis cuenta con la autorización de directora y codirectoras de la misma y de la Comisión Académica del programa. Dichas autorizaciones constan en el Servicio de la Escuela Internacional de Doctorado de la Universidad de Extremadura.

2023

Agradecimientos

*En especial, quiero agradecer a mi directora de Tesis, la **Dra. María del Carmen Gómez Jiménez** la confianza que depositó en mí en el desarrollo de esta tesis doctoral. Su apoyo y confianza en mi trabajo y su capacidad para guiar mis ideas ha sido un aporte invaluable, no solamente en el desarrollo de esta tesis, sino también en mi formación como investigadora. Las ideas propias, siempre enmarcadas en su orientación y rigurosidad, han sido la clave del buen trabajo que hemos realizado juntas, el cual no se puede concebir sin su siempre oportuna participación. Tras años de trabajo e inquietudes vividas juntas, como directora se ha ganado mi lealtad, admiración y seriedad en la investigación, consiguiendo siempre los objetivos que se propone.*

*También quiero dar las gracias a mis codirectoras de Tesis, la **Dra. Mercedes Gallardo** de la Universidad de Vigo y la **Dra. Juana Labrador** de la Escuela de Ingenierías Agrarias de Badajoz por sus valiosas correcciones, sugerencias, así como ideas e hipótesis durante el desarrollo de este trabajo.*

*En los últimos años, el **Dr. Miguel Ángel Paredes** nos dejó, pero siempre estará presente en cada uno de nuestros trabajos, ayudándonos como lo hacía en la recogida y preparación del material vegetal tanto en campo como en laboratorio. Su apoyo y ánimo constante nos daban fuerzas para seguir hacia adelante.*

*Al **Dr. Jorge Corbacho** por su atención y ayuda incondicional en la preparación de algunas figuras de esta memoria.*

*A mi compañera de batalla, la **Dra. Beatriz Briegas** por haber vivido esta etapa juntas llena de momentos buenos y de dificultad, pero nada que no hayamos podido superar con el fin de crecer profesionalmente.*

*A los compañeros del INIAV de Portugal, el **Dr. Antonio Cordeiro y la Dra. Carla Inés**, por brindarme todo su apoyo y compartir ideas, hipótesis, así como material y seminarios de investigación.*

*A **D. José Luis Grosson** por toda la ayuda desinteresada que nos ha prestado desde siempre en la aportación del material vegetal utilizado en este trabajo.*

*Al **Dr. Emilio Martínez**, por su llegada reciente al grupo de investigación mostrando todo su apoyo en el desarrollo de esta memoria.*

*Al **Servicio de Apoyo a la Investigación** de la Universidad de Extremadura y al **Servicio de Cuantificación de Hormonas Vegetales** (IBMCP, Valencia) por su contribución a este trabajo. También agradecer a **D. J.C. Triviño** (Sistemas Genómicos, Valencia) por la asistencia técnica.*

*A la **Junta de Extremadura** por haber disfrutado de un contrato como Personal Científico Investigador (PCI) del proyecto del Plan Regional en la Universidad de Extremadura.*

*No podría dar por finalizado estos agradecimientos sin dedicarles unas palabras a todos aquellos que están y han estado presente a lo largo de todos estos años llenos de buenos y malos momentos, **MI FAMILIA**; gracias a mis padres, **Mari Carmen y Miguel Ángel**, por enseñarme el valor de la educación y brindarme todo su apoyo para alcanzar mis metas. Esta tesis es una forma de agradecerles que hayan creído en mí y me hayan acompañado en los momentos más difíciles. No hay palabras suficientes para agradecerles todo lo que han hecho por mí, su amor incondicional, su paciencia y su sacrificio con el que hemos conseguido cumplir este sueño. Gracias a mis hermanos, **María del Mar y Miguel Ángel,** por ser compañeros confidentes durante toda mi carrera profesional y ser mi fuente de apoyo y motivación en este logro académico. En los últimos años, gracias a mi hermana por traer al mundo a una personita muy especial, mi sobrina **Eda**, que siempre será la alegría de la casa. Su sonrisa me hace crecer y sentirme muy afortunada de tenerla con nosotros. Gracias a mi abuelos, **Carmen y Aurelio**, luchadores y dedicados a su familia, que han entregado todo a sus hijos y nietos, esos son mis abuelos. Aunque mi abuelo ya no esté con nosotros, siempre fue un pilar muy importante para mí, dándome la fuerza para lograr el triunfo y cumplir todas mis metas. Gracias a mis tías, **Mari Ángeles y Paqui,** por ser un centro de amor y apoyo constante, por ser cálida y atenta. Por demostrarme su cariño en cada oportunidad. He aprendido de ellas a no rendirme nunca e incluso a poner buena cara en los momentos más difíciles.*

*Gracias a mis suegros, **Maribel y Ramón**, por darme todo lo que tienen sin recibir nada a cambio e integrarme a la familia como si fuera una hija. En los últimos años, mi suegro nos dejó, pero siempre estará presente en cada uno de mis pasos dándome la valentía y fortaleza para conseguir este logro académico y personal que él tanto deseaba. Mi suegra, por ser la gran profesional que es, y por todo lo que me ha inculcado desde el principio, por sus consejos, directrices y experiencias transmitidas que me han llevado a cumplir mis objetivos. Simplemente, complicidad.*

*Gracias a mi cuñada **Jara,** por darme su apoyo y amor incondicional durante toda esta trayectoria. Esas muestras de cariño como si fuera una hermana y esos disfrutes juntas hacen ver la vida de una forma más amena y feliz. Gracias a **Pepa y May**, por la confianza que han depositado en mí y apoyarme en cada uno de mis pasos.*

***A mis amigas**, les agradezco cada momento compartido y cada palabra de ánimo que me han brindado en este camino. En especial, a mi amiga **Laura**, mi cómplice y "psicóloga preferida", sin sus momentos de terapia, este proyecto no hubiera sido posible, enseñándome que ante todo en la vida hay que ser feliz. Decirte que me siento inmensamente afortunada de hacerte párticipe de este logro, otro motivo por el que celebrar nuestra amistad. Siempre de mi mano.*

*Para el final dejo a la persona más importante, mi pareja **Juane,** que siempre ha estado ahí, salgan las cosas como salgan, alegrándose o preocupándose tanto o más que yo. Decirte que termina un ciclo importante en mi vida, pero también en la tuya, ya que has sido mi apoyo incondicional en este largo proceso de investigación y redacción. Gracias por creer en mí, por escucharme, por ayudarme y por estar a mi lado en los momentos de incertidumbre y de cansancio. Este logro es también tuyo, porque sin tu amor y tu paciencia, nada de esto hubiera sido posible. Que este trabajo sea solo el inicio de muchos proyectos que juntos podamos emprender.*

A todos, muchas gracias de corazón.

A mi familia

La realización de esta Tesis Doctoral ha sido posible gracias a la concesión de un contrato de Personal Científico Investigador (PCI) del proyecto de la Junta de Extremadura (IB18075).

Este trabajo se enmarca dentro de la financiación del proyecto del Ministerio de Economía y Competitividad (RTI2018-097244-B-I00) y del proyecto de la Junta de Extremadura y el Fondo Europeo de Desarrollo Regional (IB18075).

Resumen

El cuajado y el desarrollo temprano del fruto carnoso constituyen procesos determinantes del tamaño del fruto. A pesar de los significativos avances científicos en esta línea, aún existe muy poca información sobre estos procesos en el caso del olivo (*Olea europaea* L.), cultivo de primer orden para la economía española, y en particular, sobre su regulación hormonal. El objetivo general planteado en esta Tesis Doctoral ha sido estudiar los mecanismos fisiológicos y moleculares implicados en el desarrollo del fruto de olivo. Este objetivo general se ha abordado en tres apartados específicos. En primer lugar, se ha realizado un análisis citológico, hormonal y transcriptómico del desarrollo temprano del fruto de la variedad 'Picual'. Mediante RNAseq se han podido identificar genes candidatos y rutas hormonales específicas que participan en las fases de división y expansión celular durante el desarrollo temprano del fruto de olivo. En segundo lugar, para profundizar en el estudio de la regulación hormonal del proceso de desarrollo y maduración del fruto de olivo, se ha realizado un estudio comparativo de los contenidos hormonales y de la expresión de genes relacionados con hormonas durante el desarrollo en frutos de variedades de olivo con diferencias en su tamaño y forma, así como en su duración de maduración. Nuestros resultados mostraron el posible papel de las giberelinas en la coordinación del tamaño del fruto y en la progresión de la maduración del fruto, así como el papel central del ácido abscísico en la maduración del fruto de olivo. Finalmente, se ha abordado un análisis preliminar sobre la relativa importancia de las fases de división y expansión celular en el tamaño final del fruto en frutos de tres variedades de olivo durante su desarrollo. En conclusión, esta tesis contribuye a un mejor conocimiento del control transcripcional y hormonal del desarrollo del fruto de olivo, lo que podría conducir a nuevas estrategias para mejorar la calidad del fruto de olivo.

Abstract

The fruit set and early development of fleshy fruit constitute two of the main processes determining fruit size. Despite the significant scientific advances along this line, there is still little information available concerning the physiological, biochemical, and molecular bases underlying hormonal regulation of early fruit development in the olive (*Olea europaea* L.), a leading crop for the Spanish economy. The overarching aim in the present doctoral thesis is to analyse the physiological and molecular mechanisms involved in olive fruit development. This general objective has been approached in three specific sections. Firstly, a cytological, hormonal, and transcriptomic analysis was made of early fruit development of the "Picual" cultivar. By RNAseq, candidate genes have been proposed, and specific hormonal pathways involved in the cell-division and cell-expansion phases during early development of the olive fruit were identified. Secondly, for an in-depth study of the hormonal regulation of olive fruit development and ripening, a comparative study was made of the hormonal contents and the expression of genes related to hormones during fruit development of olive cultivars differing in fruit sizes and shapes as well as in ripening duration. The results indicate the possible role of gibberellins in the coordination of the fruit size and in the progression of ripening as well as the essential role of abscisic acid in olive fruit ripening. Finally, a preliminary analysis was made concerning the relative importance of the cell-division and cell-expansion phases in the final size of the fruits of the three olive cultivars during their development. In conclusion, this thesis contributes to a fuller knowledge of the transcriptional and hormonal control of olive fruit development, which could result in new strategies to improve fruit quality in the olive.

Índice

Índice

Abreviaturas

Abreviaturas

A

ABA	...	Ácido Abscísico
ACC	...	Ácido 1-aminociclopropano-1-carboxílico
ABC	...	ATP-binding cassette
AGP	...	Proteína rica en arabinogalactanos
AGPase	...	Enzima biosintética de almidón
ARFs	...	Factores de respuesta a auxina
AVG	...	Aminoetoxivinilglicina
ARR	...	Reguladores de respuesta a citoquininas
ABA 8-OH	...	Ácido abscísico 8'-hidroxilasa
AOS	...	Aleno óxido sintasa
AAO3	...	ABSCISIC ALDEHYDE OXIDASE 3
ADC	...	Arginina descarboxilasa
AOase	...	Acetilornitina desacetilasa
ACAULIS5	...	Termospermina sintasa
ACS	...	ACC sintasa
ACO	...	ACC oxidasa
ABI5	...	Factor de transcripción bZIP
AMT	...	Transportador de amonio
ANT	...	AINTEGUMENTA; factor de transcripción
ARGOS	...	Auxin-Regulated Gene Involved in Organ Size
AP2/ERF	...	APETALA 2/ethylene responsive factor
ARID/BRIGHT	...	Factor de transcripción
aleta	...	*inflorescencia fasciada*
APC/C^{CCS52A}	...	Complejo promotor de anafase / ciclosoma^{CCS52A}
AmRAD	...	Antirrhinum RADIALIS
AtRL2	...	Arabidopsis R*AD-like 2*
Aux / IAA	...	Factores auxina / ácido indol-3-acético
amiRNA	...	Artificial microRNA
AHP	...	Actividad histidina fosfatasa
ANS	...	Antocianidina sintasa (ABA)
AREB1	...	Elemento de unión a ABA

B

BG	...	Glucano 1,3-β-glucosidasa
β-GAL	...	β-galactosidasa
BRs	...	Brasinoesteroides
BRI1	...	BR insensitive 1; receptor BR
BAK1	...	*SERK2;* BRI associated kinase
BIN2	...	BR insensitive 2
BZR	...	Brasinazol resistant
BES1/BZR1	...	Factor de transcripción
bZIP	...	Basic lecine zipper; factor de transcripción
BB	...	Big Brother
bHLH	...	Basic helix-loop-helix; factor de transcripción

C

CAL	...	Callosa sintasa
cDNA	...	Ácido desoxirribonucleico copia
CDK	...	Quinasa dependiente de ciclina
CES	...	Celulosa sintasa
CKs	...	Citoquininas
CKI	...	Proteína inhibidora de CDK
CKX	...	CK oxidasa/deshidrogenasa
CYC	...	Ciclinas
CYP707	...	Ácido abscísico 8'-hidroxilasa
CS2	...	Chorismate synthase 2
cox-6A	...	Cytochrome c oxidase subunit 6a protein
CYP735A	...	CK hydroxylase; citoquinina hidroxilasa
CTR1	...	CONSTITUTIVE TRIPLE RESPONSE1
CRK29	...	Cysteine-rich receptor-like protein kinase 29
C3H2	...	ZF CCCH domain-containing; TF
C value	...	DNA content
COI1	...	Señalización JA-Ile en el núcleo
Ct	...	Ciclo umbral
CLV	...	CLAVATA
C2H2	...	Zinc-finger; TF
CNR	...	CELL NUMBER REGULATOR
CSR	...	CELL SIZE REGULATOR

C	...	Frutos climatéricos
CDF	...	CYCLIN DOF FACTOR
CDPK	...	Proteína quinasa dependiente de calcio
CHL P	...	Geranilgeranil reductasa
CHS	...	Chalcona sintasa
CHI	...	Chalcona isomerasa
4CL	...	4-cumarato-CoA ligasa
C4H	...	Cinamato 4-hidroxilasa

D

DPA	...	Días post-antesis
DNA	...	Ácido desoxirribonucleico
DIR15	...	Dirigent protein 15-like protein
DAD2	...	SL esterasa; estrigolactona esterasa
D14	...	α/β hydrolase DWARF14
DAPI	...	4,6-diamidino-2-phenylindole
DREAM	...	MYB3R-1 TF
DESeq	...	Método algorítmico expresión diferencial de genes
DAM	...	Auxin-regulated genes
DOF-ZF	...	Factor de transcripción
DEG	...	Gen expresado diferencialmente
DELLA	...	Represor de señalización de GA
DFR	...	Dihidroflavonol 4-reductasa
DXS	...	1-desoxi-D-xilulosa-5-P sintasa
DH	...	Arogenato deshidrogenasa
2-DE	...	Two-dimensional electrophoresis
3,4-DHPEA	...	Descarboximetiloleuropeína aglicona -EDA

E

EGase/CEL	...	Endo-1,4-β-glucanasa o celulasa
ERF	...	Factor de respuesta a etileno
EIN	...	Ethylene insensitive
EIL	...	EIN3-like
ETR	...	Receptor de etileno
ETO1	...	Ethylene-overproduction protein 1
EXP	...	Expansinas
EXT	...	Extensinas

E2F/DP	...	Factor de transcripción
EMS1	...	Gene encoding for LRR-RLKs family protein
ENO	...	EXECESSIVE NUMBER OF FLORAL ORGANS
EST	...	*Expressed Sequence Tag*
EDTA	...	Ácido etilendiamino tetraacético

F

FAMA	...	bHLH proteins
FDR	...	False Discovery rate; p valor
FAF	...	proteínas FANTASTIC
FUL1/FUL2	...	Factores de transcripción de la caja MADS
FSM	...	FRUIT SANT/MYB-like
FSB	...	FRUIT SANT / MYB BINDING PROTEIN
FW	...	Fresh weight
F3H	...	Flavanona 3-hidroxilasa
FAD	...	Genes de desaturación de ácidos grasos

G

GAs	...	Giberelinas
GID1	...	Giberelina insensible dwarf1
GO	...	Ontología de genes
GH3	...	Familia de genes sensibles a auxina Gretchen Hagen3
GAI1	...	*Gibberellin insensitive*; Proteína DELLA
GID2	...	Receptor señalización giberelinas
GGPPS	...	Geranilgeranil difosfato sintasa
GA3ox	...	GA 3-oxidasa
GA2ox	...	GA 2-oxidasa
GA20ox	...	GA 20-oxidasa
GRF	...	Factor regulador del crecimiento
GIFs	...	Interacting factors
GATA	...	Factor de transcripción
GRAS	...	Factor de transcripción
GBP	...	GUANYLATE-BINDING PROTEIN
GTMT	...	Gamma tocoferol metiltransferasa
GES	...	Geraniol sintasa
GE10H	...	Geraniol 10-hidroxilasa
GC-MS	...	Cromatografía de gases - espectrometría de masas

H

Homeobox	...	Factor de transcripción
HK	...	Histidina quinasa
HPAT	...	Hidroxiprolina o- arabinosiltransferasa
HDAC	...	Histona desacetilasa
HPT1	...	Homogentisato fitiltransferasa 1
HPLC	...	Cromatografía líquida de alta resolución
HPLC-MS	...	cromatografía líquida de alta resolución – masa
ESI MS	...	Electrospray ionization mass spectrometry

I

IAA	...	Ácido indol-3-acético
IP	...	Isopentenil-adenina
IPT	...	Isopentenil transferasas
ILR1	...	IAA-amino acid hydrolase; auxin homeostasis
ICE1	...	INDUCER of CBF EXPRESSION 1; bHLH TF
IQD	...	Miembro de la familia de proteínas del dominio IQ67
IMA	...	INHIBITOR OF MERISTEM ACTIVITY

J

JA	...	Ácido jasmónico
JA-Ile	...	Jasmonoil-isoleucina
JAR1	...	Jasmonoil-isoleucina sintetasa
JMT	...	Jasmonato-O-metiltransferasa

K

KT	...	Transportador de potasio
KEGG	...	Kyoto Encyclopedia of Genes and Genomes database
KNU	...	KNUCKLES

L

LAC	...	Lacasa
LOG	...	Cytokinin riboside 5'-monophosphate phosphoribohydrolase
LOX	...	Lipoxigenasa
LAX	...	Transportador de entrada de auxinas
LRR-RLKs	...	Leucine-rich repeat receptor-like kinases
LC-MS	...	Cromatografía de líquidos-espectrometría de masas

M

1-MCP	…	1-metilciclopropeno
MeJA	…	Metil jasmonato
MCX	…	Intercambio catiónico
mRNA	…	Ácido Ribonucleico mensajero
MDS1	…	Signaling peptide; receptor-like protein kinase
MF	…	Meristemo floral
MIF	…	MIni zincFinger

N

NCED	…	9-cis-epoxicarotenoide dioxigenasa (biosíntesis ABA)
NO	…	Óxido nítrico
NOS	…	NO sintasa
NR	…	Nitrato reductasa
NRT	…	Transportador de nitrato
nsLTP2	…	Nonspecific lipid-transfer protein
NC	…	Frutos no climatéricos
NSY	…	Neoxantina sintasa

O

OeUB	…	*O. europaea* ubiquitin
OeSBT	…	Phylogenetic analysis of olive SBT
OBP1	…	DOF TF
OTCase	…	Ornitina carbamoiltransferasa
OFP	…	OVATE family protein
Oeÿ-GLU	…	ÿ-glucosidasa de olivo con alta afinidad
Ovate	…	Loci de rasgos cuantitativos

P

PAs	…	Poliaminas
PG	…	Poligalacturonasa
PME	…	Pectina metilesterasa
PIN	…	Transportador de salida de auxinas
PAL	…	Fenilalanina-amoniaco-liasa
PCA	…	Análisis de componentes principales
PAO	…	Poliamina oxidasa
PYR/PYL	…	Receptores ABA
PP2C	…	Fosfatasa de tipo 2C

PRE	...	PACLOBUTRAZOL RESISTANCES; TF bHLH
P valor	...	Valor de significación estadística expresión diferencial
PIL	...	Myc-related bHLH transcription factor
PCNT115	...	Auxin-regulated genes
PLATZ	...	Factor de transcripción
PLAC8	...	Placenta-specific gene 8 protein
pPPC2	...	Promotor fosfoenolpiruvato carboxilasa
PDS1	...	4-hidroxifenilpiruvato dioxigenasa
PPO	...	Polifenoloxidasa
PR	...	Pathogenesis-related protein
PRX	...	Peroxidasa

Q

qRT-PCR	...	PCR cuantitativa en tiempo real
QTL	...	Loci de rasgos cuantitativos

R

RB	...	Proteína retinoblastoma
RGL1	...	Proteína DELLA
RNA	...	Ácido ribonucleico
RNA-Seq	...	Secuenciación masiva de transcriptoma
RNAi	...	RNA interferente o RNA de interferencia
RIN	...	Factor de transcripción MADS
RACE	...	Amplificación rápida de extremos de ADNc
RMN	...	Resonancia magnética nuclear

S

SA	...	Ácido salicílico
SAUR	...	Small auxin up RNA; Señalización de auxinas
SL	...	Estrigolactonas
SBT	...	Subtilasas
SAMDC	...	S-adenosilmetionina descarboxilasa
SAMS	...	SAM sintetasa
SCL	...	Scarecrow-like; TF
SPDS	...	Espermidina sintasa
SHT	...	Espermidina hidroxicinamoil transferasa
SAM	...	S-adenosilmetionina
SCF	...	SKP1/Cullin/F-box

SMXL	…	Suppressor of MAX2 like
SUC	…	Proteína transportadora de sacarosa
SPNS2	…	Genes transportadores de esfingolípidos
SNF2	…	Helicase-like TF or Chromatin Remodeling Protein
SMOS1	…	AP2-like ethylene-responsive type TF
SMR	…	Siamese-related family genes; cell cycle
SCREAM2	…	Factor de transcripción bHLH33
SPCH	…	bHLH proteins
SNP	…	Polimorfismo de un solo nucleótido
SlCCS52A	…	Ciclo celular switch 52A
SE	…	Desviación típica real o estimada distribución muestral
SD	…	Desviación estándar
SSR	…	*Simple Sequence Repeats*
SDS-PAGE	…	Sodium dodecyl sulfate polyacrylamide gel electrophoresis

T

TF	…	Factor de transcripción
TIR1	…	Transport inhibitor response 1
tZ	…	*trans*-Zeatin
TAR4	…	Tryptophan aminotransferase protein 4
TPL	…	TOPLESS
Trihelix	…	Helicase-like TF or Chromatin Remodeling Protein
TCP	…	Factor de transcripción
TAGL1	…	Factor de transcripción de la caja MADS

U

UPHL	…	Cromatografía líquida de alta velocidad
UFGT	…	UDP glucosa-flavonoide 3-O-glucosiltransferasa

V

VOZ	…	Factor de transcripción
VTE5	…	Proteína biosíntesis tocoferol
VTE3	…	Vitamina E defectuosa 3
VTE1	…	Tocoferol ciclasa
v/v	…	Percent volume/volume

W

WUS	...	*WUSCHEL*
WT	...	Alelo de tipo silvestre
w/v	...	Percent weight/ volume

X

XTH	...	Xiloglucano endotransglucosilasa/hidrolasa

Y

YUCCA10	...	Síntesis de auxinas
ÿ-GLU	...	ÿ-glucosidasa

Z

ZNT	...	Transportador de zinc
Z	...	Zeatina
ZOX	...	Zeatin O-xylosyltransferase
ZOG	...	Zeatin O- glucosyltransferase
ZF	...	Zinc finger TF
Zm1	...	MYB-R2R3 TF
ZISO	...	Isomerasa de la vía biosintética de carotenoides
ZA	...	Zona de abscisión

Introducción general

I. Introducción general

1. Crecimiento, desarrollo y maduración del fruto

1.1. Crecimiento temprano del fruto

1.1.1. El fruto de tomate como modelo de estudio durante el crecimiento y desarrollo

En las plantas con flores, los frutos son órganos cruciales ya que protegen las semillas durante su desarrollo y permiten su dispersión después de la maduración. Los frutos también forman una parte esencial de la dieta humana y contribuyen en gran medida a la salud humana al proporcionar una gran variedad de compuestos, que incluyen principalmente fibra, vitaminas y compuestos fenólicos (Mauxion et al., 2021). Entre los frutos que se producen a nivel mundial, el tomate es uno de los más consumidos. El fruto del tomate *(Solanum lycopersicum)* es una fuente baja en calorías con altas cualidades nutricionales ya que contiene licopeno, ácido ascórbico, flavonoides y potasio (Mauxion et al., 2021). Además de sus propiedades bioquímicas específicas y la importancia de los nutrientes, con un ciclo de vida corto y una alta producción de semillas, el tomate se ha convertido en un modelo ampliamente utilizado para la investigación sobre la fisiología y el desarrollo de frutos carnosos, un nicho que no puede ser llenado por la clásica planta modelo Arabidopsis *(Arabidopsis thaliana),* que da lugar a un fruto seco en silicua. La silicua crece después de la fertilización, con poca diferenciación tisular, hasta que alcanza su longitud final y luego entra en un programa de senescencia (Mauxion et al., 2021). Sin embargo, el crecimiento del fruto carnoso del tomate va acompañado de una importante diferenciación tisular, seguida de la entrada en un complejo programa bioquímico, la maduración, que hace que el fruto sea atractivo y listo para dispersar semillas (Gómez et al., 2013).

La gran diversidad genética presente tanto en tomates silvestres como cultivados proporciona una reserva extensa de recursos disponibles para estudios genéticos y el descubrimiento de rasgos concretos (Rothan et al., 2019). Especialmente, la domesticación del tomate, que provocó las modificaciones de una amplia gama de caracteres morfológicos y fisiológicos en comparación con sus ancestros, resultó en una gran diversidad en el peso

y la forma del fruto (Bergougnoux, 2014), proporcionando así sistemas experimentales clave para estudiar la determinación del crecimiento. La variabilidad en el peso del fruto se ejemplifica muy bien al comparar la silvestre *Solanum pimpinellifolium*, que produce frutos que pesan alrededor de 1 g, con la especie *S. lycopersicum var. Lycopersicum*, con frutos que pueden llegar a tener más de 1 kg. A pesar de esta enorme variabilidad en el tamaño del fruto obtenida a través de la domesticación, los cambios celulares subyacentes y las redes genéticas aún se conocen poco. La mayor parte del conocimiento sobre las redes moleculares que regulan el crecimiento del fruto se deriva del estudio de la hoja de Arabidopsis, un modelo que resultó muy valioso para definir este proceso (Vercruysse et al., 2020). Con los rápidos avances en la secuenciación, la genética cuantitativa y las tecnologías de edición de genes, ahora es posible identificar directamente los componentes y las conexiones de las redes reguladoras y potencialmente modificarlos en cultivos para la reproducción (Mauxion et al., 2021). Estas tecnologías son fácilmente aplicables al tomate, lo que convierte a esta planta en un excelente modelo para diseccionar las redes genéticas que determinan el crecimiento del fruto.

1.1.2. Tamaño final del fruto: proceso altamente regulado desde el desarrollo del ovario hasta la maduración del fruto

1.1.2.1. Aumento del número de carpelos / lóculos

Dado que el fruto se deriva del ovario preexistente después de la fertilización, se puede esperar que una alteración en el tamaño del ovario pueda afectar el tamaño final del fruto (Mauxion et al., 2021). Una primera posibilidad para producir frutos más grandes, modificando el tamaño del ovario, está bien ejemplificado en la variedad *Bistec* de tomate. En esta variedad, el número de lóculos, las cavidades derivadas de carpelos fusionados que albergan las semillas, alcanza hasta diez, dando lugar a un fruto que pesa aproximadamente 1 kg, mientras que los tomates pequeños silvestres o los cultivares de frutos pequeños solo contienen dos lóculos (Rodríguez et al., 2011). Este aumento en el número de lóculos, correspondiente al número de carpelos, se determina tan pronto como comienza el desarrollo y la organización del meristemo floral (MF) (Mayer et al., 1998; Xu et al., 2015). Dos mutaciones naturales, *número de lóculos* (*Lc*) y *fascinated* (*fas*), controlan principalmente el número de lóculos en el tomate. *Lc* y *fas* se ven afectados

en los genes ortólogos de Arabidopsis *WUSCHEL (WUS)* y *CLAVATA3 (CLV3)*, respectivamente, que están implicados en la organización de los meristemos. En Arabidopsis, *WUS* codifica un factor de transcripción involucrado en el mantenimiento de la identidad de las células madre dentro del meristemo apical del brote (SAM) (Laux et al., 1996). Una sobreexpresión de *AtWUS* produce flores con órganos supernumerarios que carecen de los órganos más centrales (Xu et al., 2005). En tomate, dos polimorfismos de un solo nucleótido (SNP) en la región del gen ortólogo putativo, *SlWUS*, son responsables del aumento en el número de lóculos en el mutante *Lc* (Muños et al., 2011). La aparición de estos SNP suprime la unión del represor transcripcional *AGAMOUS* que regula negativamente a *WUS*, como en Arabidopsis (Liu et al., 2011).

Como resultado, la expresión de *SlWUS* aumenta en los botones florales de *Lc*, lo que a su vez puede permitir el mantenimiento de una población de células madre más grande, dando como resultado un mayor número de lóculos (Knaap et al., 2014; Chu et al., 2019). Un segundo locus importante para la determinación del número de lóculos en tomate es el locus *fas* que alberga una modificación en el promotor de *CLAVATA3, SlCLV3* (Xu et al., 2015). En Arabidopsis, *CLV3* codifica un glicopéptido involucrado en la restricción del tamaño del meristemo a través de la activación del receptor quinasa *CLV1* (Ohyama et al.,2009). El mutante *clv3* con pérdida de función produce SAM y MF agrandados con flores supernumerarias (Clark et al., 1995). En Arabidopsis, la producción de mutantes dobles demostró que un bucle de retroalimentación negativa *WUS / CLV3* determina la organización y el número de órganos florales (Schoof et al., 2000). Curiosamente, *SlCLV3* muestra un patrón de expresión similar al de *SlWUS* (Chu et al., 2019), y los loci *Lc* y *fas* tienen efectos sinérgicos sobre el número de lóculos y, por lo tanto, en el tamaño del fruto cuando estos se combinan. La presencia del locus *fas* solo aumenta la ramificación de la inflorescencia además del número de lóculos (Xu et al., 2015). La regulación de *SlCLV3* a través del enfoque de RNAi muestra fenotipos similares, pero también tiene efectos deletéreos, como el desarrollo de ovarios dentro del ovario inicial (Chu et al., 2019). Además, *SlCLV3* está regulado en un fondo *fas*, lo que muestra que la mutación *fas* implica una pérdida parcial de la función de *SlCLV3* (Chu et al., 2019).

En un estudio llevado a cabo por Chu et al. (2019) se demostró una tendencia positiva entre el número de lóculos y el tamaño de MF como resultado de los efectos de *Lc* y *fas*. Dos mutantes adicionales, fasciado y ramificado (*fab*) y la inflorescencia fasciada (*aleta*), también muestran meristemos agrandados y flores fasciadas con más órganos florales que producen frutos más grandes como consecuencia de la presencia de carpelos adicionales (Xu et al., 2015). Los genes que subyacen a estos fenotipos en los mutantes *fab* y *fin* corresponden a *CLV1* y una arabinosiltransferasa, respectivamente. En *fab*, se encontró una mutación sin sentido en *CLV1*, y, en *fin*, se encontraron mutaciones sin sentido y deleciones que conducían a la ausencia de transcripciones en una hidroxiprolina o- arabinosiltransferasa (HPAT). En Arabidopsis, *CLV1* codifica un receptor quinasa que se une a *CLV3* para restringir la expresión de *WUS* (Fletcher, 1999). El rescate de mutantes de arabinosiltransferasa por un *CLV3* arabinosilado mostró que *CLV3* debe estar completamente arabinosilado para realizar su función (Xu et al., 2015). En Arabidopsis, la importancia de las modificaciones de arabinosa es menos clara, ya que los mutantes nulos para los genes HPAT no tienen un fenotipo *clv* (MacAlister et al., 2016). Las mutaciones *fab* y *fin* tienen un efecto aditivo y, por tanto, actúan en la determinación del tamaño del meristemo a través de la vía *WUS/CLV*. La pérdida de función del gen número excesivo de órganos florales (*SlENO*) da como resultado un aumento del tamaño del MF, lo que lleva a la producción de frutos multiloculares más grandes, un fenotipo que es mucho más pronunciado en un contexto de mutación *Lc* (Fletcher, 1999). *SlENO* codifica un factor de transcripción que pertenece a la superfamilia apetala2 / factor de respuesta al etileno (AP2/ERF), que regula directamente *SlWUS* (Fletcher,1999). Durante la domesticación del tomate, se seleccionó una deleción de 85 pb en el promotor *SlENO*, lo que provocó una reducción de su expresión y, por tanto, frutos más grandes (Fletcher, 1999). Entre los genes involucrados en la determinación del número de lóculos se encuentran los siguientes: inhibidor de la actividad del meristemo (*SlIMA*) y KNUCKLES (*SlKNU*) que codifican respectivamente, un MIni zincFinger (MIF) y un factor de transcripción perteneciente a la familia de proteínas C2H2 zinc-finger (Sicard et al., 2008; Bollier et al.,2018). La pérdida de función de *SlIMA* y *SlKNU* aumenta el tamaño del fruto a través de un aumento en el número de carpelos, mientras que la sobreexpresión conduce a una disminución en

el tamaño del fruto. Junto con TOPLESS, estas dos proteínas forman un complejo transcripcional que recluta histona desacetilasa 19, para regular negativamente la expresión de *SlWUS* y, por lo tanto, deteriorar la actividad de las células madre dentro del MF (Bollier et al., 2018).

En tomate, el control del tamaño del meristemo por la vía *WUS-CLV* es, por tanto, esencial para la determinación del tamaño del fruto a través de la regulación del número de lóculos. Este rasgo ha sido seleccionado durante el proceso de domesticación para producir grandes plantas frutales mediante la modulación de señalización *WUS-CLV*, principalmente a través de mutaciones en elementos reguladores *cis* (Yuste-Lisbona et al., 2020; Wang et al., 2021).

1.1.2.2. División celular en el ovario y el fruto

Control de la división celular durante el desarrollo del ovario

Durante el desarrollo de las flores, la división celular es el principal impulsor del crecimiento dentro del ovario. La modificación espacial de la velocidad o duración de la división celular en el ovario influirá así en su tamaño final y, en consecuencia, en el tamaño final del fruto (Mauxion et al., 2021). Tres loci de rasgos cuantitativos (QTL), *fs8.1*, *sun* y *ovate*, que controlan el alargamiento del fruto dentro del germoplasma de tomate cultivado, están involucrados en la regulación del número de células a lo largo de diferentes ejes de crecimiento del ovario, siendo *fs8.1* el único eficaz para aumentar finalmente el peso del fruto (Rodríguez et al., 2011; Sun et al., 2015).

El locus *fs8.1* está presente en el procesamiento de tomates, denominados tomates cuadrados (Ku et al., 2000). En las plantas que albergan el locus *fs8.1*, el índice de forma del fruto, correspondiente a la relación entre el diámetro longitudinal y el ecuatorial, es diferente al de las plantas que albergan el alelo de tipo silvestre (*WT*) y conduce a frutos más alargados y pesados (Sun et al., 2015). Este efecto de *fs8.1* se origina en el alargamiento del ovario a través del aumento del número de células en la dirección próximo-distal, sin ningún cambio en la dirección mediolateral. En la dirección abaxial-adaxial, también se encontró un mayor número de capas de células en el fruto, lo que posiblemente condujo a un pericarpo más grueso. Si bien el tamaño de las células no se alteró en el ovario, las células fueron más pequeñas en el

pericarpo del fruto maduro de los frutos *fs8.1*. Hasta ahora, la identidad del gen subyacente al locus *fs8.1* sigue siendo desconocida (Sun et al., 2015).

Otros dos QTL importantes que controlan el alargamiento del fruto: son *sun* y *ovate*, que contrariamente a *fs8.1,* no conducen a un aumento del peso del fruto (Wu et al., 2011, 2015). *Ovate* confiere una forma de pera a los frutos aumentando el número de células en la dirección proximo-distal y disminuyendo el número de células en la dirección medio lateral en el ovario, lo que conduce a un aumento del extremo proximal del fruto (Knaap et al., 2002). En *sun*, se forman frutos alargados, que contienen más células a lo largo de la dirección próximo-distal dentro del pericarpo y la columela, mientras que se producen menos células en la dirección mediolateral en la columela y el tabique (Wu et al., 2011). En cuanto a *ovate* y *fs8.1*, los cambios en *sun* ocurren durante el desarrollo del ovario, pero el alargamiento del fruto se promueve principalmente poco después de la antesis. Se han identificado los genes subyacentes a *ovate* y *sun*, que corresponden respectivamente a un miembro de la proteína de la familia OVATE (OFP) propuesta para regular la organización del citoesqueleto (Liu et al., 2002; Hackbusch et al., 2005) y a un miembro de la familia de proteínas del dominio IQ67 (IQD) que está involucrado en la transducción de señales de Ca^{2+} y el tráfico celular (Abel et al., 2005; Xiao et al., 2008). En *ovate*, la mutación da como resultado un codón de parada prematuro (Liu et al., 2002; Hackbusch et al., 2005), mientras que en *sun* el fenotipo es causado por una duplicación intercromosómica que conduce a un aumento de la expresión de *SlSUN* (Jiang et al., 2009). Un homólogo de *SlSUN* también puede subyacer a la variación de la forma del fruto en pepino (Pan et al., 2017).

En conclusión, *sun*, *ovate* y *fs8.1* controlan diferentes mecanismos que regulan la elongación de los ovarios y frutos que actúan sobre diferentes características espaciales y temporales de la división celular. La interacción sinérgica entre estos tres loci sugiere que estos tres genes están implicados en distintas vías que pueden converger en un nodo común para la regulación del patrón de órganos próximo-distales (Wu et al., 2015; Wang et al., 2019). Recientemente, se demostró que una aplicación de auxina durante el desarrollo del ovario conduce a frutos alargados en forma de pera como resultado de cambios celulares similares a los efectos de *ovate* (Wang et al.,

2019). Sin embargo, la forma en que estos tres genes involucrados en la determinación de la forma del fruto ejercen su papel en el control del patrón de división celular aún requiere una mayor profundización en su investigación.

El proceso de domesticación del tomate ha dado como resultado la selección de plantas que presentan una gran variabilidad en la forma de los frutos, pero también en la obtención de frutos de mayor tamaño. En el tomate se han identificado unos 30 QTL relacionados con el tamaño / peso del fruto (Grandillo et al., 1999). El locus *fw2.2* es responsable de hasta el 30% de la variación del peso del fruto (Alpert and Tanksley,1996). El gen subyacente al locus *fw2.2*, *SlFW2.2*, codifica una proteína que pertenece a la familia multigénica regulador de número de células (*CNR*) y que contiene un motivo de la proteína del gen 8 específico de la placenta (*PLAC8*), el cual se prevé que sea importante para la localización en la membrana de la proteína (Guo et al., 2010). Dos alelos diferentes, un 'alelo de fruto grande', presente en los tomates más actuales, y un 'alelo de fruto pequeño', heredado de los ancestros del tomate silvestre, difieren principalmente de los polimorfismos en la región reguladora del gen y conducen a diferencias espaciales y temporales de expresión (Frary, 2000). El alelo del "fruto grande" se expresa en una fase temprana durante el desarrollo del fruto, mientras que el alelo del "fruto pequeño" se expresa más tarde y se mantiene durante más tiempo (Cong et al., 2002). En las plantas que albergan el alelo del 'fruto grande', el ovario es más grande, principalmente debido a un aumento en el número de células, pero sin ningún cambio en el tamaño celular, lo que demuestra que *SlFW2.2* participa en la regulación del número de células (Frary,2000). Además, en la etapa temprana del desarrollo del fruto, el índice mitótico aumenta, sin ningún cambio en el tamaño de las células registrado en la placenta y el pericarpo, y se correlaciona negativamente con la expresión de *SlFW2.2* (Cong et al., 2002; Cong and Tanksley, 2006). El incremento en la división celular, no seguido por una modificación del grosor del pericarpo, podría indicar que *SlFW2.2* actúa como un regulador negativo de las divisiones celulares anticlinales. En varias especies de plantas, los ortólogos de *SlFW2.2* también participan en la regulación del tamaño de los órganos reproductores, como es el caso del maíz (*Zea mays*), donde la sobreexpresión de *ZmCNR1* conduce a la formación de órganos pequeños (Guo et al., 2010).

A pesar de que se han llevado a cabo muchos estudios sobre *FW2.2*, el mecanismo de acción por el cual dicha proteína de membrana puede regular negativamente el número de células y, por lo tanto, el tamaño del fruto, así como los cambios exactos que ocurren a nivel celular (tasa de división celular, duración de la división celular...), todavía no se conocen.

En muchos casos, estos homólogos potenciales de genes/QTL también se describieron en otras especies de plantas. En este sentido, se han encontrado homólogos de *FW2.2* en papaya (*Carica papaya*), melocotón (*Prunus persica*), vid (*Vitis vinifera*), en los que están asociados con los QTL de peso del fruto, y también en physalis (*Physalis floridana*) o arroz (*Oryza sativa*) en los que regulan las hojas, los órganos florales, las bayas, el tamaño de la semilla, y la altura de la planta, respectivamente (Beauchet et al., 2021).

Control de la división celular durante el desarrollo del fruto

Comenzando con el mismo grupo de células dentro del ovario, una modificación de la tasa de división celular o la duración después de la antesis también puede afectar el tamaño final del fruto. Entre los QTL relacionados con el peso/tamaño del fruto, *fw3.2* es el segundo en importancia que controla la masa del fruto de tomate (Chakrabarti et al., 2013). El estudio de líneas casi isogénicas que difieren por el alelo en *fw3.2* ha revelado que el aumento en el tamaño del fruto aparece durante la fase de desarrollo del fruto. En la etapa madura, el análisis citológico mostró un aumento en el número de capas de células dentro del pericarpo, lo que conduce a frutos más grandes, mientras que el tamaño de las células permanece sin cambios (Chakrabarti et al., 2013). El aumento en el número de capas de células y el retraso en la maduración del fruto sugieren una *SlKLUH* extensión del período de división celular. El gen subyacente a *fw3.2* se identificó como un ortólogo de *AtKLUH/CYP78A5*, que se ha demostrado que controla el tamaño de los órganos en Arabidopsis y que codifica un citocromo P450 (Anastasiou et al., 2007; Chakrabarti et al., 2013). En plantas que llevan el alelo de fruto grande de *fw3.2*, se propuso una mutación en esta región para conducir a un aumento en la expresión del gen *SlKLUH*. Sin embargo, recientemente, el establecimiento del pangenoma después de una secuenciación de lectura prolongada de 100 líneas de tomate diferentes, reveló que el aumento de la expresión de *SlKLUH* es causado por una

duplicación en tándem del gen en el locus *fw3.2* (Alonge et al., 2020). Este efecto de dosificación de genes en *fw3.2* se confirmó mediante el uso de la edición del genoma CRISPR-Cas9 dirigida a una o varias copias de *SlKLUH* (Alonge et al., 2020). Varios ortólogos de *SlKLUH* también pueden regular la masa del fruto, ya que, en el caso del chile, se ha encontrado un QTL *fw3.2* asociado con *KLUH*, como en el tomate (Chakrabarti et al., 2013). Asimismo, en las hojas de maíz, el ortólogo de *SlKLUH*, *ZmPLA1*, desencadena una fase prolongada de división celular que permite una mayor producción de biomasa y un mejor rendimiento de semillas cuando se sobreexpresa (Sun et al., 2017).

Efecto de la alteración de la maquinaria del ciclo celular

El control correcto del número de células durante el desarrollo de la flor o del fruto es, por tanto, un componente clave para el control del tamaño final del fruto (Mauxion et al., 2021). Una forma de estudiar el impacto de la división celular en el crecimiento del fruto es apuntar directamente a los genes que regulan el ciclo celular. La progresión a lo largo de las fases sucesivas del ciclo mitótico está controlada por complejos de proteínas heterodiméricas formadas por una subunidad catalítica denominada quinasa dependiente de ciclina (*CDK*) y una subunidad reguladora ciclina (*CYC*). El complejo *CDK-CYC* está altamente regulado a nivel postranscripcional por proteólisis, fosforilación o unión de proteínas reguladoras (De Veylder et al., 2007). Sin embargo, alterar fuertemente la expresión de los reguladores del ciclo celular puede promover la tasa, la duración o el patrón de división celular, pero también alterar la expansión celular, lo que a menudo no conduce a un aumento en el tamaño del fruto, mostrando así la interconexión existente entre estos dos procesos (Mathieu-Rivet et al., 2010; Czerednik et al., 2012). La función de ganancia y pérdida de *SlCCS52A* (ciclo celular switch 52A), que codifica una parte proteica del complejo promotor de anafase / ciclosoma^{CCS52A} (APC/C^{CCS52A}) que se dirige a las ciclinas para su destrucción mediante proteólisis, conduce a un fenotipo de fruto similar, es decir, una reducción de tamaño pero que difiere a nivel celular. De hecho, la regulación de *SlCCS52A* altera la expansión celular sin afectar la división celular, mostrando la participación solo después de la fase de proliferación celular (Mauxion et al., 2021). El estudio cinético de las líneas de ganancia de función

en el crecimiento del fruto reveló un grado de expansión celular en las últimas etapas del desarrollo del fruto y una reducción de la división anticlinal supuestamente para promover el aumento del volumen del fruto (Mathieu-Rivet et al., 2010). Este grado de expansión celular se vio acompañado de un mayor nivel de ploidía, lo que respalda el papel propuesto de la endorreduplicación en la promoción del crecimiento.

1.1.2.3. Alteración de la expansión celular

La expansión celular comienza inmediatamente después del cuajado del fruto en las células del mesocarpo y se extiende hasta la maduración (Cheniclet, 2005; Xiao et al., 2009; Pabón-Mora and Litt, 2011; Renaudin et al., 2017), siendo responsable de un rápido y significativo aumento del tamaño del fruto. Entre los QTL que controlan la masa del fruto, *fw11.3* puede suponer hasta un 8 % de la variación del peso del fruto (Grandillo et al., 1999). El gen regulador de tamaño celular (*CSR*) subyace en el locus *fw11.3* (Mu et al., 2017). *SlCSR* codifica una proteína de función desconocida con un bajo nivel de expresión en el fruto que tiene lugar solo después de la fase de división celular. El análisis citológico de líneas casi isogénicas mostró un aumento en el grosor del pericarpo como resultado de un aumento en el tamaño de las células del mesocarpo sin ningún cambio en el número de capas celulares (Mu et al., 2017). La expresión del alelo mutado en el fondo *WT* destacó que el alelo que aumenta el peso del fruto codifica una proteína truncada que actúa como un alelo dominante que participa en el aumento de peso. El gen ortólogo de *SlCSR* en Arabidopsis pertenece a las cuatro proteínas FANTASTIC (FAF) implicadas en la regulación del tamaño de SAM a través de una regulación negativa de *AtWUS* (Wahl et al., 2010). Es probable que *SlCSR* y *AtFAF* compartan la misma función bioquímica dentro de la célula, pero en tejidos diferentes (Mu et al., 2017). Sin embargo, esta función todavía requiere más estudios, así como la supuesta participación de *SlCSR* que se ha basado en datos de coexpresión, en la acción antagonista de auxina y citoquinina sobre el agrandamiento celular (Mu et al., 2017).

En el tomate, la regulación positiva de varios factores de transcripción pertenecientes a la familia '*factor regulador del crecimiento*' (*GRF*) provocó efectos pleiotrópicos, incluyendo cotiledones más cortos, flores grandes (Cao et al., 2016). En estas plantas que expresan niveles más altos de *SlGRF1* a *5*,

el tamaño y el peso del fruto aumentan como resultado de un mayor tamaño de las células epidérmicas (Cao et al., 2016). Se cree que los genes *SlGRF* regulan el crecimiento por diferentes medios, ya que se observan fenotipos opuestos en el tamaño celular en los cotiledones y frutos de los mutantes *SlGRF1* a *5*. Estas diferencias también se observan en las hojas de Arabidopsis, con *AtGRF1* y *AtGRF2* controlando el tamaño celular, mientras que *AtGRF5* regula la proliferación celular (Kim et al., 2003; Horiguchi et al., 2005).

Las líneas de sobreexpresión para el factor de transcripción putativo, *FRUIT SANT/MYB-LIKE1* (*SlFSM1*) albergan frutos más pequeños (Machemer et al., 2011) caracterizados por un pericarpo más delgado como resultado de una expansión celular disminuida. En estas plantas, la expansión celular en las hojas y el hipocótilo también se ve afectada, lo que demuestra que *SlFSM1* actúa como un supresor de la expansión celular en varios órganos. Los ortólogos más cercanos de *SlFSM1*, *Antirrhinum RADIALIS* (*AmRAD*) y *Arabidopsis RAD-like 2* (*AtRL2*) están involucrados en las asimetrías y en la obtención de flores radialmente simétricas, respectivamente (Corley et al., 2005; Baxter et al., 2007). La búsqueda de las proteínas asociadas de *SlFSM1* permitió la identificación de *FRUIT SANT/MYB BINDING PROTEIN 1* (*SlFSB1*) y se encontró que *SlMYB1* interactúa con *SlFSB1* (Machemer et al., 2011). Sobre la base de este estudio de interacción, utilizando las proteínas del tomate y la red del modelo *AtRAD* en Arabidopsis, se propuso una competencia de unión de *SlFSB1* por *SlFSM1* y *SlMYB1* como el mecanismo implicado en la regulación de la expansión celular diferencial durante el desarrollo del fruto (Corley et al., 2005; Machemer et al., 2011).

En algunos casos, la alteración en el grosor del pericarpo puede desacoplarse del tamaño del fruto. En este caso, la pérdida de función de la proteína de unión a guanilato 1 (*SlGBP1*) induce una disminución del grosor del pericarpo a través de una disminución del tamaño celular; sin embargo, el tamaño final del fruto permanece sin cambios (Musseau et al., 2020). En estas plantas, la diferencia en el grosor del pericarpo solo aparece después de 20 DPA, y se acompaña de una parada temprana de la expansión celular y la vuelta al estado de división de las células, lo que indica que *SlGBP1* está involucrado en el mantenimiento del programa de diferenciación en células del pericarpo a través de un mecanismo aún desconocido.

1.1.2.4. Regulación hormonal del crecimiento del fruto

Auxina y división celular

La modificación de genes implicados en la regulación hormonal puede afectar el tamaño del fruto, ya que durante el crecimiento del fruto se producen cambios importantes en el contenido de hormonas (Mariotti et al., 2011). Durante los estadios previos a la antesis en Arabidopsis, los factores auxina/ácido indol-3-acético (*Aux/IAA*) reprimen la señal de auxina secuestrando el factor de respuesta auxina (*ARF*), actuando como factores de transcripción que regulan la expresión de genes de respuesta a auxina. Por tanto, el ovario permanece en una fase de letargo, en la que se inhibe la actividad de división celular (Weijers et al., 2005). La fertilización desencadena un aumento en el contenido de auxinas, lo que conduce a la destrucción de *Aux/IAA* y la liberación de *ARF*, que luego están disponibles para transcribir sus genes diana y, en consecuencia, desencadenar la reanudación del proceso de división celular (Padolfini et al., 2007). En el tomate, el tratamiento del ovario no polinizado con auxina puede simular la fecundación y conduce al desarrollo de frutos partenocárpicos (Gustafson,1936). El aumento de la concentración de auxinas en el interior del ovario después de la polinización es un desencadenante importante del crecimiento del ovario (Mariotti et al., 2011). En el tomate, la familia *ARF* consta de 22 proteínas (Zouine et al., 2014). La expresión de *SlARF9* se desencadena por la polinización y alcanza la máxima expresión a los 6 DPA, obteniéndose un patrón similar en lo que respecta a la acumulación de auxinas en el fruto (Mariotti et al., 2011). La función de pérdida y ganancia de *SlARF9* da como resultado frutos más grandes y más pequeños, respectivamente (De Jong et al., 2015). Tanto en las etapas tempranas como en las maduras, las líneas de ARNi de *SlARF9* muestran una disminución en el tamaño de las células, así como más capas de células en el pericarpo. Por el contrario, los frutos de la línea *pTPRP-SlARF9* presentan un aumento temprano en el tamaño de las células y una disminución en el número de capas de células en las etapas posteriores. Por tanto, *SlARF9* parece actuar como un regulador negativo para ajustar la división celular durante el crecimiento del fruto (De Jong et al., 2015). Sorprendentemente, también se ha podido demostrar que la disminución en la expresión de *SlARF5*, utilizando un amiRNA, conduce a un fenotipo de fruto

pequeño, similar a lo que ocurre con la sobreexpresión de *SlARF9* (Liu et al., 2018). No se observaron diferencias obvias en la morfología del fruto durante la división temprana de las líneas *amiSLARF5*, pero en etapas posteriores el pericarpo contenía menos capas de células, debido a un período más corto de división celular, así como células más grandes en comparación con las plantas *WT*. Por tanto, *SlARF5* podría ser un regulador positivo de la división celular (Liu et al., 2018). La auxina también puede modular la regulación de genes sensibles a auxina a través de la acción de proteínas represoras como *SlIAA17* (Su et al., 2014). *SlIAA17* se expresa altamente en el fruto a 10 DPA cuando comienza la expansión celular y su expresión disminuye gradualmente hasta la etapa de ruptura. Este pico de expresión corresponde a uno de los picos bimodales de auxina que se producen a los 10 y 30 DPA (Gillaspy et al., 1993). El estudio de *SlIAA17* utilizando un enfoque de ARNi ha demostrado que la disminución de la expresión de este gen conduce a la producción de frutos más grandes a través de un aumento del tamaño celular del pericarpo sin que exista modificación del número de capas celulares (Su et al., 2014). *SlIAA17* interactúa con varias proteínas *ARF*, incluida *SlARF5* (Su et al., 2015). La disminución de la expresión de *SlIAA17* y *SlARF5* que conduce al fenotipo opuesto podría corroborarse con una función represora de *SlIAA17* en *SlARF5 (*Mauxion et al., 2021). Con todo ello, el papel de la auxina en la regulación del crecimiento del fruto no está claro y, dependiendo de la etapa de desarrollo del fruto, parecen estar involucradas diferentes proteínas sensibles (Mauxion et al., 2021).

Giberelinas (GA) y expansión celular

Numerosos estudios han demostrado el importante papel de la GA en la regulación del crecimiento del fruto mediante la utilización de mutantes o por la aplicación de tratamientos exógenos de esta fitohormona (Groot et al., 1987; Fos et al., 2001). En cuanto a la auxina, el tratamiento de ovarios no polinizados con GA conduce a la formación de frutos partenocárpicos (Wittwer et al., 1957). Varios estudios han demostrado que las vías de auxina y GA están interconectadas ya que el tratamiento con GA induce un aumento en el contenido de auxina y, a su vez, la auxina induce la biosíntesis de GA (De Jong et al., 2009). Sin embargo, GA parece estar involucrada principalmente en el proceso de expansión celular en el fruto. Paclobutrazol

resistencia 2 (*PRE2*), que pertenece a la familia de factores de transcripción bHlH, es inducido por GA y participa en la respuesta de la planta a GA (Zhu et al., 2017). Las líneas de sobreexpresión de *SlPRE2* muestran un ligero aumento en el diámetro del fruto, mientras que las líneas con pérdida de esta función muestran una disminución en el tamaño del fruto (Zhu et al., 2019). En las líneas de ARNi para *SlPRE2*, el tamaño de las células del mesocarpo se reduce, lo que conduce a un pericarpo más delgado. *SlPRE2* parece mostrar una función similar a *AtPRE1*, ya que ambas proteínas están implicadas en el alargamiento celular a través de la respuesta moduladora de GA (Lee et al., 2006; Hao et al., 2012; Zhu et al., 2019). La regulación de otro factor de transcripción implicado en la vía GA, *SlGRAS2*, conduce a una reducción del tamaño de las células del pericarpo y, por tanto, a la obtención de frutos más pequeños (Li et al., 2018). *SlGRAS2* se expresa desde la pared del ovario en antesis hasta el fruto 10 DPA. En las líneas de ARNi dirigidas a *SlGRAS2*, la pared del ovario es más delgada, pero no se ha observado ningún cambio en el número final de capas celulares en el pericarpo, lo que muestra la participación de *SlGRAS2* en la regulación de la expansión celular. En estas líneas, se inhiben tanto la biosíntesis de GA como las vías de transducción de señales (Mauxion et al., 2021).

Diferentes estudios han revelado que el aumento de la expresión del factor de transcripción factor dof de ciclina 4 (*SlCDF4*) bajo el control del promotor fosfoenolpiruvato carboxilasa (*pPPC2*) utilizado para una expresión específica de frutos, con mayor expresión durante la fase de expansión celular (Fernández et al., 2009), conduce a la producción de frutos más grandes debido a un aumento tanto del número de capas como del tamaño de las células (Renau-Morata et al., 2020). En estas plantas, el contenido de hormonas se ve modificado, existiendo un mayor contenido de GA y niveles menores de auxinas. Así, *SlCDF4* puede desempeñar un papel doble en la síntesis de auxina y GA, regulando de esta manera tanto la división como la expansión celular. El aumento del tamaño del fruto y del contenido de GA ya había sido observado con la sobreexpresión de otro miembro de la familia *SlCDF3* (Renau-Morata et al., 2017), aunque no se ha llegado a describir su efecto a nivel celular.

Interacción fitohormonal durante el desarrollo temprano del fruto

La auxina y la GA poseen funciones únicas durante la fructificación, así como durante la posterior división y expansión celular, por lo que está claro que la interacción entre ambas fitohormonas permite la corregulación de los procesos de polinización y fertilización del fruto (Matthew and Giovannoni, 2021; Figura 1). La comunicación auxina-GA se facilita a través de la acción de las proteínas auxina/indol-3-ácido acético (*Aux/IAA*) y el factor de respuesta de auxina (*ARF*), mientras que los productos de la familia de genes sensibles a auxina Gretchen Hagen3 (*GH3*) funcionan para mantener la homeostasis mediante la conjugación de moléculas de auxina libres (Li et al., 2016a, 2016b; Luo et al., 2018). Los elementos *Aux/IAA*, como *IAA9* y la familia de genes *ARF*, son parte integral de la regulación del cuajado del fruto (Wang et al., 2005), así como también en otros procesos vegetativos y reproductivos. Los *ARF* individuales actúan como factores de transcripción con propiedades distintas y superpuestas, y han sido ampliamente investigados tanto en Arabidopsis como en tomate (Matthew and Giovannoni, 2021). Así, cuando los niveles de auxina son altos, las proteínas *Aux/IAA* se ubiquitinan y se mantienen en niveles bajos a medida que los *ARF* forman homodímeros a través de sus C terminales, uniéndose a las regiones AuxRE de las secuencias promotoras de los genes diana, activando o reprimiendo así las respuestas impulsadas por auxina. Por el contrario, niveles bajos de auxina promueven la unión de los *ARF* a las proteínas *Aux/IAA*, que reclutan correpresores *TOPLESS* (*TPL*) y suprimen la actividad del *ARF* (Li et al., 2016a, 2016b; Luo et al., 2018). Además, los *ARF* interactúan con otros factores de transcripción y productos genéticos, incluido el represor de señalización de *GA DELLA*. En tomate, *SlARF7* tiene la capacidad de dimerizar tanto con *SlIAA9* como con *SlDELLA* a través de dos regiones diferentes de unión a proteínas, y ambas interacciones evitan la transcripción de genes inductores del crecimiento antes de la fertilización (Matthew and Giovannoni, 2021). Específicamente, una interacción *SlARF7-SlIAA9* inhibe la biosíntesis de GA y el metabolismo de las auxinas mediante la inhibición de la expresión de *GA20ox1/GA3ox1* y *GH3.2*, y los complejos *SlARF7-SlIAA9* y *SlARF7-SlDELLA* previenen la activación transcripcional de genes que promueven el cuajado. Sin embargo, tras la fertilización, el óvulo libera auxina y GA y, respectivamente, promueven la ubiquitinación y la degradación de *SlIAA9* y *DELLA*, lo que libera a *SlARF7*

para regular positivamente las respuestas relacionadas con auxina y GA (Li et al., 2016a, 2016b; Hu et al., 2018). La capacidad de los ARF para interactuar con una gran cantidad de productos génicos es crucial para facilitar la interacción entre auxina y GA. Además, la variación entre los diferentes *Aux/IAA* y *ARF* dentro de una planta es clave para permitir que la auxina y la GA corregulen múltiples procesos que sustentan el cuajado. En este sentido, tanto *SlIAA9* como *SlIAA27* comparten un alto grado de homología de secuencia y median la sensibilidad a la auxina en el tomate, por ejemplo, pero *SlIAA27* es claramente necesario para la fertilidad del polen y los óvulos, mientras que *SlIAA9* media la expresión de genes que promueven el crecimiento posterior a la fecundación (Bassa et al., 2012; Hu et al., 2018).

El etileno y el ácido abscísico (ABA) también demuestran la capacidad de influir en la polinización y la fertilización a través de su interacción con auxina y GA, así como entre sí mismos. Varios estudios han demostrado que después de la polinización se produce un estallido transitorio de etileno en los ovarios de tomate. Ello es debido a que los genes *ACS [*Ácido 1-aminociclopropano-1-carboxílico (ACC) *sintasa]* y *ACO (ACC oxidasa)* se regulan positivamente para facilitar la senescencia de algunos tejidos florales. Sin embargo, este pico de etileno disminuye dentro de las 12h posteriores a la polinización y, además, a medida que disminuyen las emisiones de etileno se produce el progreso del cuajado del fruto (Llop-Tous et al., 2000; Pattison et al., 2015). Otros estudios en flores de tomate también han revelado que, durante la polinización, la comunicación entre el etileno y la auxina regula la germinación del grano de polen y el crecimiento del tubo polínico, ya que tanto los precursores de etileno, la expresión de la biosíntesis de etileno y los genes de respuesta al mismo (receptores de etileno *ACC sintasa* y *ETR*, respectivamente) aumentan en los granos de polen antes de la antesis (Kovaleva et al., 2017; An et al., 2020). De hecho, la función de los receptores de etileno como reguladores negativos de las respuestas de etileno es consistente con respuestas de etileno reducidas en presencia de proteínas receptoras elevadas. Por otra parte, la auxina se acumula tanto en el estigma como en el extremo del tubo polínico después de la polinización, mientras que las emisiones de etileno (que también aumentan dentro del estigma) aceleran la degeneración de los tejidos de transmisión que conducen al ovario, redistribuyendo los nutrientes a los tejidos circundantes dentro del

pistilo y proporcionando una baja ruta de resistencia del tubo polínico (Matthew and Giovannoni, 2021). Además, el etileno juega un papel en asegurar que solo un tubo polínico deposite dos gametos masculinos en el ovario, ya que la activación de los genes *EIN1* y *EIN2* dentro de la vía de señalización del etileno induce la muerte de la segunda célula sinérgica y cesa cualquier señal atractiva por un segundo tubo polínico (An et al., 2020). Las emisiones de etileno también antagonizan la biosíntesis de GA, ya que el etileno suprime *SlGA20ox* y estabiliza las proteínas *DELLA*. Por el contrario, el bloqueo de la percepción del etileno permite que la acumulación de GA aumente y proceda a inducir la partenocarpia (Kumar et al., 2014; Shinozaki et al., 2015). Asimismo, en flores de sandía sin polinizar, se observó que una fuerte biosíntesis de etileno y ABA se correlacionaba con una mayor expresión de proteínas *DELLA* e *IAA9*, lo que suprimía los niveles de GA y auxina para mantener el ovario en un estado latente protegido antes de la fertilización (Hu et al., 2019). Sin embargo, se ha demostrado que después de la fertilización en muchos frutos carnosos, incluido el tomate, la auxina regula negativamente el etileno (Shinozaki et al., 2015). De hecho, aunque los elementos de la vía de señalización del etileno, como los factores de respuesta al etileno (*ERF*), aumentan brevemente tras la fertilización, los genes asociados con el etileno y el ABA se reprimen junto con el cuajado del fruto (Kumar et al., 2014; Matthew and Giovannoni, 2021).

Curiosamente, las señales de etileno y ABA interactúan entre sí antes y durante la polinización. Así, en un estudio llevado a cabo en flores de higo se ha observado que un aumento en la biosíntesis de ABA a través de la expresión de *NCED1* precede a un aumento simultáneo en la expresión de *ACS*, de modo que ambas fitohormonas aumentan antes de la polinización (Chai et al., 2017). También en petunia tanto el ABA como el etileno co-regulan el transporte de agua en los tubos polínicos durante la fase de crecimiento del microgametofito (*Petunia hybrida*) (Kovaleva et al., 2017).

Otras fitohormonas como las citoquininas (CK), los brasinoesteroides (BR) y el ácido jasmónico (JA) han demostrado la capacidad de influir en la fertilización y la iniciación del fruto de algunas angiospermas. Tanto las CK como los BR generalmente aumentan después de la fertilización, y hay evidencia en el caqui japonés de que la aplicación exógena de BR puede

aumentar significativamente el cuajado (McAtee et al., 2013; Kumar et al., 2014; Baghel et al., 2019). Las CK también demostraron ser funcionales junto con la auxina y la GA durante el inicio del cuajado de frutos tanto en pepino polinizado como partenocárpico (*Cucumis sativus*) (Li et al., 2014).

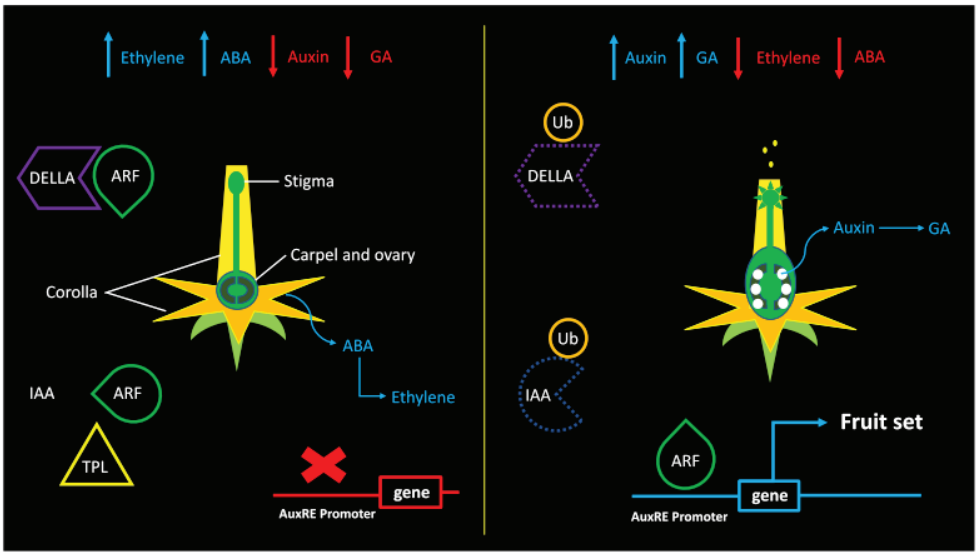

Figura 1. Resumen del cuajado de frutos carnosos y el papel de la polinización en el tomate. (a) Antes de la polinización en el tomate, el cuajado de frutos se inhibe en condiciones de bajo nivel de auxina y GA, ya que los *ARF* se unen a los *Aux/IAA (IAA)* que reclutan correpresores *TPL* para evitar que los *ARF* se unan a los promotores de sus genes diana. La actividad *ARF* también se reprime a través de interacciones con otras proteínas, como *DELLA*, mientras que la síntesis de etileno y ABA antagoniza los niveles de auxina y GA para mantener el ovario en estado latente. (b) Después de la polinización y la fertilización, los niveles de etileno y ABA disminuyen en muchos tejidos dentro de la flor, lo que permite que aumente la biosíntesis de auxina y GA. Los niveles más altos de auxina y GA promueven la ubiquitinación y la degradación de los *IAA* y *DELLA*, lo que permite que los *ARF* se unan a los promotores de genes diana y estimulen el inicio del cuajado (Matthew and Giovannoni, 2021).

Además, dentro del transcriptoma de frutos cuajados, Li et al. (2014) advirtieron una superposición significativa entre los genes que responden a la auxina y los que responden a los BR, lo que sugiere que estos últimos también podrían influir en la coordinación de la producción de frutos en el pepino. Los estudios llevados a cabo en tomate, sugieren que la percepción de JA es necesaria para la transcripción de *SlMYB21*, la cual está involucrada en el desarrollo de micro y megagametofitos antes de la fertilización. De hecho, las plantas mutantes incapaces de responder a JA, o con una

expresión atenuada de *SlMYB21*, experimentaron un desarrollo anómalo del pistilo y del polen que no favorecían el crecimiento del tubo polínico (Niwa et al., 2018).

1.2. Desarrollo y maduración del fruto

1.2.1. Desarrollo del fruto

El desarrollo del fruto en el tomate y muchas otras especies comienza después del cuajado y cesa antes de la maduración, aunque ciertas especies como la uva (*Vitis vinifera*) inician la maduración antes de que el crecimiento haya cesado por completo (Matthew and Giovannoni, 2021). El crecimiento del órgano del fruto se puede dividir en fases discretas de división celular y expansión celular. Así, después de la polinización, el tomate, la uva y la fresa inician una división celular temprana: una fase que puede durar desde unos pocos días hasta más de una semana. Después de esta fase de división el crecimiento posterior del fruto se debe principalmente a la expansión celular (Matthew and Giovannoni, 2021). Las silicuas de Arabidopsis muestran de manera similar una fase temprana de división celular, aunque esto es seguido por un período de división y expansión celular combinadas (Matthew and Giovannoni, 2021). En manzana se caracteriza por una combinación inicial de división y expansión celular, con la división celular disminuyendo para permitir una fase posterior de expansión celular predominante (Matthew and Giovannoni, 2021). En el caso del tomate, un fruto carnoso modelo, la regulación de la división y la expansión celular es similar a la del inicio de la formación del fruto donde la auxina y la GA son las principales fitohormonas reguladoras (Matthew and Giovannoni, 2021). Para comprender mejor las áreas de regulación diferencial entre la proliferación celular y las fases de agrandamiento, se puede asumir que la regulación de la división celular generalmente se lleva a cabo por la auxina sintetizada dentro de la semilla, mientras que la expansión está mediada por una combinación de auxina y GA tanto de la semilla como de los tejidos placentarios (Crane, 1964; Ozga et al., 1992; Pattison and Catalá, 2012). La importancia de la auxina y la GA durante el crecimiento del fruto se ha establecido en múltiples especies de plantas: un aumento en los niveles de auxina después del cuajado da como resultado tasas más altas de división celular en frutos de pepino jóvenes (Li et al., 2014), siendo además la auxina la principal hormona que afecta al

tamaño del fruto en manzana (Devoghalaere et al., 2012). Además, varios genes que codifican componentes de señalización de auxinas se expresaron diferencialmente 8 DAP entre dos líneas de maíz (*Zea mays*) con diferentes tamaños de granos. Los granos grandes contenían niveles significativamente más altos de auxina y estaban más enriquecidos en genes involucrados en el desarrollo del grano, lo que sugiere que las plantas de maíz que producen granos más grandes podrían haber experimentado fases más largas de proliferación celular (Ma et al., 2019). Asimismo, niveles elevados de auxina estimulan de manera similar la división celular en tomates con deficiencia de GA (líneas mutantes *gib-3*) durante el crecimiento temprano, mientras que la aplicación de GA a plantas insensibles a la auxina (líneas mutantes *dgt*) presenta un efecto mínimo en la división celular, lo que respalda la idea de que la auxina es principalmente necesaria para la fase temprana de proliferación celular (Liu et al., 2016). Con respecto a GA, *GA3ox* se expresa durante el desarrollo de la silicua en Arabidopsis en el replum, el funículo y el receptáculo (Hussain et al., 2020), y tres genes distintos del receptor de GA (*CaGID1b.1, CaGID1b.2, CaGID1c*) se expresan en pimiento dulce durante el desarrollo del fruto con el fin de unirse a *CaGAI* (una proteína DELLA) en presencia de GA (Ya-Cong et al., 2016).

1.2.1.1. División celular

La señalización de auxina y la interacción auxina-GA son elementos clave que influyen en el crecimiento del fruto, y estas vías dependen de las actividades de *Aux/IAA*, *ARF* y *GH3* (Matthew and Giovannoni, 2021). En estudios llevados a cabo en manzanas se ha observado que la expresión de *GH3.1* se eleva durante la división celular para mantener los niveles de auxina libre, y *MdARF106* se encuentra entre varios *ARF* de *Malus* que predominan en el desarrollo del fruto (Devoghalaere et al., 2012). Diferentes *ARF* participan en distintas fases de crecimiento, así Liu et al. (2016) observaron que un grupo de cuatro *ARF* sensibles a auxina/GA (*SlARF6, 8, 10 y 16*) actúan de manera redundante para restringir la división celular en el pericarpo de tomate en el crecimiento temprano después del cuajado. Sin embargo, tras la acumulación de auxina, las transcripciones de los cuatro genes *ARF* son el objetivo de miR160 y miR167 para la represión, lo que promueve la división celular temprana del pericarpo. Por el contrario, la aplicación de GA a tomates

insensibles a la auxina promueve la expresión de los *ARF 6, 8, 10 y 16*, lo que, dado el papel de GA en la promoción de la expansión, podría sugerir que una combinación de acumulación de GA y expresión elevada de *ARF* favorece la expansión celular sobre la división durante el desarrollo posterior del fruto (Liu et al., 2016). Los *ARF 10 y 16* también muestran capacidad de respuesta a miR160 y miR167 en melocotón, aunque el tratamiento con auxina sintética reguló negativamente la transcripción de micro-ARN y dio como resultado una expresión elevada de *ARF* (Shi et al., 2017). En tomate, *SlARF9* también regula negativamente la división celular, ya que las plantas transgénicas con niveles elevados de ARNm de *SlARF9* experimentan tasas más bajas de división celular y producen frutos más pequeños en comparación con las plantas de tipo silvestre y las líneas de represión de *SlARF9* (De Jong et al., 2015). Además, la represión o silenciamiento de *SlARF7* induce la acumulación tanto de auxina como de GA, lo que promueve la expansión celular prematura e inhibe la división celular (Kumar et al., 2014). La presencia de *ARF* redundantes con roles en la restricción de la división celular y la facilitación de la transición a la expansión celular es consistente con el programa de desarrollo del tomate, donde la división y la expansión están estrechamente segregadas. Las diferencias aparentes entre el crecimiento del fruto en el tomate y el melocotón, junto con la variación en la forma en que los diferentes frutos regulan la división y expansión celular, subraya el potencial de un sistema compuesto por GA, ARF y miARN asociados como objetivo de investigación para comprender mejor la expansión única del fruto en perfiles de diversas e importantes especies (Matthew and Giovannoni, 2021).

Más allá de los ARF, que actúan como reguladores positivos clave durante la señalización de auxinas, son de interés los genes sensibles a auxinas que afectan negativamente a la división celular. Entre estos se encuentran genes que codifican transportadores de cassettes de unión a ATP (*ABCB*), miembros de la familia GRAS y proteínas que funcionan en la maquinaria de histona desacetilasa (*HDAC*) (Huang et al., 2017; Ofori et al., 2018; Zhang et al., 2020b). En base a estos estudios es posible que en tomate los *ABCB* funcionen durante el crecimiento temprano del fruto para transportar y distribuir auxina durante la proliferación celular, ya que la división celular tiene lugar según el genotipo en las semanas 1 a 2 de la polinización,

observándose que la expresión de *SlABCB4* alcanza su punto máximo alrededor de 14 DAP (Matthew and Giovannoni, 2021). Los ensayos de co-inmunoprecipitación también han revelado que los *ABCB* pueden interactuar directamente con las proteínas *PIN* (transportadores de salida de auxina) en Arabidopsis, por lo que es plausible que se produzca una interacción similar en el tomate a través de *SlABCB4* (Ofori et al., 2018). Sin embargo, las proteínas dentro de la familia GRAS parecen tener un efecto opuesto en las respuestas de auxina y GA, ya que la sobreexpresión de *SlGRAS24* no solo afecta a la germinación del grano de polen y el crecimiento del tubo polínico, sino que también suprime la división celular y la expansión en frutos de tomate (Huang et al., 2017). Finalmente, estudios recientes sugieren la participación de modificaciones del epigenoma en la regulación hormonal del crecimiento del fruto. En este sentido, para el caso del pepino, el locus *SF2* codifica un homólogo de *AtHDC1* que funciona como un componente importante del complejo HDAC, y su expresión es más alta en tejidos meristemáticos que experimentan tasas elevadas de división celular. *SF2* apunta específicamente y reprime genes que suprimen las respuestas a la señalización de auxina, GA y CK, y las tasas de división celular se reducen significativamente en mutantes *sf2* (Zhang et al., 2020b). Estas observaciones recientes con respecto a la intersección de las vías hormonales y las modificaciones del epigenoma en la regulación de la división y el crecimiento de las células del fruto presentan una oportunidad para conocer en profundidad el control regulatorio en este proceso.

1.2.1.2. Expansión celular

Durante el inicio de la expansión celular del fruto de tomate, el aumento de los niveles de auxina y GA de la semilla promueve la expresión de *GA3ox* y *GA20ox* dentro de los tejidos del fruto a fin de aumentar las concentraciones celulares de GA bioactiva (McAtee et al., 2013; Kumar et al., 2014). La capacidad de auxina para estimular la biosíntesis de GA se ha demostrado también en la pera, donde la aplicación exógena de 2,4-D (un imitador de auxina sintética) puede estimular la expresión de *GA20ox* y *GA3ox*, aumentar la acumulación de GA bioactivo en el tejido del fruto y regular positivamente ambos procesos de división y expansión celular (Cong et al., 2019). Después de su aumento y liberación, la GA promueve la expansión celular de forma

sinérgica junto con la con auxina en una variedad de frutos carnosos como la ciruela (*Prunus subg. Prunus*) y la fresa silvestre (*Fragaria vesca*) (Matthew and Giovannoni, 2021). Así, en estudios con ciruela se ha demostrado que durante el proceso de desarrollo del fruto tiene lugar la regulación de la expresión de tres represores similares a DELLA (*PslGAI, PslRGL y PslRGA*) con el fin de controlar el momento de la señalización de GA. La expresión tanto de *PslRGA* como de *PslRGL* es más alta en el pico de división celular del fruto, lo que sugiere que los niveles de GA se mantienen relativamente bajos durante este tiempo (Matthew and Giovannoni, 2021). Sin embargo, durante la fase de crecimiento del fruto, cuando la expansión celular es máxima, la expresión de los tres DELLA es baja, lo que concuerda con la participación de GA (El-Sharkawy et al., 2017). En el caso de la fresa silvestre se ha observado que, en las células del receptáculo, disminuye un represor similar a DELLA (*FaRGA*) durante la transformación de fruto verde a fruto de color blanco, coincidiendo con una transición de la división celular a fase de expansión junto con una biosíntesis elevada de GA (Csukasi et al., 2011). Liao et al. (2018) también observaron que la auxina controla de manera única la división celular, así como la longitud y el ancho del fruto en la fresa silvestre. Sin embargo, tras la regulación positiva de GA mediada por auxina, tanto la auxina como la GA co-regulan el tamaño del fruto al promover tanto el alargamiento como la expansión celular. Por otra parte, la auxina y la GA también parecen mediar en la duración de la etapa de desarrollo del fruto frente a la de maduración mediante la interacción con el ABA, la principal hormona de maduración en la fresa. En este sentido, tanto la auxina como la GA afectan la expresión de NCED (biosíntesis de ABA) y CYP (degradación de ABA), y los niveles elevados de auxina y GA durante el desarrollo regulan positivamente *FveCYP707A4a* para promover la degradación de ABA. Sin embargo, durante el inicio de la maduración, los niveles reducidos de auxina y GA permiten que la acumulación de ABA aumente y autocatalice su propia biosíntesis a través de la regulación positiva de *FveNCED* (Liao et al., 2018).

Además de auxina y GA, la entrada de CK y BR también puede influir en la división y expansión celular, aunque la magnitud del efecto varía entre las diferentes especies de angiospermas. Los niveles endógenos de CK pueden aumentar proporcionalmente con el crecimiento del fruto en ciertas especies, y se ha descrito que la aplicación exógena de BR (junto con GA) aumenta la

tasa de división celular y expansión en frutos de uva (Kumar et al., 2014; Baghel et al., 2019). Por otra parte, en estudios llevados a cabo en kiwi (*Actinidia deliciosa*) se ha puesto de manifiesto que las CK reemplazan a la auxina como la principal fitohormona que afecta al crecimiento del fruto (Nardozza et al., 2020). Dichos autores, sometieron al kiwi a condiciones de carencia de carbono, lo que provocó un impacto directo sobre el tamaño del fruto, dando lugar a frutos más pequeños con expresión atenuada de enzimas biosintéticas de CK, tales como isopenteniltransferasas (*IPT*) y *CYP735A*. Asimismo, en kiwi los niveles de transcripción de las expansinas también fueron más bajos en los frutos con una acumulación reducida de CK, en consonancia con las CK que contribuyen al agrandamiento celular mediante la regulación de las enzimas modificadoras de la pared celular (Nardozza et al., 2020). En base a estos estudios se ha sugerido que las CK interactúan con la auxina o la GA durante el desarrollo del fruto, como podría ser el caso de la calabaza de botella donde los genes expresados diferencialmente entre cultivares de fruto largo y corto incluyen tanto genes sensibles a la auxina como genes relacionados con la biosíntesis y el metabolismo de la CK. Específicamente se observó que la CK deshidrogenasa (CKX), que cataboliza la CK, estaba regulada negativamente en frutos cortos, lo que sugiere que la CK puede funcionar junto con (o en lugar de) la auxina y la GA para establecer el tamaño del fruto carnoso (Zhang et al., 2020a, 2020b). También se ha demostrado que las CK regulan directamente el tamaño del fruto seco en plantas como Arabidopsis. Durante el desarrollo del fruto, las CK se unen a las histidinas quinasas (HK), que donan grupos fosfato a los elementos de respuesta a través de la acción de las AHP. En consecuencia, una mutación que reduce la actividad de AHP da como resultado una insensibilidad a la CK y silicuas más pequeñas, mientras que la expresión atenuada de CKX conduce a un aumento de la CK y silicuas más grandes (Hussain et al., 2020). En Arabidopsis, así como en la fresa, los BR funcionan junto con otras fitohormonas para controlar el tamaño del fruto. Las mutaciones en múltiples enzimas dentro de la ruta biosintética de BR en Arabidopsis conducen a silicuas más cortas (Hussain et al., 2020), mientras que la regulación negativa de los receptores de BR en la fresa reduce la división celular del fruto (Baghel et al., 2019).

El JA y el etileno también contribuyen al crecimiento del fruto. Así, se ha demostrado que en flores de fresa la acumulación de JA es inicialmente alta en la flor de este fruto y refleja los perfiles de concentración de auxina y GA, de modo que disminuyen al final del desarrollo a medida que los niveles de ABA comienzan a aumentar (Matthew and Giovannoni, 2021). El hecho que la aplicación exógena de JA tenga un efecto reduciendo los niveles de ABA mediante la regulación negativa de *FaNCED1*, puede implicar que el JA actúe de manera antagónica hacia el ABA en fresa no climatérica (Garrido-Bigotes et al., 2018). Durante el desarrollo tardío del fruto y la maduración en calabaza de botella, varios *ERF* aumentaron en cultivares de plantas que produjeron frutos largos (Zhang et al., 2020a, 2020b). Los niveles reducidos de etileno durante el desarrollo del fruto en Arabidopsis también dan como resultado silicuas más pequeñas con menos semillas (Hussain et al., 2020). En definitiva, durante el cuajado del fruto, existen múltiples observaciones que indican una variedad de papeles para CK, BR y JA en el crecimiento del fruto, y probablemente en formas que varían entre especies y condiciones de crecimiento.

1.2.2. Maduración del fruto

La transición de la etapa de crecimiento del fruto a la de maduración se caracteriza por cambios en los perfiles de fitohormonas con el fin de detener por completo la expansión y promover la senescencia y la maduración en frutos secos y carnosos, respectivamente (McAtee et al., 2013; Kumar et al., 2014; Forlani et al., 2019; Fuentes et al., 2019; Kou et al., 2021; Fenn and Giovannoni, 2021; Li et al., 2021). Así, a medida que los niveles elevados de auxina, GA y CK retrasan la maduración, la biosíntesis de cada fitohormona generalmente disminuye junto con la transición a la maduración del fruto (McAtee et al., 2013; Kumar et al., 2014). Este hecho se ha demostrado en uva, donde las bayas tratadas de forma exógena con CK y GA durante el envero producen frutos más grandes y acumulan cantidades más bajas de azúcares hexosas durante la maduración. En las bayas tratadas, la regulación negativa de la biosíntesis de ABA y etileno se correlacionó directamente con cambios de color reducidos y un verdor prolongado en el pericarpo del fruto, mientras que la señalización de ABA y etileno no se suprimió en los frutos control que exhibieron una maduración imperturbable (Suehiro et al., 2019).

1.2.2.1. Maduración en frutos climatéricos vs. no climatéricos

Las fitohormonas ABA y etileno son las principales fitohormonas involucradas en la maduración de muchos frutos carnosos, si bien sus funciones reguladoras difieren significativamente entre los frutos climatéricos y no climatéricos (Kou et al., 2021; Li et al., 2021; Matthew and Giovannoni, 2021; Fan et al., 2022; Perotti et al., 2023). En frutos no climatéricos como la cereza dulce (*Prunus avium*), la fresa y la uva, la dioxigenasa de 9-cis-epoxicarotenoide (*NCED*) (Xiong y Zhu, 2003) cataliza la biosíntesis de ABA, que influye en la producción posterior de etileno, aunque normalmente esta es limitada. Generalmente, el ABA se reconoce como la principal fitohormona reguladora durante la maduración de dichos frutos (Leng et al., 2014; Iqbal et al., 2017). Los estudios en frutos no climatéricos se han llevado a cabo especialmente en fresa, donde los niveles de ABA son bajos durante la maduración temprana, ya que se suprimen las enzimas biosintéticas a la vez que la actividad de las enzimas que degradan al ABA (CYP y UGT) es relativamente alta. Conforme avanza la maduración, los niveles de ABA aumentan progresivamente a medida que *FvNCED1* y *FvABA2* también aumentan, y su acumulación alcanza su punto máximo en la etapa "totalmente roja" (Kim et al., 2019). A lo largo de la maduración en dichos cultivos, el ABA se asocia directamente con una menor acidez del fruto, cambios en el color del pericarpo (principalmente a través de la producción de antocianinas), mayores concentraciones de hexosa vacuolar y modificaciones de la pared celular que contribuyen al ablandamiento del fruto (Forlani et al., 2019).

En frutos climatéricos como el tomate y el plátano (*Musa spp*.), la maduración ocurre en asociación con un pico rápido en la biosíntesis de etileno, catalizada a través de las acciones de los genes A*CS* y *ACO*. Ambos genes codifican las enzimas terminales de la vía biosintética del etileno y están regulados positivamente además de la *SAM sintetasa* (*SAMS*), que produce el precursor de la vía del etileno SAM (Kumar et al., 2014; Palma et al., 2019). Durante el inicio de la maduración, los frutos climatéricos experimentan una fase autoinhibitoria (sistema 1) caracterizada por niveles basales de acumulación de etileno y sensibilidad reducida al etileno en la respuesta de maduración (Kumar et al., 2014). Posteriormente, se produce un rápido

aumento de las emisiones de etileno que coincide con el inicio de una fase catalítica (sistema 2), en la que el fruto experimenta una alta sensibilidad al etileno y un ciclo de retroalimentación positiva que alimenta una mayor biosíntesis de etileno.

El cambio de producción de etileno del sistema 1 al sistema 2 implica una transición de la fase de desarrollo del fruto hasta el fruto maduro durante la que tienen lugar una serie de eventos reguladores a nivel molecular (Klee and Giovannoni, 2011; Giovannoni et al., 2017). Entre estos mecanismos tienen lugar la regulación negativa del transporte de auxina a través de *RIN* y *Sl-SAUR69* para permitir alcanzar características de alta sensibilidad al etileno durante el sistema 2 (Shin et al., 2019). A medida que las emisiones de etileno aumentan considerablemente durante la transición del sistema 1 al sistema 2, los perfiles de expresión de los genes biosintéticos de señalización y de respuesta del etileno también cambian junto con numerosos genes posteriores (Carrari and Fernie, 2006; Zouine et al., 2017; Shinozaki et al., 2018). Así por ejemplo en la nectarina (*Prunus persica var. nucipersica),* la expresión de *PpACS5* se regula negativamente al final de la maduración del fruto y se reemplaza por una mayor actividad de *PpACS1* y *PpACS4* durante el sistema 2 (Zeng et al., 2015), mientras que en tomate y otros frutos se ha observado un cambio de ACS1 a ACS2 y ACS4 (El-Sharkawy et al., 2008; Forlani et al., 2019). Dado que la biosíntesis de ABA comienza antes de la liberación de etileno en frutos climatéricos y no climatéricos y que la aplicación exógena de ABA puede estimular la producción de etileno, es posible que dichos cambios en la expresión de *ACS* estén mediados en parte por ABA en especies que presentan ambas fisiologías de maduración (McAtee et al., 2013; Kumar et al., 2014; Leng et al., 2014).

Diferentes estudios ponen de manifiesto que se produce una interacción considerable entre los sistemas de señalización de etileno y auxina, así como entre ABA y auxina durante la maduración. Así, tanto en tomate como en durazno, la auxina y el etileno aumentan en proporción entre sí, y se ha demostrado que la auxina induce la biosíntesis de etileno a través de la regulación positiva de los genes *ACS* y *ACO* (McAtee et al., 2013; Kumar et al., 2014; Iqbal et al., 2017). En papaya, *CpIAA27* se regula positivamente durante la maduración, y varios genes de la familia *CpIAA* se expresan

diferencialmente tras la aplicación de inhibidores de *ACC* o de etileno (Liu et al., 2017). El ABA y la auxina, sin embargo, parecen tener un efecto antagónico neutralizador: una combinación de ABA y auxina aplicada a plátanos verdes maduros no indujo cambios en los genes asociados con la degradación de la clorofila, el metabolismo de los carotenoides o las modificaciones de la pared celular (Lu et al., 2018). Estos resultados sugieren colectivamente que el etileno y el ABA co-regulan los niveles de auxina durante la maduración. La Figura 2 representa las interacciones de las fitohormonas en los procesos de desarrollo y maduración en frutos climatéricos (C) y no climatéricos (NC).

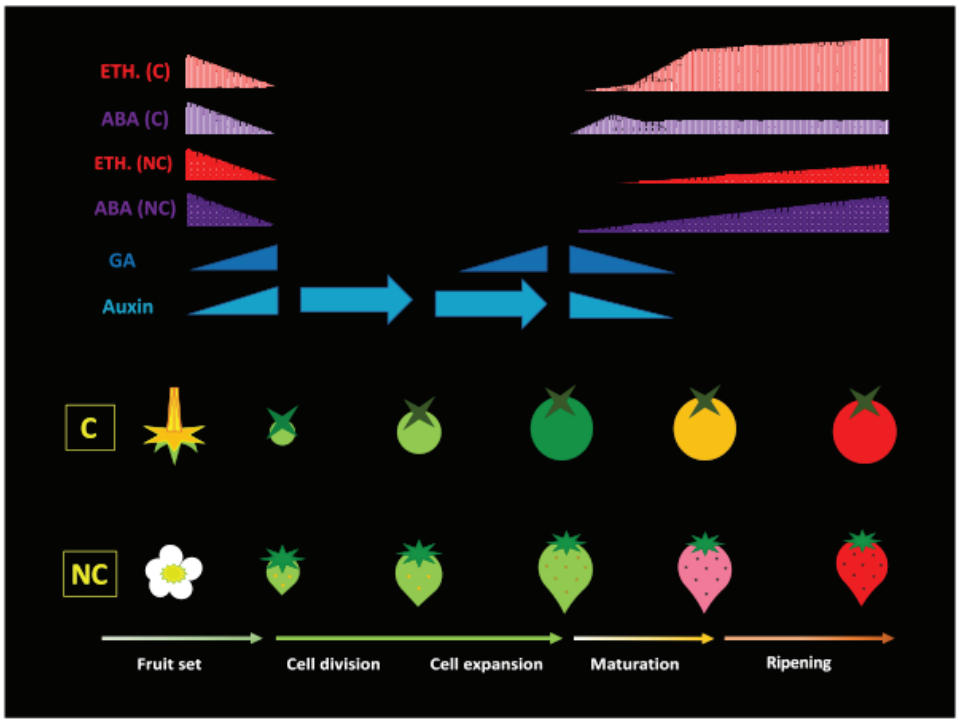

Figura 2. El cuajado y el crecimiento del fruto (división y expansión celular) están regulados de manera similar por la señalización de auxina y GA en diferentes especies de frutos carnosos. La maduración del tomate, un fruto carnoso climatérico (C), está regulado principalmente por un pico en la producción de etileno (sistema 2) que se produce después de bajas emisiones de etileno y cambios en la sensibilidad durante la maduración (sistema 1). En la fresa, un fruto carnoso no climatérico (NC), el ABA tiene una importancia central para la regulación de la maduración. Tanto en las especies climatéricas como en las no climatéricas, la síntesis de ABA precede a la del etileno e influye sobre ella (Matthew and Giovannoni, 2021).

1.2.2.2. Regulación mediante factores de respuesta al etileno (ERFs)

Dada la importancia del etileno durante la maduración, los factores de transcripción de la superfamilia APETALA2/factor de respuesta al etileno (*AP2/ERF*) han demostrado ser fundamentales para la regulación de los genes de respuesta a etileno. Los *ERF* responden tanto a etileno como a ABA, y funcionan al unirse a las regiones de la caja GCC de los genes diana modulando negativamente las respuestas de etileno (Gao et al., 2020). De forma similar a la diversidad observada entre los *ARF*, una cantidad impresionante de ERF se expresa dentro y entre los frutos: más de 70 *ERF* diferentes están codificados dentro del genoma del tomate, por ejemplo, los ERF pueden coordinar procesos como la acumulación de pigmento, el ablandamiento del fruto y el sabor/aroma en frutos climatéricos y no climatéricos (Phukan et al., 2017; Forlani et al., 2019; Gao et al., 2020). Asimismo, en melocotón, múltiples genes que codifican *AP2/ERF* se expresan diferencialmente entre los cultivares de "carne fundente" y "duro pedregoso". También en duraznos con pulpa fundente, la expresión de múltiples genes *AP2/ERF* coincide con un pico de producción de etileno durante la maduración tardía, mientras que un gen *ERF* se expresa de forma notable durante la misma etapa en el cultivar duro pedregoso (Wang et al., 2017b). Además, estos resultados revelan que los *ERF* tienen la capacidad de regulación tanto positiva como negativa. De hecho, ciertos *ERF* funcionan para regular las emisiones de etileno a través de una retroalimentación negativa. Así, en manzana, la expresión de *MdERF2* se suprime en condiciones de altos niveles de etileno, y la regulación negativa de este ERF permite mayores emisiones de etileno y una maduración acelerada. Una observación similar también fue obtenida en tomate para un *AP2/ERF* (Chung et al., 2010). En este sentido, y continuando con la manzana, cuando *MdERF2* se regula positivamente, la biosíntesis de etileno se inhibe debido a la capacidad de *MdERF2* para dirigirse al promotor de *MdACS1* y prevenir su transcripción. Además, *MdERF2* tiene la capacidad de unirse directamente a *MdERF3*, un factor de transcripción positivo para *MdACS1* (Li et al., 2016b). De manera similar, en el plátano, *MaERF11* tiene la capacidad de reprimir la maduración uniéndose al promotor de un gen diana o interactuando directamente con

un regulador positivo. Durante la maduración temprana, *MaERF11* se une a *MaHDA1* a través de un motivo 'EAR' y suprime las emisiones de etileno y el ablandamiento del fruto al prevenir la acetilación de *MaACO1* y *MaEXP2*, *7* y *8*. *MaERF11* también puede unirse a los promotores de estos genes. Sin embargo, a medida que aumentan los niveles de etileno, se inhibe la acumulación de *MaERF11* y, por lo tanto, permite la expresión de genes que promueven la producción autocatalítica de etileno y otros procesos de maduración adicionales, entre los que se encuentra el ablandamiento de la pared celular (Han et al., 2016).

1.2.2.3. Brasinoesteroides, óxido nítrico y calcio

Más allá del etileno, el ABA y el aporte de otras fitohormonas, los BR son también importantes para facilitar los efectos de la maduración. Los BR tienen la capacidad de promover la maduración, ya que su aplicación exógena puede aumentar la actividad de *ACS* y *ACO* y con ello la biosíntesis de etileno. En fresa, la expresión de *FaBRI1* (un receptor BR) aumenta notablemente desde la etapa blanca hasta la etapa roja temprana (Chai et al., 2013). En tomate, las plantas transgénicas que expresan un gen biosintético BR en algodón (*Gossypium hirsutum*) (*GhDW4*) experimentan una maduración acelerada y acumulan niveles más altos de azúcares solubles y vitamina C en el tejido de su fruto.

El gen *GhDW4* tiene un alto grado de homología con el *SlCYP90B3* de tomate, cuya expresión comienza durante la fase de madurez del fruto y aumenta a lo largo del proceso de maduración (Shu-e et al., 2015), lo que lo hace un candidato interesante en estudios fisiológicos que permitan definir mejor el papel de los BR en la maduración. La maduración de los frutos también se ve afectada por la presencia de óxido nítrico (NO) y segundos mensajeros como los iones de calcio. En estudios llevados a cabo en plátano, se ha puesto de manifiesto que la aplicación de etileno aumenta la expresión de una proteína quinasa dependiente de calcio, *MaCDPK7*. La inducción de *MaCDPK7* no solo precede a la inducción de *ACS/ACO* y al aumento posterior en la respiración típica de la maduración climatérica, sino que el bloqueo de la señalización de iones de calcio también suprime la maduración a través de la inhibición de *MaCDPK7*, *MaACS* y *MaACO* (Wang et al., 2017a, 2017b). Por el contrario, el NO (en grandes cantidades) actúa antagónicamente

retrasando la maduración. Los mutantes de tomate de raíz corta (*shr*) que sobreproducen NO experimentan una maduración retrasada, y se ha demostrado además que el NO suprime la biosíntesis de etileno en fresa, manzana y durazno a través de la nitrosilación y la inactivación de *SAMS* (Palma et al., 2019). El exceso de NO en los mutantes *shr* reprime específicamente la acumulación de ABA, como un importante regulador del etileno climatérico (McAtee et al., 2013; Kumar et al., 2014; Leng et al., 2014; Bodanapu et al., 2016).

1.2.2.4. Fenotipos de maduración influenciados por fitohormonas

Los cambios en el color del fruto ocurren a medida que las moléculas de clorofila se degradan con un aumento concomitante en la biosíntesis de compuestos de pigmento, incluidas las antocianinas y los carotenoides. Los efectos del etileno y ABA sobre el color del fruto varían ampliamente entre las especies de plantas (Matthew and Giovannoni, 2021). El etileno promueve la biosíntesis de carotenoides a través de la regulación positiva de PSY1 en el tomate, mientras que los niveles más bajos de ABA a través del silenciamiento de *SlNCED1* dan como resultado un exceso de pigmentación y niveles más altos de licopeno y β-caroteno en las bayas (McAtee et al., 2013; Kumar et al., 2014; Leng et al., 2014). En tomate, la regulación negativa de *SlNCED1* también da como resultado niveles más altos de etileno, lo que resulta en la inducción de la actividad de los factores de transcripción de la caja MADS *RIN, TAGL1, FUL1 y FUL2*, que se unen a los promotores de *ACS, ACO* y a una serie de factores de transcripción *ETR* adicionales para impulsar la vía síntesis de carotenoides (Liu et al., 2015; An et al., 2018; Li et al., 2019; McQuinn et al., 2020). El papel del etileno en la coloración de la manzana varía según el genotipo y probablemente su regulación se lleve a cabo a través de la activación de la expresión del gen MYB. Diferentes estudios llevados a cabo en arándano (*Vaccinium myrtillus*) también indican que el ABA regula positivamente la neoxantina sintasa (*VmNSY)* y la antocianidina sintasa (*VmANS*) aumentando la acumulación de antocianina (Whale et al. al., 2004; Leng et al., 2014; An et al., 2018). Las CKs y el JA también pueden influir en el color del fruto. En tomate, la regulación negativa de *SlIPT4*, que cataliza la biosíntesis de CK, da como resultado frutos de color naranja que no acumulan licopeno. En consecuencia, la expresión del gen que codifica ZISO,

una isomerasa de la vía biosintética de carotenoides, disminuye en las líneas SlIPT4-RNAi mientras que aumenta la transcripción de *SlPSY1*, lo que indica la interacción de las CK con la señalización de etileno (Zhang et al., 2018a, 2018b). Otros estudios llevados a cabo en diferentes frutos también han puesto de manifiesto que el metil jasmonato aumenta durante la maduración en manzana, pera y mango (*Mangifera indica*) (Kumar et al., 2014), pudiendo promover específicamente la biosíntesis de licopeno en el tomate (Liu et al., 2015).

El ablandamiento del fruto se logra a través de la acción de las enzimas que modifican la pared celular, cuyos patrones de expresión ocurren de manera específica para cada especie. Así, el etileno induce la metilesterasa, la poligalacturonasa y la pectato liasa para catalizar la despolimerización de la pectina en el tomate y el kiwi (Iqbal et al., 2017; Wang et al., 2019). Las expansinas y las β-galactosidasas también se acumulan en el tomate en maduración, mientras que la endo-poligalacturonasa funciona específicamente en el melocotón de "carne fundente", pero no en el "duro pedregoso" permitiendo así el ablandamiento (Forlani et al., 2019). Al igual que ocurre con el color del fruto, los efectos del etileno y ABA (o una combinación de ambos) también varían entre las diferentes especies. Así, en el plátano, el etileno y el ABA estimulan sinérgicamente el ablandamiento del fruto, mientras que la presencia de ABA durante la modificación de la pared celular en el tomate conduce a una mayor firmeza del fruto (McAtee et al., 2013; Kumar et al., 2014).

Las cualidades duales de dulzura y acidez exclusivas de muchos frutos surgen de los cambios en la acumulación de ácidos y azúcares libres solubles. Diferentes estudios han demostrado que la presencia de ABA se correlaciona con la acumulación de azúcares en las bayas de uva y la absorción de hexosas dentro de las vacuolas de la manzana. Además, la sobreexpresión de un elemento de unión a ABA en el tomate (*SlAREB1*) tiene un impacto favorable en la calidad organoléptica del fruto maduro (Kumar et al., 2014; Leng et al., 2014). La sobreexpresión de *SlAREB1* conduce específicamente a niveles más altos de ácido cítrico, málico y glutámico en bayas verdes inmaduras, verdes maduras y rojas maduras. Los niveles de glucosa y fructosa vacuolar también fueron más altos en las líneas de sobreexpresión a través de la regulación

positiva de una sacarosa sintasa y una invertasa vacuolar (Bastías et al., 2011; Bastías et al., 2014).

Es probable que los cambios en los niveles de azúcar y acidez ocurran al mismo tiempo, ya que la hidrólisis de almidón y el metabolismo del carbono mediante el ciclo TCA están estrechamente acoplados. Además, ambos procesos se modifican fuertemente durante la maduración, a medida que aumenta la resistencia a la pérdida de los esqueletos de carbono. Teniendo en cuenta esta red, es probable que el etileno, el ABA e incluso la auxina tengan alguna influencia durante la modificación de la descomposición del almidón y el metabolismo de los ácidos orgánicos impulsada por la maduración. De hecho, existen fuertes correlaciones a nivel molecular entre las transcripciones relacionadas con la maduración y los cambios en el metabolismo del carbono a través del ciclo TCA. En este sentido, la supresión de *NCED* está vinculada a una regulación descendente paralela de genes que inducen cambios en el ciclo TCA, y el aumento de las emisiones de etileno refleja aumentos en citrato, malato y hexosas en durazno (Batista-Silva et al., 2018). Asimismo, antes de la maduración, la auxina juega un papel importante durante el desarrollo del fruto al influir en la acidez y la acumulación de azúcar. Por otra parte, la expresión reducida de *SlARF4* en el tomate afecta la señalización temprana de auxina y da como resultado frutos jóvenes con mayor cantidad de clorofila por plástido y niveles más altos de almidón en el tejido del pericarpo (Matthew and Giovannoni, 2021). El aumento de clorofila en los plástidos dota a los frutos afectados de mayores capacidades fotosintéticas, lo que les permite acumular más almidón para su posterior hidrólisis y alcanzar mayores niveles de sólidos solubles. *SlARF4*, que se expresa en el pericarpo durante el desarrollo del fruto aproximadamente 25 DAP y que normalmente disminuye durante el inicio de la maduración, también reprime las acciones de *SlAGPase* (una enzima biosintética del almidón) (Sagar et al., 2013). Además, la actividad de las auxinas durante la maduración puede regular negativamente enzimas involucradas en la modificación del ciclo de TCA, lo que reduce las tasas de respiración del fruto y, en algunos casos, aumenta la acidez mediante la promoción de la acumulación de succinato, malato y citrato (Batista-Silva et al., 2018).

Al igual que el control de los niveles de azúcar y acidez, el conocimiento actual sobre la regulación del aroma y el sabor de los frutos es limitado, pero se establece que el ABA, el etileno, el JA y también el ácido salicílico (SA) pueden estar implicados en este aspecto de la maduración. Así, las emisiones de etileno influyen en la actividad de la alcohol deshidrogenasa en melón (*Cucumis melo*), y se ha demostrado que la biosíntesis y liberación atenuada de etileno reduce las emisiones de compuestos orgánicos volátiles en melón y también en manzana, reduciendo con ello el aroma del fruto (Ayub et al., 1996; Kumar et al., 2014; Iqbal et al., 2017). El ABA también afecta a la biosíntesis de flavonoides en arándanos (*Vaccinium spp.),* mientras que, en tomate, el JA influye en los niveles de poliaminas y *SlSAMT* cataliza la biosíntesis de SA en salicilato de metilo mejorando así el sabor del fruto maduro (Tieman et al., 2010; Kumar et al., 2014).

2. El olivo

2.1. Generalidades

El olivo, *Olea europaea L.*, pertenece a la familia botánica *Oleaceae*, que comprende especies de plantas distribuidas por las regiones templadas y tropicales del mundo. Las plantas de esta familia son principalmente árboles y arbustos, a veces trepadores. Muchas de ellas producen aceites esenciales en sus flores o frutos, algunos de los cuales son utilizados por el hombre. De entre los 29 géneros de esta familia, los que tienen interés agronómico son *Fraxinus* (fresno), *Jasminum* (jazmín), *Ligustrum* (aligustre), *Phillyrea* (agracejo), *Syringa* (lilo), y sobre todo *Olea* (Heywood, 1978).

Se han catalogado unas 33 especies en el género *Olea*. La especie *Olea europaea L.* incluye todos los olivos cultivados y también los acebuches u olivos silvestres. Existen diferencias de opinión sobre cómo subclasificar dentro de la especie, pero en la revisión más reciente y completa de Green (2002) se considera que los olivos cultivados pertenecen a la subespecie *europaea*, variedad *europaea,* mientras que los olivos silvestres (acebuches) también pertenecen a la subespecie *europaea* pero se incluyen dentro de la variedad *sylvestris*.

La especie *Olea europaea L.,* a la que pertenece el olivo, es una angiosperma dicotiledónea y la única especie de la familia *Oleaceae* con fruto comestible.

El olivo es un árbol perennifolio longevo que crece hasta 15 m en su madurez. Su vida útil suele ser superior a 500 años, y los árboles de más de 2000 años todavía se cultivan en numerosas regiones (Baldoni and Belaj, 2009). El sistema de raíces del olivo es generalmente poco profundo, ya sea que se propague por semilla o por esqueje, penetrando solo 90-120 cm en los suelos. El sistema de brotes es denso y pueden crecer de forma colgante en algunos cultivares, o erguidos en otros. Las hojas de olivo son opuestas, gruesas y coriáceas. Alcanzan su tamaño final en 2 semanas y viven de 2 a 3 años (Martin et al., 2005). La inflorescencia forma racimos que salen de las axilas de las hojas de los ramos fructíferos (ramos de un año de edad). Las flores son pequeñas y constan de cuatro sépalos verdes fusionados, cuatro pétalos blanco-amarillentos, dos estambres y dos carpelos (Fabbri et al., 2004), son generalmente hermafroditas y polinizadas por el viento . El ovario posee cuatro óvulos y el estilo muy corto. Los frutos son drupas oblongas con una superficie lisa y cerosa, su tamaño y forma dependen de la variedad específica (Seifi et al., 2015).

El primer foco de domesticación del acebuche, que da lugar al olivo, se establece en Oriente Medio hace unos 6000 años (Kaniewski et al., 2012). Debido al gran valor de su fruto para la extracción de aceite, el cultivo de olivo fue extendiéndose por toda la cuenca Mediterránea donde las condiciones climáticas y edáficas eran favorables para su desarrollo (Carrión et al., 2010). La llegada del cultivo del olivo a la Península Ibérica no se conoce con exactitud, aunque se piensa que se produjo sobre el siglo II a.C. durante el dominio romano (Arambarri,1992), o incluso con anterioridad (Tindall, 2002). Durante este período de difusión parece ser que los primeros olivicultores de cada zona seleccionaron en sus bosques de acebuche los individuos más sobresalientes por su productividad, tamaño del fruto, oleosidad y adaptación al medio. La propagación vegetativa ha mantenido las características de estos cultivares inicialmente seleccionados que constituyeron las primeras variedades (Barranco et al., 2017).

Al igual que en otros muchos países olivareros, el material vegetal del olivo cultivado en España se caracteriza por estar compuesto por un gran número de variedades, todas ellas muy antiguas y que presentan unas zonas de difusión restringidas en torno a sus posibles lugares de origen. Además, estas

variedades aparecen con denominaciones diferentes en las distintas zonas donde se cultivan y, en ocasiones, se aplica la misma denominación a variedades distintas (Barranco et al., 2017).

En total se han encontrado 272 variedades cultivadas de olivo en España. De estas 24 variedades son consideradas como principales, entendiendo por variedades principales aquellas que son base de plantaciones y su superficie plantada es la dominante en alguna comarca teniendo importancia a nivel nacional (Barranco et al., 2017). La Fig. 3 representa la distribución geográfica de las variedades de olivo dominantes en España. En Extremadura, la superficie real estimada es de ≈ 267.083 hectáreas (67.974 hectáreas en Cáceres y 199.109 hectáreas en Badajoz), que supone casi el 10% de la superficie nacional de olivar, siendo la tercera Comunidad Autónoma en orden a su superficie de olivar y superada sólo por Andalucía y Castilla la Mancha (Fuente: Anuario de estadística 2021 del Ministerio de Agricultura, Pesca y Alimentación).

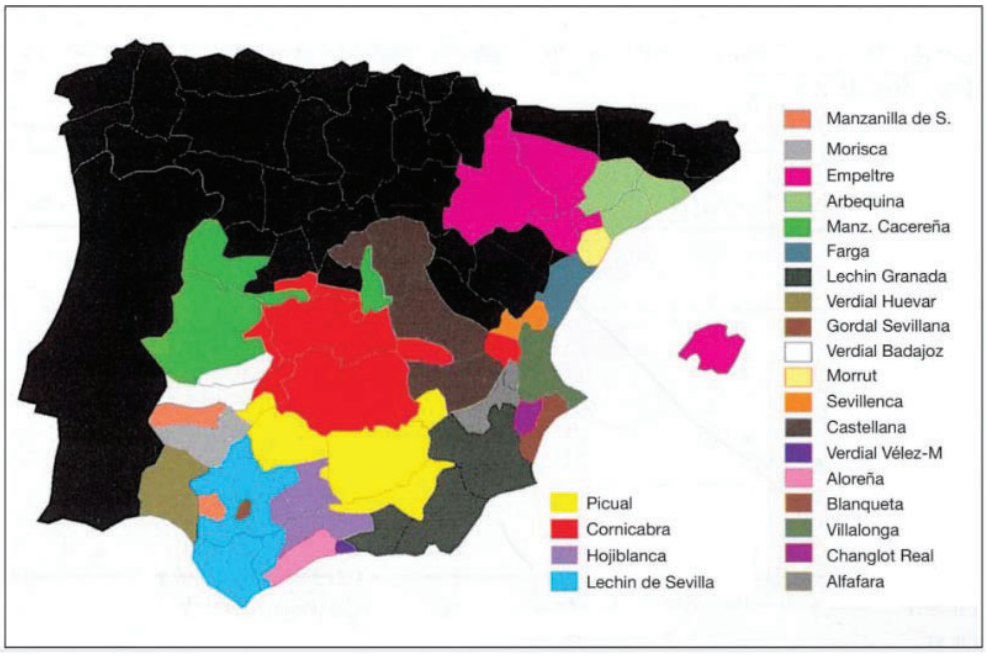

Figura 3. Distribución geográfica de las variedades de olivo dominantes en España (Barranco et al., 2017).

2.2. Importancia del Olivo

El olivo cultivado (*Olea europaea* L. subsp. *europaea* var. *europaea*) es una de las especies arbóreas más importantes de la cuenca mediterránea, representando no sólo el 90% de los olivares del mundo sino también el 90% de la producción mundial de olivos. Sólo España, Italia y Grecia producen alrededor del 75% del aceite de oliva a nivel mundial, y junto con Turquía y Túnez son los cinco mayores productores del mundo (Rugini et al., 2011). En 2021, el cultivo del olivo ocupaba 10,3 millones de hectáreas en todo el mundo con una media anual de producción cercana a los 23 millones de toneladas de aceitunas, destinadas tanto a la producción de aceite de oliva como al consumo de aceituna de mesa (FAOSTAT, 2023).

La producción mundial de aceite de oliva se estima en 3 millones de toneladas, ocupando el sexto lugar en la producción mundial de grasas vegetales líquidas, superada por la soja, semillas de algodón, cacahuetes y girasol. La producción de aceite de oliva no es constante a lo largo de los años, debido a la tendencia de esta especie a la alternancia que está determinada por factores genéticos y ambientales (Rugini et al., 2011).

La mayoría de los olivares del mundo se cultivan en condiciones extensivas de secano con densidades de hasta 150 olivos/ha y escasa mecanización, y se encuentran ubicados en las zonas dedicadas a la olivicultura más antigua, que utilizan cultivares locales. En los últimos años, la producción de aceitunas se ha incrementado como consecuencia del desarrollo de olivares modernos, la intensificación de olivares tradicionales y la expansión de la olivicultura por nuevas áreas de producción (Fernández-Escobar et al., 2012).

España es el mayor productor de aceite de oliva de la Unión Europea, haciendo que esta permanezca en primera posición en la producción mundial, a pesar de las oscilaciones que puede presentar debido a las malas condiciones climáticas o a la vecería del propio cultivo (Barranco et al., 2017). La Encuesta de Superficies y Rendimientos de cultivos (ESYRCE 2019) recoge una importante superficie de olivar (2.733.620 ha) en España, de las cuales el 93,1% (2.543.827 ha) son de olivar de almazara, el 2,8% (76.120 ha) son olivar de mesa y el 4,2% (113.674 ha) son de olivar de doble aptitud.

En el olivo, se han desarrollado diferentes programas de mejora genética sobre la identidad de los cultivares o el desempeño agronómico, así como por la cantidad y distribución de su variabilidad genética, siendo ello crucial para ampliar la base genética de nuevos cultivares (Belaj et al., 2004; Leon et al., 2004; De la Rosa et al., 2013; Rallo et al., 2018; Belaj et al., 2020). Hasta ahora, los programas de cruzamiento se han realizado solo entre cultivares, pero el uso de olivos silvestres en cruces futuros introducirá una variabilidad útil, ya que los genotipos silvestres pueden contener características raras o ausentes en el germoplasma del olivo cultivado (Baldoni and Belaj, 2009). Los primeros programas de cruzamiento en olivo se desarrollaron entre 1960 y 1971 en Israel (Lavee,1990) e Italia (Bellini et al., 2002); desde entonces, más de 50 países mantienen alrededor de 100 colecciones de aceitunas regionales, nacionales e internacionales (Belaj et al., 2016; Bartolini, 2018).

Actualmente, los programas de mejora genética del olivo mediante cruzamientos intervarietales o interespecíficos se llevan a cabo principalmente en España, Israel y Australia (Baldoni and Belaj, 2009; Belaj et al., 2020). Entre los estudios intervarietales más destacados en España, está el nuevo cultivar 'Chiquitita', derivado de un cruce entre 'Picual' y 'Arbequina'. Este nuevo cultivar se caracteriza por su producción temprana, alto contenido de aceite y alta eficiencia de rendimiento, mientras que su bajo vigor, copa compacta y ramas colgantes lo hacen muy adecuado para siembra de alta densidad (Rallo et al., 2008).

El olivo tiene una alta variación genética intra-específica con un tamaño de genoma de aproximadamente 1.800 Mb (Loureiro et al., 2007). Esta característica sirve para analizar procesos biológicos de interés biotecnológico, tales como el metabolismo fenólico y lipídico durante el desarrollo del fruto (Alagna et al., 2009; Galla et al., 2009; Bianco et al., 2013), así como el de los terpenoides y esteroles (Stiti et al., 2007). Directa o indirectamente, todos estos procesos afectan a la calidad del aceite de oliva, así como a su perfil nutricional. Los datos genómicos en olivo están aumentando gracias a los avances en el mapa genómico que se han realizado en esta planta (De la Rosa et al., 2003; Wu et al., 2004). De hecho, se ha secuenciado el ADN de todo el plastoma de "Frantoio", un cultivar italiano (Mariotti et al., 2010). Al mismo tiempo, gran número de ESTs han sido

identificadas recientemente en olivo, generando 261485 EST (Alagna et al., 2009), 443811 EST (Gil-Amado and Gomez-Jimenez, 2013; Parra et al., 2013), 291958 EST (Bazakos et al., 2015) y 465000 EST (Alagna et al., 2016) mediante la técnica de pirosecuenciación 454, además de 1132 EST utilizando la hibridación sustractiva de supresión (Galla et al., 2009), así como 2 millones de EST utilizando las tecnologías de pirosecuenciación Sanger y 454 (Muñoz-Mérida et al., 2013), 140357776 EST usando Illumina (Iaria, et al., 2016), lo que es importante para extender el catálogo de transcritos de olivo con el fin de facilitar el descubrimiento de genes, el análisis funcional de los mismos y, en definitiva, la mejora molecular.

La transformación genética ha surgido como una poderosa herramienta para la mejora genética de los árboles frutales, permitiendo la introducción de rasgos seleccionados en cultivares élite en un corto período de tiempo, como ha sido el caso de los cultivares 'Canino' y 'Moraiolo' (Rugini et al., 1995). Algunos rasgos importantes como la resistencia a hongos, la floración o la composición lipídica han sido manipulados con éxito mediante la transformación genética de embriones somáticos de origen juvenil o adulto, lo que demuestra el papel potencial que esta tecnología podría tener en la mejora del olivo. En este sentido, se han desarrollado diferentes procedimientos de transferencia genética en olivo como biobalística y *Agrobacterium tumefaciens*, utilizando explantes de embriones somáticos en ambos casos. *Agrobacterium rhizogenes* también se ha utilizado para obtener plantas quiméricas de olivo con raíces transgénicas (Palomo-Ríos et al., 2021).

Todos estos métodos y técnicas de reproducción permiten aumentar el número y el tamaño de los frutos, incrementar el contenido y la calidad del aceite (composición de ácidos grasos, contenido de fenoles, etc.), reducir la alternancia, enanizar o modificar la arquitectura del árbol para facilitar la poda y cosecha mecánicas, mejorar la resistencia a las plagas, en particular la mosca del olivo, *Bactrocera oleae*, y enfermedades tales como la mancha del pavo real, causada por *Spilocaea oleagina*, *Verticillium wilt*, *Verticillium dahliae* y el nudo del olivo, *Pseudomonas savastanoi*. También se han llevado a cabo estudios encauzados a mejorar la tolerancia al frío para permitir el cultivo de olivo en áreas más frías y

promover la autofertilidad para reducir la dependencia de los polinizadores (Baldoni and Belaj, 2009).

2.3. El fruto

El fruto del olivo, la aceituna, es un fruto pequeño cuya forma varía de esférica a elipsoidal o alargada, con diversos grados de asimetría y un ápice redondeado o puntiagudo. Los extensos recursos genéticos disponibles para el olivo muestran una amplia variabilidad de muchos caracteres del fruto de olivo (Rallo et al., 2018; Bazakos et al., 2023). En particular, el tamaño del fruto del olivo difiere varias veces entre las variedades cultivadas (Barranco 1999). Además de la alta variabilidad genética del tamaño del fruto del olivo (De la Rosa et al., 2008; 2013; Belaj et al., 2020), recientemente, se ha demostrado que el peso del fruto de olivo también está sujeto a variación genética, sugiriendo que este rasgo es poligénico (Moret et al., 2023).

Normalmente, los frutos de variedades cultivadas miden de 1–4 cm de largo, 0.5–2 cm de diámetro, y pueden pesar hasta 10 g de peso fresco y 2.5 g de peso seco. Por el contrario, los frutos de variedades silvestres suelen ser mucho más pequeños, 0.5 a 1.5 cm de largo, inferior a 1 cm de ancho y peso inferior a 2 g. Existe una tendencia a que los cultivares con frutos más pequeños se destinen a la producción de aceite y los que tienen frutos más grandes se destienen para uso de mesa. Muchos frutos son de aptitud doble y el tamaño no es un determinante estricto de uso. En el estado maduro, la aceituna es negra, negro-violácea o rojiza, pero en muchos casos se cosecha antes, en estado verde para alcanzar propiedades organolépticas valoradas por el consumidor (Rapoport et al., 2016; Barranco et al., 2017).

Botánicamente la aceituna es una drupa, tal como la almendra, el albaricoque, la ciruela, la cereza y el melocotón. Se trata de un fruto (Figura 4) con una sola semilla compuesto por tres tejidos principales: endocarpo, mesocarpo y exocarpo, siguiendo cada uno de estos tejidos una forma muy distinta de crecimiento y diferenciación durante el desarrollo del fruto. El conjunto de estos tejidos se denomina pericarpo y tiene su origen en la pared del ovario. Los tejidos del fruto se desarrollan a partir del ovario mediante los procesos de división, expansión y diferenciación celular, a partir de la fecundación y del cuajado inicial (Rapoport et al., 2016; Barranco et al., 2017).

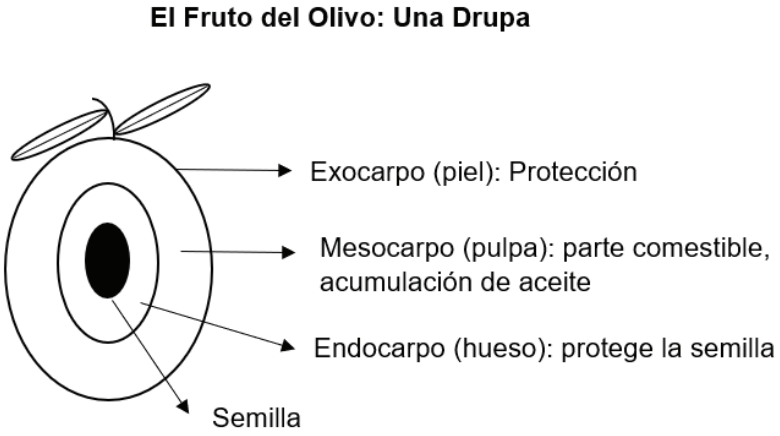

Figura 4. Estructura del fruto de olivo: exocarpo la piel o capa exterior, mesocarpo la pulpa o carne y endocarpo, el hueso. El conjunto de estos tres tejidos se denomina pericarpo.

El *endocarpo* o hueso empieza a crecer a partir de la fecundación y aumenta en tamaño durante los dos meses siguientes. En su estado maduro, el endocarpo está compuesto enteramente por células esclerificadas. Estas células deben su dureza a la deposición de una gruesa pared secundaria con un alto contenido de lignina. Desde el inicio del desarrollo del fruto, las esclereidas empiezan a diferenciarse en el endocarpo entre células no diferenciadas. Este proceso ocurre de un modo gradual y espaciado al principio y más intenso después. Mientras el endocarpo aumenta su tamaño, también se aumenta el número y la proporción de esclereidas así como su grado de esclerificación. El endocarpo crece hasta que la mayoría de esclereidas han iniciado su proceso de esclerificación, lo que implica una diferenciación estructural que impide la expansión y división celular. Al finalizar su crecimiento en tamaño, el endocarpo sigue aumentando la deposición de lignina y el endurecimiento durante un período de varios meses (Hammami et al., 2013; Rapoport et al., 2013). En el ovario en floración existe un anillo de haces vasculares marcando la separación entre el endocarpo y el mesocarpo. Con la conversión del ovario en fruto, los haces vasculares aumentan en tamaño y desarrollan muchas conexiones entre sí con el fin de importar agua y sustancias para formar el fruto. Los surcos que aparecen en el hueso del fruto maduro se forman alrededor de estos haces y son característicos en cada cultivar (Barranco et al., 2017).

El *mesocarpo* o pulpa también empieza a desarrollarse a partir de la fecundación, pero mientras la expansión del endocarpo se detiene a los dos meses, el mesocarpo sigue creciendo hasta la maduración. Las células del mesocarpo son parenquimáticas, poco diferenciadas pero con una gran capacidad de crecimiento. Estas células son isodiamétricas y forman una malla uniforme y bastante compacta. Del exterior al interior del mesocarpo existe un incremento progresivo en el tamaño celular. Durante el desarrollo del mesocarpo las células parenquimáticas experimentan un gran aumento en tamaño, alcanzando 40-50 veces el tamaño que tenían en el ovario. También, y según el cultivar, se forman algunas esclereidas aisladas dentro del mesocarpo, pero esto ocurre en número muy reducido y con menor grado de esclerificación en comparación con el endocarpo. El aceite se acumula en el citoplasma de estas células parenquimáticas, formándose pequeños cuerpos lipídicos que posteriormente se unen entre sí (Rangel et al., 1997). En el primer período de crecimiento del mesocarpo, a partir de la fecundación, intervienen los procesos de división y expansión celular. En las primeras 6 a 8 semanas después de la floración se producen la mayoría de las células del mesocarpo. La expansión celular es tan notable en este período que, aunque las células se dividen y su tamaño se reduce en un primer momento como consecuencia de la división, el tamaño celular aumenta. A partir de los dos meses y hasta la maduración ocurre el mayor incremento en tamaño celular, aproximadamente el 80%, acompañado por un incremento muy reducido en número celular (división celular). En esta segunda fase, la expansión celular está acompañada por la acumulación de aceite. Estudios comparativos de cultivares con frutos de tamaños diversos, indican que las diferencias entre cultivares están determinadas por el número de células formadas en el mesocarpo, mientras que el tamaño celular es similar entre ellos (Hammami et al., 2011). Las diferencias entre cultivares aparecen ya en el ovario, antes de la formación del fruto, siendo más grandes generalmente los ovarios de cultivares de fruto mayor y estando compuestos por más células pero de tamaño similar (Rosati et al., 2011).

El *exocarpo* o epicarpo, piel del fruto, está compuesto principalmente por la epidermis con su cutícula y unas cuatro capas subepidérmicas parecidas al mesocarpo pero con diferentes pautas de crecimiento (Hammami and Rapoport, 2012). La cutícula es fina en la época de floración y polinización,

cuando el ovario se encuentra todavía protegido por los pétalos, pero rápidamente se desarrolla para formar una gruesa capa protectora. Algunos estomas se forman en la epidermis para posteriormente convertirse en lenticelas, regiones que posiblemente actúan en el intercambio de gases. Las lenticelas son más visibles durante las etapas verdes maduras del crecimiento del fruto; su número y tamaño es un carácter varietal (Rapoport et al., 2016; Barranco et al., 2017).

Coincidiendo con la formación del fruto, e íntimamente interrelacionados entre sí, el óvulo funcional se desarrolla para formar la semilla. El embrión ocupa casi todo el volumen de la semilla. La cubierta seminal, derivada del tegumento, que representaba el tejido principal del óvulo, es fina y dura y atravesada por numerosos haces vasculares. Entre las cubiertas seminales y el embrión se encuentra una fina capa de endospermo con alto contenido de almidón (King, 1938).

2.4. Desarrollo y maduración del fruto

2.4.1. Desarrollo del fruto

El desarrollo del fruto de olivo es una combinación de eventos bioquímicos y fisiológicos que ocurren bajo un estricto control genético e influenciados por varias condiciones ambientales (Connor and Fereres, 2005; Conde et al., 2008). Tiene una duración de 4 a 5 meses e incluye cinco fases principales (Figura 5), que involucran la división celular, la expansión celular y el almacenamiento de metabolitos. La primera fase de fertilización y fructificación se caracteriza por una rápida división celular temprana que promueve el crecimiento del embrión (0-30 DPA); la segunda fase de desarrollo de la semilla, implica el primer período de rápido crecimiento del fruto, caracterizado por el escaso desarrollo del mesocarpo y el intenso crecimiento del endocarpo como resultado de la división y expansión de la actividad celular de la semilla/hueso (30-60 DPA); en la tercera fase de endurecimiento de la semilla/hueso, el crecimiento del fruto se ralentiza a medida que las células del endocarpo dejan de dividirse y se esclerifican (60-90 DPA); la cuarta fase de desarrollo del mesocarpo, representa el segundo gran período de crecimiento del fruto, debido a la expansión de las células carnosas preexistentes y a la acumulación intensa de aceite (90-

150 DPA). Finalmente, la fase de maduración, es la última etapa de desarrollo, en la que el color del fruto cambia de verde lima oscuro a verde/púrpura más claro (desde 150 DPA), como consecuencia de la degradación de la clorofila (Conde et al., 2008).

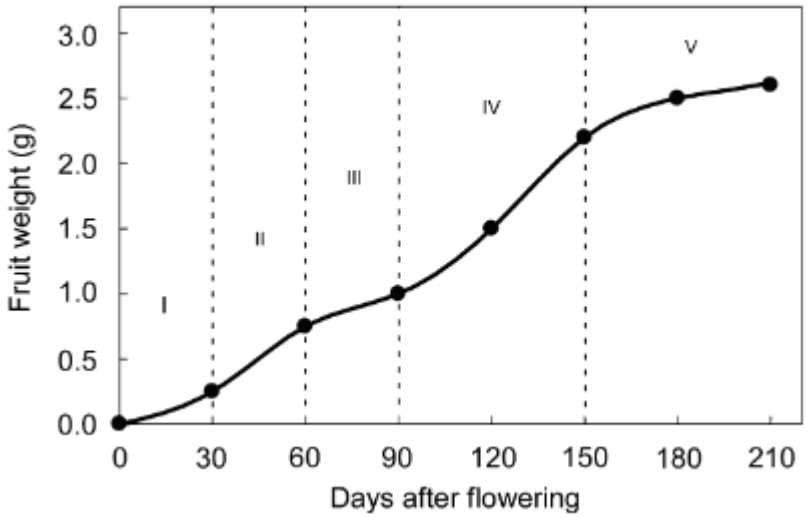

Figura 5. Crecimiento del fruto de olivo y sus etapas de desarrollo. Etapa I, fecundación del fruto y cuajado; Etapa II, desarrollo de la semilla; Etapa III, endurecimiento de la semilla/hueso; Etapa IV, desarrollo del mesocarpo; Etapa V, maduración (Lavee, 1996).

El tamaño del fruto es una característica varietal regulada por el número de células, el tamaño de éstas y el volumen de los espacios intercelulares. En una variedad dada el tamaño del fruto varía notablemente entre los diferentes años y árboles en función de la carga del árbol y de la disponibilidad de agua durante el crecimiento del fruto (De la Rosa et al., 2013; Bartolini et al., 2014; Rallo et al., 2018). En la evolución normal del crecimiento del fruto, la carga del árbol, es decir el número de aceitunas por árbol, es posiblemente el principal factor determinante del tamaño del fruto en condiciones determinadas de medio y cultivo. En olivo existe una relación negativa entre el número de frutos por árbol y el peso del fruto (Barranco et al., 2017).

Las diferencias en la disponibilidad de asimilados, debido a la carga de cultivo en el árbol, influyen en el patrón de maduración del fruto (Inglese et al., 1999). Diferentes ramas del mismo árbol pueden tener diferentes cargas de

frutos y esto puede contribuir a los patrones de crecimiento y maduración no uniformes que ocurren en muchos cultivares de olivo (Shulman and Lavee 1979; Inglese et al., 1999). Acebedo et al. (2000) estudiaron la distribución diferencial de frutos y la producción de aceite en dos cultivares que difieren en el hábito de crecimiento: uniformemente abierto 'Picual' y cerrado 'Arbequina'. Los frutos de ramitas desarrollados en la parte superior del árbol produjeron más del triple de la cantidad de aceite producido a partir de frutos del interior sombreado. Además, también observaron diferencias en los patrones de floración y fructificación: 'Arbequina' desarrolló flores y frutos más fértiles por ramita pero de menor tamaño, y el cuajado de frutos en lugar del tamaño del fruto representó la productividad diferencial entre las áreas del dosel, mientras que ocurrió lo contrario con 'Picual'.

La síntesis de ácidos grasos en las células del mesocarpo determina el rendimiento graso de la aceituna. La reacción que promueve la formación de triglicéridos es un paso previo en dicha síntesis, por lo que se puede emplear para cuantificar la acumulación temporal de lípidos. En olivo, se ha obtenido que la acumulación se inicia durante la fase de detención del crecimiento del fruto y concluye al comienzo de la maduración. Estos datos parecen confirmar estudios previos sobre el rendimiento graso de la aceituna que indican que la cantidad de aceite por aceituna alcanza su máximo en torno al comienzo de la maduración. Las fluctuaciones a partir de esta época se deben fundamentalmente a variaciones en el contenido de humedad de la pulpa (Barranco et al., 2017).

Existen dos fuentes de hidratos de carbono para el crecimiento del fruto y la biosíntesis de lípidos en el olivo. La fuente principal son los azúcares translocados en el floema desde las hojas maduras hasta los lugares de almacenamiento mientras que la fuente secundaria viene dada por los azúcares formados por la fotosíntesis en los propios frutos. Las aceitunas permanecen verdes durante un período considerable y conservan los cloroplastos activos incluso cuando cambian de color a medida que se acercan a la madurez. Así, mientras que la clorofila se localiza mayoritariamente en el exocarpo, el mesocarpo contiene cantidades significativas de fosfoenol piruvato carboxilasa (Sánchez, 1994), la enzima de fijación de CO_2 de las vías fotosintéticas CAM y C4.

Durante el período de desarrollo, se requiere una intensa respiración mitocondrial de azúcares importados del floema para sostener inicialmente la división y el crecimiento celular, y posteriormente, durante un período considerable, para llevar a cabo la síntesis de aceite. Debido a este intenso metabolismo y a la impermeabilidad de la cutícula del fruto, el CO_2 se acumula en altas concentraciones en el espacio libre de células del fruto. Después del equilibrio de CO_2/CO_3, la fosfoenol piruvato carboxilasa citosólica cataliza la fijación de bicarbonato en oxalacetato, que se convierte en malato por acción de la malato deshidrogenasa. El malato puede descarboxilarse mediante enzimas málicas citosólicas o mitocondriales para producir piruvato y CO_2. Este último se fija fotosintéticamente en triosa-fosfato en los cloroplastos del fruto durante el período de luz. La fotosíntesis de los frutos, por lo tanto, juega un papel importante en la refijación del CO_2 producido por la respiración mitocondrial de los fotoasimilados importados del floema (Sánchez and Harwood, 2002).

Las comparaciones del intercambio de CO_2 en la luz y la oscuridad (Proietti et al., 1999) revelan que los frutos jóvenes a plena luz del sol pueden fijar hasta el 80% del CO_2 respirado, y la proporción se reduce gradualmente a cero hacia la madurez a medida que se pierde la clorofila. Estos autores también reportaron que la provisión de CO_2 para la fotosíntesis fue considerable, con un Ci interno siempre >400 µmol mol^{-1} y aumentando a 800 µmol mol^{-1} durante la segunda mitad del período de llenado de frutos, cuando la conductancia del exocarpo cayó al perderse los estomas y espesarse la cera cuticular. Sin embargo, los datos disponibles sobre el balance de CO_2 no permiten estimar la contribución general que hace la refijación al crecimiento del mesocarpo durante el ciclo estacional. Así, si la refijación reduce significativamente la dependencia del crecimiento del fruto de la tasa de asimilación actual, eso puede ayudar a explicar por qué la carga de fruto no tiene un efecto aparente en la tasa fotosintética de la hoja (Proietti, 2000), una retroalimentación fuente-sumidero que se ha observado en muchas plantas de cultivo. Más tarde, Proietti et al. (2006) estudiaron los efectos de la relación hoja-fruto durante diferentes etapas de crecimiento del fruto en brotes anillados o no anillados, sobre el desarrollo del fruto, la síntesis de aceite y procesos relacionados, como la translocación de asimilados y la tasa fotosintética neta. El anillado se utilizó para estudiar los

efectos de la acumulación de asimilados en el brote porque, al bloquear el haz del floema, también se bloquea la translocación de los fotosintatos producidos en las hojas. De esta forma, el fruto en desarrollo sólo puede derivar asimilados de su brote. Si el anillado se realiza en unas pocas y muy pequeñas ramas, como se describe en el trabajo de Proietti et al. (2006), no se provocan efectos colaterales significativos sobre el crecimiento general del árbol y la acumulación de reservas. Teniendo en cuenta que en otros estudios el anillado de ramas fructíferas no provocó una variación en la tasa fotosintética neta y que en este estudio (Proietti et al., 2006) las diferencias no siempre fueron significativas, parece que en el olivo se produce una inhibición por retroalimentación en presencia de relaciones fuente-sumidero elevadas. Además, los resultados también sugieren que los efectos de la relación fuente-sumidero sobre la tasa fotosintética neta podrían depender de la interacción entre la fase fenológica de los árboles (actividad de los frutos, tejidos de reserva, ápices vegetativos como sumideros, cambios según la fase de desarrollo) y del clima que varía durante la temporada (Proietti et al., 2006).

El olivo, al igual que las plantas superiores, necesita nutrientes equilibrados tanto en forma de macronutrientes (C, H, O, N, P, K, S, Ca, Mg) como de micronutrientes (Fe, Zn, Mn, Cu, B, Cl) para un buen crecimiento y producción del fruto. Otros nutrientes (C, H y O) pueden obtenerse mediante la absorción del aire y el suelo. Sin embargo, la falta de N, P y K en el suelo conduce a una reducción del rendimiento (Sarrwy et al., 2010; Rodrigues et al., 2012). Las condiciones ambientales desfavorables como la aridez y la salinidad pueden alterar la absorción de nutrientes e interrumpir el crecimiento y desarrollo del fruto (Bustan et al., 2013). Iqbal et al. (2022) realizaron un análisis tanto de suelo como de hojas en cuatro etapas fenológicas diferentes (floración, cuajado, crecimiento y maduración del fruto). Los resultados revelaron que el macronutriente evaluado en hoja y suelo varió significativamente entre variedades, etapas fenológicas y año de crecimiento. Además, los resultados indicaron que el nivel de N disminuyó desde el cuajado (1,56 %) hasta la etapa de crecimiento del fruto (1,47 %). Los contenidos de N, P y K en la hoja y el suelo se encontraron más altos antes de la floración (etapa 1) y se agotaron después de la recolección del fruto (etapa 5), independientemente de las variedades de aceituna. Sin

embargo, las variedades de alto rendimiento mostraron nutrientes más bajos después de la cosecha de frutos. Por lo tanto, el contenido de N en la hoja y el suelo disminuyó gradualmente durante el crecimiento y desarrollo del fruto. Mientras que el contenido de K en la hoja y el suelo disminuyó drásticamente desde la maduración del fruto. En general, la tendencia de agotamiento de nutrientes mostró que diferentes genotipos de olivo con fluctuaciones estacionales necesitan P para el cuajado, N antes y después del cuajado y K después del endurecimiento del hueso o en las etapas de acumulación de aceite de forma gradual durante el crecimiento y desarrollo del fruto.

La consideración de ciclos alternos de producción para la optimización de la aplicación de N, P y K en olivo es necesario para lograr una producción más eficiente, una mejor calidad de aceite y minimizar las consecuencias ambientales (Gucci et al., 2010; Bustan et al., 2011, 2013). Además, la estrategia de riego junto con la nutrición foliar de N, Ca, Zn y B durante la iniciación y la inducción de las flores podría recomendarse para olivares en regiones áridas, semiáridas y subtropicales con los mismos problemas de desarrollo de yemas florales que la variedad 'Shengeh' (Tadayon and Hosseini, 2022).

Muchos investigadores, incluido Swietlik (2002), mencionaron los efectos beneficiosos del ácido giberélico (GA_3) y los elementos nutritivos, especialmente Zn, en el rendimiento y la calidad del fruto de diferentes cultivos. Además, el uso de GA_3 como regulador de crecimiento para promover el tamaño y controlar la caída de frutos fue estudiada por Arteca (1996). Swietlik (2002) afirmó que las aplicaciones de Zn al suelo no son muy efectivas debido a que las raíces de los cultivos frutales ocupan capas profundas del suelo y el Zn no se mueve fácilmente en el suelo. Por lo tanto, este autor indica que las pulverizaciones foliares de Zn son más efectivas. Debido a que no se ha publicado ningún estudio sobre el efecto del ácido giberélico en el tamaño del fruto de olivo, y existen informes sobre el efecto del Zn en las características del fruto de olivo, Ramezani and Shekafandeh (2009) estudiaron la posibilidad de aumentar el tamaño del fruto así como el rendimiento y mejora de las características del fruto del cultivar de olivo 'Shengeh' mediante tratamiento con ácido giberélico

y sulfato de zinc aplicado durante el crecimiento del fruto. Los resultados mostraron que el peso del fruto aumentó con las concentraciones de los tratamientos GA_3 y $ZnSO_4$ que con respecto a los árboles control, debido a un aumento en el tamaño del fruto. La pulverización de GA_3 a una concentración de 30 ppm fue más eficaz para mejorar el rendimiento que la pulverización de GA_3 a otras concentraciones. Así, estos tratamientos aceleraron el crecimiento del fruto del olivo, y también aumentaron tanto el tamaño del fruto como el rendimiento total por árbol, permitiendo un aumento de su valor económico.

Las condiciones ambientales pueden determinar el tamaño del fruto al afectar la actividad mitótica, la expansión celular o ambas (Denne, 1960; Bergh, 1985; Costagli et al., 2003; Gucci et al., 2009; De la Rosa et al., 2013; Bartolini et al., 2014; Rallo et al., 2018). En este sentido, Trentacoste et al. (2016) investigaron la influencia de la irradiación en el desarrollo del fruto de olivo demostrando que el peso del fruto, el mesocarpo y el contenido de aceite aumentan desde la base hasta la parte superior del dosel, lo que sugiere una relación lineal con la irradiación. De lo contrario, el peso y la composición del endocarpo se ven poco afectados por la disponibilidad de luz. Los diferentes niveles de asimilación influyen en la tasa de desarrollo del endocarpo, pero no en su tamaño o composición final, lo que demuestra la fuerte actividad sumidero de este tejido. Las diferencias en el peso del mesocarpo entre la posición del dosel no se vieron influenciadas por el número de frutos, lo que indica que la competencia por el sumidero no fue un factor limitante (Trentacoste et al., 2016). Trentacoste et al. (2016) también mostraron que la composición del mesocarpo estaba influenciada por el número y el tamaño de las células: el 51 y el 67 % de la variación del contenido de aceite entre la posición del fruto se debió a cambios en el número y tamaño de las células del mesocarpo, respectivamente. Así, el número de células y la tasa de expansión celular durante las últimas fases de crecimiento del fruto parece jugar un papel importante en la importación de asimilados en el olivo (Gillaspy et al., 1993; Génard et al., 1999), pero también en otros frutos como el tomate (Bertin et al., 2003). Recientemente, Reale et al. (2019) estudiaron la influencia de la disponibilidad de luz en el desarrollo del fruto de olivo. Además, investigaron el almacenamiento de aceite en las células del mesocarpo durante las diferentes etapas del desarrollo del fruto

y en diferentes condiciones de luz. Finalmente, compararon el comportamiento de dos cultivares italianos 'Leccino' y 'Frantoio' para verificar la presencia de posibles diferencias. Los resultados demostraron que la influencia de la disponibilidad de luz en el desarrollo del fruto depende del cultivar. En Leccino, el peso fresco y seco, el porcentaje de materia seca, el diámetro del grano y del fruto, el espesor del mesocarpo y el tamaño de las células del mesocarpo fueron mayores en los frutos expuestos a la luz que en los cultivados a la sombra. En Frantoio, las diferencias entre frutos de luz y sombra se observaron a los 140 DAP en el diámetro del grano y del fruto, así como en el peso seco y fresco, las cuales fueron mayores en los frutos expuestos a la luz. Leccino, por tanto, mostró una mayor sensibilidad a la disponibilidad de luz.

La humedad del suelo ha demostrado ser crítica para el desarrollo y la composición del fruto en olivo, ya que induce cambios en el tamaño, maduración, acumulación de aceite y calidad del mismo (Costagli et al., 2003, Gucci et al., 2007, Servili et al., 2007). A su vez, el grado de déficit de agua influye en el rendimiento, en el tamaño del fruto, en el peso del mesocarpo, en la proporción de mesocarpo frente a endocarpo, en la concentración fenólica y en las propiedades sensoriales del aceite (Moriana et al., 2003, Gomez-Rico et al., 2007; Lavee et al., 2007). El efecto del estado hídrico del árbol sobre el tamaño del fruto también parece depender de la cantidad de frutos que produce el árbol (Gucci et al., 2007). En este sentido, Rapport et al. (2004) demostraron que un déficit hídrico temprano alteró selectivamente el crecimiento del mesocarpo y el endocarpo y que la capacidad del endocarpo para recuperarse una vez que se alivió el estrés fue mayor que la del mesocarpo. En la capa del mesocarpo el déficit de agua redujo el tamaño de las células y no su número.

Existe un gran interés por la aplicación de técnicas de gestión de riego deficitario regulado (RDI), ya que reducen la cantidad de agua utilizada. Algunas experiencias con riego deficitario regulado (RDI) en olivo han demostrado que es posible lograr ahorros de agua y el tratamiento de riego no afectó a la composición de ácidos grasos, ni a la producción de aceite (Puertas et al., 2011).

Varios estudios sobre el crecimiento del fruto de olivo se han centrado en el estudio del fenómeno de histéresis como una importante herramienta de gestión implantada en la agricultura en los últimos años. Scalisi et al. (2020) examinaron la histéresis entre el diámetro del fruto y la presión de la hoja en dos cultivares de olivo bajo diferentes regímenes de riego. En relación con esta técnica, Khosravi et al. (2021) presentaron el primer estudio sobre la medición continua del diámetro transversal del fruto de olivo con la descripción de la histéresis del fruto según la variación diaria de déficit de presión de vapor. El objetivo específico de este estudio fue describir en continuo el crecimiento de la variedad de olivo 'Frantoio' mediante extensómetro automático. Además, se utilizó el color del fruto 'envero' para detectar la transición entre las fases de crecimiento del fruto.

2.4.2. Maduración del fruto

La maduración del fruto de olivo se caracteriza por cambios intensos en la fisiología del fruto, tales como alteraciones del color, derivadas de variaciones en los compuestos pigmentarios (clorofila, flavonoides y carotenoides), modificaciones de la textura, relacionadas con cambios en la composición de la pared celular o turgencia y variaciones metabólicas en cuanto a carbohidratos y a la producción de otros compuestos orgánicos que afectan a las propiedades organolépticas como valor nutricional, aroma y sabor (Conde et al., 2008; Skodra et al., 2021).

Las antocianinas son pigmentos de carácter flavonoide responsables de la coloración rojo-violácea que adquiere el fruto de olivo. El contenido de antocianinas aumenta desde el inicio del envero, alcanza un máximo y permanece posteriormente constante (Conde et al., 2008). En frutos que permanecen en el árbol y sobremaduran, el contenido en antocianinas desciende ligeramente (Barranco et al., 2017).

La acumulación de antocianinas constituye un índice fundamental de madurez aplicado a muchos tipos de fruto, incluido el olivo (Martinelli et al., 2012). El índice de madurez propuesto para el olivo por Uceda y Frías (1975) tiene en cuenta el color de la piel y de la pulpa de los frutos y oscila entre el verde intenso y el negro. Este índice si bien ha alcanzado una amplia aceptación entre los diferentes autores, también ha sido criticado como

subjetivo, equívoco y carente de uniformidad entre cultivares a menos que se combine con parámetros directamente asociados con la bioquímica de la maduración, como es el caso del contenido de antocianinas y la firmeza del fruto (Garcia and Yousfi, 2005; Vinha et al., 2005).

La firmeza es un rasgo de calidad importante de las aceitunas de mesa procesadas, que se ve muy afectada por la textura del fruto crudo, siendo la estructura de la pared celular primaria, y la composición de la lámina media los principales factores que determinan este parámetro (Coimbra et al., 1996). El etileno está estrechamente relacionado con los cambios de textura en frutos climatéricos (Vicente et al., 2007), pero no se puede excluir su papel en el ablandamiento de frutos no climatéricos (Villareal et al., 2016). La textura del fruto implica una serie de alteraciones organizadas en la pared celular, que están genéticamente programadas, pero también vienen influenciadas por factores ambientales y reguladores del crecimiento. Las paredes celulares del pericarpo del fruto son estructuras dinámicas y organizadas, pero también muy complejas. Están compuestas por fibrillas de celulosa (cadenas de 1,4-β-D-glucano) embebidas en hemicelulosa y la red resultante se embebe a su vez en una matriz de pectina (caracterizada por un alto contenido de residuos de ácido galacturónico, 1,4-α- D-GalA) y proteínas, estando también presentes compuestos fenólicos y algunos iones (Carpita and Gibeaut, 1993; Brummell, 2006). Las paredes celulares también están involucradas en la regulación del crecimiento celular, en la presión de turgencia y en la difusión de material a través del apoplasto; además, liberan moléculas de señalización, contribuyen al soporte mecánico, sirven como barreras al ataque biótico (Vicente et al., 2007; Cantu et al., 2008) y contribuyen a las respuestas de estrés abiótico (Tenhaken, 2015). En el pericarpo, las paredes celulares contienen pectina, hemicelulosas y celulosa, mientras que la lignina se encuentra principalmente cerca del hueso (Galanakis, 2011).

Kafkaletou et al. (2019) llevaron a cabo un estudio para conocer si los frutos recolectados en la etapa inmadura y tratados con etileno, son más firmes que los grupos control, determinando los principales cambios de textura en los frutos tratados. Este estudio, demuestra por primera vez el efecto reafirmante del etileno y los respectivos cambios en la pared celular de las aceitunas. El

hecho de que los frutos de la variedad 'Konservolia' respondieran a altos niveles de etileno confirma la percepción del etileno en estos frutos no climatéricos. Asimismo, los rápidos cambios observados en la textura hacen que el fruto sea candidato para estudios moleculares relacionados con la remodelación de la pared celular (Rose and Bennett, 1999), mientras que otros tratamientos podrían discriminar entre respuestas de estrés biótico y abiótico (Vilanova et al., 2017).

Los compuestos fenólicos alcanzan su contenido máximo en los frutos durante la etapa verde, disminuyendo drásticamente a partir de entonces durante la etapa de maduración (color negro) (Rotondi et al., 2004). La rápida disminución del contenido fenólico que ocurre durante la fase de maduración negra probablemente se correlacione con el aumento observado de la actividad de las enzimas hidrolíticas durante este período (Amiot et al., 1989). En el fruto de olivo, el principal compuesto fenólico es la oleuropeína, un éster heterosídico del ácido elenólico unido al 3,4-dihidroxifeniletanol o hidroxitirosol (Panizzi et al., 1960; Amiot et al., 1989). Este compuesto es muy abundante en los frutos jóvenes pero sus niveles disminuyen rápidamente durante la maduración (Amiot et al., 1986); esta disminución se acompaña de un aumento de otros compuestos fenólicos, tales como ciertos flavonoides (Vásquez et al., 1974; Solinas et al., 1975) y verbascósido, un éster heterosídico de ácido cafeico y de 3,4-dihidroxifeniletanol identificado previamente en aceite de oliva. La concentración del hidroxitirosol aumenta a medida que el fruto madura, como resultado de la degradación de la oleuropeína durante la maduración del fruto, debido a la mayor actividad de algunas enzimas hidrolíticas durante la maduración, siendo el hidroxitirosol el principal fenol en el fruto maduro (Amiot et al., 1989; Esti et al., 1998; Dağdelen et al., 2013).

Retrasar o anticipar el tiempo de cosecha puede ser crucial para mantener los derivados de la oleuropeína en el aceite de oliva (debido a las diferencias en su distribución entre el aceite y las fases acuosas) y equilibrar el sabor amargo y picante en el aceite (Esti et al., 1998; Caponio et al., 2001; Skevin et al., 2003). Por ello, una cosecha temprana da como resultado la producción de un aceite de oliva rico en compuestos fenólicos y generalmente de valor nutricional y características sensoriales superiores, pero con un bajo

contenido de aceite que puede implicar caracteres intensos, como un alto amargor y un exceso de picante, que son indeseables en algunos casos. Mientras que, una cosecha tardía conduce a mayores rendimientos de aceite, pero a una reducción en su calidad (Kafkaletou et al., 2021). Además, se ha observado que los compuestos fenólicos juegan un papel importante en la defensa de las plantas contra patógenos e insectos. La mosca *Bactrocera oleae* es la plaga de insectos más dañina de los olivos y afecta fuertemente al desarrollo y a la producción de frutos. Se han realizado varios estudios sobre la influencia del ataque de la mosca de olivo sobre los compuestos fenólicos del aceite de oliva (Gomez-Caravaca et al., 2008; Tamendjari et al., 2009; Medjkouh et al., 2016,2018; Mraicha et al., 2010). Según los análisis cualitativos y cuantitativos de los perfiles fenólicos realizados, el verbascósido, tirosol e hidroxitirosol fueron los compuestos más afectados por *Bactrocera oleae*. El ataque de la mosca se correlacionó significativamente con el peso de los frutos, pero no con los compuestos fenólicos (Medjkouh et al., 2018).

El contenido en azúcares reductores y solubles totales desciende conforme avanza el desarrollo y maduración del fruto, siendo menor dicho descenso al final del proceso de maduración momento en que sus valores permanecen prácticamente constantes. Entre dichos azúcares se han identificado como mayoritarios glucosa, como componente principal, fructosa, manitol y sacarosa, y como minoritarios xilosa y ramnosa. La relación entre el contenido de aceite y azúcar en el fruto de olivo en maduración ha sido estudiada por Donaire et al. (1975, 1977) que midieron el contenido de azúcar total durante el período de maduración del fruto. También Borbolla et al. (1955) y Fernández-Bolanos et al. (1982, 1983) midieron azúcares totales e individuales (glucosa, fructosa, sacarosa y manitol), pero solo al principio y al final del período de desarrollo del fruto, mientras que Fernández-Bolanos et al. (1982) también identificaron xilosa y ramnosa en el fruto, pero no midieron sus cantidades.

La variedad de olivo 'Kadesh' se caracteriza por un contenido muy bajo de aceite (Lavee, 1978). Incluso en la maduración negra completa, el contenido de aceite de los frutos no llega a superar el 8% frente al 20-22% en 'Manzanillo' y el 14-16% en 'Uovo di Piccione'. Para obtener una mejor

comprensión de la base metabólica de esta cantidad inusualmente baja de aceite, Wodner et al. (1988) estudiaron el contenido de azúcar del fruto a lo largo del proceso de crecimiento y maduración y determinaron su relación con el contenido de aceite durante este período. También Patumi et al. (1990) informaron que existe una relación positiva entre el contenido de aceite y los compuestos precursores que son responsables de la biosíntesis de lípidos durante la maduración del fruto en olivo. En su estudio, indicaron que el bajo contenido de aceite de algunas variedades de olivo podría atribuirse a la disminución de las cantidades de carbohidratos o a los efectos del malato y el citrato en la biosíntesis de lípidos. Según Wodner et al. (1987), la acumulación de aceite depende de la capacidad de las distintas variedades de olivo para metabolizar los sustratos. Otros autores también observaron el papel particular de los ácidos del ciclo de Krebs, especialmente los ácidos málico y cítrico, en la acumulación de aceite (Patumi et al., 1990). A su vez, Nergiz and Engez (2000) encontraron una correlación negativa entre los contenidos de azúcar y aceite en algunas variedades de olivo durante la maduración.

Los ácidos orgánicos son uno de los componentes menores del fruto de olivo y su cantidad es del 1,5% de la parte carnosa. Los ácidos orgánicos que juegan un papel importante en la actividad metabólica son los productos formados durante la síntesis y degradación de otros componentes del fruto como es el caso de los carbohidratos (Cunha et al., 2001). Los ácidos málico y cítrico que afectan al color de la aceituna son los principales ácidos orgánicos que se encuentran en ella. En este sentido, existen algunos estudios publicados por Nergiz and Ergönül (2009, 2010) donde investigaron los cambios en los contenidos de aceite, azúcar y ácidos orgánicos en las variedades de olivo Domat, Memecik y Uslu durante el proceso de maduración. Más recientemente, Arslan and Özcan (2011) estudiaron los cambios en las concentraciones de ácidos orgánicos en frutos de olivo de la variedad Gemlik según la fecha de cosecha y el área de cultivo.

La calidad del aceite de oliva se ve afectada principalmente por el estado de maduración del fruto. Los aceites de elevada calidad se obtienen cuando los frutos están frescos y sanos, y cuando se recolectan en el punto óptimo de maduración. Con el fin de establecer el período óptimo de cosecha, se han

desarrollado varios estudios basados en la caída de frutos, el contenido de aceite, el color, la fuerza de desprendimiento, así como la tasa de respiración de los frutos (Maxie et al., 1960; Solinas et al., 1975,1988; Vlahov, 1976; Fontanazza,1993; Ranalli et al., 1998). El rendimiento de aceite es de suma importancia económica y debe considerarse, junto con los índices de calidad, para determinar el inicio de la cosecha. Por ello, Dag et al. (2011) evaluaron y determinaron el período óptimo de recolección en relación con el rendimiento y el nivel de maduración de los frutos 'Souri' y 'Barnea', cultivados en condiciones intensivas. Así mismo, Camposeo et al. (2013) evaluaron el momento óptimo de recolección de cuatro cultivares de olivo (Arbequina, Arbosana, Coratina y Urano®) para cosecha continua, siguiendo los cambios estacionales de los índices de maduración más fiables y desarrollando un modelo para conocer el índice de desprendimiento, determinado mediante el índice colorimétrico más rápido. Los datos obtenidos en este estudio son los primeros disponibles para el nuevo cultivar italiano Urano®. Estos resultados enfatizan la importancia de establecer una prioridad de criterios para elegir el tiempo de cosecha teniendo en cuenta en primer lugar la máxima eficiencia mecánica, el máximo aceite cosechable y la máxima calidad del aceite.

Después de la maduración del fruto, muchas especies de árboles frutales sufren una masiva abscisión natural de los frutos. En olivo, la abscisión de frutos maduros depende de la activación de la zona de abscisión (ZA) ubicada entre el pedicelo y el fruto, y los patrones de abscisión de frutos maduros difieren entre cultivares (Gómez-Jiménez et al., 2010; Parra-Lobato and Gómez-Jiménez, 2011).

2.5. Aplicación de tecnologías "ómicas" en el desarrollo y maduración del fruto

Se ha demostrado que la secuenciación del genoma, las estrategias transcriptómicas, proteómicas y el perfil metabólico del olivo contribuyen a una mejor comprensión para identificar genes, proteínas y metabolitos durante el desarrollo y maduración del fruto de olivo (Biton et al., 2015; Skodra et al., 2021). Los primeros esfuerzos de secuenciación y ensamblaje del genoma de olivo se realizaron para *Olea europaea L.* subsp. *europaea* cv. 'Farga' y *Olea europaea L.* subsp. *sylvestris* mediante el enfoque de

escopeta (shotgun) del genoma completo utilizando la tecnología de lectura corta de Illumina (Cruz et al., 2016). A pesar de que, ambos ensamblajes del genoma se caracterizan por el alto número de contigs, con la ayuda del Consorcio Internacional del Genoma del Olivo se lograron anclar una gran cantidad de estos andamios (scaffolds) a 23 pseudocromosomas a través de un mapa genético y, por lo tanto, proporcionaron el primer anclaje cromosómico con anotación funcional en todo el genoma de oleaster, el olivo silvestre (Unver et al., 2017). Debido a que los genomas de olivo silvestre y domesticado tienen el mismo número de cromosomas y un tamaño similar, este ensamblaje de genoma es una valiosa contribución a los estudios de genética de poblaciones y transcriptómica como genoma de referencia.

Recientemente y gracias a la enorme mejora tecnológica de las plataformas de secuenciación de lectura larga (PacBio y Oxford Nanopore), se publicaron dos ensamblajes más de genoma de olivo de los cultivares 'Arbequina' y 'Picual' (Jiménez-Ruiz et al., 2020; Rao et al., 2021). En este sentido, Jiménez-Ruiz et al. (2020) estudiaron la evolución del genoma de olivo durante el proceso de domesticación realizando el ensamblaje del genoma de novo del cv. 'Picual', uno de los cultivares de olivo más populares. A su vez Rao et al. (2021) generaron un nuevo borrador del genoma del cv. 'Arbequina' con calidad suficiente para estudios de genoma completo en especies de olivo. Ambos estudios lograron mejorar notablemente la calidad de los borradores de genoma existentes.

2.5.1. Estudios transcriptómicos en el desarrollo y maduración del fruto

Hasta la fecha, se han obtenido numerosos estudios transcriptómicos de algunos genes de olivo que participan en funciones específicas, como es el caso de la maduración del fruto de olivo (Skodra et al., 2021). En particular, comprender la regulación de los patrones evolutivos de la síntesis de ácidos grasos durante el desarrollo y la maduración del fruto, así como la respuesta a varios factores externos, puede ayudar a construir las bases para la manipulación genética con el objetivo de producir frutos y aceites de calidad desde el punto de vista bioquímico, nutricional y organoléptico (Rallo et al., 2018). En este sentido, se encontró que la mayor expresión de transcritos asociados con la biosíntesis de ácidos grasos y con el ensamblaje de los

triacilgliceroles almacenados estaba estrechamente relacionada con el patrón de acumulación de ácidos grasos en frutos de olivo. Además, las transcripciones relacionadas con la biosíntesis de proteínas estructurales se correlacionaron con las divisiones celulares rápidas durante el crecimiento del fruto y mantuvieron la expresión más alta (Skodra et al., 2021). Asimismo, se realizó un análisis muy extenso entre dos cultivares de olivo diferentes comparando el transcriptoma de sus frutos (cv. 'Coratina' con alto contenido en fenoles y cv. 'Tendellone' como una variante natural carente de oleuropeína) durante dos etapas de desarrollo, 45 y 135 días después de la floración (Alagna et al., 2009). Un análisis SSR anterior indicó una distancia genética muy alta entre los dos cultivares y discrepancias en su patrón de acumulación de biofenoles (Sarri et al., 2006). Además de este trabajo, se propuso un vínculo entre los niveles de transcripción de geranilgeranil reductasa (CHL P) y la concentración de tocoferoles durante el proceso de maduración del pericarpo de olivo (Sarri et al., 2006). Tratando de examinar el efecto de la maduración en la capacidad antioxidante, se evaluaron los niveles de transcripción de OeCHL P de once cultivares de olivo diferentes mediante análisis qRT = PCR en dos etapas de desarrollo de los frutos (Muzzalupo et al., 2011). Los datos obtenidos revelaron que la expresión de CHL P se indujo notablemente durante el proceso de maduración de manera independiente del cultivar. Este estudio también mostró que la concentración de fenoles se redujo mientras que el nivel de tocoferol se estimuló con la maduración (Muzzalupo et al., 2011).

Es importante destacar que el fruto de olivo contiene cantidades significativas de tococromanoles que se conocen como potentes antioxidantes lipofílicos y que además son nutrientes dietéticos esenciales como es el caso de la vitamina E (Schneider, 2005). Los tocoferoles y los tocotrienoles son compuestos bien conocidos por sus efectos beneficiosos para la salud, que se encuentran comúnmente en varios frutos incluido el olivo (Chun et al., 2006). Numerosos estudios han revelado varias respuestas fisiológicas a los tococromanoles que pueden ser relevantes para la promoción de la salud y la prevención o tratamiento de algunas enfermedades crónicas (Sen et al., 2007). El α-tocoferol representa hasta el 68–89% del contenido total de tocoferoles en olivo, según el cultivo y la etapa de desarrollo (Muzzalupo et al., 2011). Se ha descrito una gran

diversidad en la concentración de tococromanoles en el fruto de olivo, destacando el impacto de factores genéticos y ambientales en la composición de estos compuestos (Hassapidou and Manoukas, 1993; Bruno et al., 2009; Muzzalupo et al., 2011; Bodoira et al., 2015). Existe poca información sobre la vía biosintética de la vitamina E en cultivos de árboles frutales, incluido el olivo (Georgiadou et al., 2015). En este estudio (Georgiadou et al., 2015), los perfiles de expresión génica temporal de alta resolución de los genes biosintéticos de tococromanol se determinaron en paralelo con el contenido de las ocho formas de vitamina E durante 17 etapas de desarrollo del fruto de olivo en el árbol. Georgiadou et al. (2016) determinaron los perfiles de transcripción temporal de los genes biosintéticos de tocoferol y tocotrienol y la cuantificación del contenido de proteína VTE5 en paralelo con la composición del tococromanol y la capacidad antioxidante durante años consecutivos. El objetivo a largo plazo es la regulación de la vía biosintética de los tococromanoles para aumentar su contenido durante la recolección del fruto de olivo para la producción de aceite de oliva.

Más tarde, Sezer and Taskin (2017) presentaron por primera vez las transcripciones completas que codifican las enzimas biosintéticas de vitamina E de tejidos de mesocarpo de frutos utilizando el método de amplificación rápida de extremos de ADNc (RACE). A su vez, caracterizaron la estructura de los genes 4-hidroxifenilpiruvato dioxigenasa (PDS1), homogentisato fitiltransferasa 1 (HPT1), vitamina E defectuosa 3 (VTE3), tocoferol ciclasa (VTE1) y gamma tocoferol metiltransferasa (GTMT), responsables de la biosíntesis de tocoferoles. En esa caracterización, se observó que PDS1 se encontraba en todos los organismos mientras que HPT1, VTE3, VTE1 y GTMT se encontraban en organismos fotosintéticos. Además, aislaron el ARN total de los tejidos del mesocarpo disecados del fruto recolectado en intervalos de 15 días. Se compararon los niveles de expresión de genes usando RT-PCR cuantitativa y se determinó el contenido de tocoferoles usando la técnica de cromatografía líquida de alta resolución-detección de fluorescencia (HPLC-FLD) durante la maduración del fruto en el cultivar Ayvalık. Los resultados arrojaron una alta expresión de OeHPT1, OeVTE3, OeVTE1 y OeGTMT en frutos jóvenes. Sin embargo, el ARNm de OePDS1 no mostró cambios de expresión significativos durante la

maduración. El contenido de α-tocoferol varió entre 26,78 y 21,05 mg/100 g y fue más alto en las primeras etapas de desarrollo del fruto. Además, los estudios de expresión y contenido de tocoferoles revelaron que la biosíntesis de tocoferoles en olivo es más activa en las primeras etapas de maduración del fruto.

Con el fin de decodificar las rutas de los flavonoides a través del desarrollo del fruto de olivo, se estudió la expresión de genes relacionados, incluida la fenilalanina-amoniaco-liasa (PAL), la chalcona sintasa (CHS), la flavanona 3-hidroxilasa (F3H), la dihidroflavonol 4-reductasa (DFR), la antocianidina sintasa (ANS) y la UDP glucosa-flavonoide 3-O-glucosiltransferasa (UFGT), junto con la concentración de compuestos flavonoides y antocianinas (Martinelli et al., 2012). La concentración de flavonoides aumentó en frutos jóvenes, mientras que las antocianinas se acumularon en la maduración, en particular en el tejido del epicarpo, al mismo tiempo que aumentaba la regulación de UFGT. Además, PAL, CHS, F3H y UFGT estaban regulados positivamente en las primeras etapas del desarrollo del fruto; se indujo DFR en el epicarpo al inicio del cambio de color, mientras que las transcripciones de ANS fueron extremadamente abundantes en una etapa más avanzada. Estos datos sugirieron que DFR y ANS, junto con UFGT, podrían representar elementos clave en la regulación de la biosíntesis de antocianinas en aceitunas (Martinelli et al., 2012). La investigación adicional en este campo se concentró en los niveles de ARNm de 35 transcritos de olivo que se definieron mediante análisis RT-qPCR en frutos de cultivares de olivo con una concentración baja y alta en compuestos fenólicos ('Dolce d'Andria' y 'Coratina ', respectivamente) y en tres etapas diferentes del desarrollo del fruto (Alagna et al., 2012). Los transcritos que participan en la biosíntesis de fenoles mostraron una correlación relativa con las concentraciones de estos compuestos, lo que indica un ajuste transcripcional de las vías que pueden corresponder. Principalmente, OeGES, OeDXS, OeDH y OeGE10H, que codifican geraniol sintasa, 1-desoxi-D-xilulosa-5-P sintasa, arogenato deshidrogenasa y geraniol 10-hidroxilasa, respectivamente, se observaron solo en fruto de olivo a los 45 días después de la floración. Se sugiere que estos compuestos puedan tener un papel importante durante la maduración del fruto en la acumulación de secoiridoides (Alagna et al., 2012).

Otra investigación sobre la transcriptómica de olivo se centra en la reconstrucción del transcriptoma de novo de los frutos de olivo junto con un análisis de expresión completa entre muestras de 'Leucocarpa', una variedad de olivo caracterizada por un apagado en el color de la piel en plena madurez, y 'Cassanese' utilizada como planta control a los 100 y 130 días después de la floración usando tecnología Illumina RNA-seq (Iaria et al., 2016). En este momento, 3792 y 3064 transcripciones se expresaron, respectivamente, en los genotipos 'Leucocarpa' y 'Cassanese' de manera diferente, de un total de 103. 359. Diferencias significativas en los perfiles de transcripción de flavonoides y antocianinas, que incluyen chalcona isomerasa (CHI), chalcona sintasa (CHS), 4-cumarato-CoA ligasa (4CL), cinamato 4-hidroxilasa (C4H), fenilalanina amoniaco liasa (PAL) y antocianidina sintasa (ANS), surgieron tanto durante la maduración del fruto como en relación con los genotipos. Finalmente, la abundancia de transcripciones de factores de transcripción de tipo MYB, MYC y WD40 fue mayor en el cultivar 'Cassanese' que en 'Leucocarpa' y también estuvo directamente relacionada con la acumulación de antocianinas (Iaria et al., 2016).

2.5.2. Estudios proteómicos en el desarrollo y maduración del fruto

La proteómica permite la identificación y cuantificación del contenido de proteínas de las células, tejidos u organismos utilizando tecnologías analíticas. Está demostrado que las alteraciones fenotípicas del fruto pueden describirse suficientemente a través de cambios en el proteoma en lugar de genoma o transcriptoma, ya que la producción y regulación de proteínas son directamente afectadas por numerosos factores ambientales. En consecuencia, el análisis proteómico puede ofrecer una visión sobre la respuesta del fruto a diversos estímulos ambientales y, por lo tanto, contribuir a los mecanismos de maduración (Karagiannis et al., 2016). Debido a su alto contenido en compuestos fenólicos y lipídicos, los tejidos del olivo (hojas, frutos) son difíciles de manipular durante la extracción de proteínas y dan lugar a extractos de baja calidad.

A fin de mitigar estos problemas, se sugiere tratar el tejido de olivo con ácido tricloroacético (TCA) al 10 % de acetona en polvo antes de la extracción de proteínas para proporcionar una eliminación eficaz de contaminantes orgánicos solubles en agua y ofrecer patrones 2-DE de buena calidad (Wang

et al., 2003; Wang et al., 2004). Antes de 2010, se realizaron varios estudios de proteínas/enzimas en olivo, centrándose en los alérgenos del polen, el almacenamiento de semillas, la calidad del aceite y las respuestas al estrés (Wang et al., 2010). Aunque se detecta un gran número de proteínas en muestras de aceituna, una pequeña proporción de ellas se identifica en base a datos sobre organismos homólogos secuenciados.

Varias proteínas de olivo exhibieron patrones de acumulación específicos de tejido durante el desarrollo del fruto; así, se detectaron proteínas similares a la taumatina en la pulpa de la aceituna, mientras que las proteínas de almacenamiento, las oleosinas y las histonas fueron más abundantes en las semillas (Steve et al., 2011). En las primeras etapas de maduración, los procesos de endurecimiento del hueso incluyen una alta acumulación de proteínas de almacenamiento de semillas. El primer informe de proteínas de almacenamiento de semillas de olivo fue realizado por Wang et al. (2001) utilizando SDS-PAGE, inmunotransferencia y secuenciación N-terminal. También se afirmó que la síntesis de proteínas de almacenamiento de semillas se intensificó junto con el desarrollo de la semilla, lo que subyace a una estricta regulación genética del desarrollo del endospermo. Además, Zamora et al. (2001) estudiaron el perfil proteico de los frutos de dos cultivares de olivo diferentes ('Picual' y 'Arbequina') durante la maduración y señalaron un compuesto polipeptídico de 4,6 kDa como uno de los constituyentes más significativos del mesocarpo de olivo usando SDS-PAGE y análisis de aminoácidos. Asimismo, se demostró una correlación positiva entre el contenido de aceite y de proteína durante la maduración.

Otros estudios basados en proteínas se centran en el contenido de lipoxigenasa (LOX) debido a su participación en la formación de aldehídos de seis carbonos, responsables del aroma del aceite de oliva virgen. La LOX es un polipéptido con una masa molecular superior a 100 kDa que se encuentra en el fruto de olivo y, junto con otras enzimas, como la alcohol deshidrogenasa, la hidroperóxido liasa de ácidos grasos y la polifenol oxidasa, son responsables de numerosas características organolépticas (Montealegre et al., 2014). La polifenol oxidasa y la peroxidasa podrían definir la etapa de desarrollo del fruto, ya que sus concentraciones parecen aumentar durante los procesos de maduración (Ebrahimzadeh et al., 2003).

Otro estudio también reveló que una ÿ-glucosidasa está involucrada en la transformación de los glucósidos fenólicos presentes en el mesocarpo de olivo, creando compuestos metabólicos secundarios que participan en la maduración del fruto de olivo (Romero-Segura et al., 2012). Más tarde, se ha aislado y caracterizado funcionalmente una ÿ-glucosidasa de olivo con una alta afinidad (Oeÿ-GLU) para desglicosilar la oleuropeína (Koudounas et al., 2015). También Cirilli et al., (2017) llevaron a cabo un experimento para conocer el papel de las familias de genes polifenoloxidasa (PPO), peroxidasa (PRX), ÿ-glucosidasa (ÿ-GLU), así como sus actividades enzimáticas en la acumulación de compuestos fenólicos durante el desarrollo del fruto de olivo en condiciones de riego total o de secano. Además, Badad et al. (2021) destacaron por primera vez la huella de metilación del ADN de la actividad de la lipoxigenasa Linoleato 9S en la biosíntesis de compuestos aromáticos volátiles. Este estudio revela el estado de metilación del genoma de olivo durante la maduración del fruto mediante secuenciación por inmunoprecipitación (MeDIP-seq).

Tras el análisis proteómico comparativo, se han llevado a cabo numerosos estudios sobre las etapas de desarrollo o abscisión de olivo. Así, Bianco et al. (2013) estudiaron las alteraciones del proteoma correlacionadas con la maduración del fruto de olivo (cv. 'Coratina') mediante proteómica comparativa 2-DE junto con el análisis de espectrometría de masas. Los datos de este trabajo indicaron que se alteraron 247 proteínas a lo largo del desarrollo, mientras que se identificaron 68 proteínas. En particular, las proteínas relacionadas con la multiplicación celular aumentaron durante el desarrollo temprano del fruto, mientras que las ATPasas vacuolares, las anexinas y las proteínas del citoesqueleto regularon la expansión celular en etapas posteriores. La información sobre varias proteínas asociadas con el metabolismo y la biosíntesis de ácidos grasos se deriva del trabajo proteómico sin gel no publicado de Bianco and Perrotta (2016) en frutos de 'Chondrolia Chalkidikis' varvia nano-LC acoplado al espectrómetro de masas HDAM Orbitrap. En este trabajo se identificaron 3258 proteínas, de las cuales 350 se acumularon diferencialmente entre las dos etapas finales de maduración de los frutos (etapa verde vs. negra). Investigaciones adicionales sobre los procesos de maduración del fruto de olivo, junto con la secuencia completa del genoma de olivo cultivado, aportarán datos importantes sobre

los procesos que ocurren durante la maduración de olivo (Bianco and Perrotta,2016).

2.5.3. Estudios metabolómicos en el desarrollo y maduración del fruto

Los procesos de maduración implican variaciones en el perfil metabólico de los frutos, principalmente relacionadas con la biosíntesis de ácidos grasos y fenoles. Hasta la fecha, utilizando tecnologías de metabolómica, varios grupos de investigación han podido identificar y monitorizar varios metabolitos que están presentes durante el crecimiento del fruto de olivo, brindando así información sobre su metabolismo y fisiología (Michailidis et al., 2017). En términos de estructura y función, los metabolitos se agrupan en metabolitos primarios y secundarios (Deborde et al., 2017). Ambos pueden evaluarse a través de una variedad de métodos analíticos, como resonancia magnética nuclear (RMN) y cromatografía de gases o líquidos, junto con varios sistemas de espectrometría de masas (GC-MS, LC-MS). Los efectos beneficiosos para la salud del aceite de oliva están altamente correlacionados con su abundancia en metabolitos, especialmente compuestos fenólicos, como tirosol, hidroxitirosol y oleuropeína (Tuck, Hayball 2002). El perfil de metabolitos de diversos tejidos de olivo (hojas, raíces, semillas y frutos) está disponible en la actualidad debido a los avances recientes en la extracción e identificación de metabolitos totales. Este conocimiento puede ofrecer oportunidades para comprender las respuestas de las plantas bajo numerosas condiciones o interpretar procedimientos biológicos complejos, incluida la maduración de los frutos. Un ejemplo aplicable es ofrecido por Di Donna et al. (2010), quienes propusieron que la determinación del perfil de metabolitos secundarios en hojas de olivo podría usarse como marcador para la diferenciación de cultivares. Específicamente, utilizando HPLC combinado con el enfoque ESI MS, se identificaron 12 compuestos fenólicos, oleósido, verbascósido, oleuropeína, lingstrosido, glucósido de hidroxitirosol, en cinco cultivares ('Carolea', 'Cassanese', 'Coratina' 'Nocellara' y 'Leccino'). En base a ello y utilizando dos aplicaciones supervisadas de reconocimiento de patrones, junto con técnicas de análisis discriminante lineal y modelado suave independiente de analogía de clase, se ha logrado predecir de manera efectiva el cultivar y la zona de cultivo de cada muestra.

Las respuestas fisiológicas de los frutos de olivo en condiciones de estrés abiótico y biótico también podrían describirse a través de cambios en el metabolismo; Los tejidos del fruto de olivo parecen producir metabolitos implicados en la adaptación/resistencia a condiciones adversas. Martinelli et al. (2013), utilizando GC-MS, detectaron 176 metabolitos en frutos de olivo, de los cuales 57 estaban relacionados con el estrés hídrico. Este trabajo indicó además que 19 metabolitos se vieron afectados negativamente por el estrés hídrico, incluidos azúcares, polioles y ácidos grasos. Del mismo modo, Machado et al. (2013) concluyeron que el riego durante la maduración de los frutos de cv. 'Cobrancosa' influyó negativamente en la calidad del aceite obtenido debido a la disminución del contenido de fenilpropanoides, alcoholes fenólicos, secoiridoides y flavonoides. En otro estudio de riego, se encontró que 46 metabolitos del mesocarpo diferían significativamente en la cv 'Leccino' con riego y sin riego, seguido de alteraciones en la expresión de genes relacionados con las vías metabólicas de los polifenoles, como la chalcona sintasa (CHS), la fenilalanina amoníaco liasa (PAL) y la dihidroflavonol reductasa (DFR) (Martinelli et al., 2012). En particular, se informó de un aumento en el contenido de polifenoles y antocianinas en frutos sin riego, seguido de una mayor actividad de PAL en las primeras etapas de desarrollo, posiblemente relacionado con mecanismos activados por estrés durante la maduración. La acumulación de transcripciones de CHS y DFR aumentó principalmente en los epicarpos de los frutos no irrigados durante las últimas etapas de maduración, sirviendo en los procesos de pigmentación del fruto. El ácido shikímico, el ácido galacturónico, la alosa y la L-asparagina aumentaron drásticamente en las muestras irrigadas, lo que indica un posible retraso en los procesos de maduración de los frutos relacionado con niveles más altos de riego (Martinelli et al., 2012).

El proceso de maduración del fruto de olivo implica la activación de varias vías metabólicas que conllevan la producción de polifenoles y ácidos grasos, lo que afecta en gran medida a la calidad del aceite de oliva (Servili et al., 2016). Las concentraciones de ácidos grasos trans, saturados, monosaturados y poliinsaturados se encuentran fuertemente relacionadas con el estado de maduración del fruto e indican el momento óptimo de cosecha (Gómez-González et al., 2011; Cecchi et al., 2013). Asimismo, se ha demostrado que el contenido de ácidos grasos varía significativamente en diferentes

cultivares de olivo ('Arbequina', 'Gordal', 'Manzanilla', 'Picual' y 'Picudo') siendo el cultivar 'Picudo' el que exhibe un aumento continuo en el contenido total de aceite en todas las etapas de maduración (Gómez-González et al., 2011). En otro estudio identificaron, mediante análisis HPLC/DAD/ESI/MS, 20 compuestos fenólicos diferentes durante la maduración de tres cultivares toscanos típicos, 'Frantoio', 'Moraiolo' y 'Leccino' (Cecchi et al., 2013). En todos estos frutos se excluyó la presencia de lignanos y la forma dialdehídica de la descarboximetiloleuropeína aglicona (3,4-DHPEA-EDA). Además, en términos de fenoles totales, 'Moraiolo' fue siempre el cultivar con mayor abundancia; la reducción fenólica fue apenas apreciable en 'Frantoio', mientras que para 'Moraiolo' y 'Leccino' la disminución estuvo casi inversamente relacionada con el tiempo de maduración (Cecchi et al., 2013). Por otra parte, también se investigó la dinámica de acumulación de escualeno y esteroles durante la maduración del fruto en los cultivares 'Picual' y 'Arbequina' así como en dos selecciones de mejora derivadas de cruces entre ellos (Fernández-Cuesta et al., 2013). Esta investigación reveló cambios significativos en los contenidos de escualeno y esteroles en frutos cosechados de septiembre a noviembre, pero prácticamente no hubo diferencias entre los frutos cosechados en noviembre y diciembre (Fernández-Cuesta et al., 2013).

Las modificaciones en el perfil fenólico de los frutos durante la maduración están fuertemente correlacionadas con cada cultivar y definen, en gran medida, la calidad del aceite extraído. El contenido fenólico de varios cultivares españoles ('Cornicabra', 'Arbequina', 'Picudo', 'Morisca', 'Picual' y 'Picolimón') durante el desarrollo del fruto fue evaluado por Gomez-Rico et al. (2008) usando un HPLC-MS. Así, durante la maduración del fruto de olivo, disminuye el contenido de oleuropeína en frutos maduros de numerosos cultivares; el nivel de estado estacionario de oleuropeína se correlacionó negativamente con el contenido de verbascósido, que tiende a acumularse en frutos maduros (Gómez-Rico et al., 2008; Dagdelen et al., 2013). Estos metabolitos, junto con el hidroxitirosol, determinan características organolépticas importantes de los frutos, como su sabor (Dagdelen et al., 2013). Adicionalmente, se ha identificado una gran variedad de compuestos fenólicos en los frutos de olivo, presentando variaciones en su contenido según el cultivar y el estado de madurez; esto puede conducir a la

categorización de los cultivares en grupos según su perfil fenólico y, como resultado, su calidad (Gómez-Rico et al., 2008). En otro estudio, también se cuantificó etanol por HS-SPME-GC-FID en frutos de tres cultivares de olivo ('Picual', 'Hojiblanca' y 'Arbequina') durante la maduración, mostrando que su concentración aumenta rápidamente cerca de la fecha de cosecha (contenido de etanol varió entre 0,56 y 59 mg/kg), y su síntesis está fuertemente regulada a nivel genético (Beltrán et al., 2015). La acumulación de etanol se intensificó a medida que los frutos de olivo maduros permanecían en el árbol debido a la respiración anaeróbica del fruto. Por último, se han puesto de manifiesto las variaciones en el contenido de triterpenoides pentacíclicos durante la maduración del fruto mediante un análisis HPLC-UV/vis en frutos de dos cultivares de olivo ('Picual' y 'Cornezuelo') (Peragón, 2013). Además, Peragón (2013) identificó ácido oleanólico y ácido maslínico en los frutos, los cuales aumentaron significativamente sus concentraciones durante las primeras etapas del crecimiento y desarrollo del fruto, lo que demuestra su papel en la fisiología del fruto, incluyendo su respuesta a factores abióticos y bióticos.

La correlación del metaboloma y los datos transcripcionales en varios tejidos de olivo proporciona una visión integral de la expresión génica y el metabolismo que podría dilucidar el complejo proceso de maduración de los frutos. En este sentido, Xiaoxia et al. (2020) combinaron análisis metabolómicos y transcriptómicos para caracterizar la interacción entre la expresión génica y la producción de metabolitos en frutos, hojas viejas y nuevas del cultivar 'Leccino'. En este análisis, se identificaron 3049 genes recién anotados; 2350 genes fueron anotados funcionalmente, y los genes más regulados estaban relacionados con el metabolismo de los ácidos grasos. También, Liu et al. (2021) combinaron ambas estrategias realizando un análisis integrado del metabolismo de ácidos grasos y del transcriptoma involucrado en el desarrollo del fruto de olivo para mejorar la composición de aceite. En este estudio identificaron un total de 34 ácidos grasos mediante cromatografía de gases-espectrometría de masas (GC-MS) y estudiaron todas las transcripciones del metabolismo de los ácidos grasos durante el desarrollo del fruto de olivo, incluida la glicólisis, la síntesis de ácidos grasos, la síntesis de triacilglicerol y la degradación de los ácidos grasos.

Como tejidos distintos, las hojas de olivo y los frutos revelan variaciones metabólicas específicas del tejido, ya que los frutos sintetizan una gran cantidad de ácidos grasos (el ácido oleico y el ácido palmítico son los más dominantes), mientras que las hojas se caracterizan por una abundancia de flavonoides y fenilpropanoides (Rao et al., 2016). Recientemente, Bruno et al. (2019) aplicaron un análisis transcriptómico comparativo en los frutos del cultivar 'Carolea' cultivados a diferentes altitudes (10, 200 y 700 m). Se detectó una regulación positiva importante de los genes de desaturación de ácidos grasos (FAD) que están específicamente implicados en la vía biosintética de los ácidos grasos insaturados junto con una regulación negativa de los genes implicados en la formación de secoiridoides en los frutos cultivados a mayor altitud (700 m). El análisis de RNA-seq reveló que los genes OeFAD2.2 y FAD6 estaban regulados positivamente en frutos morados que crecían a 700 m, mientras que el gen OeFAD7 estaba regulado positivamente en frutos que crecían a 10 m de altitud. En las áreas de cultivo de menor altitud, la biosíntesis de fenoles mejoró, mientras que la producción de oleuropeína fue mayor en los frutos que crecieron a 700 m. Estos resultados sugirieron que la estabilidad de los ácidos grasos y los fenoles, principalmente del grupo de los secoiridoides, se promueve a gran altitud, mientras que a menor altitud se prolonga la biosíntesis de fenoles.

En estudios previos se han caracterizado los genes de desaturación de ácidos grasos de olivo implicados en la composición de ácidos grasos insaturados del aceite de oliva en los cultivares Picual y Arbequina (Hernández et al., 2005, 2009, 2016, 2020; Parvini et al., 2016). Sin embargo, el control genético de su variabilidad entre los cultivares de olivo aún es poco conocido. Por ello, se amplió el estudio a los cultivares de una colección núcleo previamente desarrollada (Core 36) con una amplia diversidad genética (Belaj et al., 2012), lo que permitió identificar dos cultivares de olivo con contenido de ácido linoleico muy contrastado: Klon-14 y Abu Kanani. Estos dos cultivares se utilizaron además para determinar los niveles de expresión de genes que codifican ácidos grasos desaturasas en los tejidos del mesocarpo durante el desarrollo y la maduración del fruto de olivo, con el fin de investigar su participación en la regulación del contenido de ácido oleico y linoleico. Los niveles de expresión del gen de desaturación de ácidos grasos, junto con el análisis de lípidos, sugieren que no solo estaba controlada por OeFAD2-2 y

OeFAD2-5, sino también por las diferentes especificidades de las enzimas aciltransferasa extraplastidiales.

En olivo también se han podido describir cuatro genes que codifican el SAD soluble: OeSAD1 (Haralampidis et al., 1998), OeSAD2, OeSAD3 (Parvini et al., 2016) y OeSAD4 (Contreras et al., 2020). Con respecto a las desaturasas unidas a la membrana, Hernández et al. (2005, 2009, 2020) han aislado y caracterizado cinco genes que codifican oleato desaturasas microsomales (OeFAD2-1 a OeFAD2-5), mientras que hasta el momento solo se ha descrito un gen OeFAD6 (Banilas et al., 2005; Hernández et al., 2011). Además, se han caracterizado cuatro miembros de la familia del gen de la linoleato desaturasa de olivo, dos microsomales (OeFAD3A, Banilas et al., 2007; OeFAD3B, Hernández et al., 2016) y dos plastidiales (OeFAD7-1, Poghosyan et al., 1999).; OeFAD7-2, Hernández et al., 2016).

Por otra parte, a medida que avanza la maduración del fruto se produce una activación progresiva de la actividad lipolítica que los hace más sensibles a las infecciones patógenas y daños mecánicos (Gutiérrez et al., 1999; Salvador et al., 2001). Así, los genes FAD en olivo mostraron una diferenciación funcional diversa en la morfología de los diferentes tejidos, el desarrollo del fruto y las respuestas al estrés. Entre ellos, OeFAB2.8 y OeFAD2.3 estaban regulados positivamente y OeADS.1, OeFAD4.1 y OeFAD8.2 estaban regulados negativamente bajo la infección provocada por *Verticillium dahliae* y estrés por frío. Este estudio presenta un análisis exhaustivo de los genes FAD a nivel de genoma completo y proporcionará nuevas perspectivas para la mejora de la calidad del aceite o la tolerancia al estrés de los olivos (Niu et al., 2022).

Objetivos

II. Objetivos

El **objetivo general** planteado en esta Tesis Doctoral ha sido estudiar los mecanismos fisiológicos y moleculares implicados en el desarrollo del fruto de olivo (*Olea europaea* L.).

Para el desarrollo de este objetivo general se llevaron a cabo los siguientes **objetivos específicos**:

1. Caracterizar, a nivel transcriptómico y hormonal, el desarrollo temprano del fruto de olivo.

2. Profundizar en el estudio de la regulación hormonal del proceso de desarrollo y maduración del fruto de olivo. Realizar un estudio comparativo de los contenidos hormonales y de la expresión de genes relacionados con la biosíntesis y señalización hormonal durante el desarrollo en frutos de variedades de olivo con diferencias en su tamaño y forma, así como en su duración de maduración.

3. Estudiar la posible relación entre el tamaño final del fruto y el área de las células del mesocarpo del fruto durante el desarrollo del fruto en olivo. Para ello, se utilizaron frutos de variedades de olivo con diferente tamaño de fruto, como la variedad de aceituna de mesa 'Manzanilla Sevillana' y las variedades de aceite 'Arbequina' y 'Picual'.

Capítulo I

Caracterización de la dinámica del transcriptoma durante el desarrollo temprano del fruto en olivo

Capítulo I

Characterization of transcriptome dynamics during early fruit development in olive

Abstract

In the olive (*Olea europaea* L. subsp. *europaea* var. *europaea*), a leading oil crop worldwide, fruit size and yield are determined by the early stages of fruit development. However, few detailed analyses of this stage of fruit development are available. This study offers an extensive characterization of the various processes involved in olive fruit early growth (cell division, cell cycle regulation, and cell expansion). For this, cytological, hormonal, and transcriptional changes characterizing the phases of early fruit development were analysed in olive fruit of the cv. 'Picual'. First, the surface area and mitotic activity (by flow cytometry) of fruit cells were investigated during early olive fruit development, from 0 to 42 days post-anthesis (DPA). The results demonstrate that the cell division phase extends up to 21 DPA, during which the maximal proportion of 4C cells (63.2%) in olive fruits was reached at 14 DPA, indicating that intensive cell division was activated in olive fruits at that time. Subsequently, fruit cell expansion lasted as much as 3 weeks more before endocarp lignification. Moreover, auxin, GA_4 and ABA have higher relative importance in the phase when olive fruit growth depends mainly on cell expansion, while CKs (*trans*-Zeatin, *t*Z) and SA were greater during the phase of more intense cell division. Finally, the molecular mechanisms controlling the early fruit development were investigated by analysing the transcriptome of olive flowers at anthesis (fruit set) as well as olive fruits at 14 DPA (cell division phase) and at 28 DPA (cell expansion phase). Sequential induction of the cell cycle regulating genes is associated with the upregulation of genes involved in cell wall remodelling and ion fluxes, and a shift in plant hormone metabolism and signalling genes during olive fruit early development. This occurs together with transcriptional activity of subtilisin-like protease proteins together with transcription factors potentially involved in early fruit growth signalling. This gene expression profile, together with hormonal regulators, will help clarify gene regulatory

networks during early olive fruit development. In practical terms, it will aid in designing specific approaches for crop breeding and engineering, facilitating the development of the table-olive and olive-oil industry.

Keywords: cell division; cell expansion; flow cytometry; fruit growth; hormone; olive; ploidy; transcriptome

1. Introduction

The olive tree (*Olea europaea* L. subsp. *europaea* var. *europaea*) produces fruit that rank among the world's leading oil crops (Baldoni and Belaj, 2009). Genetically, it is typically diploid (2n = 2X = 46), though many studies have polyploidy (Rugini et al., 1996; Besnard et al., 2008). Its genome size is approximately 1,800 Mb (Loureiro et al., 2007). Technically a fleshy drupe from hermaphroditic flowers, the fruit is commonly called a 'stone fruit' because the seed coat is enclosed in a stone-hard, lignified endocarp (Conde et al. 2008). The olive fruit has two parts: the flesh, of maternal origin; and the embryo, of different genetic origins that account for variations in certain characteristics of the oil composition in different environments (Breton and Bervillé, 2013).

The size increase of the olive fruit depends on two distinct mechanisms: (1) young fruit growth (cell division and expansion) before endocarp lignification (early fruit growth), and subsequently, (2) fruit pulp growth (cell expansion) after endocarp lignification (late fruit growth). As the young olive fruit accumulates water, its cells swell and also rapidly proliferate. The first signal of fruit differentiation, the hardening of the stone, results from the appearance of sclerenchymous cells. This early developmental feature of the fruit becomes patent some 50 days following ovary fertilization, as most of the nutritional resources become mobilized at this early stage while the other parameters tend to slow down (Conde et al., 2008; Breton and Bervillé, 2013). After this early stage and until fruit ripening, fruit pulp growth is due solely to cell expansion, and oil starts to accumulate. The oil content and composition are determined by the cultivar with little environmental influence, whereas other compounds (phenols and sterols) depend more on the environment (Breton and Bervillé, 2013). Because of in the increasing oil content during fruit pulp growth, which can reach 30% (fresh weight) at full

ripening (Breton and Bervillé, 2013), and due to the high commercial value of the oil, most studies to date have attempted to elucidate the molecular bases of olive fruit ripening (Alagna et al., 2009, 2012; Galla et al., 2009; Martinelli and Tonutti, 2012; Parra et al., 2013; Parvini et al., 2015; Inês et al., 2018; Mougiou et al., 2018; Bruno et al, 2019; Carbone et al., 2019; Xiaoxia et al., 2020; Briegas et al., 2020; Liu et al., 2021; Rao et al., 2021). Other studies have identified candidate genes associated with early fruit development or flower development in olive (Haloamides et al., 1998; Martsinkovskaya et al., 1999; Hatzopoulos et al., 2002; Banilas et al., 2005, 2011; Poghosyan et al., 2005; Gomez-Jimenez et al. 2010; Alagna et al., 2016), but the transcriptomic control of changes associated with early fruit development in olive remains unknown.

In fleshy fruit, early development requires a precise orchestration of cell division, cell expansion, and cell differentiation by integrating endogenous signals and various environmental cues (Gillaspy et al., 1993; Mauxion et al., 2021). Fruit growth begins immediately after the ovary is pollinated, triggering vigorous cell division. This cell division is the primary driver for growth within the ovary. Spatial changes in cell division rate or duration within the ovary thus holds sway over the final fruit size (Mauxion et al., 2021). In tomato (*Solanum lycopersicum*), a model system for fleshy fruit development (Quinet et al., 2019; Mauxion et al., 2021), the prime factors controlling ultimate tomato fruit size are cell division as well as cell expansion (Bertin et al., 2005; Cheniclet, et al., 2005; Pećinar et al., 2021). Moreover, in many species, including tomato, the transition from cell division to expansion phases is accompanied by endoreduplication (Cheniclet et al., 2005; Chevalier et al., 2011, 2014; Pirrello et al., 2018; Farinati et al., 2021). Because cell size for a certain cell type generally proves proportional to the quantity of nuclear DNA, an effective strategy of cell growth is endoreduplication, as often occurs in differentiated cells that are large or metabolically highly active (Edgar and Orr-Weaver, 2001). An understanding of the interaction involving endoreduplication, cell division, and cell expansion processes is vital for predicting the appearance of key morphological traits (fruit size, shape, mass, and texture). In olive, however, the ploidy levels during early fruit development have not yet been explored, and several questions remain regarding not only the rate and duration of cell division during early fruit

development but also its relative importance on the final fruit size. According to previous studies analysing the olive fruit histology by qualitative (cross-section) methods, cell division and cell expansion occur concomitantly in the first phase of fruit growth, i.e. 6-8 weeks after anthesis (Rallo and Rapoport, 2001; Rosati et al., 2012; Trentacoste et al., 2012). However, no available studies have investigated the mitotic activity of olive fruits by flow cytometry during early fruit development. Recently, it has been demonstrated that under water stress during the fruit pulp growth (cell expansion) in olive, even though olive fruit growth appears to stop, stress-induced cell division occurs, and the final size of the olive fruit is not severely diminished when the trees are irrigated again during the period of fruit pulp growth (Hernández-Santana et al., 2021).

In recent years, notable progress has been made in understanding the molecular mechanisms that coordinate the interaction of transcriptional control and hormonal activity in early fruit development (Catalá et al., 2000; Lemaire-Chamley et al., 2005; Mounet et al., 2009; Wang et al., 2009; Ando et al., 2012; Kang et al., 2013; Pattison et al., 2015; Farinati et al., 2021). The modification of genes that act in hormonal regulation can alter fruit size, given that hormone contents can undergo major shifts during fruit growth (Mauxion et al., 2021). In fact, using mutants or exogenous treatments, many studies have indicated the decisive role of hormones for early fruit-growth regulation (Atta et al., 1999; Fos et al., 2001; Fu et al., 2008; Mariotti et al., 2011; Wang et al., 2019a). In olive, we have previously demonstrated that exogenous brassinosteroid (BR) application promoted the early fruit growth, whereas the blocking of BR synthesis with brassinazole (Brz) slowed down the fruit growth rate (Corbacho et al., 2018). Moreover, our data have provided new findings on the role of BRs in modulating the composition and gene expression of sterols and sphingolipids, these being lipophilic membrane components essential for cellular functions during early olive fruit growth (Corbacho et al., 2018; Inês et al., 2019). This latter study also revealed the up-regulation of β-sitosterol biosynthesis by BR at the transcriptional level during early olive fruit growth. Likewise, in a previous study, we have demonstrated that free endogenous polyamines (PAs) may regulate olive-flower anthesis mainly through S-adenosyl methionine decarboxylase (SAMDC) enzyme activity and expression gene localized in the ovary; the

same study has indicated that PAs appear to correlate positively with cell division during early fruit development in olive (Gomez-Jimenez et al., 2010). Nevertheless, knowledge remains scant on the hormone content and composition of olive fruits during early fruit development.

An understanding of the molecular mechanisms of early olive fruit development will be particularly relevant in developing targeted approaches for breeding and engineering crops and specifically in accelerating advances in the table-olive and oil-olive industry. The purpose of the present study was to gain a more complete picture of gene expression and hormonal control during early fruit development in olive. For this, we analysed the cytology, ploidy, and transcriptome dynamics associated with early fruit development in combination with data on hormonal content. The cell area and mitotic activity, by flow-cytometric analysis, in the developing olive fruits were first investigated in order to characterize the duration of the cell division and cell expansion phases. Next, transcriptional and hormonal changes in olive fruit were investigated during early fruit development as a means of establishing candidate genes associated with distinct phases of early development. Specific potential genes and their associated hormonal pathways were determined to participate in the phases of cell division and expansion during olive fruit early development.

2. Materials and Methods

2.1. Plant material and cytological study

Olive trees (*Olea europaea* L. subsp. *europaea* var. *europaea*) of the 'Picual' cultivar 20 years old in an orchard under drip irrigation (fertigation with suitable liquid fertilizers) near Badajoz (Spain) were studied. From these trees, flowers were collected at the anthesis stage (0 days post-anthesis, DPA) and fruits were sampled at 7, 14, 21, 28, 35 and 42 DPA, spanning a time from the fruit set to the time of endocarp lignification, and using 500 flowers or fruits for each developmental stage during the 2018-2019 growing seasons (Gomez-Jimenez et al., 2010; Corbacho et al., 2018; Inês et al., 2019). Harvested flowers and whole fruits of 'Picual' olive were weighed, and the longitudinal and equatorial diameters were measured at different developmental stages (Figure I.1). Flowers plus whole fruits at different stages

of development were frozen in liquid nitrogen and then stored at -80ºC until analysed.

In the cytological study, at least three biological replicates were made at each stage. For this, samples were sliced 0.3 to 0.6 mm thick and quickly fixed in ethanol-acetic acid (3:1, v/v) for 2h at ambient temperature. Then the samples were rinsed 3 times using 70% ethanol, dried using an ethanol series, and finally embedded in Technovit 7100 (Kulzer). Sections 30 µm thick used for confocal imaging were stained for 2 min with Calcofluor White M2R (Wyeth, http://www.wyeth.com, 0.1% w/v in distilled water), a fluorescence brightener commonly used in the visualization of crystalline cellulose in plant cell walls (Gahan, 1984), rinsed with distilled water, mounted with a cover slip in DABCO mounting medium, and sealed with nail polish. Fruit cells and pericarp thickness were examined using a confocal laser-scanning microscope (model Fluoview-BX50, Olympus). For microscopy, the cell size (cell area) and pericarp thickness (cross-section) were determined using a CellProfiler image analysis system (Lamprecht et al., 2007).

2.2. Flow cytometry analysis

The cell division period was precisely determined by using flow cytometry with nucleus ploidy profiles taken from ovaries and fruits by the method recommended elsewhere (Loureiro, 2009). The samples of 0.1-0.2 g fresh weight were diced into 0.5 ml using a razor blade and placed in ice-cold buffer (0.2 M Tris-HCl, 4 mM $MgCl_2$, 2 mM EDTA, 86 mM NaCl, 10 mM metabisulphite, pH 7.5, and 1% Triton X-100), then filtered through a 30-µm nylon mesh, and finally stained using 4,6-diamidino-2-phenylindole (DAPI). Next, the distribution of the nuclear-DNA content was run through a FACS CantoII flow cytometer, and the data recorded were analysed using FACSDiva 6.1.2 software (BD Biosciences, Franklin Lakes, NJ, USA). For each stage, 4 biological replicates, with 10,000 nuclei each, were undertaken per stage. The DNA content (C value) of the olive fruit cells was submitted to flow cytometry with the use of internal calibration standards (Loureiro, 2009). The C values were determined following Dolezel et al. (2007): 2C DNA (pg) = (mean of the problem sample G1 peak × 2C DNA content of the standard [pg])/mean of the standard G1 peak.

2.3. RNA extraction, library preparation and sequencing

The extraction of the total RNA from ovaries and fruits samples was performed as in Gomez-Jimenez et al. (2010). For each sample, three biological replicates were collected of the same developmental stage. Tissue frozen at -80ºC was milled to powder in liquid nitrogen prior to the addition of the buffer (2 mL buffer: 1 g tissue). The RNA quality tests were performed with the Agilent 2100 Bioanalyzer (Agilent Technologies, Santa Clara, CA, USA) employing an RNA 6000 Pico assay kit (Agilent Technologies). This RNA was used in RNA-seq and quantitative RT-PCR (qRT-PCR) analyses.

We isolated the poly(A)+ mRNA fraction from the total RNA and obtained cDNA libraries following the recommendations of Illumina. In short, poly(A)+ RNA, after being isolated on poly-T oligo attached magnetic beads, was chemically fragmented before reverse transcription and cDNA generation. Next, conducting the end-repair process of the cDNA fragments, we added a single 'A' base to the 3' end, and afterwards the adapters were ligated. Finally, we purified the products and enriched them with PCR to compile the final indexed double-stranded cDNA library. We checked the quality of the libraries using a Bioanalyzer 2100, High Sensitivity assay. The quantity within the libraries was assessed by real-time PCR in LightCycler 480 (Roche). Before cluster generation in cbot (Illumina), we performed an equimolar pooling of the DNA libraries and then sequenced the pool using paired-end sequencing (100 x 2) with an Illumina HiSeq 2000 sequencer. We ordered RNA-seq analysis to Sistemas Genómicos (Valencia, Spain). We sequenced 3 independent biological replicates per sample, each replicate consisting of an equilibrated pool of 3 RNAs.

Quality control checks of raw sequencing data were performed with FastQC 0.11.7. The generated reads were cleaned using the Trimgalore 0.6.2 method (http://www.bioinformatics.babraham.ac.uk/projects/trimgalore/).
Subsequently, all samples were combined, and the complexity of the reads was reduced by removing duplicates and low-quality reads using Picard tools 2.9.2 and Samtools 1.9 algorithms (Li et al., 2009) (>Q20). Reads were mapped to the *Olea europaea* var. sylvestris genome as the reference [*Olea europaea* var. sylvestris Annotation Report (nih.gov)]. Each sample was then mapped with the latest bowtie2 2.3.3 version (Langmead and Salzberg, 2012).

The reads of good quality (Phred > 20) were selected to increase the resolution of the count expression. Finally, the expression inference was evaluated by means of the count of properly paired end reads by transcript.

2.4. Differential expression

For the study of differential gene expression and normalization gene expression using library size, the DESeq 1.36 algorithm was used (Love, 2014). This method is based in a negative binomial distribution. The genes with a fold change of less than -2 or greater than 2, and a p adjust by FDR<0.05 were considered differentially expressed (Benjamini and Hochberg, 1995). A functional enrichment study was performed using the information obtained from pFam and uniprot database. This study is based on a hypergeometric distribution using the statistical software R. The principal-component analysis (PCA) was analyzed using the methods described in DESeq using the normalize counts of gene expression obtain from this method. Differential expression was made for each comparison. Then, specific gene expression each comparison was obtained using venn diagram (https://bioinfogp.cnb.csic.es/tools/venny/). KEGG data was accessed using AnnotationHub (Yu et al., 2012; Morgan and Shepherd, 2019). The RNA-seq results by qRT-PCR were validated as indicated in Briegas et al. (2020). The primers employed are shown in Table I.S1. ClustalW (Thompson et al., 1994) in MEGA11 software (http://www.megasoftware.net) was used to align the protein sequences.

2.5. Quantification of plant hormones

We used a pool of 100-mg fresh weight/sample for each measurement split into 3 independent biological replicates per sample. The plant hormones were quantified as described by Briegas et al. (2020).

3. Results

3.1. Morphological and cytological changes during early fruit development in olive

To explore the early fruit development in olive, we monitored weight, longitudinal and equatorial diameters, and size of cells in an olive cultivar 'Picual' with large sized and elongated fruits. As shown in Figure I.1, the olive fruit, after ovule fertilization (concomitant with anthesis), showed a highly reproducible growth progression in terms of increases in weight, longitudinal and equatorial diameters, index shape, and growth rate up to 42 DPA, followed by a period of endocarp lignification for fruit under the experimental conditions used (Figure I.1A-F). Immediately following fertilization, the developing fruits grew more in length than in width (Figure I.1C,D), resulting in an increase in the fruit-shape index (Figure I.1E). This trend is characteristic of the elongated fruit shape of 'Picual' olive, and consequently its fruit size/weight augmented 128-fold (± 6.0) from anthesis to 42 DPA. Greater cell size was apparent in both the epicarp and mesocarp (pericarp) cells of the fruit during the early stages (0-42 DPA) (Figure I.1H-I). In fact, the epicarp- and mesocarp-cell area in the pericarp of one ovary at anthesis increased 5- and 13-fold, respectively, in the developing fruit at 42 DPA. Pericarp cells expanded at similar rates (cell area/day) for 21 DPA. From 21 to 28 DPA, cell expansion in the pericarp was dramatic, with the cell expansion rate doubling up to 42 DPA. Variations in pericarp thickness were linked mainly to variations in mesocarp cell size (Figure I.1G-I). Thus, the 128-fold increase in olive fruit weight up to 42 DPA was related to a 7-fold increase in longitudinal diameter, a 5-fold increase in equatorial diameter, and a 13-fold increase in mesocarp cell size.

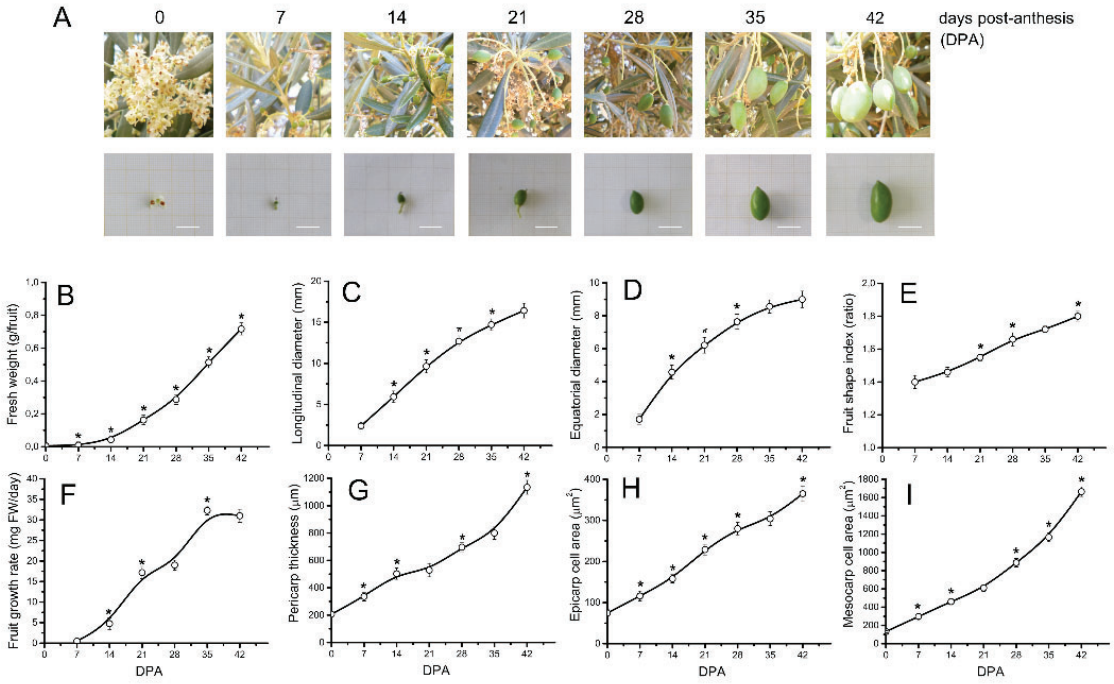

Figure I.1. Growth of 'Picual' olive fruits. (A) Morphological changes of olive fruit during early fruit development. Increase in 'olive fruit length and diameter as a function of days post anthesis (DPA). (B) Changes in fresh weight (FW) (g fruit^{-1}), (C) longitudinal diameter (mm), (D) equatorial diameter (mm), (E) fruit-shape index, (F) growth rate (mg FW day^{-1}), (G) pericarp thickness (mm), (H) epicarp cell size (µm^2) and (I) mesocarp cell size (µm^2) of developing olive fruit at 0, 7, 14, 21, 28, 35, and 42 DPA. Fruit-shape index is length-to-width ratio of the fruit. The cell area of fruit mesocarp and epicarp cells was measured during early fruit development (staining was with Calcofluor White) using confocal microscopy. Asterisks indicate statistically significant changes based on unpaired Student's *t* test ($P<0.05$) from the preceding point. Data are means ± SE ($n \geq 20$). Scale bar 10 mm. DPA: Days Post-Anthesis.

3.2. Ploidy level during fruit early development in olive

Cell division during early olive fruit development was characterized by flow cytometric analysis of the nuclear-DNA contents from 0 to 42 DPA (Figure I.2). At anthesis (0 DPA) and the 7 DPA stage, most of the nuclei were 2C (88% and 65.2% of total nuclei, respectively) and only a low proportion of endoreduplicated nuclei >4C was found (0.8 % and 1.3 % of total nuclei; respectively, Figure I.2).

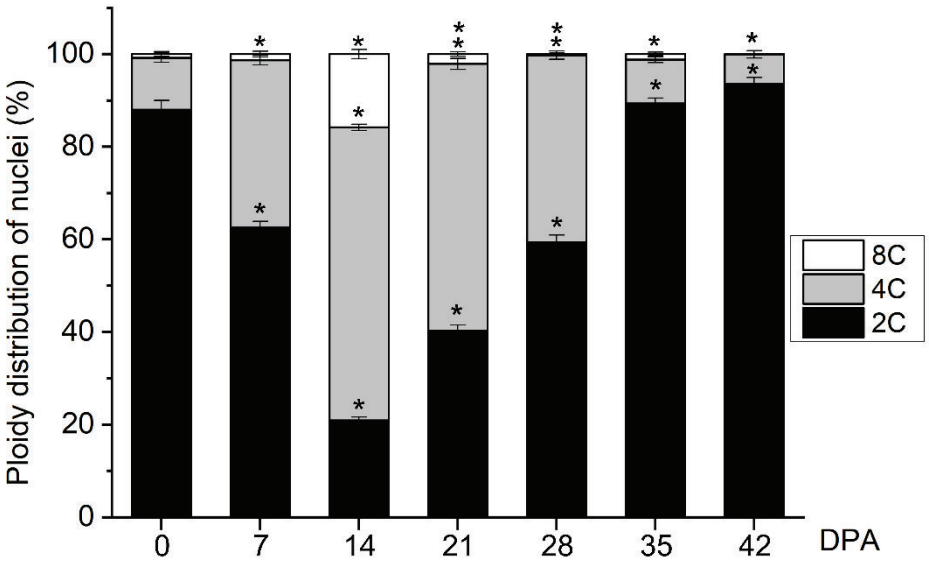

Figure I.2. Nuclear ploidy levels from olive fruits during early development. The percentage of nuclei in 2C, 4C, and 8C are shown from 0 to 42 DPA in the developing fruits. Each point is the average of four samples. Asterisks denote significant differences based on unpaired Student's *t* test ($P < 0.05$) from the preceding point and bars are ± SE.

From 0 to 14 DPA, the proportion of 4C cells increased with time, while the proportion of 2C cells decreased in olive fruits. At 14 DPA, an early stage of fruit development, 4C cells represented the highest proportion of cells in the olive fruits (63.2%) indicating intensive cell division, while the proportion of 8C cells increased in comparation to that in fruits at 7 DPA (1.3% and 15.8% of total nuclei at 7 and 14 DPA, respectively, Figure I.2). Given that the 4C nuclei population involves not only mitotic diploid cells in the G2/M phase (4C) as well as tetraploid endoreduplicated cells (4n), it was assumed that the nuclei displaying higher ploidy levels (>4C) occur exclusively by endoreduplication (i.e. successive cycles of DNA replication without mitosis) (Breuer et al., 2010). A population of 8C cells observed in olive fruit at 14 DPA could indicate that an initial cell division phase was associated with endoreduplication activity in olive fruit at this time. By contrast, at 28 DPA, cell division was not activated in the fruits based on the increased ratio of 2C to 4C DNA levels relative to that at 21 DPA (Figure I.2). The 2C cells represented 40.3% and 59.4% of the cells, and the 4C cells represented 57.6% and 40.4% of the cells in the fruits at 21 and 28 DPA, respectively. The 8C cells represented 2.1% and 0.3% of the cells in the fruits at 21 and 28 DPA,

respectively. From 28 to 42 DPA, most of the nuclei were 2C (59.39, 89.3%, and 93.5% of total nuclei of fruits at 28, 35, and 42 DPA, respectively), while only a low proportion of 4C and 8C nuclei was detected in these fruits (Figure I.2). Thus, the results show that the maximal proportion of 4C cells (63.1%), which is an indirect estimate for cell division, in olive fruits was reached 14 DPA, indicating that intense cell division was activated in the fruits at this time.

3.3. Overall transcriptional changes during early fruit development in olive

Based on our cytological and ploidy analyses of early fruit development (Figures I.1-2), to ascertain the molecular mechanism of early fruit growth in olive, we compared the transcriptome, using RNA-seq, of whole 'Picual' olive fruit at selected stages of early fruit development: 0 DPA (P0, anthesis, fruit set), 14 DPA (P14, cell division, mostly dividing cells) and 28 DPA (P28, post-mitotic cell expansion, mostly expanding cells). The use of these three samples (P0, P14, and P28) of developing 'Picual' olive fruit, which represent critical physiological changes during early fruit development, allowed the preferential identification of post-mitotic cell expansion related genes (Figure I.3A).

The RNA-Seq analysis averaged 40 million reads per sample, of which 78% mapped to the 132,819 annotated transcripts from the *Olea europaea* var. *sylvestris* reference genome. From the three olive samples, we performed a PCA using transformed read counts (see Methods). The three biological replicates for each sample clustered together, thus indicating that the expression levels among replicated samples were closely associated (Table I. S2, Figure I.S1). A total of 24,168 differentially expressed genes (DEGs) related to early fruit development in olive were identified (Figure I.3B, Tables I.S3-S6). Among the 24,168 DEGs, 16,943 genes were development responsive in the first comparison (between the fruit at 14 DPA and 0 DPA, P14 vs. P0), and 7,225 were development responsive in the second comparison (between fruit at 28 DPA and 14 DPA, P28 vs. P14) (Figure I.3B, Tables I.S3-S6).

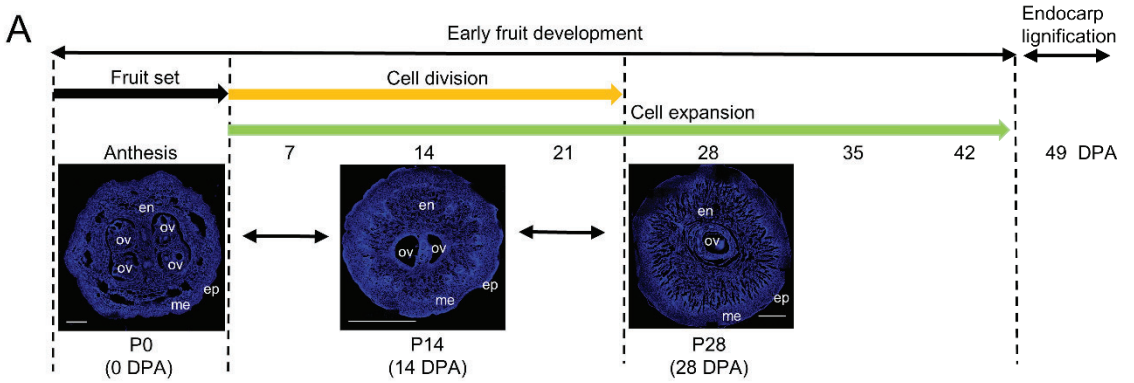

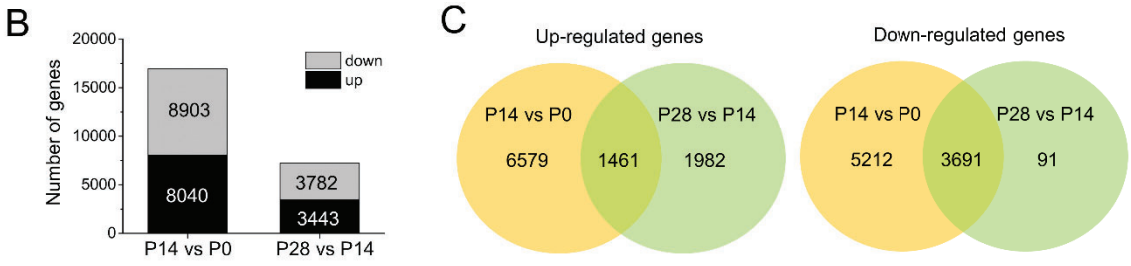

D

Specific genes at anthesis (fruit set)

LOC111402396	subtilisin-like protease SBT5.4
LOC111374547	stress-induced protein KIN2-like
LOC111402646	auxin-responsive protein SAUR50-like
LOC111365791	ethylene-responsive transcription factor WIN1-like
LOC111380840	E3 ubiquitin-protein ligase MIEL1-like
LOC111370065	sodium/calcium exchanger NCL1-like
LOC111381330	protein IQ-DOMAIN 1-like, transcript variant X3
LOC111396530	transcription factor IBH1
LOC111367290	transcription factor bHLH87, transcript variant X2
LOC111401715	vignain-like
LOC111411160	WAT1-related protein At1g09380-like
LOC111376679	probable E3 ubiquitin-protein ligase BAH1-like
LOC111402520	ABC transporter G family member 9
LOC111367772	COP1-interactive protein 1-like, transcript variant X2
LOC111383887	cellulose synthase-like protein D4

Specific genes at 14 DPA (cell division phase)

LOC111399703	subtilisin-like protease SBT4.15
LOC111399011	aspartic proteinase CDR1-like
LOC111391077	ethylene-responsive transcription factor ERF110-like
LOC111390480	transcription factor MYB8-like
LOC111385282	beta-galactosidase 14-like
LOC111404076	laccase-7-like
LOC111398706	EG45-like domain containing protein
LOC111397047	MADS-box protein SOC1-like, transcript variant X4
LOC111407314	probable WRKY transcription factor 35
LOC111393013	MADS-box protein AGL42-like, transcript variant X6
LOC111396190	NAC transcription factor 29-like
LOC111377905	hexose carrier protein HEX6-like
LOC111392847	protein LITTLE ZIPPER 3-like
LOC111396650	FAM10 family protein At4g22670-like, transcript variant X2
LOC111398732	LRR receptor-like serine/threonine-protein kinase GSO1

Specific genes at 28 DPA (cell expansion phase)

LOC111389777	chorismate synthase 2, chloroplastic-like
LOC111411422	dirigent protein 15-like
LOC111377292	putative expansin-B2
LOC111365434	cytochrome c oxidase subunit 6a, mitochondrial-like

Figure I.3. Design of RNA-seq analysis and olive fruit genes during early fruit development. (A) Cross-sections of ovaries at anthesis stage (P0) and developing fruits at 14 DPA (P14) and 28 DPA (P28) used in RNA-seq analysis. Micrographs showing changes in fruit surface during early fruit development, stained with Calcofluor White. Calcofluor White staining of cellulose indicated the cell wall; en endocarp, ep epicarp, me mesocarp, ov ovule. Scale bar 50 μm in P0, and 500 μm in P14 and P28. (B) Distribution of genes differentially expressed during early fruit development (P14 vs. P0, and P28 vs. P14 comparisons). (C) Overlap of up-regulated and down- regulated fruit genes during early olive fruit development. This figure shows that 1461 were up-regulated in both comparisons and that 3691 were down-regulated in both comparisons. (D) Specific genes differentially expressed during early fruit development. Top 15 genes at anthesis (P0), and at 14 DPA (P14).

In the first comparison (P14 vs. P0), 8,040 genes were up-regulated, and 8,903 were down-regulated in fruit at 14 DPA. In the second comparison (P28 vs. P14), 3,443 genes were up-regulated, and 3,782 were down-regulated in fruit at 28 DPA (Figure I.3B, Tables I.S3-S6). A comparison of the genes which were development responsive during early fruit development indicated that 1,461 were up-regulated in both comparisons, and that 3,691 were down-regulated in both comparisons (Figure I.3C, Tables I.S7-S8). Thus, most of the 24,168 DEGs display a distinct temporal expression consistent with the succession of the different phases of early fruit development (Figure I.3C, Tables I.S3-S6).

Additionally, we identified 162 transcripts could be considered as fruit-set specific (specific genes at anthesis) among the transcripts expressed in the fruit at 0 DPA (fruit set) since they were not detected in other fruit development stages analysed (Table I.S9), including homologues of stress, cell wall, transport, cell division, transcription factor (TF) and hormone-related genes. An appreciable proportion (almost 30%) of them encode proteins with unknown functions or present no homology with any known genes. Similarly, among the transcripts expressed in the olive fruit at 14 DPA (mostly dividing cells), 67 transcripts could be considered to be cell division specific (specific genes at 14 DPA) (Table I.S9). These mainly included genes involved in cell growth processes such as cell wall synthesis and modification, sugar and organic acid transport and metabolism, and hormonal metabolism and signaling. Particularly evident was the transition between 14 and 28 DPA. Among the transcripts expressed in the fruit at 28 DPA (post-mitotic cell expansion), only four transcripts (*CS2*, *DIR15, EXPB2* and *cox-6A*) could be considered to be cell expansion specific (specific genes at 28 DPA) since they were not detected in other fruit-development stages analysed (Table I.S9): (1) *CS2* coding for chorismate synthase 2 protein controlling a key step in the shikimate pathway and catalyses the transformation of 5-enolpyruvylshikimate 3-phosphate to chorismate, which serves as the initiator metabolite for the synthesis of aromatic amino acids and secondary metabolites (the pathway 'phenylalanine, tyrosine, and tryptophan biosynthesis' and other pathways) (Macheroux et al., 1999); (2) *DIR15* coding for dirigent protein 15-like protein which is involved in cell wall metabolism (Paniagua et al., 2017); (3) *EXPB2* coding for the expansion of B2 protein, which is involved in cell expansion and other developmental events during

which cell wall modification occurs (Kende et al., 2004); and (4) *cox-6A* coding for cytochrome c oxidase subunit 6a protein, involved in the pathway oxidative phosphorylation, which is part of energy metabolism (Fontanesi et al., 2008).

Moreover, to validate our RNA-seq results, we performed qRT-PCR to determine the levels of *OeCS2*, *OeDIR15*, *OeEXPB2,* and *Oecox-6A* expression across the three samples, which showed exclusively a significant expression level in the fruit at 28 DPA (Figure I.S2). Thus, the evidence for *CS2*, *DIR15, EXPB2* and *cox-6A* gene expression exclusively in the expanding fruit at 28 DPA, where they are presumed to allow fruit growth by starting the synthesis of aromatic metabolites and the endocarp lignification as well as modifying cell wall properties, suggests that CS2, DIR15, EXPB2 and cox-6A could play a role in post-mitotic cell expansion mechanisms, after cell division arrest, during early olive fruit growth. Thus, we identified a large number of specific genes, implying that they may play unique roles in the different developmental phases. They were considered to be prime candidates for further molecular research on the programmes of cell division and expansion in olive fruit and their regulation.

3.4. Gene ontology functional enrichment analysis of differentially expressed genes

To gain an overall view concerning the functions and processes altered during early olive fruit development, we classified the DEGs using the Gene Ontology (GO) database. Furthermore, we assigned GO accessions to the DEGs based on similar sequences in known proteins available in the UniProt database in addition to InterPro as well as the Pfam domains that these contain. To study the function of DEGs, we focused on the common and specific DEGs at different developmental stages. We found several GO classifications to be over-represented in genes having greater or lesser transcript accumulation during early olive fruit development. The GO terms 'Transcription', 'ATP binding', and 'Integral component of membrane' were most represented among the categories of biological processes (Figure I.4, Tables I.S10-S13), molecular functions (Figure I.5, Tables I.S10-S13), and cell components (Figure I.6, Tables I.S10-S13), respectively.

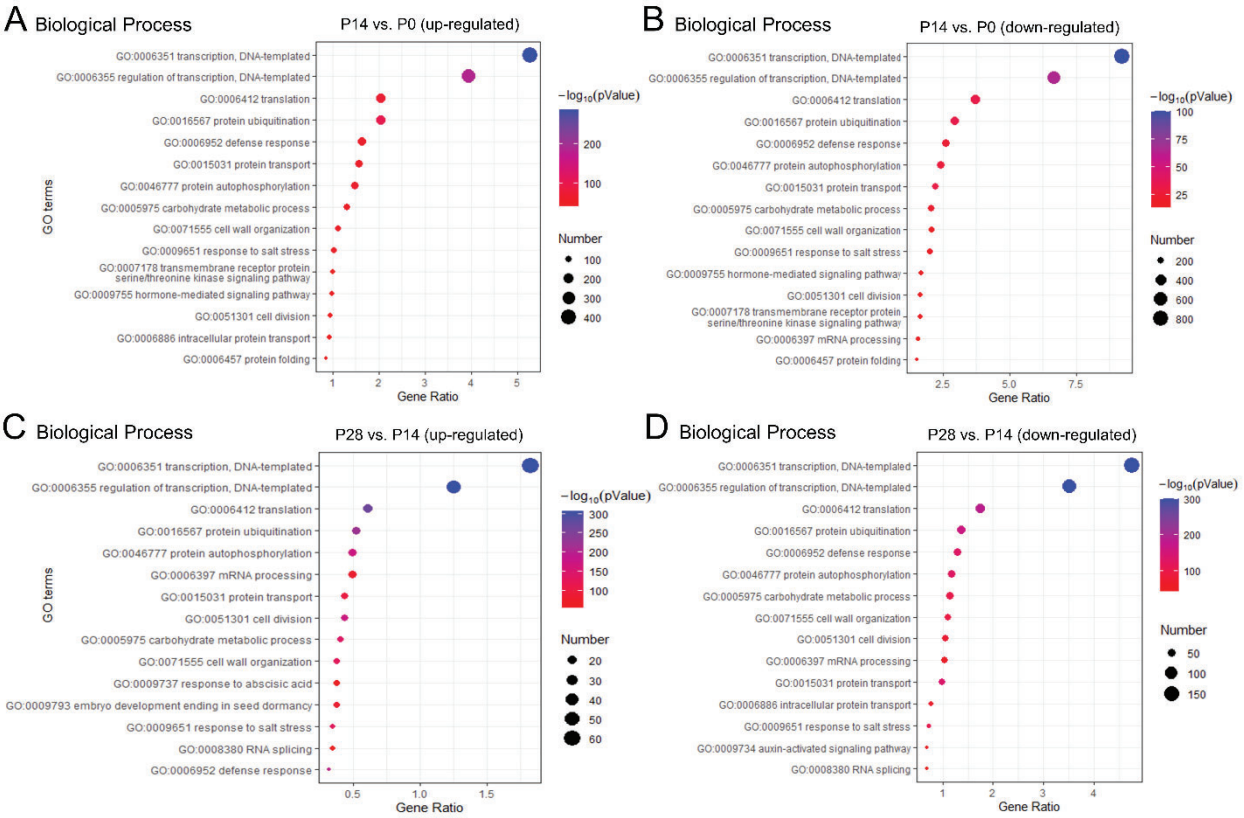

Figure I.4. Functional analysis of DEGs during early olive fruit development. The enrichment analysis of GO 'biological process' terms based on DEGs in the olive flowers at anthesis stage (P0), and the developing fruits at 14 (P14) and 28 (P28) DPA. (Top 15). (A) Bubble Plot of GO 'biological process' terms in the GO annotations of the genes of the 8040 transcripts with increased transcript accumulation, (B) and of the genes of the 8903 transcripts with decreased transcript accumulation in the P14 vs. P0 comparison; and (C) Bubble Plot of GO 'biological process' terms in the GO annotations of the genes of the 3443 transcripts with increased transcript accumulation, and (D) of 3782 transcripts with decreased transcript accumulation in the P28 vs. P14 comparison. The Y-axis and X-axis denote GO name and gene ratio, respectively. The colour of each bubble represents -$\log_{10}$ (p value), and each bubble size represents the count of DEGs. Additional information is presented in Tables I.S10-S13.

Within the 'Biological process' category, a number of GO classifications proved to be over-represented in genes which had augmented transcript accumulation in fruit at 14 DPA versus 0 DPA (Figure I.4A). The over-represented group in the dividing olive fruit (14 DPA) having the greatest

number among the DEGs was 'Regulation of transcription', 'Translation', 'Protein ubiquitination', 'Defense response', 'Protein transport', 'Protein autophosphorylation', 'Carbohydrate metabolic process', 'Cell wall organization', 'Response to salt stress', 'Transmembrane transport', 'Hormone-mediated signaling pathway', and 'cell division' (Figure I.4A).

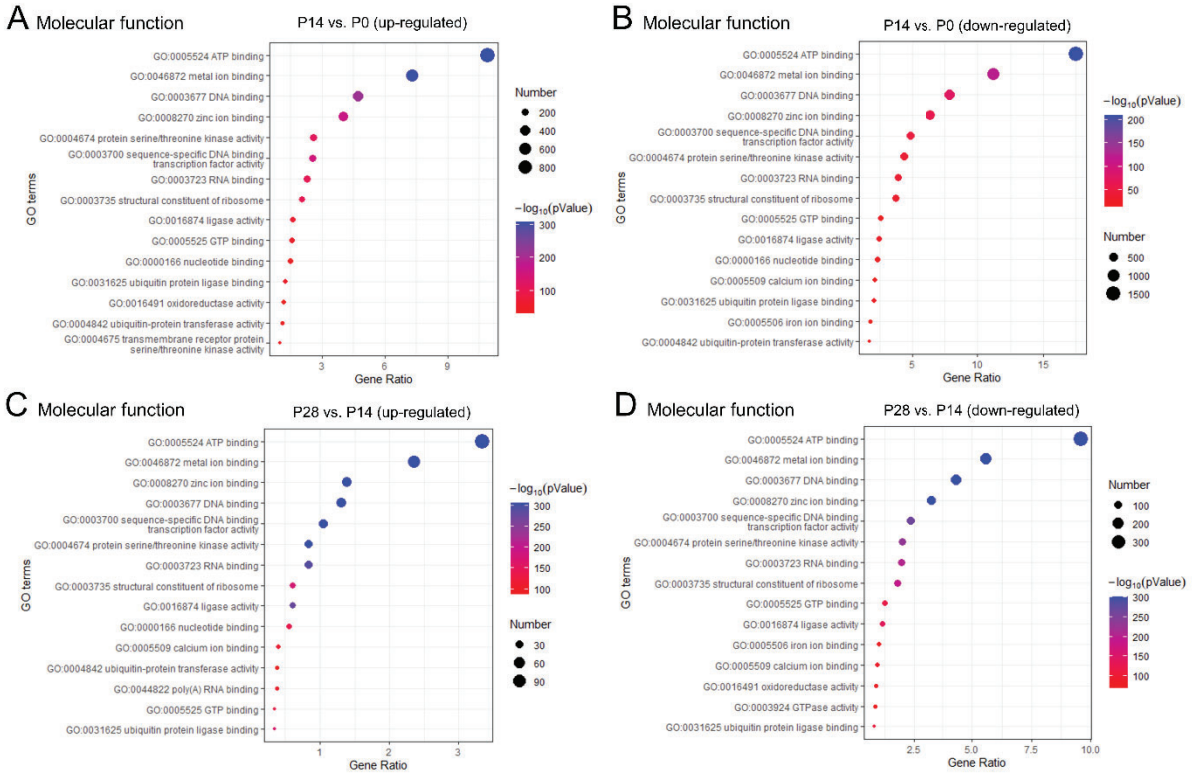

Figure I.5. Functional analysis of DEGs during early fruit development in olive. The Top 15 enrichment analysis of GO 'molecular function' terms based on DEGs in olive flowers at anthesis stage (P0), and the developing fruits at 14 (P14) and 28 (P28) DPA. (Top 15). (A) Bubble Plot of GO 'molecular function' terms in the GO annotations of the genes of the 8040 transcripts with increased transcript accumulation, (B) and of the genes of the 8903 transcripts with decreased transcript accumulation in the P14 versus. P0 comparison; and (C) Bubble Plot of GO 'molecular function' terms in the GO annotations of the genes of the 3443 transcripts with increased transcript accumulation, and (D) of 3782 transcripts with decreased transcript accumulation in the P28 versus. P14 comparison. The Y-axis and X-axis denote GO name and gene ratio, respectively. The color of each bubble represents -$\log_{10}$ (p value), and each bubble's size of represents the count of DEGs. Additional information is presented in Tables I.S11-S14.

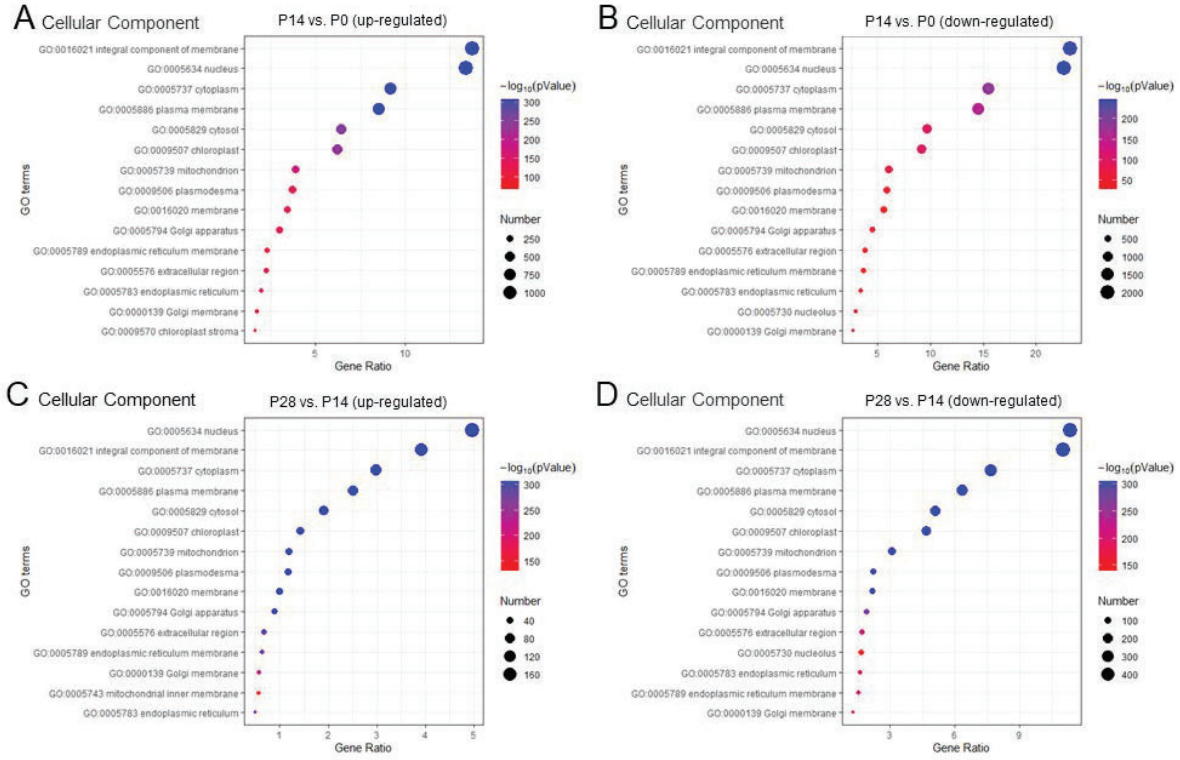

Figure I.6. Functional analysis of DEGs during early fruit development in olive. The Top 15 enrichment analysis of GO 'cellular component' terms based on DEGs in olive flowers at anthesis stage (P0), and the developing fruits at 14 (P14) and 28 (P28) DPA. (Top 15). (A) Bubble Plot of GO 'cellular component' terms in the GO annotations of the genes of the 8040 transcripts with increased transcript accumulation, (B) and of the genes of the 8903 transcripts with decreased transcript accumulation in the P14 versus. P0 comparison; and (C) Bubble Plot of GO 'cellular component' terms in the GO annotations of the genes of the 3443 transcripts with increased transcript accumulation, and (D) of 3782 transcripts with decreased transcript accumulation in the P28 versus. P14 comparison. The Y-axis and X-axis denote GO name and gene ratio, respectively. The color of each bubble represents -$\log_{10}$ (p value), and each bubble's size of represents the count of DEGs. Additional information is presented in Tables I.S11-S14.

Remarkably, the expanding olive fruit (28 DPA) also bore a significant representation of transcripts associated with 'Regulation of transcription', 'Translation', 'Protein ubiquitination', 'Protein autophosphorylation', 'mRNA processing', 'Protein transport', 'Cell division', 'Carbohydrate metabolic process', and 'Cell wall organization' (Figure I.4C). Thus, GO terms including 'Regulation of transcription', 'Protein ubiquitination', 'Protein autophosphorylation', 'Protein transport', 'Carbohydrate metabolic process'

and 'Cell wall organization' were enriched in both lists of genes (Figure I.4), indicating that the same biological processes might necessitate different gene sets in different phases during early fruit development in order to support their activities.

Marked differences were nevertheless detected between the two lists of enriched GO terms. That is, GO terms associated with the 'Regulation of cell cycle', 'Regulation of cell shape', 'Regulation of growth', 'Positive regulation of GTPase activity', 'Cell redox homeostasis', and 'Response to cadmium ion' were strongly enriched in the genes most highly expressed in the dividing olive fruit at 14 DPA compared to the fruit at 0 DPA (Tables I.S10-S13). Meanwhile differences with respect to other enriched GO terms included 'mRNA splicing' and 'Transmembrane receptor protein serine/threonine kinase signaling pathway', which underwent enrichment in genes of higher expression in the expanding fruit at 28 DPA at with the dividing fruit at 14 DPA (Tables I.S10-S13), suggesting that such biological processes may be associated with distinctions in cell division/expansion.

In an effort to trace back to the pathways, such as 'Oxidative phosphorylation', 'Tryptophan metabolism', 'Pentose and glucuronate interconversions', and 'Spliceosome' (Figures I.7-I.10), which were closely involved in the transition between 0 and 14 DPA, the whole DEGs set was examined through the Kyoto Encyclopedia of Genes and Genomes (KEGG).

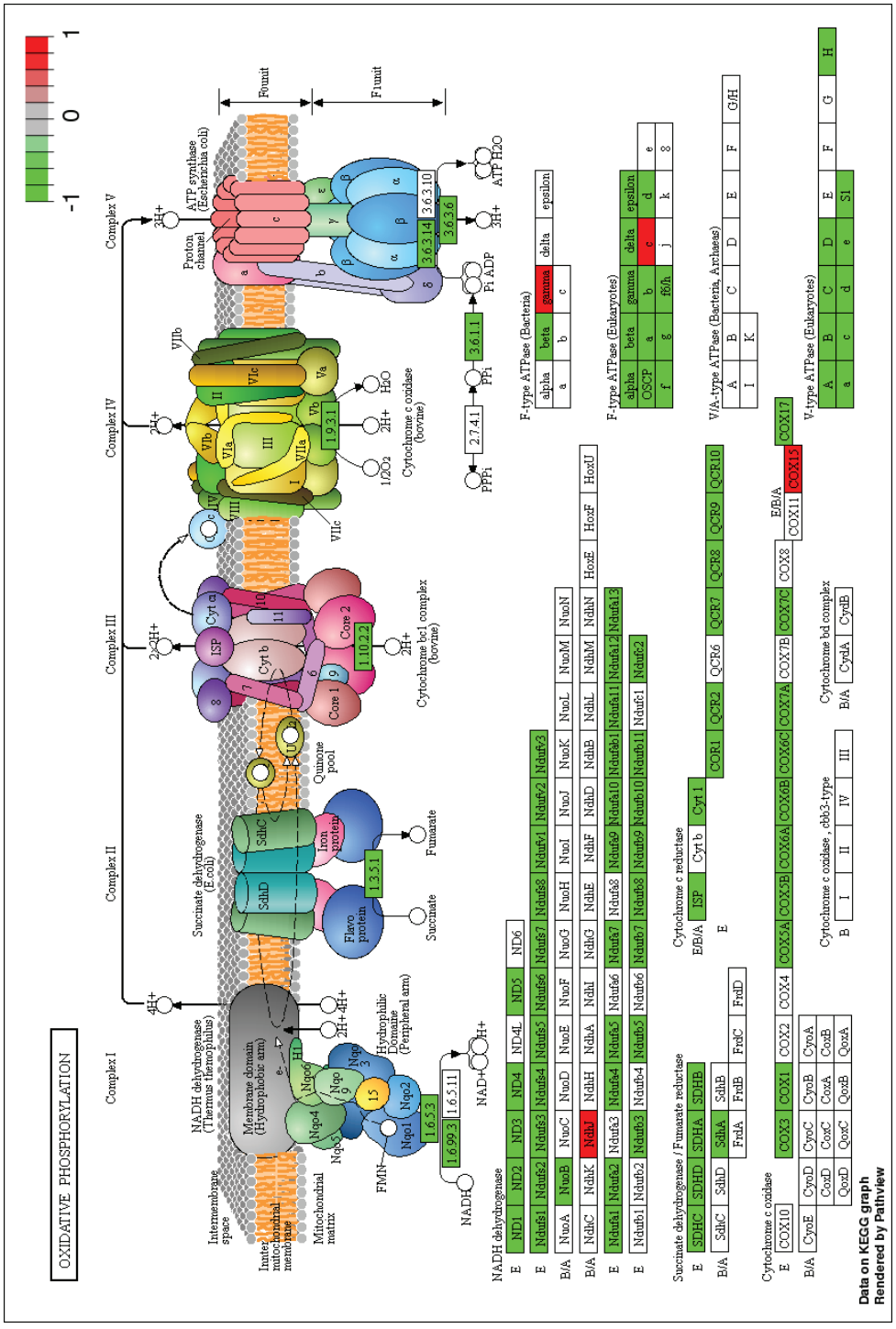

Figure I.7. Graphic representation of the oxidative phosphorylation pathway by KEGG. Boxes colored in red or green represent the EC number of the enzymes encoded by up- or down-regulated genes in the P14 versus P0 comparison (fruit at 14 DPA versus fruit at 0 DPA), respectively, generated by this study that are homologous to genes involved in the oxidative phosphorylation pathway.

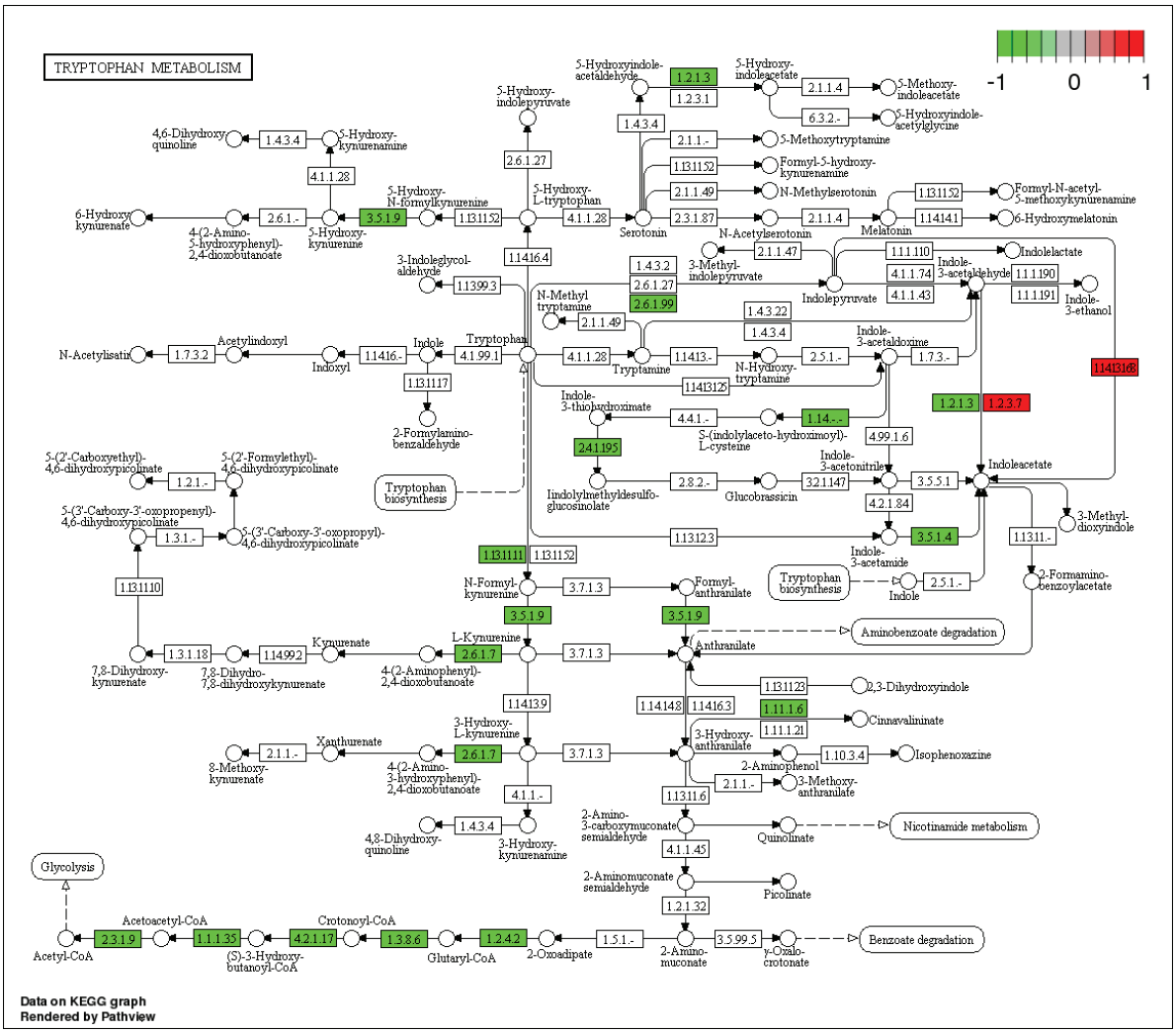

Figure I.8. Graphic representation of the tryptophan metabolism pathway by KEGG. Boxes colored in red or green represent the EC number of the enzymes encoded by up- or down-regulated genes in the P14 versus P0 comparison (fruit at 14 DPA versus fruit at 0 DPA), respectively, generated by this study that are homologous to genes involved in the tryptophan metabolism pathway.

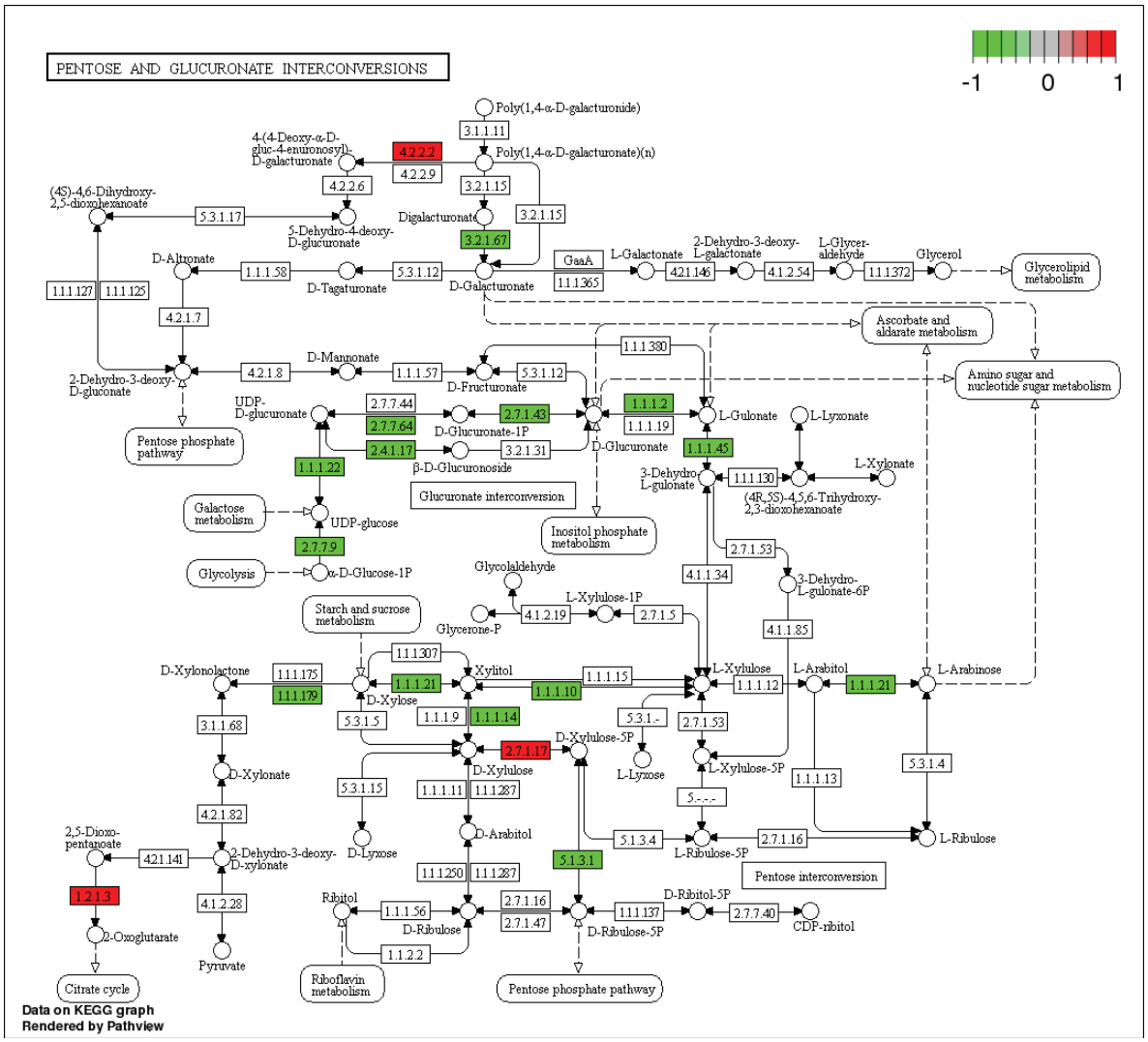

Figure I.9. Graphic representation of the pentose and glucuronate interconversions pathway by KEGG. Boxes colored in red or green represent the EC number of the enzymes encoded by up- or down-regulated genes in the P14 versus P0 comparison (fruit at 14 DPA versus fruit at 0 DPA), respectively, generated by this study that are homologous to genes involved in the pentose and glucuronate interconversions pathway.

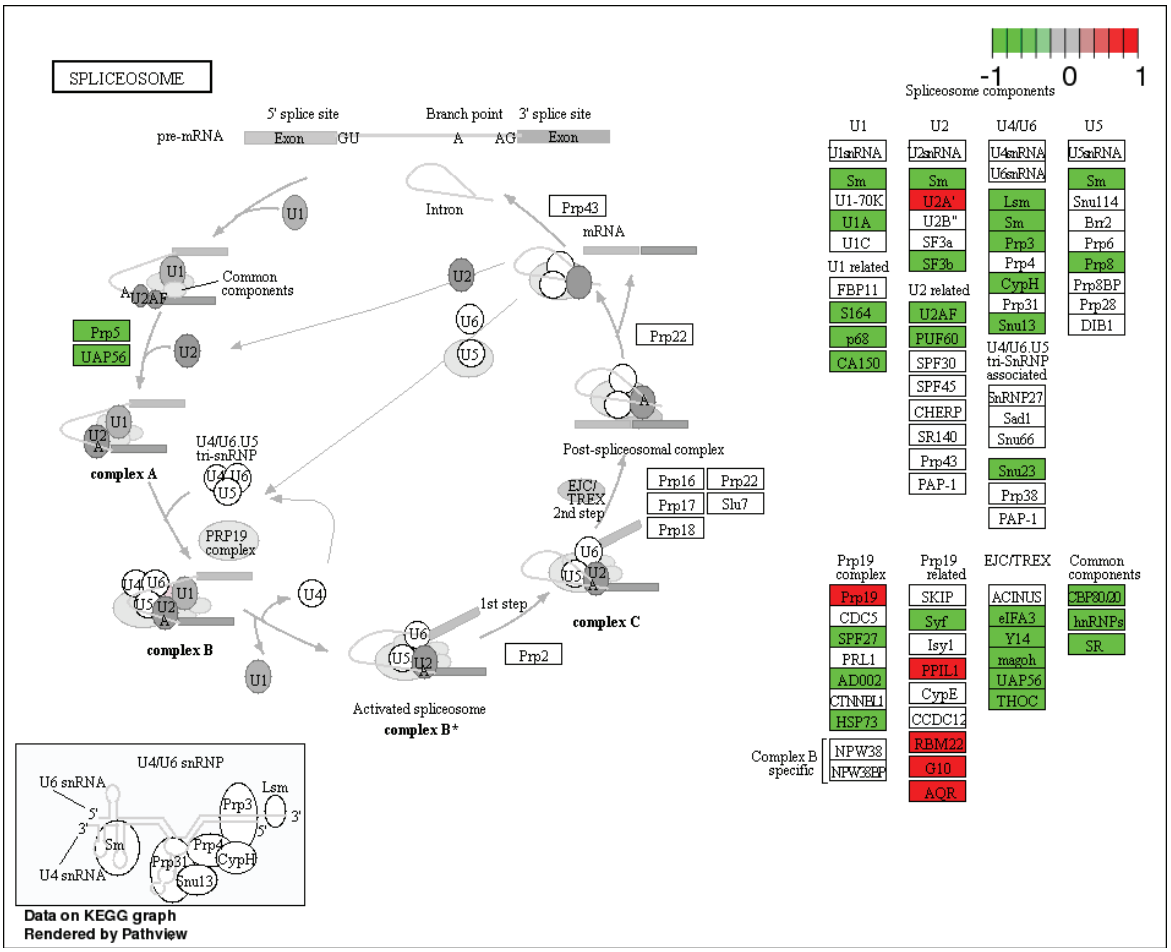

Figure I.10. Graphic representation of the spliceosome pathway by KEGG. Boxes colored in red or green represent the EC number of the enzymes encoded by up- or down-regulated genes in the P14 versus P0 comparison (fruit at 14 DPA versus fruit at 0 DPA), respectively, generated by this study that are homologous to genes involved in the spliceosome pathway.

Likewise, this also revealed significantly enriched pathways in the transition between 14 and 28 DPA: endocytosis (Figure I.S3), protein processing in endoplasmic reticulum (Figure I.S4), cell cycle (Figure I.S5), plant hormone signal transduction (Figure I.S6), zeatin biosynthesis (Figure I.S7), porphyrin and chlorophyll metabolism (Figure I.S8), phenylalanine, tyrosine and tryptophan biosynthesis (Figure I.S9), purine metabolism (Figure I.S10), pyrimidine metabolism (Figure I.S11), fructose and mannose metabolism (Figure I.S12), galactose metabolism (Figure I.S13), fatty acid biosynthesis (Figure I.S14), and valine, leucine, and isoleucine degradation (Figure I.S15).

3.5. Characterization of cell cycle-related genes associated with early fruit development in olive

An examination of our current data set corroborates the development-induced accumulation of transcripts presumably participating in the basic cell cycle machinery, including DEGs that encode cyclins (CYC, 48 genes), cyclin-dependent kinases (CDKs, 8 genes), CDK inhibitor proteins (CKIs, 10 genes), homologues of the retinoblastoma (RB) protein (2 genes), and the E2F TFs (4 genes) during early olive fruit development (Figures I.11-12, Table I.S14).

CYCs, the regulatory subunits of their respective CDKs, constitute major components in the cell cycle progression machinery. In fact, certain cyclins are discontinuously expressed over the cell cycle, as their synthesis as well as their degradation prove strictly programmed (Bulankova et al., 2013). This raises the question as to whether the intense cell division phase during early olive fruit development involves the utilization of specific cyclins. A total of 48 cyclins were included in our data set and were retained for further phylogenetic analysis, of which 5 are A-type, 4 are B-type, 2 are C-type, 16 are D-type, 2 are L-type and 2 are U-type cyclins (Figure I.11C, Table I.S14). Among the 48 genes, 16 (3 A-type, one B-type, 6 D-type, one L-type and one U-type cyclins) were up-regulated exclusively in olive fruit at 14 DPA compared with 0 DPA (P14 vs. P0 comparison), and 5 (one C-type, 3 D-type, and one U-type cyclins) were up-regulated exclusively in olive fruit at 28 DPA compared with 14 DPA (P28 vs. P14 comparison), whereas 16 genes (2 A-type, 3 B-type, one C-type, 7 D-type, one L-type cyclins and 2 cyclin 2-like) were up-regulated in both comparisons (Figure I.11A,B). Among the latter, the most abundant proved to be a CYCD3;1 and a CYCD6;1 proteins.

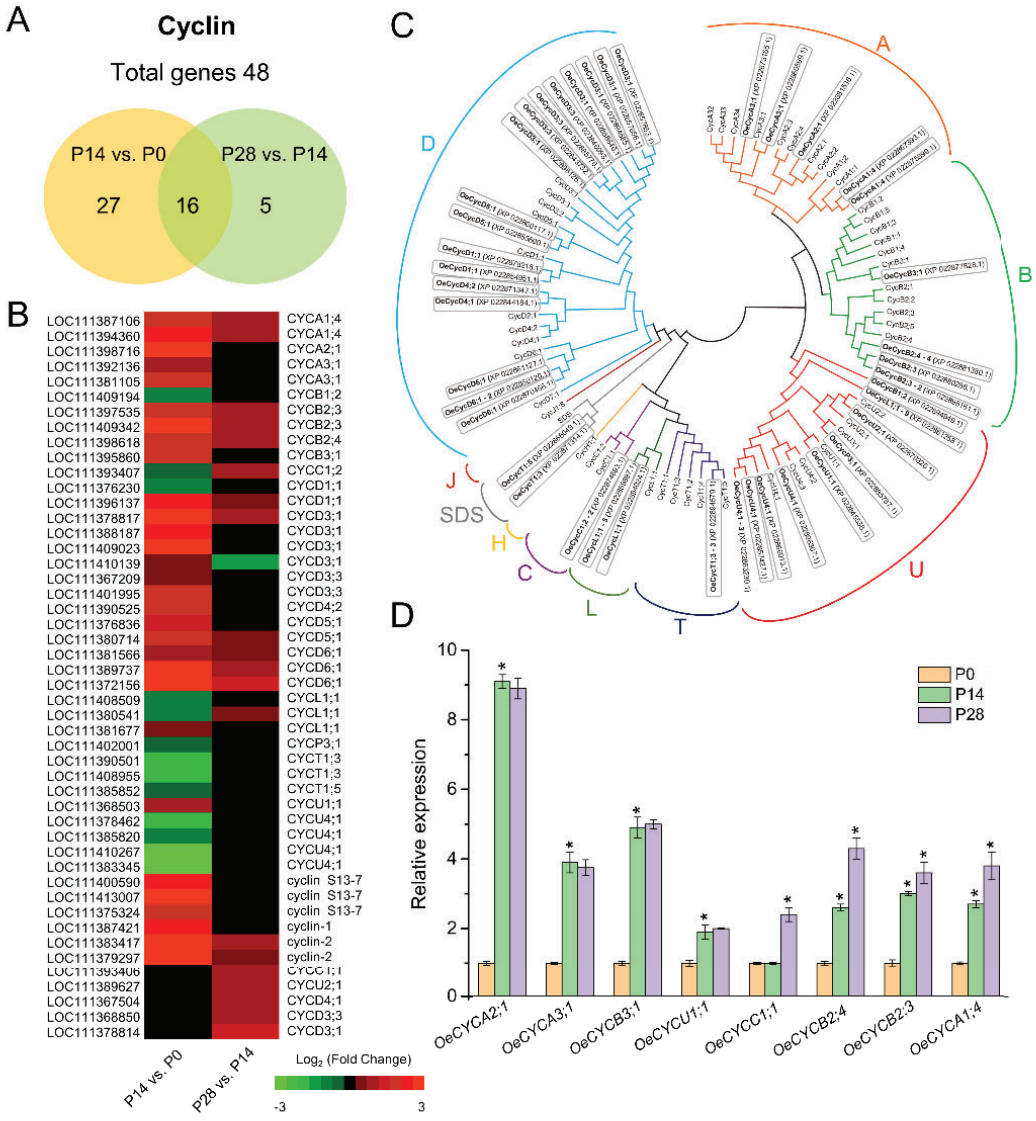

Figure I.11. Differential gene expression of *CYC* genes during early olive fruit development. (A) Venn diagram showing numbers of overlapping *CYC* genes in both the fruit at 14 DPA (P14) versus fruit at 0 DPA (P0), and in the fruit at 28 DPA (P28) versus fruit at 14 DPA (P14) comparisons. (B) Expression values are represented in a heatmap as Log_2 Fold Change in the P14 versus P0 comparison, and the P28 versus P14 comparison, and the colour key is indicated at the bottom. (C) Phylogenetic analysis of olive *CYC* with other *CYC* genes. The sequences included in this alignment are from olive (*Olea europaea* var. sylvestris Annotation Report; https://www.ncbi.nlm.nih.gov/genome/annotation euk/Olea europaea var. sylvestris/100/), and Arabidopsis (http://www.arabidopsis.org/). The CYC proteins studied from our work are enclosed in an open box. (D) Expression of 8 selected CYC genes in olive fruits at 0 (P0), 14 (P14) and 28 (P28) DPA. Analysis of transcript levels of genes by quantitative RT-PCR. Genes and their primers are shown in Table I.S1.

Relative expression values were normalized to the lowest expression value taken as 1. The data represent the mean values (±SEs) of duplicate experiments from three independent biological samples. Statistical significance compared with the preceding point was determined using Student's *t test*. *P< 0.05. Additional information on the *CYC* genes is presented in Table I.S14.

Additionally, our data demonstrated that 11 cyclins genes (one B-type, one D-type, one L-type, one P-type, 3 T-type, and 4 U-type cyclins) were down-regulated in the olive fruit at 14 DPA compared with 0 DPA, and only one cyclin gene (D-type) was exclusively down-regulated in the olive fruit at 28 DPA compared with 14 DPA, whereas 2 (one C-type and one L-type cyclin) were down-regulated exclusively in olive fruit at 28 DPA compared with 14 DPA (P28 vs. P14 comparison) (Figure I.11, Table I.S14). Moreover, differences in expression among different A-type (A1 vs. A2 and A3) cyclins and different B-type (B2 vs. B3) cyclins during early fruit development make it possible to discriminate olive fruits that have an arrested cell division phase. Expression of A2, A3, B3, and U1 cyclins in olive fruit is restricted to intensive cell division activity during early fruit development. For further analysis of CYC family genes, a qRT-PCR analysis was conducted to assess the expression of 8 members of this family in fruits at 0, 14, and 28 DPA (Figure I.11D). The qRT-PCR test in the dividing olive fruit corroborated the enrichment in A2, A3, B3, and U1 cyclin genes as well as the enrichment of A1 and B2, and C1 cyclin genes in the expanding olive fruit (Figure I.11D). We hypothesise that the differences in time of expression of cyclin A2 and A3 versus cyclin A1 as well as of cyclin B3 versus cyclin B2 may reflect specific functions during olive fruit development, including A-, B-, and D-type CYCs.

Similarly, only one member of CDK family (*CDKC1*) was up-regulated exclusively in olive fruit at 14 DPA compared with 0 DPA, whereas 6 of the 8 members of CDK family were down-regulated exclusively in olive fruit at 14 DPA compared with 0 DPA (P14 vs. P0 comparison) (Figure I.12A; Table I.S14). Of particular interest is one member of CDK family, homologous to CDKB1 (Weimer et al., 2016), which proved to be up-regulated in both comparisons (Figure I.12A; Table I.S14). In addition, one gene homologous to CKI3 and two genes homologous to SMR6 were exclusively transcribed in the dividing fruit at 14 DPA, whereas one gene homologous to SMR9 was up-regulated in both comparisons.

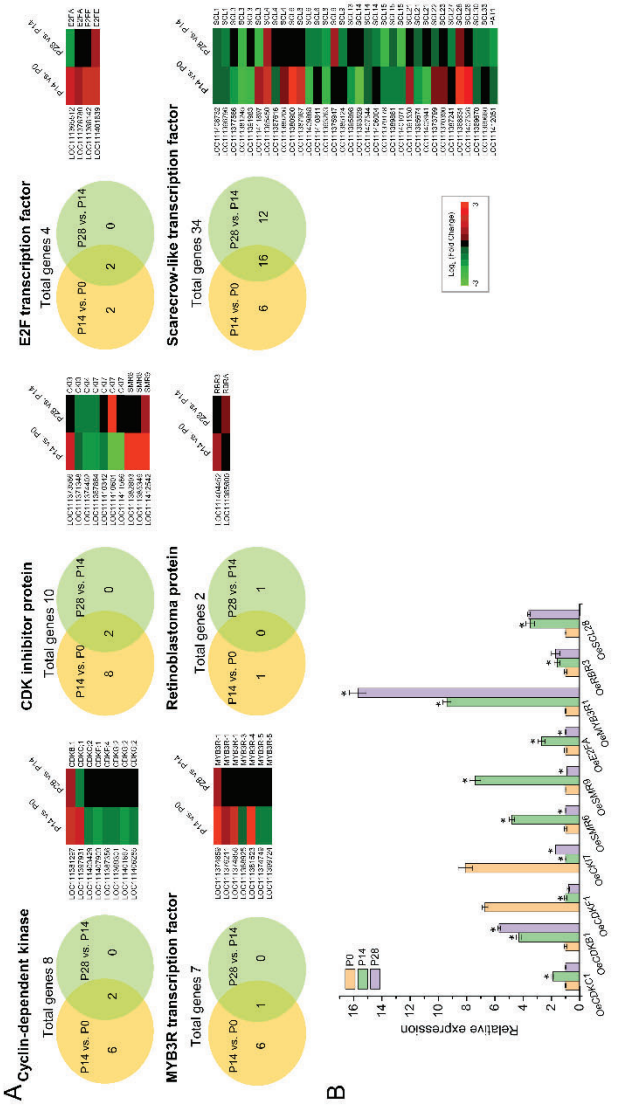

Figure I.12. Differential gene expression of candidate cell cycle-related genes during early olive fruit development. (A) Venn diagram representing overlap between differential expressed genes *CDK, CKI, E2F, MYB3R, RBR*, and *SCL* in both the comparison of fruit at 14 DPA (P14) versus fruit at 0 DPA (P0), and the comparison of fruit at 28 DPA (P28) versus fruit at 14 DPA (P14). Expression values are represented in a heatmap as Log_2 Fold Change in the P14 versus P0, and the P28 versus P14 comparisons, and the colour key is indicated at the bottom. (B) Expression of cell cycle-related genes in olive fruits at 0 (P0), 14 (P14) and 28 (P28) DPA. Analysis of transcript levels of cell cycle-related genes by qRT-PCR. Genes and their primers are shown in Table I.S1. Relative expression values were normalized to the lowest expression value taken as 1. The data represent the mean values (±SEs) of duplicate experiments from three independent biological samples. Statistical significance compared with the preceding point was determined using Student's *t test*. *P< 0.05. Additional information on the cell cycle-related genes is presented in Table I.S14.

By contrast, 5 of the 10 members of CKI family were down-regulated exclusively in olive fruit at 14 DPA compared with 0 DPA, whereas only one *CKI7* gene was down-regulated in both comparisons during early fruit development (Figure I.12A, Table I.S14). Additionally, our data demonstrate that one member of RB protein family homologous to *RBR3* was transcribed exclusively in the dividing olive fruit at 14 DPA, while one gene homologous to *rbrA* was transcribed exclusively in the expanding olive fruit at 28 DPA (Figure I.12A; Table I.S14).

Regulation of the cell cycle and endocycle by TFs proves to be upstream of the cyclins and CDKs. Furthermore, E2F, OBP1 (DOF TF), and THREE MYB REPEAT (MYB3R) TFs have been found to be primary regulators of the cell cycle (Komaki and Sugimoto, 2012). Differential expression patterns of other cell cycle-related genes were investigated during olive fruit early development, including E2F, MYB3R and SCARECROW-LIKE (SCL) TFs (Figure I.12A, Table I.S14), of which we randomly examined 10 genes and confirmed their expression patterns using qRT-PCR (Figure I.12B). E2Fs are known to target genes involved in DNA repair and chromatin dynamics at the transition between G1 and S phase. In our analysis, two members of E2F TF family homologous to E2FA and E2FE were found to be up-regulated in olive fruit at 14 DPA (P14 vs. P0), whereas one other gene homologous to E2FE was up-regulated in both comparisons during early olive fruit development (Figure I. 12; Table I.S14).

3.6. Differing hormonal composition and gene expression patterns during early fruit development in olive

According to our previous data, GO enrichment identified hormone-mediated signalling pathways that may be key during early olive fruit development (Figure I.4). Firstly, investigating a potential relationship between early fruit development and hormonal composition, we examined the hormone profiles of indole-3-acetic acid (IAA), gibberellins [(GAs), GA_1 and GA_4], cytokinins [(CKs), *trans*-Zeatin (*t*Z)], abscisic acid (ABA), jasmonic acid (JA), and salicylic acid (SA) during early olive fruit development. This is the first report available on the direct measurement of these hormones during early fruit development in olive. As shown in Figure I.13, all detected hormones decreased during the first 14 days of fruit development in olive

fruit, except *t*Z, SA, and IAA. In particular, our results reveal that the *t*Z levels rose during the first 14 days of fruit development, only to disappear later from 14 to 28 DPA in olive fruit. SA levels also rose from the anthesis stage to fruit at 14 DPA, and fell later by 46% in fruit at 28 DPA, while IAA levels rose during early fruit development, reaching a maximum at 28 DPA.

The hormone profiling revealed that the olive flower at anthesis stage (fruit set) is characterized by high levels of JA and GA_1 (Figure I.13). In fact, JA was the most abundant in olive flower at anthesis, but JA levels sharply fell during early fruit development (Figure I.13). Similarly, upon fertilization, a decrease of GA_4, and ABA levels accompanied by a loss of GA_1 were detected in olive fruit at 14 DPA. By contrast, at 28 DPA, the fruit showed the highest peak of hormones with a rise in IAA, GA_1, GA_4, and ABA levels from 14 to 28 DPA, while the *t*Z content was undetected in the fruit at 28 DPA. Notably, GA_1 was absent from the fruit at 14 DPA but was enriched at 28 DPA (Figure I.13), suggesting a specific association between this hormone and the cell expansion phase in olive fruit development. Hence, we related *t*Z, SA, IAA, GA_1, GA_4, and ABA to early olive fruit growth. More specifically, zeatin *t*Z and SA were relatively more important during intense cell division, whereas IAA, GA_1, GA_4, and ABA were found to have greater relative importance during the period when fruit growth proves to depend primarily on cell expansion.

Here, we show that, upon fertilization, the olive fruits grow as cell division prevails over expansion associated with high levels of *t*Z and low levels of GA_4 (loss of GA_1). At 28 DPA, the loss of *t*Z and high levels of GA (GA_1 and GA_4) in olive fruit boosts fruit growth mainly in terms of cell expansion, concomitantly with a rise in the level of IAA.

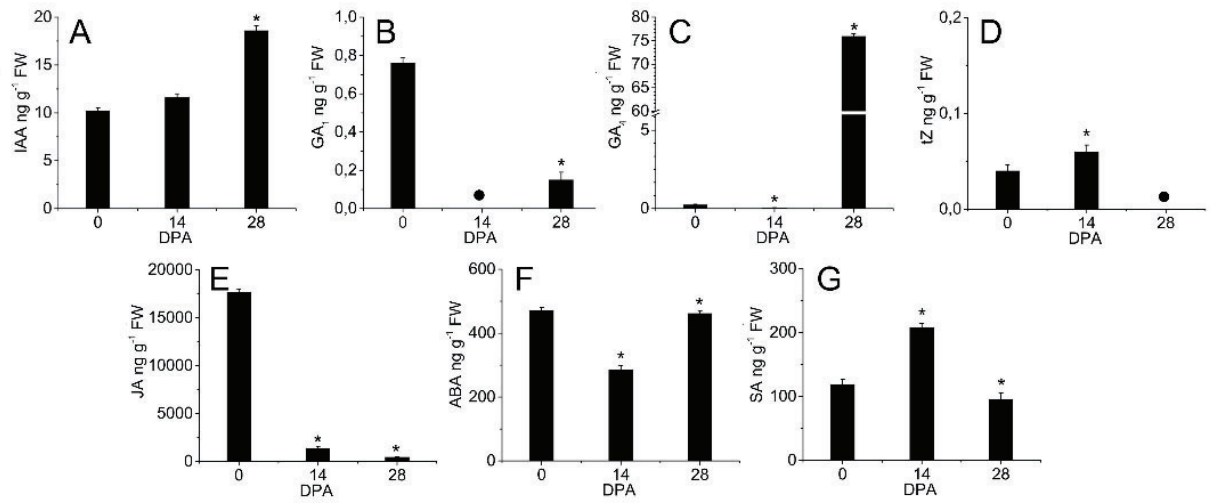

Figure I.13. Profiles of (A) indole-3-acetic acid (IAA), (B) gibberellin 1 (GA_1), (C) gibberellin 4 (GA_4), (D) *trans*-Zeatin (*tZ*), (E) jasmonic acid (JA), (F) abscisic acid (ABA), and (G) salicylic acid (SA) levels in olive fruits at 0 (P0), 14 (P14) and 28 (P28) DPA during early fruit development. Hormone levels not detected are indicated by a black dot (•). Data are the means ± SD of three biological replicates with three technical repeats each. Statistically significant differences based on unpaired Student's *t-test* at $p < 0.05$ are denoted by an asterisk.

Next, in an effort to determine the way in which gene expression related to hormone signalling is correlated with the hormone accumulation during early olive fruit development, we used RNA-seq technology to analyse the transcriptomic profiling of genes involved in hormone signalling and metabolism. Among the 623 DEGs related to plant hormone metabolism and signalling (Table I.S15), those related to auxin (164 genes), ethylene (141 genes) and ABA (78 genes) were the most represented, followed by those related to GA (48 genes), CKs (46 genes), PAs (35 genes), JA (31 genes), SA (22 genes) oxide nitric (NO, 29 genes), BRs (21 genes) and strigolactones (SL, 8 genes). Olive fruit undergoes a significant increase in IAA-, CK-, GA-, PA- and BR-related expression during early fruit development. This suggests a regulatory function and/or interactions among these hormones within the olive fruit. The expression patterns found in these pathways were analysed using hierarchical clustering (Figure I.S16).

We noted a divergence in auxin-related gene expression for cell division versus cell expansion during early olive fruit development (Figure I.14; Table I.S15; Figure I.S16). Transcripts involved in IAA synthesis, such as a transcript encoding tryptophan aminotransferase protein 4 (TAR4) was up-regulated in the dividing fruit at 14 DPA (P14 vs. P0), but IAA levels did not significantly differ in fruit between 14 DPA and 0 DPA (Figure I.14; Table I.S15; Figure I.S16). In addition, *YUCCA10* was down-regulated in both comparisons during early fruit development, but not with consistently the highest IAA levels detected in the fruit at 28 DPA (Figure I.14). The IAA-amino acid hydrolase genes (*ILR1-like 1*, *ILR1-like 3*, and *ILR1-like 5*), involved in auxin homeostasis, are exclusively overexpressed in the dividing fruit at 14 DPA. Auxin-amino acid hydrolase may provide local concentrations of auxin within the fruit during early development. However, expression levels for the auxin conjugating enzymes *GH3.6*, *GH3.9* and *GH3.10* were also found to be boosted in the dividing fruit at 14 DPA (P14 vs. P0) during early fruit development. Furthermore, these *GH3.6* and *GH3.9* genes show down-regulated expression in the expanding fruit at 28 DPA (P28 vs. P14) during early olive fruit development, consistently with the highest IAA levels detected in the fruit at 28 DPA (Figure I.14; Table I.S15; Figure I.S16). In addition, the *GH3.1* gene shows down-regulated and up-regulated expression in the fruit at 14 DPA (P14 vs. P0) and at 28 DPA (P28 vs. P14), respectively, during early fruit development (Figure I.14; Table I.S15; Figure I. S16). Several transcripts related to auxin transport and signalling also displayed increases during early olive fruit development (Figure I.14; Table I. S15; Figure I.S16). In our study, transcript levels for two auxin efflux carriers, *PIN1* and *PIN7,* rose in the dividing fruit at 14 DPA and lowered in the expanding fruit at 28 DPA, while *PIL2*, *PIL6* and *PIL7* expression showed the opposite expression, suggesting that the latter participates in the transition from cell division to expansion during early olive fruit development. However, transcripts encoding auxin influx carrier-like protein (*LAX2*, *LAX4* and *LAX5*) increased exclusively in the dividing fruit at 14 DPA during early development, indicating altered auxin distribution in the fruit at this time.

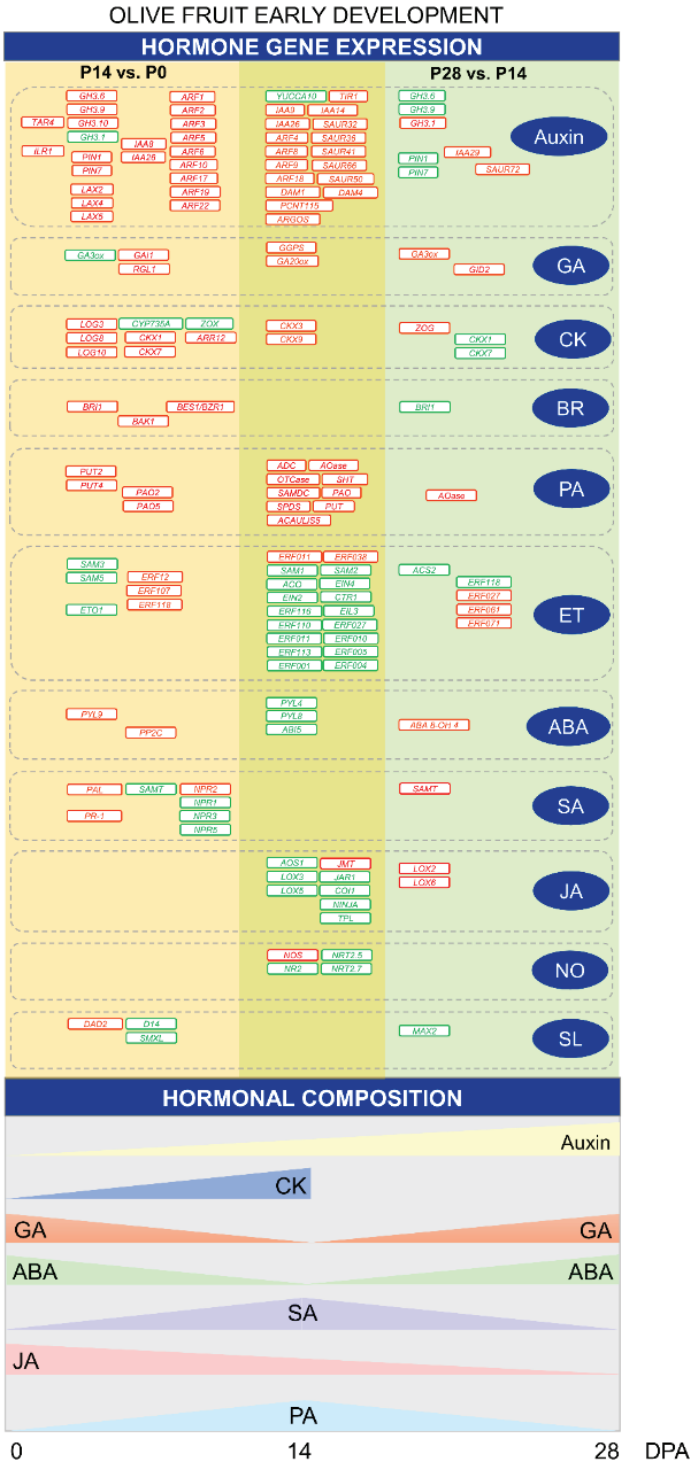

Figure I.14. Summary figure including hormonal composition and the most important DEGs during early fruit development in olive. DEGs in red color represents genes that increased its expression and DEGs in green color represents genes that decreased its expression. The middle column of the figure represents DEGs in common in both comparisons. Additional information on the hormone-related genes is presented in Table I.S15.

In addition, genes specifying auxin signalling components (*TIR1*, *IAA9, ARF4*, *ARF8*, *ARF9*, *ARF18*, and *SAUR50)* were up-regulated in both comparisons, while other genes (*IAA8, IAA26, ARF1*, *ARF2*, *ARF3*, *ARF5*, *ARF6 ARF10*, *ARF17*, *ARF19* and *ARF22)* were exclusively up-regulated the dividing olive fruit at 14 DPA (P14 vs. P0), and still others (*IAA29* and *SAUR72)* were exclusively up-regulated in the expanding olive fruit at 28 DPA (P28 vs. P14) during early olive fruit development. Conversely, we detected numerous auxin-regulated genes which were down-regulated during early fruit development (*IAA14*, *IAA26*, *SAUR32*, *SAUR36*, *SAUR41*, *SAUR62*, *SAUR66, ARGOS*, *DAM1*, *DAM4*, and *PCNT115*, among others) (Figure I.14; Table I.S15; Figure I.S16).

In the case of GA, our data suggest that GA synthesis is up-regulated by *GGPS*, coding geranylgeranyl pyrophosphate synthase (GGPS), and *GA20ox*, coding GA 20-oxidase, these two genes active during early olive fruit development. Meanwhile, *GA3ox* (GA 3-oxidase), which is a transcript involved in a late GA biosynthetic step, was down-regulated in the dividing fruit at 14 DPA (P14 vs. P0) and up-regulated in the expanding fruit at 28 DPA (P28 vs. P14), consistently with the highest GA (GA_1 + GA_4) levels detected in olive fruit at 28 DPA (Figures I.14; Table I.S15; Figure I.S16). These results suggest that GA3ox is the major late-step enzyme responsible for the high-level accumulation of GA_4 detected in the fruit at 28 DPA, whereas the complete absence of GA_1 observed in the dividing fruit at 14 DPA may be attributed to the expression of the *GA2ox* gene, which is a transcript involved in the deactivation of bioactive GAs. Additionally, we show that GA signalling is regulated by *GAI1* and *RGL1* (DELLA proteins) exclusively during the first 14 days of fruit development (P14 vs. P0) and later by *GID2* receptor during the latest 14 days of fruit development (P28 vs. P14) (Figure I.14; Table I.S15; Figure I.S16).

It bares noting that we found the up-regulation of the expression of three different cytokinin riboside 5'-monophosphate phosphoribohydrolase genes (*LOG3*, *LOG8,* and *LOG10)* during the first 14 days of olive fruit development (P14 vs. P0). LOG converts inactive CK nucleotides to the biologically active free-base forms, which is consistent with the highest *t*Z levels detected at 14 DPA in olive fruit (Figure I.14; Table I.S15; Figure I.S16).

By contrast, both *CYP735A* (CK hydroxylase), which catalyses the biosynthesis of trans-zeatin (*t*Z), as well as *ZOX*, which encodes zeatin O-xylosyltransferase involved in CK conjugation, were exclusively down-regulated in the dividing olive fruit (P14 vs. P0) (Figure I.14; Table I.S15; Figure I.S16). However, transcripts encoding for another zeatin conjugating enzyme *ZOG* (zeatin O-glucosyltransferase) increased exclusively in the expanding olive fruit at 28 DPA during early fruit development, consistently with the loss of *t*Z detected in the olive fruit at 28 DPA (Figure I.13). These results suggest local transcriptional control of the CK biosynthesis and conjugation rather than transport from other tissues. Bioactive forms of CKs are, in turn, deactivated by CK oxidase/dehydrogenase (CKX), and, thereby, regulate the amount of bioactive CK. In the present study, *CKX1* and *CKX7* gene expression were up-regulated in the P14 versus P0 comparison, and down-regulated in the P28 versus P14 comparison, while *CKX3* and *CKX9* gene expression were up-regulated in both comparisons, suggesting that the deactivation of CK may actively occur during early olive fruit development (Figure I.14; Table I.S15; Figure I.S16). Similarly, several transcripts related to CK signaling were also differentially expressed during early fruit development. Of these, 7 are gene-encoding members of the A-ARR family (*ARR5*, *ARR6*, *ARR8*, *ARR15*, *ARR17*), but only one is a gene-encoding member of the B-ARR family (*ARR12*). The up-regulation of the expression of cytokinin-responsive *ARR12* TF exclusively in the dividing olive fruit at 14 DPA (P14 vs. P0) suggests that the *ARR12* gene activates CK-responsive gene expression during the fruit growth phase to ensure a prevalence of cell division over cell expansion.

In the case of BR, we also showed that 3 *BRI1* receptor kinase, 2 *BAK1 (SERK2)* co-receptors, and 3 *BES1/BZR1* factor transcription were exclusively up-regulated in the dividing fruit at 14 DPA (P14 vs. P0), while only a different receptor *BRI1* gene was exclusively up-regulated in the expanding fruit at 28 DPA (P28 vs. P14, Table I.S15; Figure I.S16), suggesting that the up-regulation of receptor *BRI1* may be required for olive fruit development. Furthermore, genes encoding key genes related to PA biosynthesis, transport, conjugation, and degradation, including *ADC* (arginine decarboxylase), *AOase* (acetylornithine deacetylase), *OTCase* (ornithine carbamoyltransferase), *ACAULIS5* (thermospermine synthase), *SAMDC* (S-adenosylmethionine decarboxylase), *SPDS* (spermidine synthase), *SHT* (spermidine

hydroxycinnamoyl transferase), *PUT* (polyamine uptake transporter), and *PAO* (polyamine oxidase), also showed temporal regulation across the samples studied (Figure I.14; Table I.S15; Figure I.S16). This agrees with our prior study of the PA levels as well as the induction and spatial expression patterns of *SPDS* and *SAMDC* genes involved in spermidine biosynthesis during early olive fruit development (Gomez-Jimenez et al., 2010). Both the P14 versus P0, and the P28 versus P14 comparisons during early olive fruit development are apparently characterized by an active PA biosynthesis and conjugation, although the up-regulation of two different PA transporters *PUT* (*PUT2* At1g31830 and *PUT4* At3g13620) genes, and two different *PAO* (*PAO2* and *PAO5*) genes exclusively in the dividing olive fruit at 14 DPA, suggest that PA transport and catabolism may have a significant influence on the role of PA in the cell division phase during early olive fruit development. Recently, the importance of PA transporters has been shown in the regulation of flowering and senescence pathways (Pál et al., 2021). Substantial information is available on the PA transport systems in bacteria, yeast, and mammals, but the role of PA transporters in plants is only now being recognized (Pál et al., 2021). However, other PA-related genes, such as one *AOase*, were exclusively up-regulated in the fruit at 28 DPA following early fruit development (Figure I.14; Table I.S15; Figure I.S16). This protein is involved in a step of the subpathway, which is part of the L-arginine biosynthesis pathway, which synthesises L-ornithine from N (2)-acetyl-L-ornithine, required for the biosynthesis of putrescine. This suggests that an accumulation of putrescine may take part in regulating the transition from cell division to expansion during olive fruit development.

In addition, our results show that many genes encode major elements that are related to the ethylene pathway (Figure I.14; Table I.S15; Figure I.S16). In particular, 24 of the 38 DEGs involved in ethylene biosynthesis were down-regulated during early olive fruit development (Figure I.14, Table I.S15). Indeed, 5 S-adenosylmethionine synthase (*SAM1, SAM2, SAM3, SAM5*) gene, one 1-aminocyclopropane-1 carboxylic acid (ACC) synthase (*ACS*) genes, 7 ACC oxidase (*ACO*) genes, and one ethylene-overproduction protein 1 (*ETO1*) gene were down-regulated in the dividing olive fruit at 14 DPA (P14 vs. P0) , while 2 *SAMS* (*SAM1*, and *SAMS2*) genes, one ACC synthase (*ACS2*) gene, and 7 ACC oxidase (*ACO*) genes were down-regulated in the expanding olive fruit

at 28 DPA (P28 vs. P14), indicating that the early olive fruit development can apparently be characterized by an inactive ethylene biosynthesis at transcriptional level. Similarly, other genes related to ethylene signalling, such as *EIN4, EIN2, CTR1, EIL3* (EIN3-*like, EIL*), *ERF* (*ERF001*, *ERF004*, *ERF005*, *ERF010*, *ERF011*, *ERF027*, *ERF104*, *ERF110*, *ERF113*, *ERF116*, *ERF118*) among others, were also down-regulated during early olive fruit development (Figure I.14; Table I.S15; Figure I.S16). By contrast, the up-regulation of the genes related to ethylene signalling during early fruit development was also found (Figure I.14; Table I.S15; Figure I.S16): ERF011 and ERF038 were related to early olive fruit growth, whereas ERF12, ERF107, and ERF118 were likely to be associated with a period of more intense cell division, and ERF027, ERF061, and ERF071 tended to be associated with the cell expansion period.

Furthermore, 5 out of the 8 DEGs involved in ABA biosynthesis showed less transcript abundance during early olive fruit development (Figure I.14; Table I.S15; Figure I.S16), whereas other transcripts involved in ABA catabolism such as ABA 8-OH 4, which encodes ABA 8′-hydroxylase, was up-regulated exclusively in the expanding fruit at 28 DPA during early development, disagreeing with the ABA levels detected in olive fruit at this time (Figure I. 13). The present analysis also found components of ABA signalling repressed during early fruit development. Two *PYR/PYL (PYL8* and *PYL4,* ABA receptors) and one *ABI5 (*bZIP TF) were down-regulated in fruit during early development. In addition, up-regulation of ABA-related genes was found following this phase (Table I.S15). In particular, one *PYR/PYL (PYL9)* and 7 *PP2C genes* were exclusively up-regulated in the dividing fruit at 14 DPA, suggesting that this PYL9 receptor forms part of an ABA signalling unit that modulates early olive fruit growth. Similarly, several genes related to SA were up-regulated exclusively during the first 14 days of fruit development, such as *PAL*, *NPR2*, and *PR-1* and whereas another such as *SAMT, NPR1, NPR3 and NPR5* genes were down-regulated in olive fruit at 14 DPA (P14 vs. P0), consistently with the highest SA levels detected in the fruit at 14 DPA (Figure I.14; Table I.S15; Figure I.S16). On the other hand, the gene-profiling data revealed that one *SAMT* transcript, which encodes salicylic acid carboxyl methyltransferase (an enzyme responsible for biosynthesis of methyl salicylate) increased in olive fruit at 28 DPA compared with 14 DPA, in good

agreement with a loss of SA in the expanding olive fruit at 28 DPA (Figure I. 13; Table I.S15; Figure I.S16).

With regard to JA, our results suggest that *AOS1*, which encodes an allene oxide synthase (AOS) protein, is the major control point responsible for the drop of JA detected in olive fruit during early development. AOS, the second enzyme in the biosynthesis of the JA, is a regulatory point in the biosynthesis of JA (Farmer and Groossens, 2019). In addition, *LOX3* (13-LOX member) and *LOX5* (9-LOX member) genes encoding lipoxygenase members were down-regulated in the olive fruit during early development, whereas *LOX2* (13-LOX member) and *LOX6* (13-LOX member) were exclusively up-regulated in the expanding olive fruit at 28 DPA (Figure I.14; Table I.S15; Figure I.S16), suggesting that these genes modulate the distribution between 13-LOX- and 9-LOX-derived oxylipins during early fruit development. Moreover, *JMT* genes encoding a jasmonate-O-methyltransferase, which catalyses the methylation of JA into methyljasmonate (MeJA), was also up-regulated during early fruit development, suggesting that the MeJA could regulate the cell growth rate during early olive fruit development. JA conjugation with isoleucine is reportedly catalysed by jasmonoyl-isoleucine (JA-Ile) synthetase (JAR1), this being a member of the GH3 family (Li et al., 2021a). The most bioactive of the JAs is JA-Ile. The perception of JA-Ile by its coreceptor, the Skp1-Cullin1-F-box-type (SCF) protein ubiquitin ligase complex SCF^{COI1}-JAZ, derepresses the transcriptional repression of target genes in the nucleus. JA-Ile signalling participates in regulating several developmental processes, such as root growth and architecture, tuber and trichome formation, seed germination, and particularly reproductive-organ development (Huang et al., 2017). Here, we report that *JAR1*, *COI1, NINJA* and *TPL* (TOPLESS) genes were down-regulated in the olive fruit during early development (Figure I.14; Table I.S15; Figure I.S16), suggesting that these components may aids in JA-Ile signalling in the nucleus to regulate early fruit development.

On the other hand, the identification of the proteins involved in NO formation and transport in olive fruit constitutes a promising avenue of research for a better comprehension of NO physiological function during early fruit development. Here, several transcripts related to NO metabolism

were also differentially expressed during early olive fruit development, such as *NOS* genes, encoding putative NO synthase, and *NR2* genes, encoding putative nitrate reductase (NR), which were up-regulated and down-regulated during early fruit development, respectively (Figure I.14; Table I.S15; Figure I.S16). Similarly, *NRT*2.5 and *NRT2.7* genes encoding members nitrate transporter were down-regulated in the olive fruit during early development.

Finally, genes involved in the strigolactone (SL) signaling pathway, such as the receptor *DAD2* (SL esterase) was up-regulated exclusively in the dividing olive fruit at 14 DPA (P14 vs. P0), whereas the receptor *D14* (α/β hydrolase DWARF14) and the transcriptional repressor *SMXL* (SUPPRESSOR OF MAX2 LIKE) genes were exclusively down-regulated in the dividing the fruit at 14 DPA during early development, suggesting that these components act to regulate karrikins/strigolactone responses during the cell division phase of early fruit development. In contrast to this, we show that one *MAX2* gene encoding MORE AXILLARY GROWTH2 (MAX2), an F-box protein that is part of a SKP1-Cullin-F-box (SCF) ubiquitin ligase complex, was exclusively down-regulated in the expanding olive fruit at 28 DPA (Figure I.14; Table I.S15; Figure I.S16).

3.7. Signaling peptides regulating early fruit development in olive

The molecular identifications for the signalling peptides during early fruit development are still limited. Signalling peptides in the role of phytohormones control several features of plant growth and development through cell-cell communication networks, e.g. organ abscission, meristem maintenance, gravitropism, cell proliferation and differentiation, cell elongation, and defence (Ghorbani et al., 2014). These peptides can be recognized typically by membrane-embedded receptor-like kinases which activate cell signalling to govern plant growth and development. In our analysis, more than 40 genes encoding putative leucine-rich repeat receptor-like kinases (LRR-RLKs) family proteins, involved in plant peptide signalling, differed in expression level during early olive fruit development (Table I.S16). Among these, *EMS1* gene encoding for LRR-RLKs family protein was found to be exclusively detected in the dividing olive fruit. Similarly, one cysteine-rich receptor-like protein kinase 29 (CRK29) and one probable receptor-like

protein kinase At5g38990 (MDS1), involved in growth adaptation upon exposure to metal ions (Richter et al., 2018), were found to be detected exclusively in the dividing olive fruit (Table I.S16). Likewise, more than 400 genes have been found to encode putative proteases (also referred to as peptidases or proteinases), including serine proteases, cysteine proteases, aspartic proteases, and Clp proteases, among other (Table I.S17). Proteases are enzymes able to participate in almost all stages of plant life (Ghorbani et al., 2014; Stintzi and Schaller, 2022). In particular, two genes encoding for serine carboxypeptidase-like 45, and serine carboxypeptidase-like 2 were found to be detected only in the dividing olive fruit (Table I.S17), suggesting that fruit protein degradation contribute to early fruit growth in olive.

Moreover, two genes, *SBT5.4*, and *SBT4.15,* coding for subtilisin-like protease proteins (also known as subtilases; SBT), were found to be detected exclusively in the flower at anthesis (fruit set), and in the dividing fruit at 14 DPA, respectively (Table I.S16). Although previous studies have indicated that SBT-mediated processing results in the activation of peptide signals regulating stress-induced flower drop, the formation of the embryonic cuticle, and pollen development (Stintzi and Schaller, 2022), little has been reported concerning its role in early fleshy fruit development. Our analysis identified 32 putative SBT genes in olive fruit that differed in expression level during early fruit development (Figure I.15A,B), and were retained for further phylogenetic analysis (Figure I.15C). Among 32 SBT genes identified in our analysis, 11 were exclusively expressed in the dividing olive fruit at 14 DPA, while 4 were expressed only at 28 DPA (Figure I.15, Table I.S16), indicating that at least some members of SBTs play major roles during early olive fruit development. Overall, 19 SBT genes were up-regulated and 9 were down-regulated in fruit at 14 DPA compared with 0 DPA, whereas 11 SBT genes were up-regulated and 8 were down-regulated in the expanding fruit at 28 DPA compared with 14 DPA (Figure I.15, Table I.S16), of which we randomly examined five genes and confirmed their expression patterns using qRT-PCR (Figure I.15D).

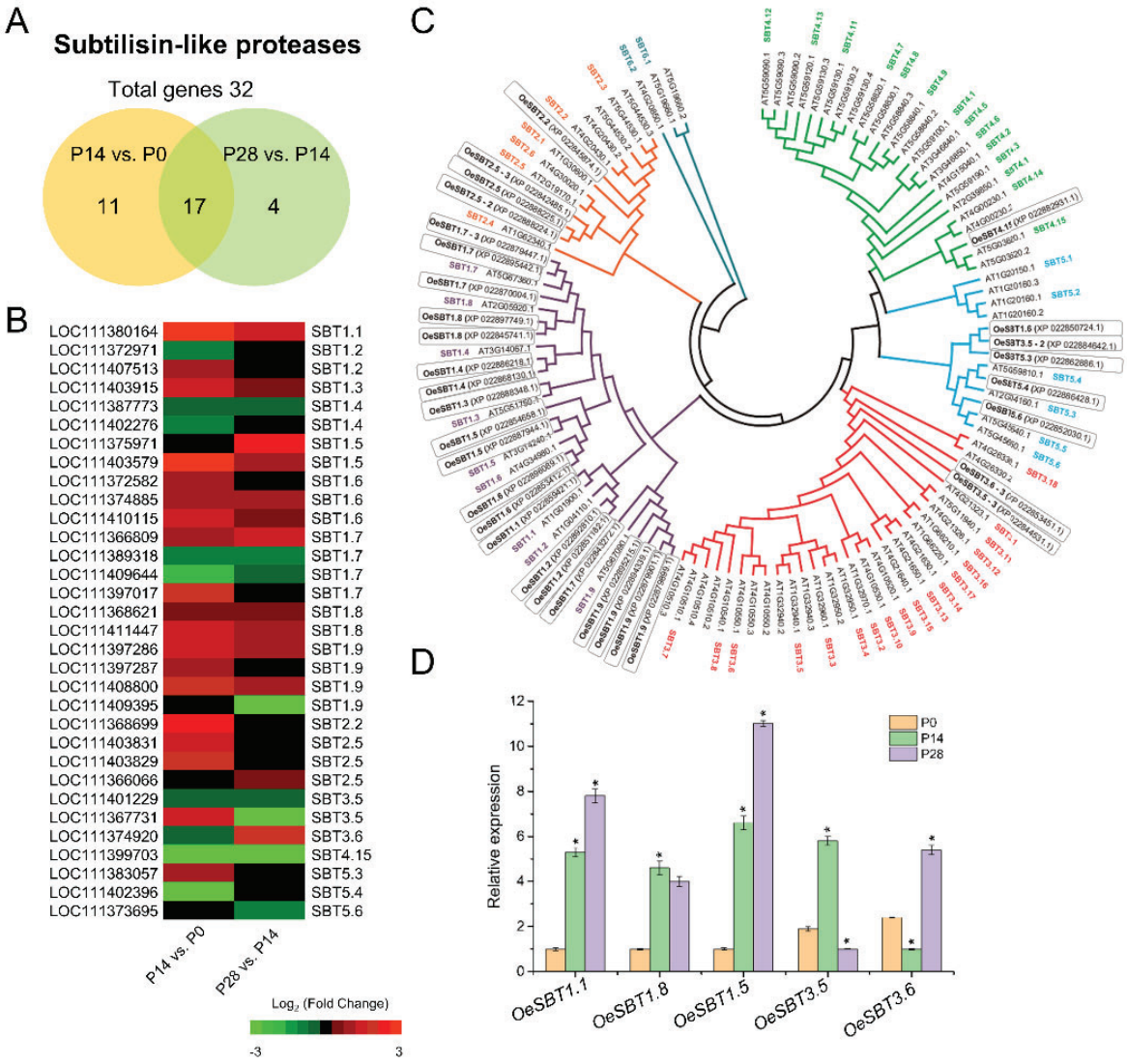

Figure I.15. Differential gene expression of subtilisin-like protease (*SBT*) genes during early olive fruit development. (A) Venn diagram showing numbers of overlapping *SBT* genes in both the fruit at 14 DPA (P14) versus fruit at 0 DPA (P0), and in the fruit at 28 DPA (P28) versus fruit at 14 DPA (P14) comparisons. (B) Expression values are represented in a heatmap as Log_2 Fold Change in the P14 versus P0 comparison, and the P28 versus P14 comparison, and the colour key is indicated at the bottom. (C) Phylogenetic analysis of olive SBT (OeSBT) with other SBT genes. The sequences included in this alignment are from olive (*Olea europaea* var. sylvestris Annotation Report; https://www.ncbi.nlm.nih.gov/genome/annotation euk/Olea europaea var. sylvestris/100/), and Arabidopsis (http://www.arabidopsis.org/). The SBT proteins studied from our work are enclosed in an open box. (D) Expression of five selected *SBT* genes in olive fruits at 0 (P0), 14 (P14) and 28 (P28) DPA. Analysis of transcript levels of genes by qRT-PCR. Genes and their primers are shown in Table I.S1. Relative expression values were normalized to

the lowest expression value taken as 1. The data represent the mean values (±SEs) of duplicate experiments from three independent biological samples. Statistical significance compared with the preceding point was determined using two-sided Student's *t-test*. *P< 0.05. Additional information on *SBT* genes is presented in Table I.S16.

Notably, we show that, after fertilization, transcripts encode SBT1.1, SBT1.3, SBT1.5, SBT1.6, and SBT1.8 are associated with both cell division and cell expansion phases, whereas the cell division phase involves mainly the gene activity of SBT1.2, SBT1.9, and SBT3.5 proteins. Furthermore, the cell expansion phase is associated with the gene activity of SBT2.5 and SBT3.6 proteins during early olive fruit growth (Figure I.15, Table I.S16). Previously, SBT3.5 and SBT6.1 proteins have been shown to promote cell expansion (Ghorbani et al., 2016), but cross-talk involving different signaling peptide pathways controlling cell expansion has not been elucidated, nor has their relation to hormonal growth control.

3.8. Transcript changes in cell wall biosynthesis and remodelling during early olive fruit development

In this study, we identified, among the DEGs, 895 genes that encode proteins with probable functions in cell wall biosynthesis and remodelling during early olive fruit development (Table I.S18), of which 300 were up-regulated and 258 down-regulated in the P14 versus P0 comparison, and 195 were up-regulated and 142 down-regulated in the P28 versus P14 comparison (Table I.S18). Overall, 119 genes were up-regulated, and 75 genes were down-regulated in both comparisons during early fruit development (Figure I.16, Table I.S18). The well-represented families included cellulose synthase (CES, 59 genes), arabinogalactan protein (AGP, 59 genes), polygalacturonase (PG, 55 genes), pectin methylesterase (PME) (53 genes), glucan 1,3-β-glucosidase (BG; 43 genes), endo-1,4-*β*-glucanase or cellulase (EGase/CEL, 41 genes), expansin (EXP, 39 genes), xyloglucan endotransglucosylase/hydrolase (XTH, 37 genes), laccase (LAC, 34 genes), β-galactosidase (βGAL, 28 genes), and extensin (EXT, 28 genes) proteins (Figure I.16; Table I.S18), implying that these cell wall-related enzymes help regulate early olive fruit development.

Examining these families, we identified genes that were up-regulated exclusively in the dividing olive fruit (14 DPA), such as genes that encode one

EXP (EXPA13), four EGase/CELs, two XTHs (XTH9, XTH10), 5 CSs (CESA2, CESA3, CESA6, CESE6, CESG2), 2 AGPs (AGP26, AGP31), 3 EXTs (EXT2, EXT3, EXT6), and 2 LACs (LAC15, LAC7) proteins (Figure I.16; Table I.S18). Similarly, we identified genes up-regulated only in the expanding olive fruit (28 DPA), such as genes encode 2 EXP (EXPA15, EXPA8), 2 EGases/CEL (CEL10, CEL25), two XTH (XTH32, XTH33), 1 CS (CESD4), 4 AGP (AGP10, AGP19, AGP20, AGP26), and 1 EXT (EXT1) proteins (Figure I.16; Table I.S18), suggesting that these cell wall-related enzymes regulate cell expansion during early fruit development in the olive. According to our RNA-Seq data, in addition to these DEGs at different developmental stages, other cell wall related family members serve as candidates for early olive fruit development (e.g. *EXPA1*, *EXPA4*, *EXPA6*, *EXPB3*, *CEL17*, *CEL11*, *CEL6*, *XTH31*, *CESA1*, *CESA4*, *CESA7*, *CESA8*, *CESD2*, *CESD3*, *CESD4*, *CESD5*, and *CESG3* genes*)* with higher expression levels in both comparisons (Figure I.16; Table I.S18).

In particular, we focused on (a) specific genes of the dividing olive fruit (14 DPA): (1) 5 genes encoding members of glycosyl hydrolase family 9 [*EGase17* (XP 022875747.1), *EGase17* (XP 022858517.1), *EGase17* (XP 022892029.1), *EGase* (XP 022848852.1), and *EGase* (XP 022865957.1)], (2) one gene encoding one member of glycosyl hydrolases family 16 [*XTH7* (XP 022894638)], (3) one gene encoding one member of LAC family [*LAC14* (XP 022894320.1)], (4) one gene encoding one member of endochitinase family [*EP3-like* (XP 022874843.1,)], and (5) one gene encoding one member of AGP family [*AGP26* (XP 022899100.1)]; as well as (b) specific genes of the expanding olive fruit (28 DPA) such as *EXPB2* (XP 022856136.1) encoding a member of EXP family proteins (Figure I.16; Table I.S18). EGase, XTH and EXP are cell wall-loosening factors expressed during the stages of maximum growth in fleshy fruit (Catalá et al., 2000; Ando et al., 2012; Pattison et al., 2015). Our gene-expression analysis reveals a sequential induction of cell wall biosynthesis and remodelling genes during early olive fruit development, and the distinctiveness of candidate genes associated with cell division in comparison with cell expansion during early fruit growth.

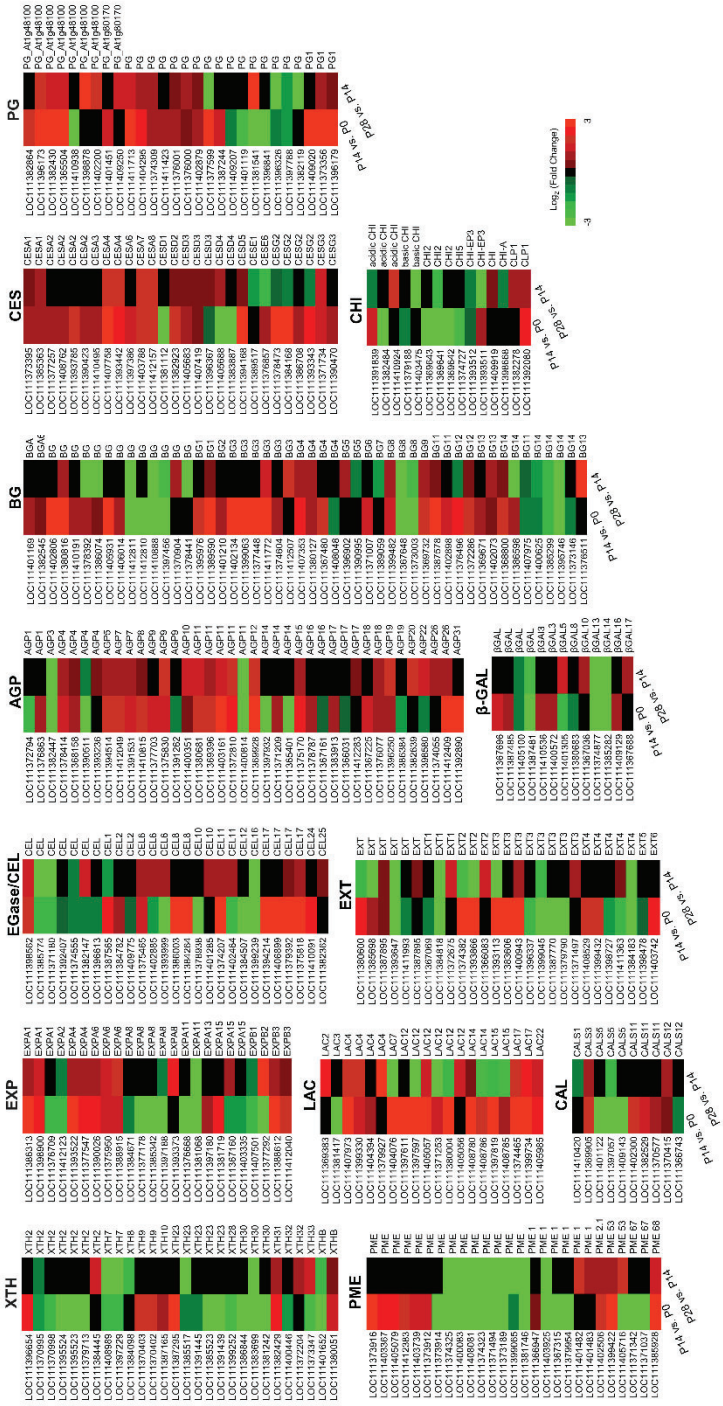

Figure I.16. Expression profile of family genes encoding various cell wall proteins during early fruit development in olive. Expression values are represented in a heatmap as Log_2 Fold Change in both the P14 versus P0 (P14 vs. P0), and the P28 versus P14 (P28 vs. P14) comparisons, and the colour key is indicated at the bottom. Additional information on the cell wall-related genes is presented in Table I.S18.

3.9. Characterization of transport-related genes associated with early olive fruit development

Furthermore, during early fruit development in olive, significant change was identified in the abundance of a subset of 1187 genes encoding channel and transporter proteins of 127 diverse families (Table I.S19). Among these, 273 were up- and 426 down-regulated in the dividing fruit (P14 vs. P0), and 162 up- and 326 down-regulated in the expanding fruit (P28 vs. P14). Likewise, of the 127 different families of channel and transporter proteins, 26 were expressed only in the dividing olive fruit including the dicarboxylate transporter, GDP-fucose transporter, membrane magnesium transporter, and nucleobase-ascorbate transporter families, 25 families (the protein EXORDIUM, protein YLS3-like, protein NRT1/PTR FAMILY, lipid-transfer protein, sulphite exporter, tetraspanin-2, glycerol-3-phosphate transporter, and glycolipid transfer protein families, among others) are regulated only in the expanding olive fruit, and 76 families (ATP-binding cassette (ABC) transporter, amino acid transporter, aquaporin, glucose-6-phosphate/phosphate translocator, hexose carrier protein, sugar transporter, boron transporter, CMP-sialic acid transporter, copper transport protein, GABA transporter, and magnesium transporter families, among others) are regulated in both developmental stages of olive fruit (Figure I.17; Table I.S19).

Among the most abundant up-regulated genes in the dividing olive fruit (P14 vs. P0), a homologue of *KT12* (AT1G60160 putative orthologue) encoding a member of the KT/KUP/HAK family of proton-coupled potassium transporters (KT) was identified, these being highly expressed also in the expanding olive fruit (28 DPA). KT12 have potential effects on cell expansion regulated by auxin (Tenorio-Berrío et al., 2018). Overall, we identified 26 genes that encode KTs fruit (Figure I.17; Table I.S19). Of these, 2 genes (*KT5*, *KT8*) were up-regulated exclusively in the P14 versus P0 comparison, one gene (*KT2*) was exclusively up-regulated in the P28 versus P14 comparison, and 2 genes (*KT6*, *KT12*) were up-regulated in both comparisons. Vigorous cell expansion occurs with greater cell-turgor pressure, this depending on the controlled import of ions to promote water influx. Given that, in plant cells, potassium is the predominant inorganic ion, K transporters and channels constitute the most plausible candidates involved in the production of

osmotic gradients through the plasma membrane and thus the molecular mediators responsible for vigorous cell expansion (Dreyer and Uozumi, 2011). However, only limited research is available concerning which channels/transporters are involved in K import during early fruit development. Another gene highly expressed in the dividing olive fruit was a homologue of *AMT3* (*AMT1;1* AT4G13510 putative orthologue), encoding a member of the ammonium transporter family fruit (Figure I.17; Table I.S19), suggesting that AMT3 may help provide ammonium nitrogen nutrition to olive fruit during early growth.

Among the 162 genes related to transport and up-regulation in the expanding olive fruit at 28 DPA, the most abundant up-regulated genes encode one nonspecific lipid-transfer protein (nsLTP2) (Figure I.17; Table I. S19), which is found in seeds and involved in the transport of the more rigid suberin monomers and sterols (Samuel et al., 2002). This result may mean that this OeLTP2 protein facilitates rapid transport of lipids to the plasma membrane in the fruit during early growth, which may then remain at the cell surface to defend against pathogens. Moreover, in the plasma membrane, sterols are found to interact with sphingolipids and phospholipids to form liquid-ordered microdomains (lipid rafts) that take part in different biological processes (Valitova et al., 2016). Recently, we have reported not only high sterol concentrations in olive fruit with actively dividing cells in the earliest developmental stages but also the appearance of β-sitosterol among the main sterols (Inês et al., 2019). Furthermore, in the present study, 3 sphingolipid transporter genes encoding SPNS2 proteins were exclusively up-regulated in the dividing fruit (Figure I.17; Table I.S19), in agreement with our prior study concerning the sphingolipid levels during early olive fruit development (Corbacho et al., 2018), whereas several phospholipid transporting ATPase genes were up-regulated in the dividing fruit at 14 DPA, and down-regulated at 28 DPA (Figure I.17; Table I.S19), indicating that these lipophilic membrane components are essential for diverse cellular functions during early olive fruit growth. Thus, the metabolism during early fruit development is highly active in this species, including alterations in membrane lipids metabolism and transport.

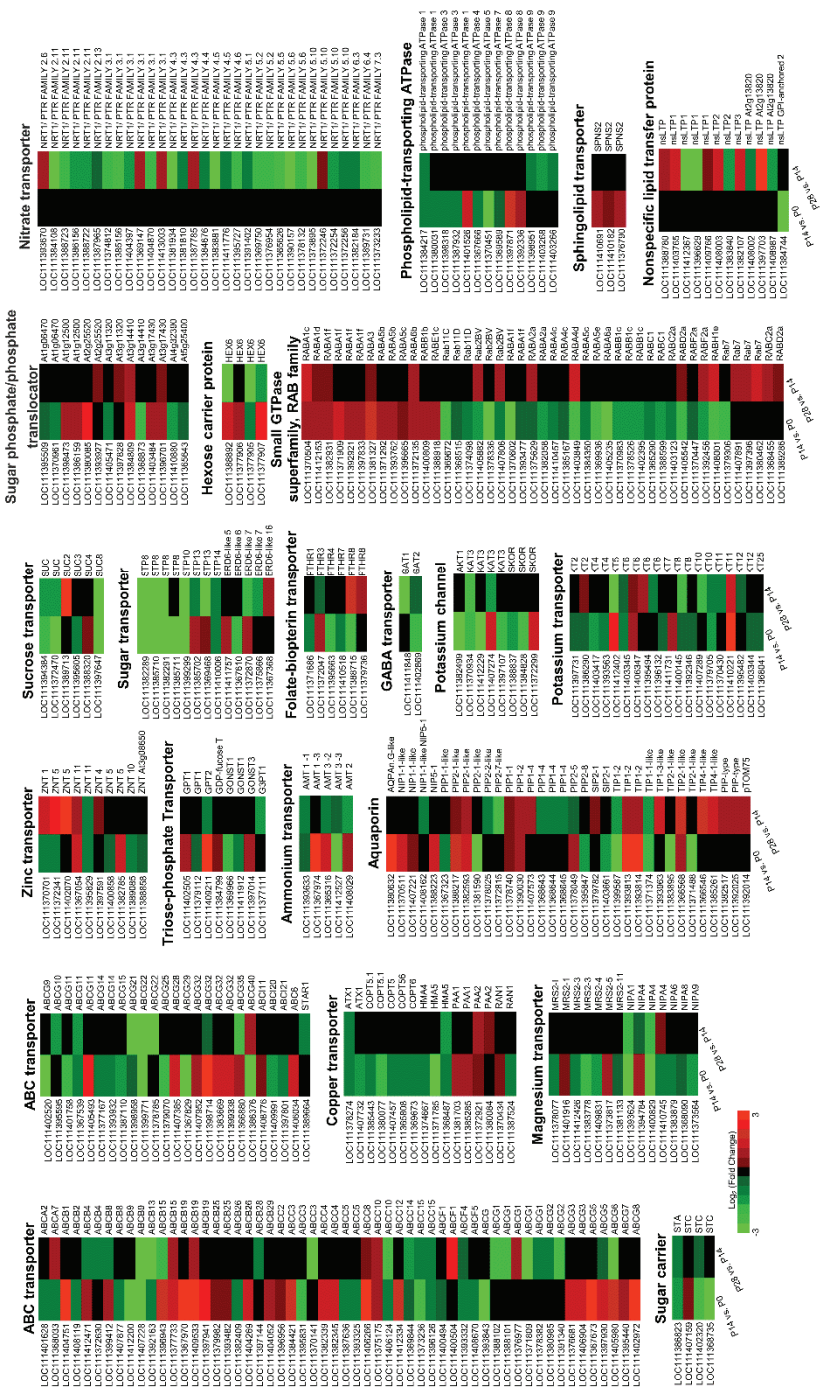

Figure I.17. Expression profile of transport-related genes during early fruit development in olive. Expression values are represented in a heatmap as Log_2 Fold Change in both the P14 versus P0, and the P28 versus P14 comparisons, and the colour key is indicated at the bottom. Additional information on the transport-related genes is presented in Table I.S19.

On the other hand, among the most abundant up-regulated genes in the expanding olive fruit, we also found one encodes zinc transporter 5, ZNT5

(Figure I.17; Table I.S19), which mediate both cellular zinc efflux and zinc sequestration into membrane-bound organelles, suggesting that homeostasis of zinc, cofactor for hundreds of TFs and enzymes, is tightly modulated by ZNT5 during early fruit development. Our data also show that one sucrose transport protein gene, *SUC2*, was up-regulated in the expanding fruit, suggesting a role for this SUC2 protein in the import of sugar from source leaves and its further accumulation in olive fruit during development. Other genes noticeably present in the expanding fruit and involved in vesicle trafficking were found to encode dynamins, kinesins, small GTPases, V-type ATPases, syntaxins and reticulons (Table I.S19). Among the high quantity of RAB-GTPase genes that we identified, only 4 (*RABA5B*, *RABA5C*, *RABB1B*, and *RABE1C*) were exclusively up-regulated in the dividing fruit, and 5 (*RABA2BV*, *RAB7*, *RABA4D*, *RABC2A*, and *RABA2A*) were exclusively up-regulated in the expanding fruit, whereas 5 RAB-GTPases were up-regulated in both developmental stages of the fruits (in both comparisons), including RABA1C, RABA1D, RABA1F, RABA3, and RABA6B (Figure I.17; Table I.S19). By contrast, none of the genes encoding a member of RAB-GTPase gene family was down-regulated in the expanding fruit (Figure I.17; Table I.S19), indicating that vesicle trafficking is among the most critical cellular activities for early olive fruit development.

3.10. Identifying transcription factors (TF) critical for early olive fruit development

Identifying new TF genes as well as their function in regulating the expression of candidate genes will aid a fuller understanding of the signalling pathways regulating early olive fruit development. Of the DEGs studied, 1,150 genes presumably encoding TFs of diverse families were differentially expressed during early fruit development in olive, most of them with a down-regulation pattern from 0 to 28 DPA (Figure I.18A; Table I.S20). In particular, 902 DEGs within the P14 vs. P0 comparison (the set of cell division-related genes), and 564 genes within the P28 vs. P14 comparison (the set of cell expansion-related genes). Our RNA-seq analysis revealed that 385 and 517 genes were up-regulated and down-regulated in the dividing olive fruit (the P14 vs. P0 comparison), respectively, while 174 and 390 genes were up-regulated and down-regulated in the expanding fruit (the P28 vs. P14 comparison),

respectively (Table I.S20). These DEGs were shown to be especially related to the TFs MYB, bHLH, ZF, homeobox domain proteins, WRKY, and bZIP families (Figure I.18A), implying that TFs from these families may take part in triggering the transcriptional cascade during early fruit development in olive.

The set of cell division-related genes is especially enriched in ZF proteins, whereas set of cell expansion-related genes was found to be rich mainly in the MYB and bHLH families (Figure I.18A). Hence, despite that two sets contained members from a number of TF families, clearly significant differences were found in each set regarding the proportion of families (Figure I.18A; Table I.S20). Also, distinct TF families make up each set: the Whirly, Trihelix and SNF2 (Helicase-like TF or CHromatin Remodeling Protein) families in the set of cell division-related genes, and the ARID/BRIGHT and VOZ families in the set of cell expansion-related genes (Figure I.18A; Table I. S20). Thus, our results indicate that the cell division phase is potentially controlled by up-regulation of E2F/DP, Whirly, TCP, and homeobox TFs, while the cell expansion phase may be controlled by up-regulation of MADS-box and GATA-binding proteins during early fruit development (Figure I.18A; Table I.S20). However, the most members of the zinc finger (ZF), the basic lecine zipper (bZIP), GRAS, WRKY, NAC, PLATZ, and AP2/ERF families were down-regulated genes during early fruit development in olive. In different gene groups from each set, the enrichment of sequence elements together with data concerning transcript abundance, provide a feasible set of TFs that are able to bind these elements and that may be valuable as a focus of future research.

Within the set of cell division-related genes (P14 vs. P0 comparison), three TFs (TFs) homologous to *AINTEGUMENTA (ANT)*, *bHLH61,* and *MYB3R-1* belonging to AP2/ERF, bHLH and MYB families, respectively, have been identified as the most abundant TFs. Indeed, these TF families were among the most widely represented class of proteins in the dividing olive fruit (Figure I.18A; Table I.S20). In addition, three bHLH (bHLH18, bHLH87, and bHLH93), and one ZF CCCH domain-containing (C3H2) protein were the most abundant TFs found in the expanding fruit (the P28 vs. P14 comparison).

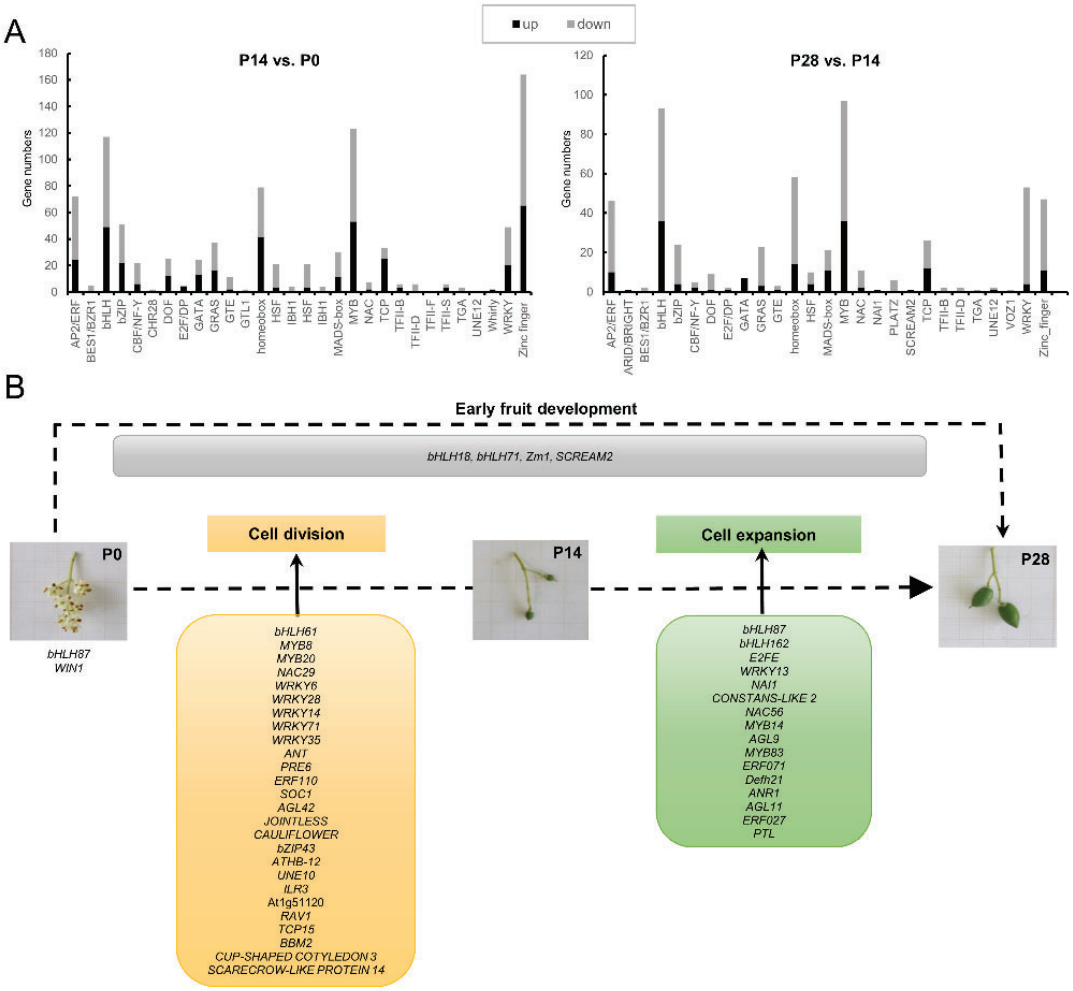

Figure I.18. Olive transcription factors (TFs) induced or repressed during early fruit development. (A) Summary of the number of significant changes in transcription factor transcripts between the different families during early fruit development in olive. Comparisons of fruit at 14 versus 0 DPA (P14 vs. P0), and 28 versus 14 DPA (P28 vs. P14) for significantly up-regulated (black) and down-regulated (grey) transcripts revealed differences in the families of TFs during early olive fruit development. (B) The TFs involved in regulating cell division and expansion phases during early fruit development in olive. The TFs (log_2FoldChange > 3, $p < 0.01$) were chosen for candidate TFs between the samples.

Furthermore, the major up-regulated differentially expressed TFs (Log_2 Fold Change >3) were identified during early fruit development. As shown in Figure 18B, 26 TFs that might be associated with cell division phase were identified, including two DOF-ZF (DOF3.4 and DOF4.7), two MYB (MY8 and MYB20), five WRKY (WRKY6, WRKY14, WRKY28, WRKY35, and WRKY71), two

MADS-box (SOC1 and AGL42), two NAC (NAC29), one AP2/ERF (ERF110) proteins, among others, while 16 TFs that might be involved in cell expansion phase, including two bHLH (bHLH87 and bHLH162), E2FE, WRKY13, NAI1, two MYB (MYB14 and MYB83), two AP2/ERF (ERF071 and ERF027) proteins, among others. We also identified four TFs that might be involved in both cell division and cell expansion phases, including two bHLH (bHLH18 and bHLH71), Zm1, and SCREAM2 (Figure I.18B). The abundance of the related transcripts suggests that these TFs play a regulatory role during early fruit development in olive.

4. Discussion

Up to the present, research on olive fruit development has concentrated mainly on the ripening process (Alagna et al., 2009, 2012; Galla et al., 2009; Martinelli and Tonutti, 2012; Parra et al., 2013; Bruno et al, 2019; Carbone et al., 2019; Xiaoxia et al., 2020; Briegas et al., 2020; Liu et al., 2021; Rao et al., 2021), and on a few genes from early developing fruit (Haralampidis et al., 1998; Banilas et al., 2005, 2011; Poghosyan et al., 2005; Gomez-Jimenez et al., 2010; Corbacho et al., 2018; Inês et al., 2019). Early fruit growth follows a complex developmental programme determined by both cell division and expansion (Gillaspy et al., 1993; Mauxion et al., 2021). In quantitative terms, little is known about these events in olive, a fleshy fruit in which substantial early growth occurs before the endocarp lignification. In the present study, this quantitative pattern is examined using cytological and ploidy analyses in early developing olive fruit of cv. 'Picual'. Our aim was to identify genes linked with cell division and cell expansion phases in early developing olive fruit through a global analysis of gene expression and hormonal content. These findings will help elucidate the molecular mechanisms that underlie early development in this fruit as well as its regulation.

Here, for the first time, we report detailed quantitative data at the ploidy level in olive fruit throughout early development. During early fleshy-fruit development, the spatial shift in the rate or time span of cell division within the ovary affects the final size of the ovary and, as a result, the final size of the fruit (Mauxion et al., 2021). In the present study, we found by flow cytometric analysis that cell division was triggered by pollination in the 'Picual' olive fruit from 0 to 21 DPA. Our data offered no evidence for cell

division in fruits from 28 to 42 DPA, and the increased fruit size/weight in this period apparently resulted from cell expansion, while both cell division and expansion coexisted at gradually increasing rates in the fruits until 21 DPA. However, longer durations of the cell division phase have been qualitatively reported in olive cultivars through 8 to 10 weeks (Rallo and Rapoport, 2001). In our study, a greater pericarp cell size was evident both in dividing cells (0-21 DPA) and in post-mitotic expanding cells (28-42 DPA) in the fruit, this notably contributing to significantly enlarged olive fruit at all the stages examined. As expected, after the cessation of cell division, pericarp cell size most rapidly increased in 'Picual' olive fruit and, indeed the maximum relative rate of cell expansion in the fruit occurred at 42 DPA, while the maximum relative rate of cell division in the fruit was found at 14 DPA. At this stage, we detected a low, but significant proportion of endoreduplicated cells up to 8C (one endocycle) in olive fruits compared with tomato fruits up to 256C or even 512C (Bergervoert et al., 1996; Joubès et al., 1999; Cheniclet et al., 2005; Bourdon et al., 2010; Chevalier et al., 2014). Endoreduplication increases ploidy in individual cells and reportedly correlates not only with high metabolic activities, cell differentiation, post-mitotic cell growth, and rapid anisotropic cell expansion, but also with the capacity to react under DNA damage (Robinson et al., 2018; Tsukaya, 2019). In particular, the ploidy increase is strongly correlated with increased cell size (Chevalier et al., 2014; Robinson et al., 2018). In tomato fruit, previous studies have reported that endoreduplication begins in developing ovaries when organogenesis-related cell division ends (Cheniclet et al., 2005; Chevalier et al., 2014). However, with the exception of some Rosaceae species (e.g. apricot, peach, and plum), endoreduplication does not occur in most of the species where fruit development lasts for a long period (over 14 weeks) of time (Bourdon et al., 2010), as is the case of the olive fruit. In the present study, we report a rapid surge in 8C nuclei after anthesis, at 14 DPA, suggesting that endoreduplication in 'Picual' olive fruit cells at 14 DPA supports their very rapid post-mitotic cell expansion from 21 DPA onwards.

To date, prime determinants of fleshy fruit growth identified by analysing transgenic lines, mutants, or the natural diversity of genotypes with altered fruit size and shape have been associated with early events affecting the pattern of cell division within the ovary prior to anthesis or in the new fruit

just after anthesis in tomato (Mauxion et al., 2021). However, molecular-genetic information on regulators associated with these events in olive fruit remain limited. CDK-CYC complexes help regulate the cell cycle (De Veylder et al., 2011; Mauxion et al., 2021). Our data indicate that specific CYC and CDKs are involved in different phases during early olive fruit development. After fertilization, the cell division phase results mainly from the gene activity of CYCA2, CYCA3, CYCB3, CYCU1, and CDKC1. The post-mitotic cell expansion phase is associated with the gene activity of CYCA1, CYCB2, and CYCC1, whereas transcripts encode CYCD3;1, CYCD6;1, and CDKB1 proteins are associated with both cell division and cell expansion phases during early fruit growth in olive, in accordance with previous studies (Joubès et al., 2000; Lemaire-Chamley et al. 2005; Fu et al., 2008; Ando et al., 2012; Kang et al., 2013; Farinati et al., 2021; Luo et al., 2021). In Arabidopsis, the M-specific CDKB1;1 constitutes the plausible candidate kinase that forms part of the mitosis-inducing factor (MIF) when it is bound to the A-type cyclin CYCA2;3, capable of inhibiting endoreduplication when it is fully active (Boudolf et al., 2009). The up-regulation of members of the cyclin D family, CYCD3;1 and CYCD6;1, during early fruit growth have been previously reported (Lemaire-Chamley et al. 2005; Fu et al., 2008; Luo et al., 2021). In fact, the cyclin D family has a major part in the regulation of the RBR/E2F pathway, activating CDK-mediated RBR phosphorylation and upsetting its interactions with E2F (De Veylder et al., 2011). A number of genes, such as *RBR3, E2FA*, and *E2FE*, notably affect the balance of mitotic and endoreduplicating cells or the number of endocycles in Arabidopsis (Ramirez-Parra and Gutiérrez, 2007), which were also up-regulated during early olive fruit development. In Arabidopsis, E2FA, a protein involved in cell cycle regulation, exerts a dual function, not only maintaining cell proliferation but also stimulating cell expansion needed in differentiating cells for the growth of organs by promoting endoreduplication (Magyar et al., 2012). This protein was exclusively expressed in the dividing olive fruit, indicating that it might be involved in the regulation of cell division during early olive fruit development.

By binding to and inhibiting cyclin-dependent kinase complexes, CKIs promote sustained endoreduplication in cells (Robinson et al., 2018). At 14 DPA, the maximum mitotic activity is associated with cell-size changes in the olive fruit pericarp followed by endoduplication and is positively correlated

with the expression of members of CKI family (*CKI3*, *SMR6* and *SMR9* genes), while the *CKI7* expression is down-regulated in the dividing olive fruit. Notably, we found that one gene homologous to AP2-like ethylene-responsive type TF (*SMOS1*), a putative orthologue of the AtSMOS1 (At2g41710) protein in Arabidopsis, is transcriptionally induced during early olive fruit development. SMOS1 is involved in the transcription activation of a specific set of SIAMESE-RELATED (SMR) family genes, encoding plant-specific CKI, and thus inhibiting cell cycle progression at G2 and promoting the onset of endoreplication (Robinson et al., 2018). In our analysis, *SMR9* exhibited a similar expression pattern as that of *SMOS1*. The transcript level of *SMR9* rose in both comparisons during early olive fruit development, leading to the hypothesis that SMOS1/SMR9 is involved in cell cycle control, quickly triggering the repression of cell division during early olive fruit growth. Recently, Nomoto et al. (2022) documented that AtSMOS1 forms a dimer with SCARECROW-LIKE28 (SCL28), a GRAS TF that in Arabidopsis plays a critical part in regulating cell size, as part of a transcriptional network downstream of the central MYB3Rs that regulates the G2 to M phase of cell cycle transition. In the present work, we have shown that early fruit growth in olive was associated with up-regulated *SCL28* and *MYB3R-1* transcripts. This suggests that *SCL28* controls cell expansion and differentiation by promoting endoreplication onset during early fruit growth. Thus, the expression of *SCL28*, *SMOS1*, and *MYB3R-1* shows to positively correlate with early fruit growth in olive, indicating that the regulation of cell division and expansion in the olive fruit can be similar to that in other systems.

In Arabidopsis, researchers have identified a small number of organ-size regulators. Notably, among the specific genes in the dividing olive fruit, two *Growth-Regulating Factor* (GRF) genes, GRF1 and GRF3, which encode a transcription activator that plays a role in the regulation of cell proliferation and size in Arabidopsis leaves (Kim and Tsukaya, 2015), abundantly accumulated in the dividing olive fruit at 14 DPA, indicating the potential roles of these genes in signaling pathways for the regulation of early olive fruit growth. A previous study has shown GRF3 to be a component in a network composed of miR396, GRFs, and their interacting factors (GIFs) contributing to at least partial regulation of meristem function by controlling cell proliferation after infection by cyst nematode (Hewezi et al., 2012). In

tomato plants expressing higher levels of *SlGRF1* to -*5*, fruit size and weight are increased as a result of an increased size of the epidermal cells (Cao et al., 2016). Our findings provide a valuable tool for unravelling the physiological function of GRF1 and GRF3 in future studies. Conversely, negative effectors of cell proliferation in Arabidopsis, such as BIG BROTHER (BB) (Vanhaeren et al., 2017), was also identified in our analysis. Here, 8 *BB* genes were up-regulated in the expanding olive fruit at 28 DPA, indicating that at least some members of BBs play a role not only in limiting the cell-proliferation stage, but also in fostering the transition towards cell differentiation and expansion in early olive fruit growth. Nevertheless, the way in which these different effectors act on the regulatory genes of the cell cycle in developing olive fruit has not been completely elucidated.

Of particular interest is also one member of AP2 family, homologous to AINTEGUMENTA (ANT), which was the most abundant TF transcript expressed in the dividing olive fruit. ANT is required in the control of cell proliferation in Arabidopsis, and regulates growth and cell numbers during organogenesis, modulating auxin biosynthesis in the ovule via regulation of YUCCA4 (Li et al., 2021b). In the present work, on the base of homology and the strong up-regulation of *ANT* exclusively in the dividing olive fruit, we hypothesise that this TF plays a major role in the regulation of cell division and size through its downstream control of auxin biosynthesis in the fruit, consistently with the IAA levels detected in the dividing fruit at 14 DPA. Previously, it has been suggested that *CYCD3;1* is a target of ANT (Wu et al., 2011). *CYCD3* genes regulate the length of the temporal period of mitotic cell division during aerial organ development, and are induced by CKs in Arabidopsis (Randall et al., 2015). According to our data, the *CYCD3;1*, *ANT*, and CK metabolism, together with signaling gene expression share a common shift during early olive fruit growth, indicating that these components may act in conserved pathways linking CKs to developmentally regulated cell division in the fruit enriched mainly in CKs (*t*Z). Indeed, our comprehensive study of varying gene expression, together with analyses of different hormonal composition unveils complex hormone control underlying early fruit growth in olive, with intricate temporal variations, implying distinct regulatory programmes. We found that the relative importance of CK (*t*Z), and SA were higher during periods of more intense

cell division, while IAA, GA_1, GA_4 and ABA had higher relative importance as cell division approaches its end, when the growth olive fruit depends primarily on cell expansion. Also, cross-talk between CKs, GAs, and auxins stimulate cell growth during early development (Lemaire-Chamley et al., 2005; Pattison et al., 2014), is also likely in developing olive fruit where co-expression of the following occurs: *YUCCA10* (auxin synthesis); *TIR1*, *IAA9*, *ARF4, ARF8*, *ARF9, ARF18,* and *SAUR50* (auxin signaling); *PIN1* and *PIN5* (auxin transport); *GGPPS* (GA synthesis); *CKX3* and *CKX9* (CK metabolism); and *HK3*, *HK4* and *ARR5* (CK signaling).

Key candidate genes functioning in CK (*LOG3*, *LOG8*, *LOG10, CKX1, CKX7,* and *ARR12*) and auxin (*LAX2*, *LAX4*, *LAX5, PIN1, PIN7, GH3.6, GH3.9, GH3.10, IAA8, IAA26, ARF1, ARF2, ARF3*, *ARF5*, *ARF6*, *ARF10*, *ARF17*, *ARF19*, and *ARF22)* metabolism and signaling showed a preferential expression in the cell division phase during early olive fruit growth, while some other candidate genes encoding proteins with roles in auxin (*PIL2*, *PIL6*, *PIL7, IAA29*, *GH3.1,* and *SAUR72)* and GA (*GA3ox, GID2*) metabolism and signaling could act in the post-mitotic cell expansion phase during early fruit growth. Free CK hydrolysed from its conjugates by CK riboside 5'-monophosphate phosphoribohydrolases (LOG) exclusively in the dividing fruit could in turn activate and coordinate the expression of cell division-related proteins (via ARR12). In the case of GA, our data indicate that GA signaling is negatively regulated by *GAI1* and *RGL1* (DELLA proteins) in the cell division phase, whereas GA signaling (*GID2* receptor) is up-regulated in the post-mitotic expansion phase during early olive fruit development. These results agree with the established notion that GA participates mainly in the cell expansion process in the fruit (Mauxion et al., 2021). Moreover, PACLOBUTRAZOL RESISTANCES 6 (PRE6), belonging to the bHLH TF family, which is involved not only in auxin, GA, and BR signaling, but also light responses regulating cell expansion in Arabidopsis (Zhang et al., 2009; Mara et al., 2010; Zheng et al., 2017), was down-regulated during early olive fruit development. The down-regulated *PRE6* expression is hypothesised to promote cell expansion through GA, auxin, and BR modulating response in olive fruit, as in Arabidopsis. In tomato, SlPRE2 and AtPRE1 proteins are involved in cell elongation through GA modulating response (Zhu et al., 2019). Thus, our data reveal that CKs as well as auxins positively affect cell division, whereas the GA

and auxin hormones display positive effects on post-mitotic cell expansion during early olive fruit development.

Auxins as well as GA reportedly serve as early signals for fruit set as well as for strong fruit growth (Pattison et al., 2014). A weakened auxin signaling as well as fainter GA stimulation have been reported to induce the change from a regular cell cycle to an endocycle (De Veylder et al., 2011). The role of auxins in early fruit growth has been amply reported (Catalá et al., 2000; Pandolfini et al., 2002). In tomato, auxin signaling appears to be a prerequisite for the expansion of the fruit locular cells (Lemaire-Chamley et al., 2005), for the negative control of the division of the fruit cells (de Jong et al., 2015), and for fruit set (de Jong et al., 2009; Wang et al., 2009). Our data reveal that the content of IAA increased progressively during early olive fruit development, and that expression levels for the auxin-conjugating enzymes, GH3.6 and GH3.9, were down-regulated in the expanding olive fruit at 28 DPA, consistently with the highest IAA levels detected in olive fruit at this time. Also, this is consistent with the accepted idea that the release of auxins produced by seeds and/or surrounding fruit tissues trigger fruit growth through cell expansion (Gillaspy et al., 1993; Lemaire-Chamley et al., 2005). In this light, we propose that an increase in auxin and GA contents as well as GA signaling stimulation trigger the shift from a regular cell cycle to the endocycle in olive fruit, whereas the two hormones, auxin and CK, could activate the cell cycle in the developing fruit, according to absolute levels, cell sensitivity, and other signaling cross-talk, such as BR (*BRI1*, *BES1/BZR1*), PA (*ADC*, *OTCase*, *SPDS*, *PUT2*, *PUT4*), NO (*NOS*), ABA (*PYL8*, *PYL9*, *ABA-8-OH*, *ABI5*), SA (*SAMT*, *SABP2*, *NPR2*), ethylene (*ERF11*, *ERF12*, *ERF38*, *ERF107*, *ERF118*, *ERF71*, *ERF38*, *ERF61*, *ERF27*), strigolactone (*DAD2*, *D14*), and signal peptides (*SBT4.15*) which apparently also participate in an intricate interaction web regulating the early fruit development in olive.

According to their expression profiles, other genes appear to be promising candidates for the main regulations in the early development of olive fruit. In our RNA-seq analysis, four TFs, SCREAM2 (or bHLH33), bHLH18, bHLH71, and Zm1 (R2R3-MYB), were identified within the differentially expressed gene set, that were all up-regulated in both the dividing and the expanding olive fruits (P14 vs. P0, and P28 vs. P14 comparisons) and thus, linkable to cell division

and cell expansion phases during early fruit development in olive. SCREAM2 (or bHLH33, a putative orthologue At1g12860) encoding a key component of core regulatory units in stomatal development probably by controlling successive roles of SPCH, MUTE, and FAMA (bHLH proteins) in Arabidopsis (Kanaoka et al., 2008). Additionally, SCREAM is INDUCER of CBF EXPRESSION1 (ICE1), a bHLH TF that positively regulates the cold-induced transcriptome and freezing tolerance (Kanaoka et al., 2008). According to our analysis, a homologue of *ICE1* is also up-regulated in both comparisons, suggesting that the two proteins prompt sequential steps in the development programme (i.e. entry, proliferation, and terminal differentiation) of the stomatal cell during early fruit development in olive. Moreover, we found that other members of bHLH TF family, including homologues of bHLH18 (a putative orthologue At2g22750) and bHLH71 (At5g46690), are induced during early olive fruit development, while bHLH61 (At5g10570) are exclusively up-regulated in the dividing olive fruit, indicating that bHLH61 might be involved in the regulation of cell division, and that bHLH87 (At3g21330) and bHLH162 (At4g20970) are exclusively up-regulated in the expanding olive fruit. These results suggest that these bHLH proteins are involved in a convergence point of early fruit development signaling, but none have been previously associated with early fruit growth. The bHLH proteins represent prime regulatory components in networks of transcription that control several biological processes, such as fruit and flower development (Liljegren et al., 2004; Tani et al., 2011; Wang et al., 2019b). Therefore, changes in the temporal distribution of these proteins could lead to unexpected cross-talk in the regulatory network of genes.

Moreover, bHLHs and MYBs or bZIPs bind to DNA as either homodimers or heterodimers, multiplying the feasible regulatory combinations (Ezer et al., 2017). In this context, also, MYB and bZIP TFs are members of TF families abundantly represented in the developing olive fruit. In the dividing olive fruit, our results demonstrated up-regulation of 33 (MYB20, MYBS3, among others) out of 122 MYB genes identified, and 17 (bZIP11, bZIP44, among others) out of 49 bZIP genes identified, while 20 (MYB14, MYB83, among others) MYB genes and 4 bZIP (bZIP6, bZIP11, bZIP18, and RF2b) genes were up-regulated in the expanding olive fruit. We should not disregard the possibility that bHLH proteins act as an interaction partner for MYB or bZIP

TFs in regulating genes involved in processes downstream during early growth in the olive fruit. More research is needed in order to determine whether or not these bHLH TFs participate jointly with MYB or bZIP proteins in the signaling of developing olive fruit. From this perspective, MYB TFs appear to take part in controlling the cell cycle not only in animals, but also in plants and other higher eukaryotes (Ambawat et al., 2013). MYB factors are involved in regulating the transcription of cyclin genes via MYB recognition elements in cyclin promoters (Ito et al., 2001). Our RNA-Seq analysis showed that the up-regulation of MYB3R-4 (3R-MYB, AT5G11510.1), which activates mitotic gene expression and CK response (Furuya et al., 2021), and MYB3R-5 (3R-MYB, AT5G02320.1), which is member of DREAM complex (Chen et al., 2017), are probably associated with the cell division phase, while the up-regulation of MYB3R-1 (3R-MYR, AT4G32730.2) is likely associated with the cell expansion phase during early olive fruit development. Additionally, members of the R2R3-MYB family have been identified in olive fruit, as in the case for Zm1, which is involved in the regulation of flavonoid biosynthesis (Franken et al., 1989). The increased expression of *Zm1* in both the dividing and expanding olive fruits suggests the involvement of Zm1 in early fruit growth. Likewise, many R2R3-MYB genes also act in signal-transduction pathways of ABA, GA, JA, and SA (Ambawat et al., 2013), supporting the contention MYB proteins constitute vital components of many hormone-mediated transcriptional cascades, such as ABA, GA, and SA, which regulate early fruit development in olive. Thus, the present study reveals novel regulators associated with early fruit growth and provides a useful resource for further characterization of the physiological functions of these regulators in olive and other plant species.

5. Conclusions

Cytological, ploidy, hormonal, and transcriptional analyses reveal the rate and duration of cell division and cell expansion phases during early olive fruit growth as well as the regulation of these phases. The present study provides evidence that CKs may regulate cell division mainly through the *ARR12* expression gene, and that CKs and SA appear to correlate positively with cell division during early olive fruit development, while GA (via *GA3ox* and *GID2*), auxin (via *PIL2*, *PIL6*, *PIL7*, *IAA29*, *GH3.1*, and *SAUR72*), and ABA (via *ABI5*) have higher relative importance in the period where fruit growth depends mainly on cell expansion. In particular, CK (*tZ*) and GA_4 present different accumulation patterns during early olive fruit development, suggesting that the *tZ* and GA_4 hormones act on early olive fruit development in opposite ways during the transition from cell division to cell expansion. Furthermore, this study offers the first detailed analysis available for an array of cellular responses under the control of gene expression leading to early fruit development in olive. Through gene expression studies, a selection was made of the candidate genes having well-known molecular roles in different biological processes affecting olive fruit growth. This gene expression profile, together with hormonal regulators, will help clarify gene regulatory networks during early olive fruit development. In practical terms, it will aid in designing specific approaches for crop breeding and engineering, facilitating the development of the table olive and olive oil industries.

Capítulo II

Regulación hormonal durante el crecimiento y maduración del fruto de olivo

Hormonal regulation during olive fruit growth and ripening

Abstract

The olive (*Olea europaea* L. subsp. *europaea* var. *europaea*) has cultivars showing a large diversity for fruit quality and yield traits. However, the hormonal mechanisms underlying the fruit growth and ripening in olive, a non-climacteric fruit species, remains largely uncharacterized. In this study, we investigated the physiological and hormonal changes as well as the expression patterns of hormone-related genes during fruit growth and ripening in two olive cultivars, 'Arbequina' and 'Picual', with contrasting in fruit size and shape as well as differing fruit ripening rate and duration. Hormonal profiling revealed that olive fruit growth involves a lowering of auxin (IAA), cytokinins (CKs) and jasmonic acid (JA) levels as well as an increase of salicylic acid (SA) levels from the endocarp lignification stage to the onset of fruit ripening in both cultivars. During olive fruit ripening, both abscisic acid (ABA) and anthocyanins levels rose, while JA levels fell and SA levels showed no significant changes in either cultivar. In contrast, differential accumulation patterns of gibberellins (GAs) were found between the two olive cultivars during fruit growth and ripening. GA_1 was not detected at either stage of fruit development in 'Arbequina', revealing a specific association between the GA_1 and 'Picual', the cultivar with large sized and elongated fruit and fast-ripening. Moreover, unlike 'Picual' fruit, 'Arbequina' fruit (slow-ripening) accumulated auxin and CKs (tZ) during olive fruit ripening, suggesting that endogenous GAs, IAA, and CKs may act in modulating olive fruit ripening duration. Overall, the trend of ABA content in olive fruit was consistent with that of the GAs, in good agreement with the upregulated *OeNCED* and *OeGGPS* gene expression levels, but in disagreement with the IAA and CK (*t*Z) profiles such that ABA and GA levels rising and the resulting elevated ABA + GA/IAA + CK ratio coinciding with olive fruit fast-ripening. Taken together, the results suggest that endogenous GA_1 levels can regulate olive fruit size and shape, as well as fruit ripening duration. Such detailed knowledge may be of help to

design new strategies for effective manipulation of olive fruit size and ripening duration.

Keywords: fruit ripening; fruit size; gene expression; hormone; olive

1. Introduction

The olive (*Olea europaea* L. subsp. *europaea* var. *europaea*), one of the most widely cultivated fruit trees worldwide for the table olive and oil purposes of its fruit, display significant phenotypic variation in olive fruit quality and yield traits (Beltrán et al., 2004, 2010; Barranco et al., 2005; Baldoni and Belaj, 2009; Gomez-Jimenez et al., 2010a; Parra-Lobato et al., 2012; De la Rosa et al., 2013; Bartolini et al., 2014; Rallo et al., 2018; Belaj et al., 2020; Rugini et al., 2020). Despite the importance of understanding the control of olive fruit size and ripening, the hormonal regulatory mechanisms underlying how olive fruit growth and ripening, as well as the relative roles of the plant hormones on different olive fruit traits remain poorly understood.

Like stone fleshy fruits, the olive fruits with varied morphologies from different olive cultivars of this species share common events in their life cycle that are crucial for their development including fertilization and fruit set, early fruit growth, endocarp lignification, late fruit growth, fruit maturation and ripening (Conde et al., 2008; Breton and Bervillé, 2013). This period can oscillate between 5 and 9 months, from the floral anthesis stage to the fully ripe fruit stage, depending on olive cultivar, climactic conditions, and cultural practices (Beltrán et al., 2004; Conde et al., 2008; Breton and Bervillé, 2013; De la Rosa et al., 2013; Mousavi et al., 2019; Belaj et al., 2020; Hamze et al., 2022). The successful fertilization of the ovule is followed by cell division and expansion, resulting in the growth of the olive fruit (Rallo and Rapoport, 2001; Rosati et al., 2012; Camarero et al., 2023). Indeed, olive fruit may either undergo growth entirely by both cell division and expansion coexisting at gradually increasing rates until 21 days post-anthesis in 'Picual' olive cultivar. Meanwhile, olive fruit cell expansion, without cell division, can last as long as 3 weeks more before endocarp lignification (Camarero et al., 2023). Subsequently, the late growth of olive fruit after endocarp lignification comprises mainly cell expansion, which is responsible for the maximum fruit size, and oil accumulation (Conde et al., 2008; Breton and Bervillé, 2013).

However, recently, it has been demonstrated that cell division is induced by water deficits in olive fruit during this late fruit growth phase (Hernández-Santana et al., 2021). Finally, olive fruit undergo a complex and highly coordinated series of events comprised in the developmental process of fruit ripening which is characterized by gradual increases in oil and anthocyanin contents (Conde et al., 2008; Martinelli et al., 2012; Breton and Bervillé, 2013). Moreover, the olive fruit ripening process depends on the olive cultivars regarding different dates of the onset of fruit ripening, as well as different fruit ripening durations and rates (Beltran et al., 2004; Barranco et al., 2005; De la Rosa et al., 2013; Gómez-Rico et al., 2008; Dag et al., 2011; Ardila et al., 2012; Camposeo et al., 2013; Rallo et al., 2018; Belaj et al., 2020). After olive fruit ripening, several olive cultivars undergo massive natural fruit abscission, making the abscission zone in olive fruit an agronomically important trait for mechanically harvested fruit (Gomez-Jimenez et al., 2010b; Parra-Lobato et al., 2017; Parra et al., 2020; Parra and Gomez-Jimenez, 2020).

Generally, olive fruits are classified as a non-climacteric fruit (Maxie et al., 1960) because previous studies found no burst of ethylene during olive fruit ripening, and ethylene treatment after harvest showed no olive fruit softening or anthocyanin synthesis (Shulman et al., 1974; Crisoto et al., 2005). However, while information regarding ethylene metabolism in olive fruits is limited, several studies have tracked fruit respiration during olive fruit ripening (Tombesi et al., 1994; García et al., 1995; Ranalli et al., 1998; Proietti et al., 1999; Nanos et al., 2002), in some cases, reporting contradictory results. Indeed, ethylene is effective in olive fruits then the ethylene inhibitors, 1-methyl cyclopropropene (1-MCP) or 1-amino ethoxyvinyl glycine (AVG), reversed the ethylene responses, but the impact of these treatments or of the exogenous ethylene depended on the olive cultivars (Rugini et al., 1982; Nanos et al., 2002; Ramin, 2007; Tsantili and Pontikis, 2004; Amini and Ramin, 2015; Kafkaletou et al., 2019; López-García et al., 2022). Moreover, the ethylene precursor level, the 1-aminocyclopropane-1-carboxylic acid (ACC), increases as olive fruit ripens (Ardila et al., 2012), suggesting thus, differential fruit ACC levels and ethylene sensitivity between olive cultivars.

Because changes in plant hormone metabolism during fleshy fruit development and ripening may be part of a mechanism controlling the

transitions from pericarp-cell expansion to ripening, hormone levels should be maintained within strict limits (McAtee et al., 2013; Kumar et al., 2014; Fuentes et al., 2019; Fenn and Giovannoni, 2021; Kou et al., 2021; Li et al., 2021; Fan et al., 2022; Perotti et al., 2023). Moreover, several studies have indicated that the regulation of fleshy fruit development in both perennial and annual crops, and therefore the final quality of fleshy fruit involves differential plant hormone levels between cultivars within the one plant species (Coelho et al., 2019; Khew et al., 2020; Lee et al., 2020; Ponce et al., 2021; Renaudin et al., 2023). In olive, although the temporal transcriptional, proteomic, and metabolic changes during olive fruit ripening in different olive cultivars (Alagna et al., 2009, 2012; Galla et al., 2012; Martinelli et al., 2012; Bianco et al., 2013; Parra et al., 2013; Parvini et al., 2015; Iaria et al., 2016; Mougiou et al., 2018; Inês et al., 2018, 2019; Bruno et al., 2019; Carbone et al., 2019; Briegas et al., 2020; Xiaoxia et al., 2020; Hernández et al., 2021; Liu et al., 2021; Rao et al., 2021) have been well reported, the accumulation dynamics of the different plant hormones during fruit ripening have not been previously described. In particular, high levels of cytokinins (CKs), gibberellins (GAs), and polyamines (PAs) have been reported in the olive developing fruits (Shulman and Lavee, 1976, 1980; Gomez-Jimenez et al., 2010a), whereas abscisic acid (ABA), salicylic acid (SA) and GAs are abundant in the olive ripe fruit (Briegas et al., 2020). In this context, the preharvest application of plant hormones to different olive cultivars has been lately described to increase fruit size and to enhance the content of bioactive components, antioxidants, among others, and thus to preserve the oxidative stability of olive fruits during storage (Corbacho et al., 2018; Blanch et al., 2018a,b; Blanch et al., 2020a,b). Recently, we have shown the first detailed analysis available for an array of cellular responses under the control of gene expression together with hormonal changes leading to early fruit growth in olive (Camarero et al., 2023). CKs and SA appear to correlate positively with cell division during early olive fruit development, while GA, auxin, and ABA have higher relative importance in the period where fruit growth depends mainly on cell expansion (Camarero et al., 2023). However, a characterization of the hormonal composition during late fruit growth in olive is still lacking.

The purpose of the present study was to investigate the hormonal regulatory mechanisms underlying olive fruit growth and ripening. For this purpose,

comparatively physiological, cytological and hormonal analyses of olive cultivars with contrasting fruit size and shape as well as ripening duration, together with the expression patterns of hormone-related genes during olive fruit growth and ripening are reported. These data provide a starting point to dissect the hormonal differences of olive fruit growth and ripening among olive cultivars. We report on the hormonal control that variation in large and elongated- versus small and round-fruit as well as fast- versus slow-ripening could be correlated to the relative presence of GA_1 in olive fruit. Collectively, our results highlight the possible role of GA in coordinating the fruit size and the progression of fruit ripening in olive, which would have relevant biological and practical implications.

2. Materials and methods

2.1. Plant material and cytological analysis

Olive trees (*Olea europaea* L. cv. 'Picual' and 'Arbequina') grown under drip irrigation and fertirrigation during the 2018 and 2019 growing seasons in an orchard near Badajoz (Spain) were studied. Fruits at five specific developmental stages (Fig.II.1A) were randomly tagged, collected, and processed as previously described (Inês et al., 2018). The two cultivars studied, 'Arbequina' and 'Picual', with different final fruit sizes and shapes (Gomez-Jimenez et al., 2010a; Ardila et al., 2012), required different days after green fruit maturation to reach their full fruit ripening (90 and 50 days, respectively). A total of 250 fruits from 10 olive trees per cultivar were used for each developmental stage. As a means of minimizing the effects related to asynchronous fruits ripening within the same tree, fruits with similar pigmentation were picked from all around the external parts of the tree canopy. Whole fruits of 'Arbequina' and 'Picual' olive cultivars were weighed, and the longitudinal and equatorial diameters were measured at different developmental stages (Fig.II.1). Fruit firmness was measured at four equatorial regions of the fruit using a penetrometer (model SMT-T-50, Toyo Baldwin, Tokyo, Japan) fitted with a 5 mm plunger. An initial group of pericarp samples from different developmental stages was used for cytological analysis, and another group was immediately frozen in liquid nitrogen and stored at -80ºC for total lipids, anthocyanins, hormones, and RNA extractions.

In the cytological study, at least three biological replicates were made at each stage. For this, samples were sliced 0.3 to 0.6 mm thick and quickly fixed in ethanol-acetic acid (3:1, v/v) for 2 h at ambient temperature. Then the samples were rinsed 3 times using 70% 226 ethanol, dried using an ethanol series, and finally embedded in Technovit 7100 (Kulzer). Sections (3 mm) cut with glass knives were stained with 0.04% (w/v) toluidine blue and photographed using a Zeiss Axiophot microscope coupled to a Spot digital camera (Diagnostic Instruments).

2.2. Extraction of total lipids and anthocyanins

Total lipids were extracted from 800 mg fruit pericarps of freeze-dried powder following Inês et al. (2018). Extracted lipids for each stage of development from three different extractions were quantified gravimetrically after evaporation until dryness under nitrogen at 40ºC. Total anthocyanins were extracted from fruit pericarps and determined according to the method reported in Piga et al. (2005). All experiments were conducted with at least three biological replicates.

2.3. Quantification of plant hormones

A pool of 100-mg fresh weight/sample was used for each measurement split into 3 independent biological replicates per sample. The plant hormones were quantified as described by Camarero et al. (2023). The hormones were analysed by electrospray ionization and targeted-SIM using a Q-Exactive spectrometer (Orbitrap detector, ThermoFisher Scientific, Spain). The concentrations of hormones in the extracts were determined using embedded calibration curves and the Xcalibur 4.1 SP1 build 48 and TraceFinder programs.

2.4. RNA extraction and quantitative real-time PCR analysis

The total RNA was extracted from fruit samples as in Briegas et al. (2020). For each sample, three biological replicates were collected of the same developmental stage. Previously published RNA-Seq data (Briegas et al., 2020) were mined for hormone metabolism and signalling related genes. qRT-PCR assays were performed with gene-specific primers (Table II. S1). The cDNA was amplified using a SYBRGreen-PCR Master kit (Applied Biosystems) containing an AmpliTaq Gold polymerase on an iCycler (BioRad Munich),

following the protocol provided by the supplier. Samples were subjected to thermal cycling conditions of DNA polymerase activation at 94ºC, 45 s at 55ºC, 45 s at 72ºC, and 45 s at 80ºC; a final elongation step of 7 min at 72ºC was performed. The melting curve was designed to increase by 0.5ºC every 10 s from 62 ºC. The amplicon was analysed by electrophoresis and sequenced for confirmation of identity. The qRT-PCR efficiency was estimated via a calibration dilution curve and slope calculation. Expression levels were determined as the number of cycles needed for the amplification to reach a threshold fixed in the exponential phase of the PCR (CT). Data were normalized for the quantity of the *O. europaea* ubiquitin (*OeUB*) gene (Gomez-Jimenez et al., 2010a). At least two to three independent RNA isolations were used for cDNA synthesis, and each cDNA sample was subjected to real-time PCR analysis in triplicate.

2.5. Statistical analysis

All the experiments were carried out in triplicate, and all data are presented as mean ± standard deviation. Variables of three replicates were compared using Tukey's multiple-range test, and a *p* value at 0.05 was considered significant.

3. Results

3.1. Physiological changes during olive fruit growth and ripening

As observed previously (Gomez-Jimenez et al., 2010a), olive cultivars, such as 'Picual' and 'Arbequina', displayed significant phenotypic variation in fruit size and shape: 'Picual' is an olive cultivar with large sized and elongated fruit, while 'Arbequina' bears small sized and round shaped fruit. In the present study, the physiological and cytological changes during fruit development in two olive cultivars, 'Arbequina' and 'Picual', were recorded (Fig.II.1). Five major developmental stages were established to define olive fruit development in 'Arbequina' and 'Picual' cultivars: 1) 'small immature fruit' with complete pit hardening, 2) 'large immature green fruit', 3) 'mature green fruit', 4) 'turning fruit' and 5) 'fully ripe fruit' (Fig.II.1). Under the experimental conditions used, mature green 'Picual' olive fruits required about 50 days for complete ripening, as indicated by the fully black colour and softening of the fruit, while mature green 'Arbequina' olive fruits required

about 90 days. Thus, a marked variability was found in the duration of the fruit ripening process between the two olive cultivars: fast-ripening cultivar ('Picual' olive cultivar) and slow-ripening cultivar ('Arbequina' olive cultivar).

The cytological observations and comparison of growth curves indicate that the developmental stages of 'Arbequina' fruit are equivalent to that of 'Picual' fruit (Fig.II.1 and 2). The fruit pericarp cells were tightly arranged in young developing fruit (stage 1) of both olive cultivars, but as the fruit pulp expanded (stages 2-4) and ripened (stage 5) the fruit pericarp cells began to lose their close connections. In the fully ripe fruit (stage 5) of both cultivars, pericarp cells had fewer points of attachment to their neighbours and air spaces developed between cells, indicating that intercellular adhesion was declining (Fig.II.1C-D).

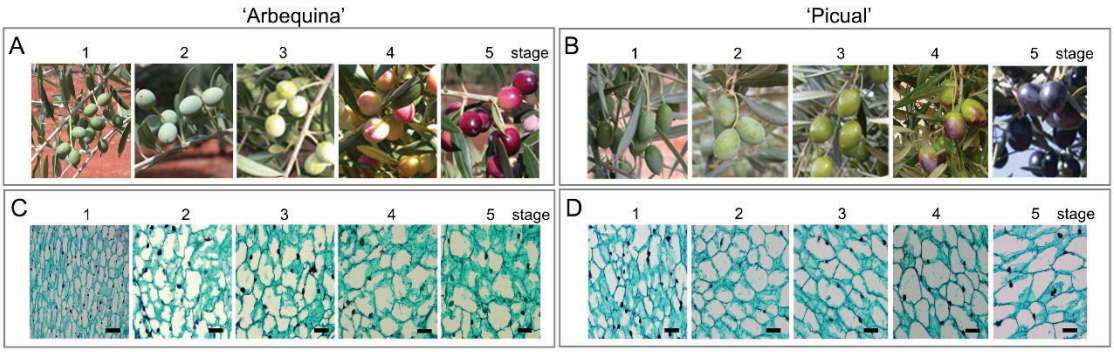

Figure II.1. Development of 'Arbequina' and 'Picual' olive fruits. Morphological changes of olive fruit of 'Arbequina' (A) and 'Picual' (B) cultivars during fruit growth and ripening. Pericarp cross-section of olive fruit of 'Arbequina' (C) and 'Picual' (D) cultivars during the stages of olive fruit development. Stage 1: 'the completed pit hardening'; Stage 2: 'the immature green' (peak of pericarp cell expansion); Stage 3: 'the mature green'; Stage 4: 'the turning' (the onset of fruit ripening); Stage 5: 'the fully ripe'. Bars = 100 μm.

'Arbequina' and 'Picual' olive fruits followed a highly reproducible progression of growth including increases in weight, longitudinal and equatorial diameters, mesocarp cell area, and pericarp thickness from developmental stage 1 to 4, while the values remained constant between stages 4 and 5 in both olive cultivars (Fig.II.2A-E).

During the pulp growth phase, olive fruit growth leads to a significant increase in fruit weight in both olive cultivars (Fig.II.2A). Consequently, the

fruit weight augmented 3-fold (a 66% of final fruit weight) in 'Arbequina' and 4-fold (a 75% of final fruit weight) in 'Picual' cultivar during this phase (Fig.II.2A).

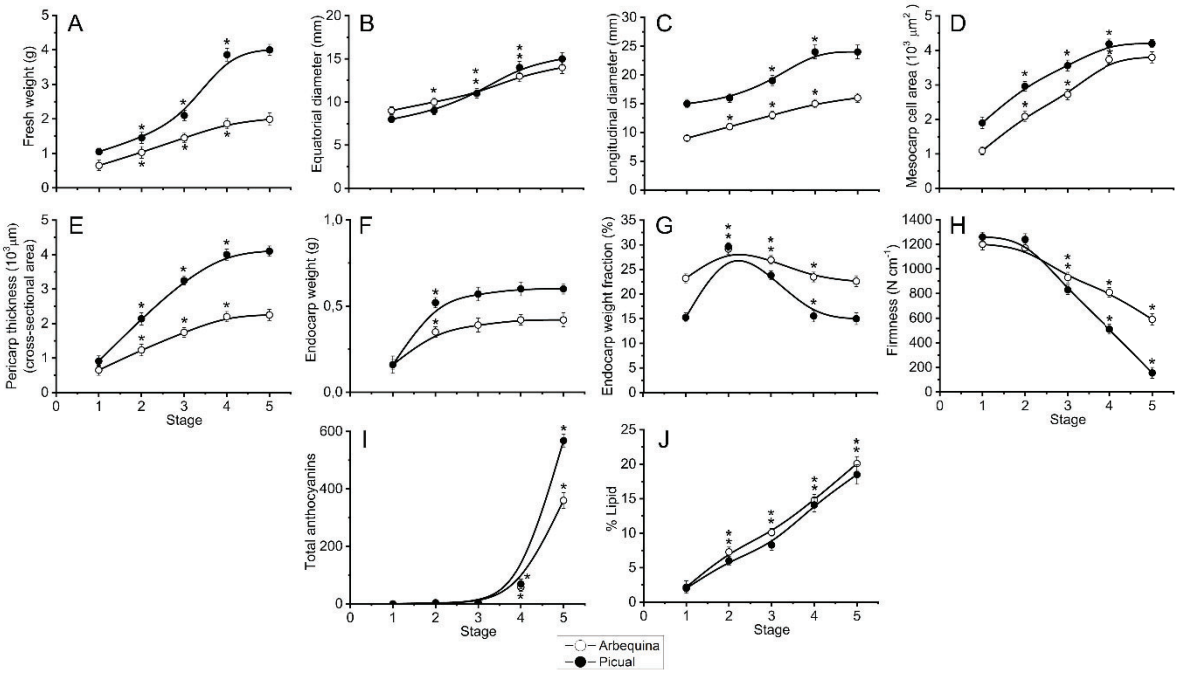

Figure II.2. (A) Changes in fresh weight (FW) (g fruit^{-1}), (B) transverse diameter (mm), (C) longitudinal diameter (mm), (D) mesocarp cell area, (E) pericarp thickness, (F) endocarp weight, (G) endocarp weight fraction, (H) firmness, (I) total anthocyanins, and (J) % lipid of the 'Arbequina' (open circles) and 'Picual' (solid circles) fruit during the stages of olive fruit development. Fresh weight, equatorial diameter, longitudinal diameter, and firmness measurements were performed on whole fruits. Anthocyanin and lipid content measurements were performed on fruit pericarps. Asterisks indicate statistically significant changes with respect to the preceding point according to Tukey's test ($P < 0.05$). Data are the means of three independent experiments ± SE.

In 'Picual' cultivar, the fruit weight was significantly higher compared with 'Arbequina' cultivar. In fact, the weight of 'Picual' fully ripe fruit is double that of 'Arbequina' fully ripe fruit. In this stage, 'Picual' fruit (cultivar with large sized and elongated fruit) is about 15 mm in transverse diameter and 24 mm in longitudinal diameter, while 'Arbequina' fruit (cultivar with small sized and round shaped fruit) is about 14 mm in transverse diameter and 16 mm in longitudinal diameter. Moreover, in 'Arbequina' cultivar, fruit length and width showed very similar trends, resulting in a rounder shape of this cultivar (Fig.II.2B,C), while in 'Picual', the fruit growth in length was more rapid than

width, resulting in the characteristic elongated shape of this cultivar (Fig.II.1 and 2B,C). During this phase, olive fruits increased their size mainly by cell expansion and thus, the fruit mesocarp cell area reached more than 60% of final mesocarp cell size in both olive cultivars (Fig.II.2D). Likewise, the endocarp weight was higher in 'Picual' than in 'Arbequina', which was consistent with the greatest fruit weight observed in 'Picual' during olive fruit growth (Fig.II.2F). However, dynamics of the endocarp weight and endocarp weight fraction (%) were found to be similar between fruit developmental stages in both olive cultivars (Fig.II.2G).

In both cultivars, olive fruit firmness decreased after the onset of ripening and reached the oversoft stage at stage 5 (fully ripe fruit), but fruit firmness rapidly decreased and was much lower in 'Picual' than in 'Arbequina' during fruit ripening (from stage 4 to 5) (Fig.II.2H). Thus, the degree of decline differed between the cultivars, resulting in unequal final fruit firmness. Conversely, total anthocyanins were undetectable before stage 3, but rapidly increased during olive fruit ripening (stages 4-5) in both cultivars and were also higher in the fully ripe fruits of 'Picual' than in those of 'Arbequina' (Fig.II.2I). Notwithstanding the observed differences in the fruit ripening between the two olive cultivars, the total lipid contents showed similar increasing trends through all developmental stages in the two olive cultivars (Fig.II.2J).

3.2. Quantitative changes of plant hormones during olive fruit growth and ripening

In an effort to elucidate the possible relationship between hormone composition and olive fruit development, the hormone profiles of IAA, GAs (GA_1 and GA_4), CKs [*trans*-Zeatin (*t*Z) and isopentenyl adenine (iP)], ABA, SA and jasmonic acid (JA) were analysed in both olive cultivars during fruit growth and ripening. The levels of hormones changed differentially within and between olive fruits of the two cultivars during fruit growth and ripening (Fig.II.3).

In both olive cultivars, the IAA content of olive fruits was greatest at the stage 1 and gradually decreased thereafter to the stage 3 (Fig.II.3A). In fact, IAA levels fell steadily to as much as 73% and 58% from stage 1 to 3, in

'Arbequina' and Picual fruit, respectively. From stage 3 to 4, the levels of IAA increased in olive fruit of both cultivars, but the IAA level continues to rise in 'Arbequina' fruit from stage 4 to 5, while the IAA level lowered by 62% in 'Picual' fruit (Fig.II.3A). Thus, endogenous IAA levels declined during fruit growth, whereas a surge was observed at the onset of ripening in both olive cultivars. However, olive fruit ripening was accompanied by a lower IAA level only in 'Picual' fruits (fast-ripening cultivar), which contained lower levels (about 30%) of endogenous IAA than 'Arbequina' fruits (slow-ripening cultivar) at fully ripe stage.

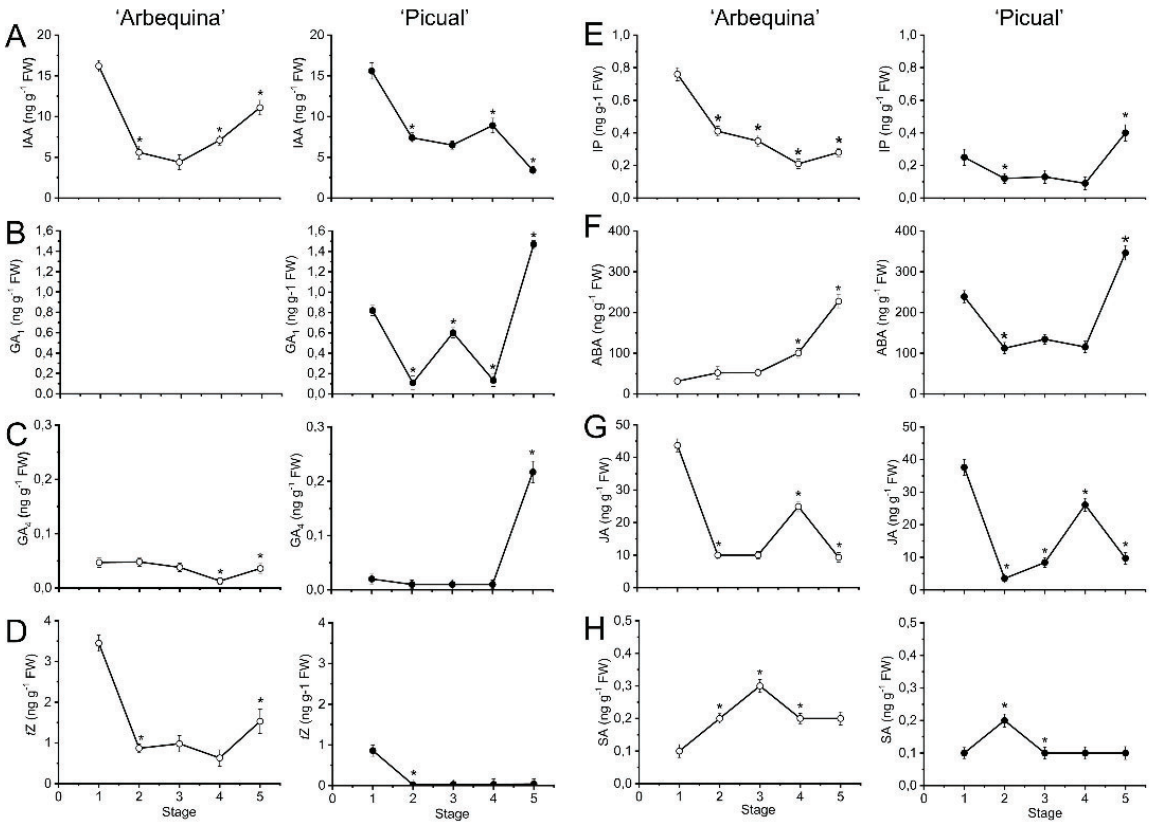

Figure II.3. Profiles of IAA (A), GA_1 (B), GA_4 (C), *t*Z (D), iP (E), ABA (F), SA (G), and JA (H) levels measured from 'Arbequina' and 'Picual' fruits during olive fruit growth and ripening. Hormone levels not detected are indicated by a black dot (•). Data are the means ± SD of three biological replicates with three technical repeats each. Statistically significant differences according to Tukey's test ($p < 0.05$) are denoted by an asterisk.

Notably, in contrast to 'Picual' fruit (cultivar with large sized and elongated fruit), GA_1 was not detected at either stage of fruit development in

'Arbequina' fruit (cultivar with small sized and round shaped fruit) (Fig.II.3B). In 'Picual' fruit, GA_1 levels fell by 87% from stage 1 to 2, while they rose 6-fold from stage 2 to 3 (Fig.II.3B). From stage 3 to 4, GA_1 levels fell up to 78% in 'Picual' fruit to rose later on, up to 11-fold between stage 4 to 5 in 'Picual' fruit (Fig.II.3B). These results identify GA_1 as the specify bioactive GA of the 'Picual' fruit (Fig.II.3B). On the other hand, in both olive cultivars, endogenous GA_4 maintained relatively low levels and unaltered during fruit growth (stages 1-3), while an increase was observed through stages 4 to 5 only in 'Picual' fruit (Fig.II.3C). Thus, unlike 'Arbequina' fruit, GA_1 and GA_4 levels rose in 'Picual' fruit at the last stage of fruit ripening (stage 5, fully ripe fruit), when the highest levels were measured (Fig.II.3B,C), and consequently, 'Picual' ripe fruits (fast-ripening cultivar) were found to contain higher levels of endogenous GAs than 'Arbequina' ripe fruits (slow-ripening cultivar), suggesting a prominent role of GAs during this process.

Similarly, the CK (*t*Z and IP) contents in olive fruit of both cultivars were high at the stage 1 and gradually decreased thereafter to the stage 5, except for *t*Z levels in 'Arbequina' fruit, which rose by 2.5-fold from stage 4 to 5 (Fig.II.3D), and for IP levels in 'Picual' fruit, which rose by 4.4-fold from stage 4 to 5 (Fig.II.3E). The levels of *t*Z were higher in the 'Arbequina' ripening fruit than in the 'Picual' ripening fruit, while the levels of IP were lower in the 'Arbequina' ripening fruit than in the 'Picual' ripening fruit. More specifically, this study indicates that the 'Arbequina' ripe fruit contained not only higher levels of IAA, but also high levels of CKs (*t*Z), suggesting that the high levels of endogenous auxins and CKs in 'Arbequina' ripe fruits are involved in a slow fruit ripening process and hence, a prolongated duration of the ripening process. Furthermore, the ABA levels increased during olive fruit ripening in both cultivars, but ABA levels of 'Arbequina' young fruits (stage 1) were low, while being greater in 'Picual' young fruits (Fig.II.3F).

In the case of JA, in 'Arbequina' fruit, JA levels fell by 77% from stage 1 to 2 to remain unaltered afterwards, while JA levels increased 2.5-fold from stage 3 to 4 and fell by 63% from stage 4 to 5. Comparable to the trend during 'Arbequina' fruit growth, JA levels fell by 91% between stages 1 and 2 in 'Picual' fruit, but then rose 7.5-fold from stage 2 to 4, to decline by 63% afterwards (Fig.II.3G). However, SA levels rose during olive fruit growth, while

they fell at maturation stage (stage 3) or the onset of ripening (stage 4), to keep constant afterwards in both olive cultivars (Fig.II.3H). Thus, these results showed that both olive cultivars presented different accumulation dynamics of plant hormones during olive fruit development, suggesting that hormonal regulatory networks differ between olive cultivars and contribute to differences in the olive fruit size and shape as well as the ripening duration.

3.3. Transcriptional regulation of hormone-related genes during olive fruit growth and ripening

To gain information concerning hormone dynamics during olive fruit development, we investigated the possibility that hormone biosynthesis and signalling genes were differentially regulated during fruit growth and ripening in the two olive cultivars. The results showed that the expression of auxin signalling genes (*OeTIR1*, *OeIAA1*, *OeARF2* and *OeSAUR*) followed a different pattern in 'Arbequina' with respect to 'Picual' fruits. That is, *IAA1* and *ARF2* genes were exclusively upregulated in 'Picual' olive fruit during fruit ripening but presented lower levels of expression in 'Arbequina' fruit (Fig.II.4).

In accordance with IAA content, *OeTIR1* and *OeSAUR* genes showed greater expression at the stages 4 and 5, respectively, during fruit ripening in 'Arbequina' fruit (Fig.II.4A,B), whereas this did not occur in 'Picual' fruit. Thus, the IAA accumulation during olive fruit ripening clearly corresponded to the up-regulation of *OeTIR1* and *OeSAUR* expression in 'Arbequina' cultivar. These data therefore support the conjecture that the two olive cultivars may differ in the auxin signalling regulation during olive fruit ripening.

The data for GAs suggest that GA synthesis was up-regulated by *OeGGPS*, coding geranylgeranyl pyrophosphate synthase (GGPS), during olive fruit ripening in 'Picual' fruit (Fig.II.5A). Meanwhile, we showed that GA signalling, regulated by *OeGID1B* receptor, was down-regulated during olive fruit ripening in both cultivars (Fig.II.5B).

In both cultivars, an increase of *CK oxidase/dehydrogenase* (OeCKX) gene expression is found in the fully ripe fruit, implying that the deactivation of CK may actively occur in olive ripe fruit (Fig.II.5C). In addition, *OeCKX* was upregulated at stages 2 and 3, in 'Picual' and 'Arbequina' fruits, respectively, parallel to the total CK content decrease.

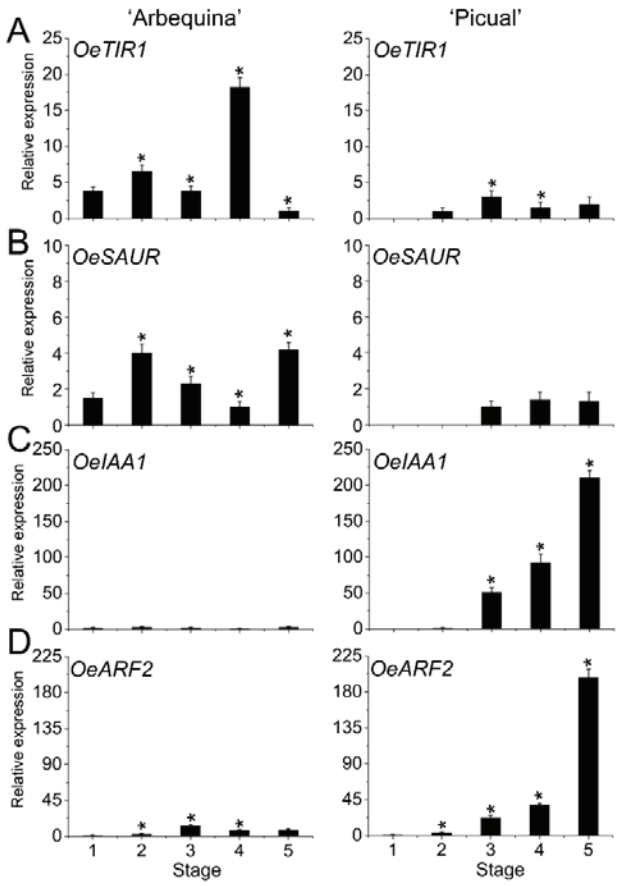

Figure II.4. Expression of different components of the auxin signalling pathways during olive fruit growth and ripening. Expression patterns of *OeTIR1* (A), *OeSAUR* (B), *OeIAA1* (C) and *OeARF2* (D) during olive fruit development and ripening in 'Arbequina' and 'Picual' cultivars. Data are the means ± SD of three biological replicates with three technical repeats each and were obtained by qRT-PCR normalized against *Olea europaea* ubiquitine. Statistically significant differences from the preceding point based on Tukey's test ($p < 0.05$) are denoted by asterisks.

Meanwhile, ABA contents increased during olive fruit ripening in both cultivars, the levels of expression of gene coding for 9-cis-epoxycarotenoid dioxygenase (NCED), involved in ABA biosynthesis, were higher during olive fruit ripening in both olive cultivars (Fig.II.6A). Other transcripts involved in ABA catabolism such as ABA 8-OH, which encodes ABA 8'-hydroxylase, was up-regulated in both olive fruits at the stage 4 (Fig.II.6B), in contrast to the ABA levels detected in olive fruit at this time. In the case of SA, the expression of *PAL1*, which are associated with the SA biosynthesis, was up-regulated during fruit ripening in 'Arbequina' fruit (Fig.II.6C), while SA level remained

almost constant. Similarly, *PAL1* was up-regulated only at the maturation stage in 'Picual' fruit parallel to the decrease in SA content.

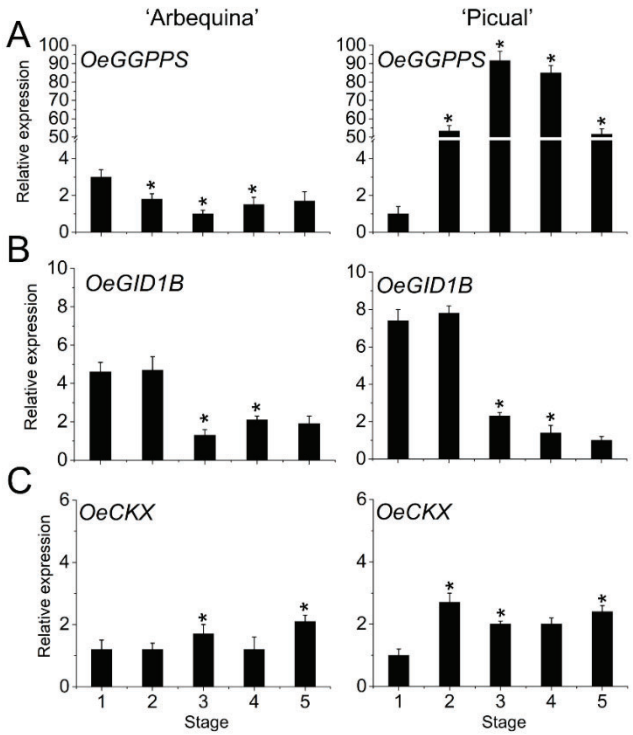

Figure II.5. Expression of *OeGGPPS* (A), *OeGID1B* (B), and *OeCKX* (C) during olive fruit growth and ripening in 'Arbequina' and 'Picual' cultivars. Data are the means ± SD of three biological replicates with three technical repeats each and were obtained by qRT-PCR normalized against *Olea europaea* ubiquitine. Statistically significant differences from the preceding point based on Tukey's test ($p < 0.05$) are denoted by asterisks.

In addition, in the present study, the expression of two genes coding for lipoxygenase (LOX) and allene oxide synthase (AOS), involved in JA synthesis, showed a pronounced increase at stage 4 in both olive cultivars (Fig.II.6D,E), in accordance with the surges in JA content observed in both cultivars at this stage, though these increases were greater in the case of the 'Arbequina' fruit. However, another gene encoding JAR1 (JASMONOYL ISOLEUCINE CONJUGATE SYNTHASE1), involved in JA-Ile biosynthesis, was upregulated at the stage 4 followed by a decrease in the expression levels up to full fruit ripening (stage 5) in 'Arbequina' fruit, while *OeJAR1* increased in 'Picual' fruit at the stage 5 (Fig.II.6F).

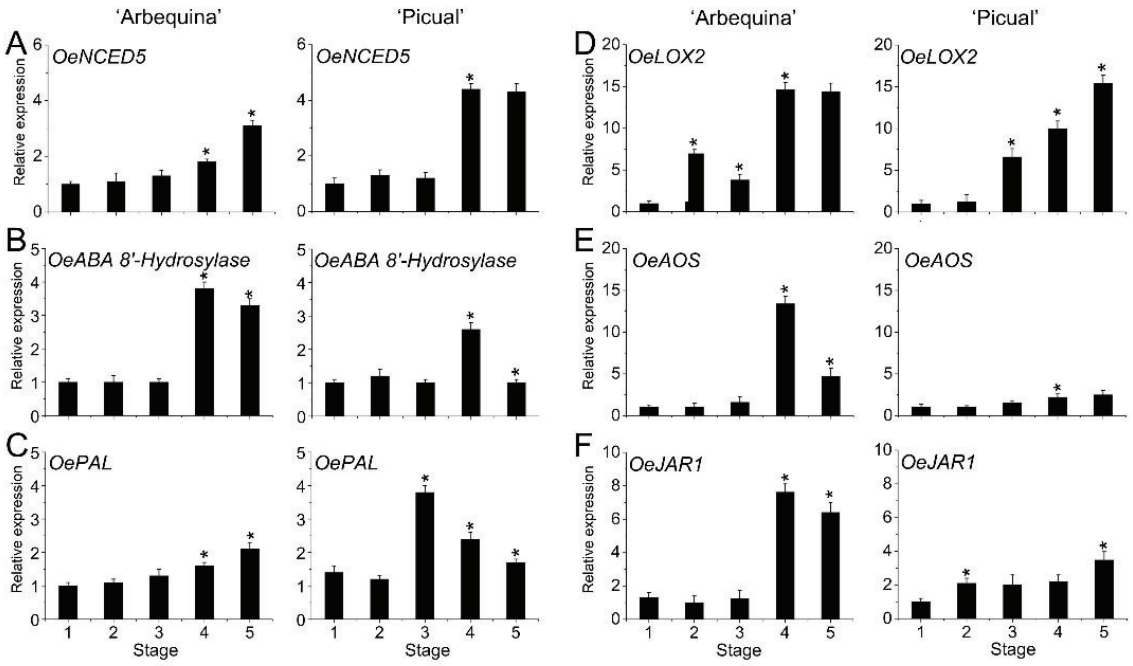

Figure II.6. Expression of *OeNCED5* (A), *OeABA 8'-OH* (B), *OePAL* (C), *OeLOX2* (D), *OeAOS* (E), and *OeJAR1* (F) during olive fruit growth and ripening in 'Arbequina' and 'Picual' cultivars. Data are the means ± SD of three biological replicates with three technical repeats each and were obtained by qRT-PCR normalized against *Olea europaea* ubiquitine. Statistically significant differences from the preceding point based on Tukey's test ($p < 0.05$) are denoted by asterisks.

Therefore, distinct accumulation patterns of hormones and expression of hormone-related genes in olive cultivars provided insights into the complex processes involved in olive fruit ripening, suggesting that distinct hormonal metabolism and signalling occur in this species during fruit ripening.

4. Discussion

Although the application of molecular and genomic approaches has been focused on the fruit development process in olive (Alagna et al., 2009, 2012; Galla et al., 2012; Iaria et al., 2016; Xiaoxia et al., 2020; Skodra et al., 2021; Liu et al., 2021; Rao et al., 2021) for the enhancement of oil yield, information concerning the hormonal changes during olive fruit development is still limited, in contrast to other non-climacteric fruits. So far, there are no studies have reported hormonal changes during fruit ripening in olive. Moreover, a key unresolved question regarding the olive fruit is whether the olive cultivars share a common ripening mechanism and, if so, which of the known plant

hormone(s) are involved. In the present study, the physiological and hormonal changes are examined in developing olive fruits of two major olive cultivars in commercial production for the oil market, 'Arbequina' and 'Picual', which differ in fruit size and shape, as well as fruit ripening rate and duration.

Olive cultivars are grouped according to intended use as oil, table and dual-use cultivars based on morphological, compositional, and organoleptic characteristics (Rallo et al., 2018). Previous works have indicated that olive cultivars are classified into two groups according to the presence or absence of massive fruit abscission after ripening (Gomez-Jimenez et al., 2010b). It bears noting that olive cultivars with massive ripe fruit abscission are characterized by a fast-ripening and a large sized fruit (e.g. 'Picual' olive cultivar), whereas olive cultivars without massive ripe fruit abscission are characterized by a slow-ripening and a small sized fruit (e.g. 'Arbequina' olive cultivar), revealing that olive fruits can be organized within two categories by using combinations of the fruit quality traits. Thus, here, we analyse hormone contents and gene expression between one olive cultivar of each category, 'Picual' and 'Arbequina', to determine whether this might reveal hormones and genes that are specifically associated with large or small fruit, as well as with fast- or slow-ripening in olive. The results showed that both olive cultivars presented different accumulation dynamics of plant hormones as well as different expression of some genes related to hormonal metabolism and signalling during key points of the stages of olive fruit development (Fig.II.7). Overall, our hormonal analysis enables similar hormone signals controlling olive fruit growth and ripening of both olive cultivars to be distinguished from those that are specific to a certain cultivar. Therefore, these findings will help elucidate the common or distinct mechanisms that underlie the hormonal regulation of olive fruit development within the species and with other plant species.

Here, the evaluation performed throughout the different development stages of olive fruit indicated a decrease of IAA, CK, and JA, and an increase of SA during fruit pulp growth in both olive cultivars. This coincided with the major increase in mesocarp cell expansion of olive fruit, i.e. 60% of final size of mesocarp cell, as well as in fruit weight resulting in the final size of fruit, which

varied greatly among the two cultivars. In addition, these growth parameters agreed with the lipid accumulation as well in both cultivars.

By contrast, throughout this pulp growth phase, the data from our study indicate that both olive cultivars presented different accumulation dynamics of GA_S, suggesting underlying differences in the olive fruit size and shape. Specifically, GA_1 was undetectable in 'Arbequina' fruit (small sized and round shaped fruit), whereas GA_1 level increased together with fruit size and weight in the 'Picual' cultivar (large sized and elongated fruit) during this phase. In addition, no significant changes of GA_4 levels showed during fruit growth in both olive cultivars. Thus, unlike small sized fruit, it is observed that GA_1 levels rose in the large sized fruit during its growth by cell expansion after endocarp lignification, indicating that the presence of GA_1 in 'Picual' fruit could be correlated to the fruit size of this cultivar in comparison to 'Arbequina' cultivar. These results agree with the established notion that GA participates mainly in the cell expansion process in the olive fruit (Camarero et al., 2023). In 'Picual' cultivar, the level of GA_1 was high at flowering and then fell during cell division phase, while the levels of GA_1 and GA_4 peaked during cell expansion phase of 'Picual' fruit early development, in agreement with the upregulated expression patterns of *OeGA3ox,* coding GA 3-oxidase (GA3ox), and *OeGID2,* coding GA receptor (Camarero et al., 2023). Likewise, in plums, during the fruit growth phase when cell expansion is greatest, expression of three DELLAs is low, consistent with involvement of GA (El-Sharkawy et al., 2017). However, the mechanisms of GA action during olive fruit growth, after the endocarp lignification stage and before the onset of fruit ripening, remain to be elucidated. In the present study, the expression of GA receptor gene *OeGID1B* did not notably change in olive fruit between cultivars, whereas the expression of the GA biosynthesis gene *OeGGPS,* coding geranylgeranyl pyrophosphate synthase (GGPS), in olive fruit increased consistently with the increase in GA_1 content at the stage 3 during fruit pulp growth in the 'Picual' cultivar. By contrast, *OeGGPS* expression was found to be repressed in the 'Arbequina' fruit from stages 1-3. Likewise, there is significant difference between olive cultivars; the *OeGGPS* expression level was higher in the 'Picual' cultivar that in the 'Arbequina' cultivar, indicating a relationship between the expression of *OeGGPS*, olive fruit cell expansion and the subsequent increase in olive fruit size. In line with this, comparison of

transcriptomic analyses between varieties of small and large grape berries have shown that differentially expressed transcripts were related mainly to auxin, ABA, ethylene, brassinosteroids (BRs), but also to GAs (Wong et al., 2016). Thus, the high expression of *OeGGPS* in 'Picual' cultivar might be correlated with the larger fruit size observed in this cultivar when compared to the 'Arbequina' cultivar, in accord with the GA accumulation profiles.

The role of GA in fruit growth by influencing cell expansion has been amply reported (Csukasi et al., 2011; 2012; McAtee et al., 2013; Fuentes et al., 2019; Perotti et al., 2023). Furthermore, previous studies have shown that the manipulation of GA levels can influence both fruit size and morphology (García-Hurtado et al., 2012; Liao et al., 2018; Chen et al., 2020; Khew et al., 2020; Renaudin et al., 2023). In present study, unlike small and round olive fruits of 'Arbequina' cultivar, it is shown that large and elongated olive fruits of 'Picual' cultivar are rich in particularly GAs (GA_1) during growth by cell expansion after endocarp lignification, suggesting that GA_1 may be involved in the pathways regulating both fruit elongation and size in olive. In strawberry, GA promotes the longitudinal elongation of strawberry fruits, compared to auxin, which increases overall fruit size (Liao et al., 2018). Similarly, in tomato, fruit shape index was increased when GA was applied, which was attributed mainly to the increased organ elongation (Chen et al., 2020). Moreover, a recent work has revealed tight connections between fruit shape variation and microtubules through integration of phytohormones, including GAs, auxin and brassinosteroids (BRs) (Li et al., 2023), but the underlying mechanisms of fruit shape variation remain largely unknown. Based on our data, we examine whether this fruit growth mechanism of the 'Picual' cultivar could be regarded as similar to that of other olive cultivars with large sized and elongated fruit or whether this is specific fruit pulp growth regulation unique to the 'Picual' cultivar. In other olive cultivars, several genes with annotated functions in GA biosynthesis and responses have been identified in the olive fruit transcriptome (Alagna et al., 2009; Galla et al 2009; Xiaoxia et al., 2020), but no available studies have investigated the hormonal contents of olive fruits during the same fruit developmental phase.

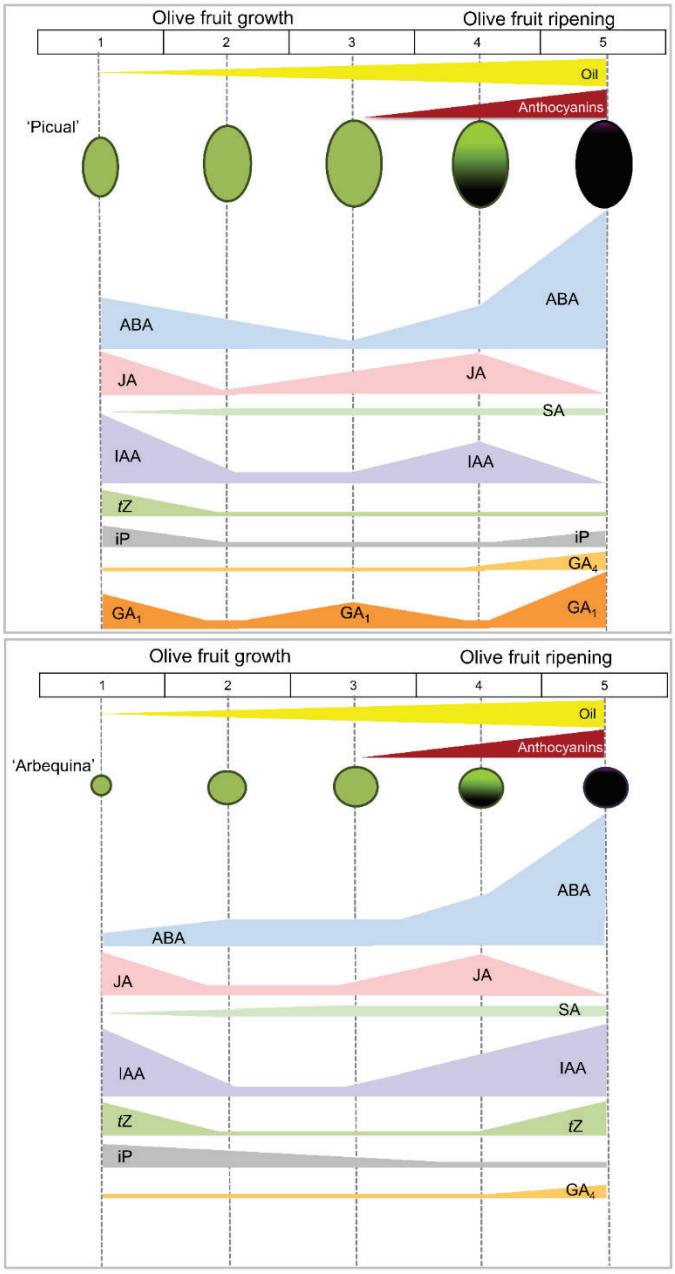

Figure II.7. Scheme representing the hormone profiling of 'Picual' and 'Arbequina' olive cultivars during the stages of olive fruit development. See text for details.

Although many questions remain unanswered regarding the physiological basis that controls olive fruit size or shape, differential accumulation patterns of GAs between the olive cultivars during olive fruit growth after endocarp lignification could explain the difference in the final fruit size and shape. This study shows, therefore, that the level of endogenous GA_1 and its biosynthesis may play a key role in the regulation of olive fruit growth, mainly by cell expansion, and eventually of olive fruit size and shape. However, further

studies are needed to determine the molecular and genomic control underlying of the regulation of GA pathways and interaction with other pathways during olive fruit growth in different olive cultivars.

The hormone profiling revealed that the olive fruit ripening process starts with an increase of ABA level in parallel with the accumulation of anthocyanins and the decline of fruit firmness in both olive cultivars, when expression of ABA related genes, such as *OeNCED5* (9-cis-epoxycarotenoid dioxygenase) and *OeABA-8OH* or *OeClCYP707As* (abscisic acid 8'-hydroxylase) also increased, suggesting that both ABA biosynthesis and inactivation were stimulated during olive fruit ripening. Generally, ABA plays a pivotal role in non-climacteric fruit ripening (McAtee et al., 2013; Kumar et al., 2014; Fuentes et al., 2019; Li et al., 2021), but this regulatory role of ABA during fruit ripening has been shown in non-climacteric as well as in climacteric fruits (Kou et al., 2021; Fan et al., 2022; Gupta et al., 2022). Our results showed that *OeNCED5* and *OeABA-8OH* are associated with ABA levels and olive fruit ripening. By contrast, in strawberry, ABA repressed the expression of *FveCYP707A4*a but promoted that of *FveNCED* during fruit ripening (Wang et al., 2017; Liao et al., 2018). The ABA catabolism gene *FveCYP707A4a* was reported to be an important crosstalk point for auxin, GA, and ABA, regulating the transition from the early growth phase to ripening phase (Liao et al., 2018). In ripening olive fruit, the upregulation of NCED is presumably sufficient to maintain ABA at levels higher than stimulated the fruit ripening in olive. In fact, in both fully ripe fruits, the most abundant hormone was ABA, but the ABA levels were higher in the 'Picual' cultivar (fast-ripening) in comparison to the 'Arbequina' cultivar (slow-ripening). NCED is the main enzyme in the ABA biosynthetic pathway in both climacteric and non-climacteric fruits (Kumar et al., 2014; Fuentes et al., 2019; Li et al., 2021; Gupta et al., 2022). Notably, levels of *OeNCED5* transcripts were more than two-fold higher in 'Picual' olive fruit than in 'Arbequina' olive fruit at the onset of fruit ripening. During peach fruit ripening, the role of *NCED* genes, including *NCED5*, were observed in cooperatively regulating the ABA response (Wang et al., 2021). Similarly, in the 'Leccino' olive cultivar, the synthesis of ABA was also stimulated throughout fruit ripening since a key enzyme encoded AAO3 (ABSCISIC ALDEHYDE OXIDASE 3) was upregulated at the onset of fruit ripening (Galla et al. 2009). The observed upregulation of

genes involved in ABA biosynthesis is consistent with a higher ABA content amply reported in other non-climacteric fruits during fruit ripening (McAtee et al., 2013; Kumar et al., 2014; Fuentes et al., 2019; Kim et al., 2019; Bai et al. 2020; Kou et al., 2021; Gupta et al., 2022; Perotti et al., 2023). Thus, it is proposed here that a considerable rise in the ABA level during olive fruit ripening might derive mainly from the increase in *OeNCED5* gene expression in both olive cultivars.

Furthermore, in previous studies, exogenous application of ABA has been reported to raise anthocyanin levels and fruit ripening (Wang et al., 2016; Jia et al., 2017; Gupta et al., 2022). However, exogenous ABA application did not show a promotion of olive fruit ripening in olive cultivars (data not shown), when ABA was included in the pre-harvest treatment at the onset of fruit ripening to produce olive fruits enriched in antioxidants (Blanch et al., 2018a). By contrast, exogenous applications of methyl jasmonate (MeJA) on olive tree have been associated with anthocyanin accumulation (data not shown) supports a role for MeJA as inducer of ripening in olive (Blanch et al., 2018b), as previously demonstrated in other non-climacteric fruits (Concha et al., 2013; Wei et al., 2017; Han et al., 2019). JA and JA-Ile contents may be crucial in the initiation of fruit ripening, and their contents begin to decline at the late ripening stage in non-climacteric fruits (Garrido-Bigotes et al., 2018; Kim et al., 2019). In the present study, a similar trend for JA level is reported, exhibiting higher concentrations of endogenous JA at the onset of olive fruit ripening followed by a decline during fruit ripening in both olive cultivars. Moreover, genes involved in the JA metabolism (*OeJAR1*) and biosynthesis (*OeLOX2* and *OeAOS*) were upregulated at the onset ripening consistent with of JA levels in olive fruits of both olive cultivars. Indeed, previous work has shown that genes involved in JA metabolism were also upregulated at the onset of fruit ripening in 'Leccino' olive cultivar (Galla et al., 2009). Although the possible role of JA in olive fruit ripening remains largely uncharacterized, the increase of JA and gene expression levels coincided with the onset of olive fruit ripening in both olive cultivars, suggesting that JA is involved in olive fruit ripening. Previously, an antagonistic relationship from the JA to the ABA pathway was proposed during non-climacteric strawberry fruit ripening (Garrido-Bigotes et al., 2018). However, it has been shown that the endogenous MeJA might stimulate ABA levels in grape berries since MeJA

activated lipoxygenase that is involved in ABA synthesis (Kondo and Fukuda, 2001), while a similar effect of MeJA on ethylene synthesis in climacteric fruits has been reported (Kondo et al., 2007; Tao et al., 2021). Our experimental data support the hypothesis that JA plays a role in the onset of olive fruit ripening through stimulation of ABA biosynthesis at the transcriptional level, but it is possible that JA acts antagonistically towards ABA in olive fruit ripening, as showed in other non-climateric fruits (Garrido-Bigotes et al., 2018).

It has been shown that the metabolism of ABA, JA and IAA differ between grape cultivars during fruit ripening (Coelho et al., 2019). Here, our results indicate that the start of the rise in ABA levels just at the onset of olive fruit ripening coincides with the higher JA and IAA levels in both olive cultivars, but an inverse relationship between IAA and GA levels was apparent between cultivars during olive fruit ripening. IAA level continues to rise in 'Arbequina' fruit during slow-ripening (from stage 4 at 5) along with the CK (tZ) accumulation, whereas the IAA level decreased concomitant with an increase of GAs (GA_1 and GA_4) in 'Picual' fruit during fast-ripening (stages 4-5). Thus, IAA and GAs present different accumulation patterns during olive fruit ripening. The fact that the slow-ripening olive cultivar accumulated IAA and CK from the onset of fruit ripening until fully fruit ripening in contrast to the fast-ripening olive cultivar in which occur GA accumulation suggested that IAA and CK retard the ripening process in the slow-ripening olive cultivar. Generally, the promotion of fruit growth by auxin and CK, and their inhibition of fruit ripening are highly conserved in plant species (McAtee et al., 2013; Fenn and Giovanoni, 2021), but recent evidence indicate that auxin and CK may play a complex role in regulating ripening through interactions with other plant hormones, supporting the activation of auxin and CK signalling during this stage (Kou et al., 2021; Mazzoni-Putman et al., 2021). In apple, it has been shown that the genotype-specific feature of auxin metabolism in maturing fruit may determine the different rates of ripening progression (Shin et al., 2016). In this regard, our results of the IAA levels in 'Picual' olive cultivar were similar to those reported in tomato, a climacteric fruit, and in strawberry, a non-climacteric fruit, where the IAA level increased at the onset of fruit ripening and then decreased during fruit ripening (McAtee et al., 2013; Fenn and Giovanoni, 2021); however, in 'Arbequina' olive cultivar, we detected no rising or falling pattern seen in those previous reports, revealing

that IAA content is high when the ripe fruits are most slowing ripening in olive. It appears that the IAA involves counteracting the ABA effect, thereby circumventing excessive ABA signal amplification. In grape, an ABA-IAA switch reportedly controls the degree to which a bunch of grapes ripens (Gouthu and Deluc, 2015), and the level of both hormones augment simultaneously in sweet cherry (Ponce et al., 2021). Moreover, genes related to IAA signaling exhibited varying expression patterns between olive cultivars, showing an increased fruit *OeTIR1* and *OeSAUR* expression associated with slow-ripening and with high IAA level, while the expression of the *OeIAA1* and *OeARF2* genes increased markedly during fruit fast-ripening. In tomato, altered *ARF2* expression leads to modified contents in ABA, CK, and SA highlighting that auxin signalling intersects hormonal signals in the regulation of fruit ripening (Mazzoni-Putman et al., 2021). Therefore, differential regulation of auxin pathway genes regulates olive fruit ripening in fast- and slow-ripening cultivars, suggesting that the auxin signalling involves different regulatory mechanisms between olive cultivars.

Previous studies have shown GAs associated with fruit ripening (Csukasi et al., 2011, 2012; El-Sharkawy et al., 2014; Teh et al., 2014; Chen et al., 2020; Alferez et al., 2021). In non-climateric fruit, GA and ABA often counteract each other in the regulation of the fruit ripening (Liao et al., 2018). In 'Picual' cultivar, GA_1 and GA_4 levels were highest at the fully ripe stage and rose ~11- and 22-fold, respectively, from the onset of fruit fast-ripening. In contrast, the relative lack of GA_1 and/or reduced GA-sensitivity in 'Arbequina' cultivar appears, at least partially, responsible for prolonged fruit ripening in this cultivar. Thus, while IAA levels exhibited a decline during olive fruit fast-ripening, the opposite pattern was detected for GA (GA_1 and GA_4), suggesting that GA play a key role in progressing olive fruit ripening, since the presence of endogenous GA in olive fruit shortened the fruit ripening duration. Similarly, high levels of GA_1 were detected through fruit ripening in other stone fruits (El-Sharkawy et al., 2014; Teh et al., 2014). However, despite a substantial increase of the endogenous GA_1 and GA_4 levels exclusively during 'Picual' fruit ripening, *OeGGPPS* and *OeGID1B* expression levels did not rise, emphasizing a complex regulation of the GA metabolism and signalling in olive developing fruits. On the other hand, GA levels increased markedly during olive fruit ripening exclusively in 'Picual' cultivar with fast-ripening,

while in 'Arbequina' cultivar (slow-ripening), IAA and CK (*t*Z) accumulated during olive fruit ripening, suggesting that GA accumulation could coordinate ripening duration by lowering auxin and CK (*t*Z) levels. In particular, GA (GA_3) and CK (*t*Z) contents exhibited fluctuations and differences between two strawberry cultivars during fruit ripening (Lee et al., 2020), highlighting the value of characterizing multiple genotype-specific fruit ripening in a species. In this work, we showed that olive fruit ripening can have opposing effects on the levels of GAs (GA_1 + GA_4) and of IAA + CK (*t*Z) for a specific olive cultivar, revealing that the genotype-specific feature of the GA_1 presence in ripening olive fruit may determine the different rate of olive fruit ripening progression. Consequently, the present study indicates that GA_1 could play a dual regulatory role, promoting first the growth of olive elongated fruit mainly by cell expansion, and a relevant role in the ripening afterwards, shortening the olive fruit ripening duration. These results agree with the findings of Chen et al. (2020) that the manipulation of GA levels can simultaneously influence tomato fruit shape and ripening, suggesting that a common regulation mechanism exists in different plant species. Furthermore, GA-deficient mutant fruits present several developmental disorders, including reduced fruit size, and delayed ripening (Serrani et al., 2007; de Jong et al., 2009; El-Sharkawy et al., 2012). Although the role of GA in the regulation of olive fruit development deserves more attention in the future, these findings lead us to hypothesise that the differences in the fruit morphology and the ripening duration observed in the two olive cultivars are, at least partially, due to variations in the GA-content and/or -responsiveness in olive fruit. Overall, our findings revelated that ripening occurs in association with a rise in IAA and *t*Z levels together with an increase of ABA in olive slow-ripening fruits, whereas GA and ABA act synergically towards fast-ripening of olive fruits. Therefore, in addition to ABA, our results indicate that IAA, CK, and GA are hormones involved in olive fruit ripening, and their regulatory roles differ between fast- and slow-ripening fruits in olive.

5. Conclusions

This detailed study was compiled to provide a comprehensive description of the hormonal regulatory mechanisms of olive fruit growth and ripening. Olive fruit ripening depends mainly on ABA, but the IAA, CK, and GA content and/or -responsiveness differ between olive cultivars during fruit ripening. Further studies are in progress to discern the relevance of these hormones in other olive cultivars. The relative lack of GA_1 and/or reduced GA-sensitivity in 'Arbequina' cultivar appears, at least partially, responsible for smaller fruit size and prolonged fruit ripening duration in this cultivar, suggesting that the fruit size and ripeness of olive can be regulated by regulating GA. However, it cannot be ruled out that other hormonal or physiological signals, not yet elucidated, can influence some aspects of the olive fruit growth and ripening process. Finally, we expect such detailed knowledge to help design new strategies to develop olive fruits with both enhanced fruit quality (fruit size) and shortened fruit ripening duration for olive cultivars.

Capítulo III

Variaciones en el tamaño celular del mesocarpo y la ploidía del fruto entre cultivares de olivo de frutos pequeños y grandes durante la ontogenia del fruto

Variations in mesocarp cell size and fruit ploidy between small- and large-fruited olive cultivars during fruit ontogeny

Abstract

Olive (*Olea europaea* L. subsp. *europaea* var. *europaea*) is one of the most economically important fruit trees worldwide. However, the mechanisms underlying olive fruit growth remain poorly understood. Here, we examine questions regarding the relative importance of cell division and expansion phases to olive fruit growth depending on the final fruit size, by measuring fruit diameters, pericarp thickness, cell area, and mitotic activity (by flow cytometry) during fruit ontogeny in three olive cultivars having different fruit size. The results demonstrate that differences in the fruit size are related to the duration of early fruit growth and the maximum growth rate between olive cultivars. Differences in fruit weight between olive cultivars were found from 35 days post-anthesis (DPA), while the increase in pericarp thickness became detectable from 7 DPA in the three cultivars. Intense mitotic activity appeared the first 21 DPA in olive fruit of the three cultivars, suggesting that olive fruit cell number is determined from 21 DPA. Moreover, olive fruit of the large-fruited cultivars enlarged due to relatively higher cell division and expansion rates during early fruit growth, and to higher expansion rates of mesocarp cells during late fruit growth compared with the small-fruited cultivar. Likewise, investigating the ploidy level, we observed that the maximum endoreduplication level in olive fruit pericarp occurred during early fruit growth in the three olive cultivars. We conclude that a combination of greater cell division capacity and a greater degree of cell expansion are involved in the increase of olive fruit size.

Keywords: cell division; cell expansion; flow cytometry; fruit growth; fruit size; olive; ploidy

1. Introduction

Fruits develop after signals from pollination and fertilization, inducing fruit set, i.e. the resumption of growth of ovaries and sometimes neighbouring tissues (Seymour et al., 2013; Sotelo-Silveira et al., 2014). The fruit growth phase relies on cell division and expansion in response to signals issued from the developing seeds (Mauxion et al., 2021). Until then, the main role of the fruit is to protect the developing seeds it contains. When the seeds have completed their development, fruit growth ceases and the fruits ripen, acquiring new characteristics that facilitate seed dispersal through a wide variety of mechanisms (Fenn and Giovannoni, 2021). The growth phase, generally the longest phase during fruit development, is crucial in determining fruit properties important to humans, such as size, shape, texture, and content. In fleshy fruits, knowledge of mechanisms associated with fruit growth and of their relationship with environmental factors aids in potential applications in agriculture (Giovannoni, 2004; Mauxion et al., 2021). Although some studies have shown that the cell division plays a critical role in the control of fruit size as well as cell expansion in tomato (Dolan and Davies, 2004; Tanksley, 2004; Bertin, 2005; Cheniclet et al. 2005; Renaudin et al. 2017; 2023), apple (Harada et al., 2005), kiwi (Cruz-Castillo et al., 1991), persimmon (Hamada et al., 2008), saskatoon (McGarry et al., 2001), strawberry (Cheng and Breen, 1992), and peach (Scorzal et al., 1991; Farinati et al., 2021), so far little data is available on the relationship between cell division and expansion and fruit size in olive.

The cultivated olive (*Olea europaea* L. subsp. *europaea* var. *europaea*) fruit is one of the most economically leading oil crops worldwide. The extensive genetic resources available for olive are illustrated by a wide variability of many characters of olive fruit (Rallo et al., 2018; Bazakos et al., 2023). In particular, olive fruit size differs up to several fold among cultivars (Barranco 1999). In addition to the high genetic diversity of olive fruit size (De la Rosa et al., 2008; 2013; Belaj et al., 2020), fruit weight is also subject to genetic variation, suggesting that this trait is polygenic (Moret et al., 2023). In terms of growth, the analysis of the olive fruit histology by qualitative methods has shown that cultivar-based fruit size was related directly to cell number and was established soon after anthesis by cell division rate in olive cultivars

(Hammami et al., 2011). Likewise, olive fruit growth and sink strength are related to cell number, not to tissue size (Rosati et al., 2020). However, few studies to date have given quantitative details on the kinetics and localization of cell division and expansion in olive fruit. Recently, we provided the first detailed quantitative analysis at the ploidy level of olive fruit during early growth (Camarero et al., 2023), showing that cell division and expansion occur simultaneously for 21 days post-anthesis (DPA) and that cell expansion alone continues thereafter for 3 weeks up to endocarp lignification about 50 DPA in 'Picual' olive cultivar (Camarero et al., 2023). Subsequently, the late growth of olive fruit after endocarp lignification consists primarily of cell expansion, which is responsible for the maximum fruit size and oil accumulation (Conde et al., 2008). However, to date, no studies available have investigated the ploidy level of olive fruit during late fruit growth.

In the present study, we consider the variability of olive fruit size in order to address the question of its dependence on cell size and ploidy during olive fruit ontogeny. For this, we made a quantitatively comparative analysis of fruit development in three olive cultivars that differed in the final fruit size. This included the cytology and ploidy analyses associated with olive fruit development in an olive small-fruited cultivar, 'Arbequina', and two large-fruited cultivars, 'Picual' and 'Manzanilla Sevillana'. Specifically, we examined the cell area and mitotic activity of the developing olive fruits by flow-cytometric analysis to determine whether cell division and/ or cell expansion is reduced in the small olive fruit, or conversely increased in the case of large olive fruit are examined. These data provide important new findings on the contribution of fruit cell size and ploidy to olive fruit size, and ultimately the control of olive fruit development.

2. Materials and methods

2.1. Plant material and morphological analysis

Three cultivars of olive (*Olea europaea* L. subsp. *europaea* var. *europaea*.) differing markedly in fruit size, i.e. 'Arbequina', 'Picual', and 'Manzanilla Sevillana', were used in this study (Fig.III.1). Olive trees of the three cultivars were grown under drip irrigation and fertirrigation during the 2019 and 2020 growing seasons in an orchard near Badajoz (Spain). From these trees, flowers

were collected at the anthesis stage (0 days post-anthesis, DPA) and fruits were sampled at 7, 14, 21, 28, 35, and 42 DPA, spanning a time from the fruit set to the time of endocarp lignification (Gomez-Jimenez et al., 2010; Camarero et al., 2023). In addition, after endocarp lignification, fruits of the three olive cultivars at specific developmental stages were randomly tagged, collected, and processed as previously described (Inês et al., 2018). A total of 500 fruits from 10 olive trees per cultivar were used for each developmental stage. To minimize the effects related to asynchronous fruits ripening within the same tree, we picked fruits with similar pigmentation from all around the external parts of the tree canopy. Flowers at the anthesis stage and whole fruits of 'Arbequina', 'Picual' and 'Manzanilla Sevillana' olive cultivars were weighed, and the longitudinal and transverse diameters were measured at different developmental stages. Flowers at the anthesis stage, and whole fruit as well as fruit pericarp samples at different developmental stages were collected for cytology and ploidy analyses.

2.2. Cytological analysis

In the cytological study, at least three biological replicates were made at each stage. Fruits were cut at the equatorial plane. For this, samples were sliced 0.3 to 0.6 mm thick and immediately fixed in ethanol-acetic acid (3:1, v/v) for 2 h at ambient temperature. The samples were rinsed 3 times using 70% 226 ethanol, dried using an ethanol series, and finally embedded in Technovit 7100 (Kulzer Sections that were 30 µm thick were used for confocal imaging and were stained for 2 min with Calcofluor White M2R (Wyeth, http://www.wyeth.com (accessed on 10 January 2020), 0.1% w/v in distilled water), a fluorescence brightener commonly used in the visualization of crystalline cellulose in plant cell walls (Gahan 1984). The samples were rinsed with distilled water, mounted with a cover slip in DABCO mounting medium, and sealed with nail polish. Fruit cells and pericarp thickness were examined using a confocal laser-scanning microscope (model Fluoview-BX50, Olympus). The cell size (cell area) and pericarp thickness (cross-section) were determined using a CellProfiler image analysis system (Lamprecht et al., 2007), as in our previous study (Camarero et al., 2023).

2.3. Flow cytometry analysis

The cell division period was precisely determined using flow cytometry with nucleus ploidy profiles taken from ovaries and fruits using the method of Loureiro (2009). The samples of 0.1-0.2 g fresh weight were diced into 0.5 mL using a razor blade and placed in an ice-cold buffer (0.2 M Tris-HCl, 4 mM $MgCl_2$, 2 mM EDTA, 86 mM NaCl, 10 mM metabisulphite, pH 7.5, and 1% Triton X-100), filtered through a 30 µm nylon mesh, and finally stained using 4,6-diamidino-2-phenylindole (DAPI). Next, the distribution of the nuclear-DNA content was analysed with a FACS CantoII flow cytometer, and the recorded data were analysed using FACSDiva 6.1.2 software (BD Biosciences, Franklin Lakes, NJ, USA). For each stage, 4 biological replicates, with 10,000 nuclei each, were prepared. The DNA content (C value) of the olive fruit cells was submitted to flow cytometry with the use of internal calibration standards (Loureiro, 2009). The C values were determined following Dolezel et al. (2007): 2C DNA (pg) = (mean of the problem sample G1 peak × 2C DNA content of the standard [pg])/mean of the standard G1 peak.

3. Results and discussion

3.1. Morphological changes during fruit development in olive cultivars

The characteristics of olive developing fruits were compared in the three olive cultivars, 'Arbequina', 'Manzanilla Sevillana' and 'Picual', which were chosen because of the different fruit sizes. As shown in Fig.III.1, the variations in the fruit weight between olive cultivars, in which the mean fruit weights at fully ripe stage ranged from 1.5 to 4.5 g, were exhibited from 35 DPA under the same grown conditions. The fruit weight difference among the three olive cultivars gradually increased as a result of growth after 35 DPA until the fruit ripening (Fig.III.1). Although the three olive fruits maintained an initial rapid increase of fruit weight, the small-fruited cultivar 'Arbequina' required about 240 DPA from anthesis until complete fruit ripening, whereas large-fruited cultivars, 'Picual' and 'Manzanilla Sevillana', required about 195 and 169 DPA, respectively, suggesting a possible antagonistic relationship between the fruit size and the duration of fruit ripening process in olive cultivars.

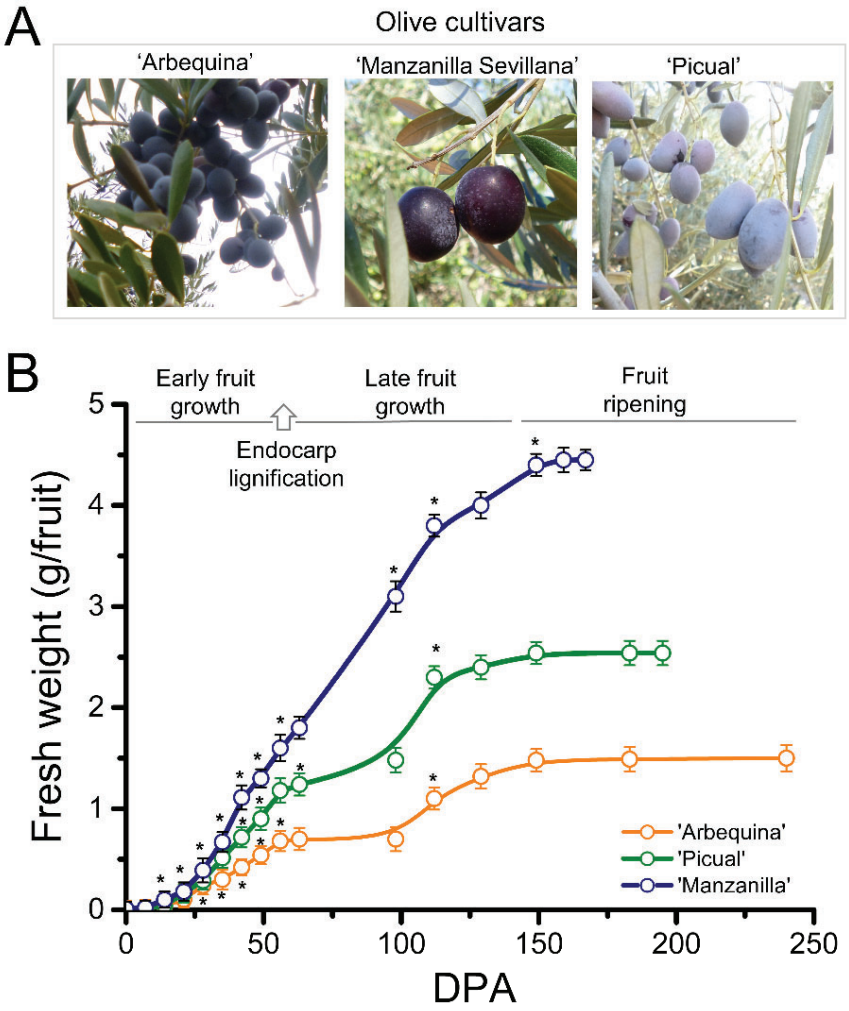

Figure III. 1. Fruit development of 'Arbequina', 'Manzanilla Sevillana' and 'Picual' olive cultivars with contrasting fruit size and shape. (A) Images of olive fruit morphology at the fully ripe stage in 'Arbequina', 'Manzanilla Sevillana' and 'Picual' cultivars at 260, 189, and 169 DPA, respectively. (B) Changes in fresh weight (FW) (g fruit^{-1}) of olive fruit during fruit growth and ripening in the three cultivars: 'Arbequina' with small and round fruit, 'Manzanilla Sevillana' with large and round-fruit and 'Picual' with large and elongated fruit. Asterisks indicate statistically significant changes with respect to the preceding point according to Tukey's test ($P < 0.05$). Data are the means of three independent experiments ± SE (n ≥ 20). DPA: Days Post-Anthesis

The growth of olive fruit has generally been divided into three stages: rapid growth with fruit size increase, fruit endocarp lignification with delayed size increase in the fruit pulp; and increase in fruit pulp size (Conde et al., 2008). The endocarp lignification of olive fruit is considered to undergo growth arrest around 50 days after pollination and fertilization (Camarero et al.,

2023). In the present study, the results were showed in two independent experiments, first from anthesis to 50 DPA (early fruit development) and second from 50 DPA to fully ripe stage (late fruit development).

3.2. Morphological changes during early fruit growth in olive cultivars

To appreciate the extent of this growth arrest about endocarp lignification of olive fruit, were measured various growth-related variables in the ovary and fruit of the three olive cultivars, at anthesis (0 DPA) and up to 42 DPA, determined according to Camarero et al. (2023). Even if the fruit weight increases are largest between 21 and 42 DPA in all olive cultivars, their growth rates maximized at 28 DPA in 'Arbequina', at 35 in 'Picual', and at 42 in 'Manzanilla Sevillana' cultivars (Fig.III.2A). In the small-fruited cultivar 'Arbequina', the olive fruit growth rate decreased after 28 DPA, but increased in large- fruited cultivars (up to 35 and 42 DPA in 'Picual' and 'Manzanilla Sevillana', respectively). This variable then decreased during the endocarp lignification in all three olive cultivars, indicating the end of the early vigorous growth period of the olive fruit. In addition, the maximum growth rate was slower in the small-fruited cultivar, 'Arbequina', that in the large-fruited cultivars, 'Manzanilla Sevillana' and 'Picual' (Fig.III.2A). This means that 'Arbequina' fruit weight augmented 64-fold from anthesis to 42 DPA, whereas both 'Picual' and 'Manzanilla Sevillana' more than doubled (an increase of 218-fold) compared with 'Arbequina' from anthesis to 42 DPA (Fig.III.1). Thus, we found variations between olive cultivars in the duration of early fruit growth and in the maximum growth rate.

Regarding the fruit shape, in 'Arbequina' and 'Manzanilla Sevillana' cultivars, fruit length and width showed similar trends during this phase, resulting in a rounder shape of these cultivars (Fig.III.2B,C), whereas, in 'Picual' with elongated fruit, the growth in length was the most rapid followed by width starting from 14 DPA, resulting in an increase in the fruit-shape index after 21 DPA (Fig.III.2D).

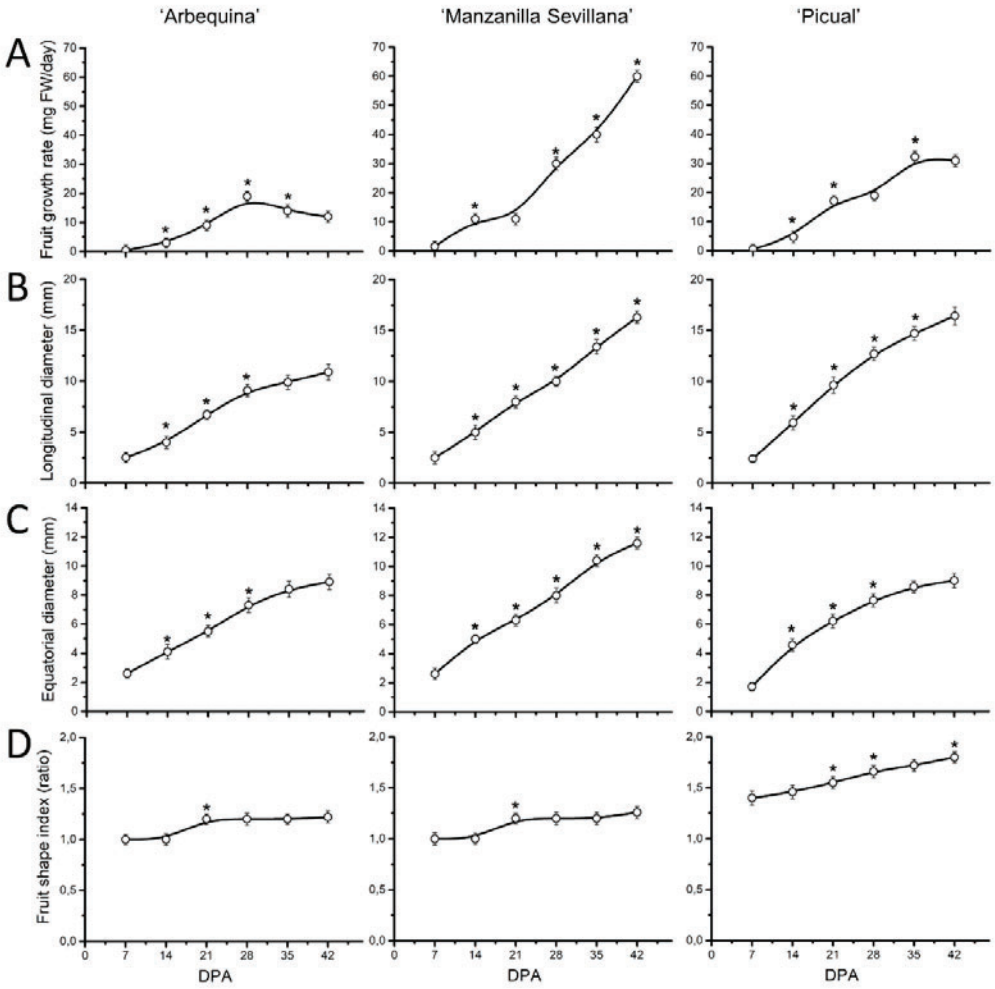

Figure III. 2. Morphological changes of olive fruit of 'Arbequina', 'Manzanilla Sevillana' and 'Picual' cultivars during early fruit development. (A) Changes in growth rate (mg FW day^{-1}), (B) longitudinal diameter (mm), (C) transverse diameter (mm), and (D) fruit-shape index of developing olive fruit at 0, 7, 14, 21, 28, 35, and 42 DPA from the three olive cultivars. Fruit-shape index is length-to-width ratio of the fruit. Asterisks indicate statistically significant changes with respect to the preceding point according to Tukey's test ($P < 0.05$). Data are the means of three independent experiments ± SE (n ≥ 20).

3.3. Cytological changes during early fruit growth in olive cultivars

To analyse the correlation between fruit size and cell size during early fruit growth, were first examined the epicarp and mesocarp cell areas, pericarp thickness, and cell expansion rate during early fruit development (Fig.III.3). In the three cultivars, the increase in pericarp thickness became detectable from 7 DPA and the area of cells in the mesocarp increased by more than 10-fold

from anthesis to 42 DPA, but the mesocarp cell area appeared to be smaller in the 'Arbequina' cultivar from 21 to 42 DPA than in the 'Manzanilla Sevillana' and 'Picual' cultivars during early fruit growth (Fig.III.3A).

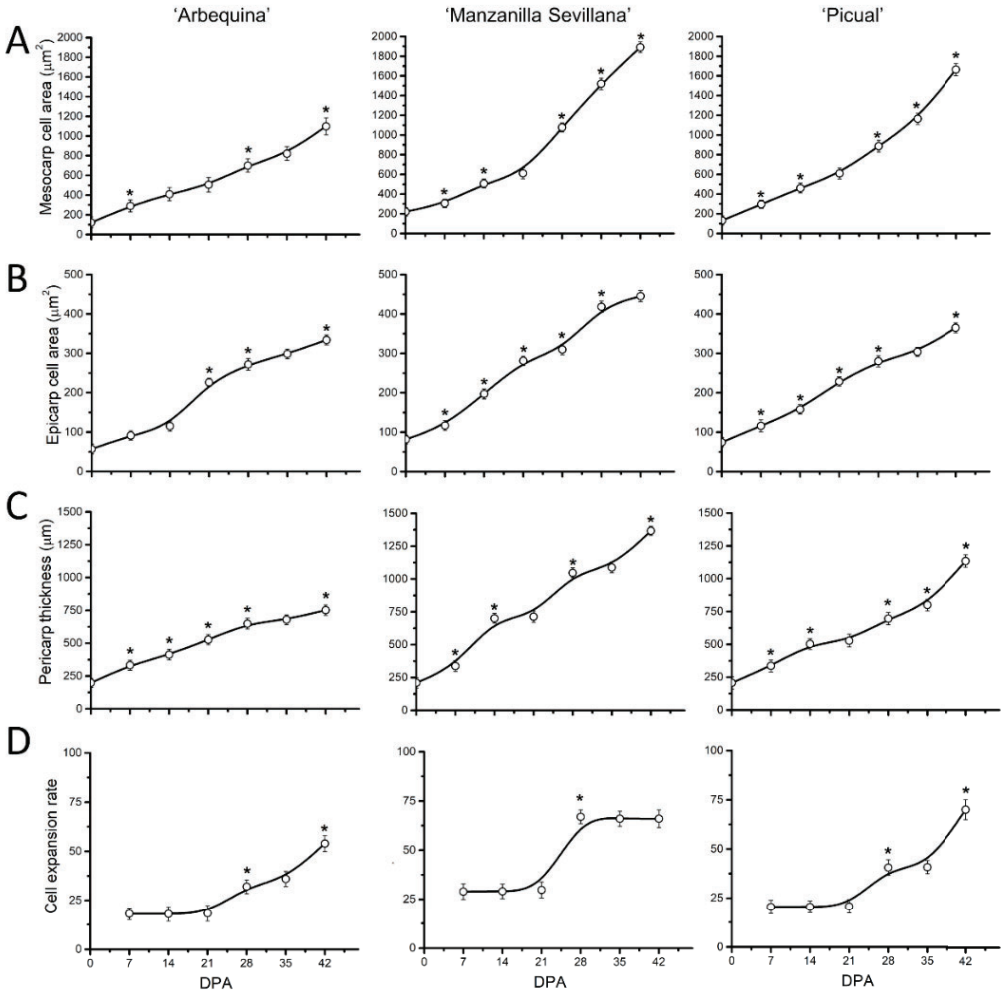

Figure III. 3. Cell parameters of olive fruit pericarp of 'Arbequina', 'Manzanilla Sevillana' and 'Picual' cultivars during early fruit development. (A) Mesocarp cell area (μm^2), (B) epicarp cell area (μm^2), (C) pericarp thickness (µm) and (D) cell expansion rate (mesocarp cell area/day) of developing olive fruit at 0, 7, 14, 21, 28, 35, and 42 DPA from the three olive cultivars. The cell area of fruit mesocarp and epicarp cells was measured during early fruit development (staining was with Calcofluor White) using confocal microscopy. Asterisks indicate statistically significant changes based on Tukey's test ($p < 0.05$) from the preceding point. Data are means ± SE ($n \geq 5$).

The highest cell expansion rates (cell area/day) occurred from 21 to 42 DPA, while pericarp cells expanded at a similar rate for 21 DPA in all three cultivars. In addition, different rates of mesocarp cell expansion from 21 to 42 DPA among cultivars led to lower cell size in Arbequina cultivar and to higher cell

size in Manzanilla Sevillana' and 'Picual' (Fig.III.3). Thus, the smaller cell size in 'Arbequina' fruit was due to a lower expansion rate rather than to a shorter period of expansion during early fruit growth.

3.4. Morphological changes during late fruit growth in olive cultivars

According to the data of fruit growth variables throughout the following fruit growth phase, the three cultivars showed the same patterns of fruit growth and diameters during this phase (Fig.III.4).

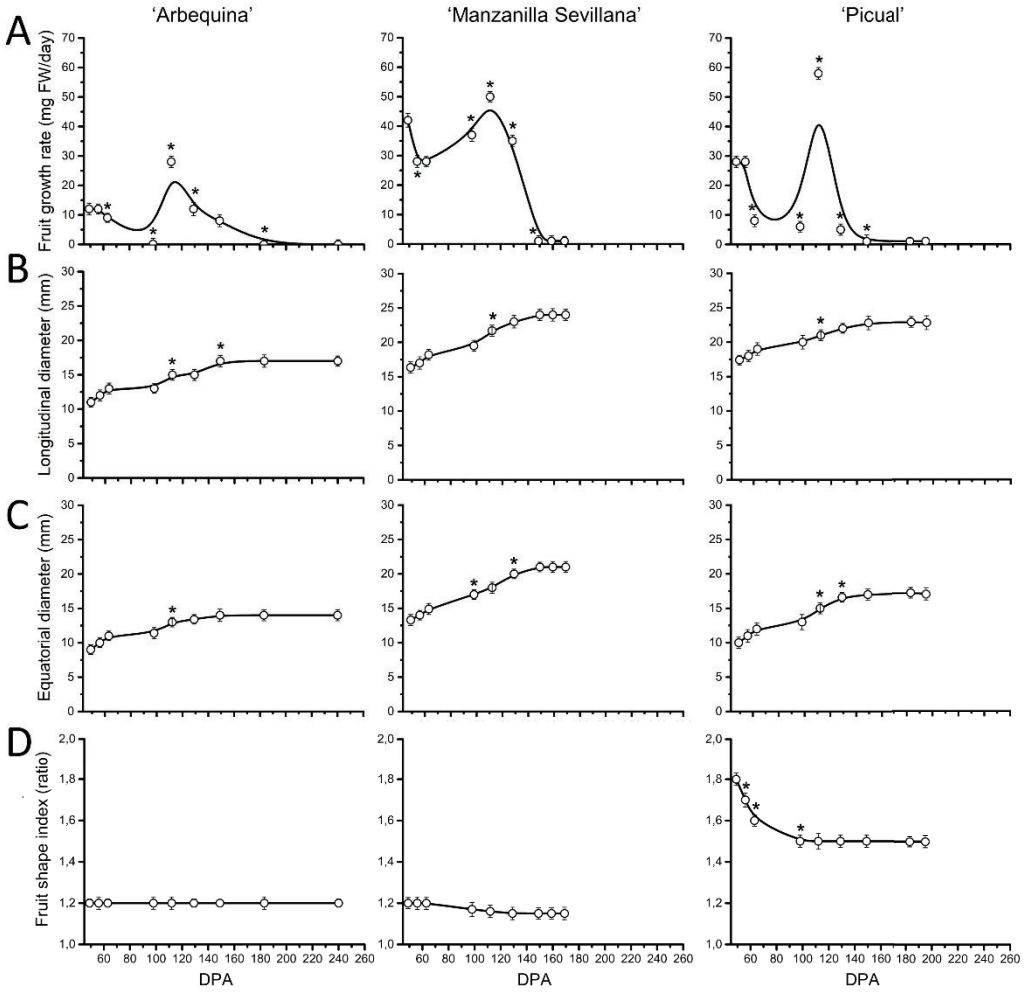

Figure III.4. Morphological changes of olive fruit of 'Arbequina', 'Manzanilla Sevillana' and 'Picual' cultivars during fruit growth and ripening. (A) Changes in growth rate (mg FW day^{-1}), (B) longitudinal diameter (mm), (C) transverse diameter (mm), and (D) fruit-shape index of developing olive fruits from the three olive cultivars. Fruit-shape index is length-to-width ratio of the fruit. Asterisks indicate statistically significant changes with respect to the preceding point according to

Tukey's test ($P < 0.05$). Data are the means of three independent experiments ± SE ($n \geq 20$).

From 56 to 98 DPA, fruit growth rates slowed, and the diameters of olive fruits grew moderately in the three cultivars. At 112 DPA, both parameters rose strongly and then levelled off at the green mature stage (Fig.III.4). In fact, a secondary increase of fruit weigh by 2.5 times (about 60% of final fruit weight) was evident at the transition between endocarp lignification and green mature stage in the three cultivars (Fig.III.1). Their fruit growth rate reached its maximum at 112 DPA followed by a decline until the green mature stage in the three cultivars, but 'Arbequina' also displayed a slower growth rate than did the other cultivars during this phase (Fig.III.4), consistent with the smaller final fruit weight recorded among olive cultivars. Likewise, the fruit diameters increased by more than 30-fold from the fruit endocarp lignification to the green mature stage in 'Arbequina' and 'Manzanilla' rounded fruits, whereas in elongated fruit of 'Picual', the increase in fruit weight was related to 22-fold increase in longitudinal diameter and a 33-fold increase in transverse diameter during this phase, resulting in a decrease in the fruit-shape index during late fruit growth in this cultivar (Fig.III.4).

3.5. Cytological changes during late fruit growth in olive cultivars

Similar variations occurred for pericarp cell areas and thickness in the three cultivars during late fruit growth (Fig.III.5A-C). The cell area in the fruit mesocarp at this final stage of olive fruit development did not differ significantly among the three cultivars (Fig.III. 5A).

In olive fruit, the pericarp thickness increased by more than 2-fold during this phase. A significant increase in the rate of mesocarp cell expansion was observed from 60 DPA in the three cultivars (Fig.III.5D), indicating that intense cell expansion occurs in olive fruit mesocarp after the endocarp lignification.

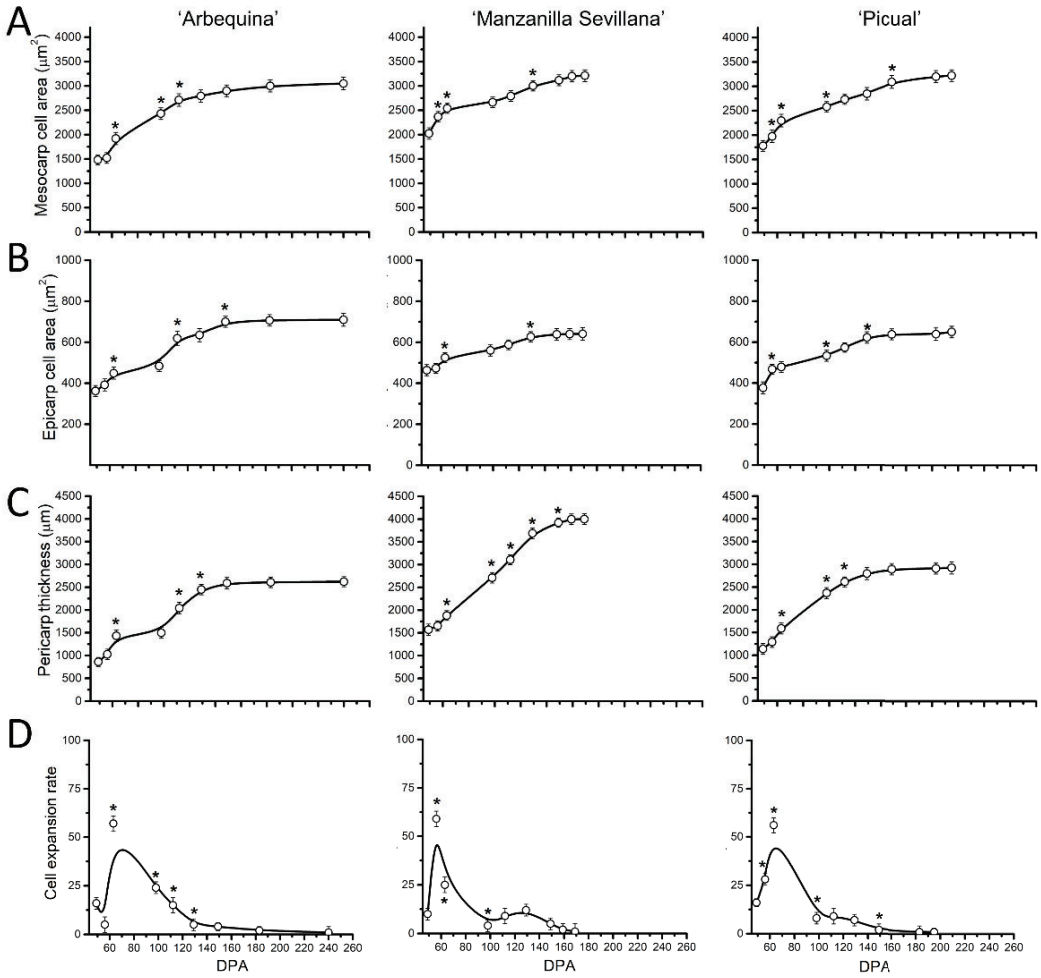

Figure III.5. Cellular parameters of olive fruit pericarp of 'Arbequina', 'Manzanilla Sevillana' and 'Picual' cultivars during fruit growth and ripening. (A) Mesocarp cell area (μm^2), (B) epicarp cell area (μm^2), and (C) pericarp thickness (µm) and (D) cell expansion rate (mesocarp cell area/day) of developing olive fruits from the three olive cultivars. The cell area of fruit mesocarp and epicarp cells was measured (staining was with Calcofluor White) using confocal microscopy. Asterisks indicate statistically significant changes based on Tukey's test ($p < 0.05$) from the preceding point. Data are means ± SE (n ≥ 5).

3.6. Ploidy analysis in developing olive fruit

Cell division activity during olive fruit development for the three cultivars was characterized by flow cytometric analysis of the nuclear DNA contents in olive fruit from 0 to 42 DPA (Fig.III.6). In olive fruit of small-fruited cultivar, the maximal proportion of 4C cells (47.8%), which is an indirect estimate for cell division, was reached at 21 DPA (Fig.III. 6A). High levels of cell division were

found afterwards at 21 DPA, but the proportion of 4C cells was lower in 'Arbequina' (47.8% for the maximum level) than in 'Manzanilla' and 'Picual' fruits (62.7% and 63.1% for the maximum level, respectively, Fig.III.6B,C). The slower division rate of 'Arbequina' fruit suggests a lower final cell number compared with 'Manzanilla' and 'Picual' fruits at this stage. Notably, at 35 DPA, the proportion of 2C cells increased while the proportion of 4C cells decreased remarkably in 'Arbequina' fruits (Fig.III.6), indicating that cell division had almost completely stopped. The 8C cells represented 9.5 and 8.2% of the cells in 'Arbequina' fruits at 21 and 35 DPA, respectively.

In large-fruited cultivars, 'Manzanilla Sevillana' and 'Picual', the analyses of cell division activity showed similar trends during early olive fruit development. From anthesis (0 DPA) to 14 DPA, the proportion of 4C cells increased with time, while the proportion of 2C cells decreased in olive fruits (Fig.III.6). At 14 DPA, 4C cells represented the highest proportion of cells in the olive fruits (62.7% and 63.1% in 'Manzanilla' and 'Picual', respectively) indicating intensive cell division, while the proportion of 8C cells increased in comparison to those in fruits at 7 DPA (15.6% and 15.8% of total nuclei at 14 DPA in 'Manzanilla' and 'Picual', respectively, Fig.III.6). By contrast, at 28 DPA, cell division was not activated in fruits based on the increased ratio of 2C to 4C DNA levels relative to that at 21 DPA (Fig.III.6). From 28 to 42 DPA, most of the nuclei were 2C (88.7%, and 93.5% of total nuclei of fruits at 42 DPA in 'Manzanilla' and 'Picual' cultivars, respectively), while only low proportions of 4C and 8C nuclei were detected in these fruits (Fig.III.6). Thus, the results showed that cell division was triggered by pollination in the Manzanilla and 'Picual' olive fruits from 0 to 21 DPA.

For a clarification of the contribution of fruit pericarp to ploidy level of whole fruit and for an evaluation of the ploidy level during late fruit growth in olive, the DNA content of nuclei isolated from pericarp was determined by flow cytometric analysis in olive fruits of the three cultivars from 7 DPA to fully ripe stage (Fig.III.7).

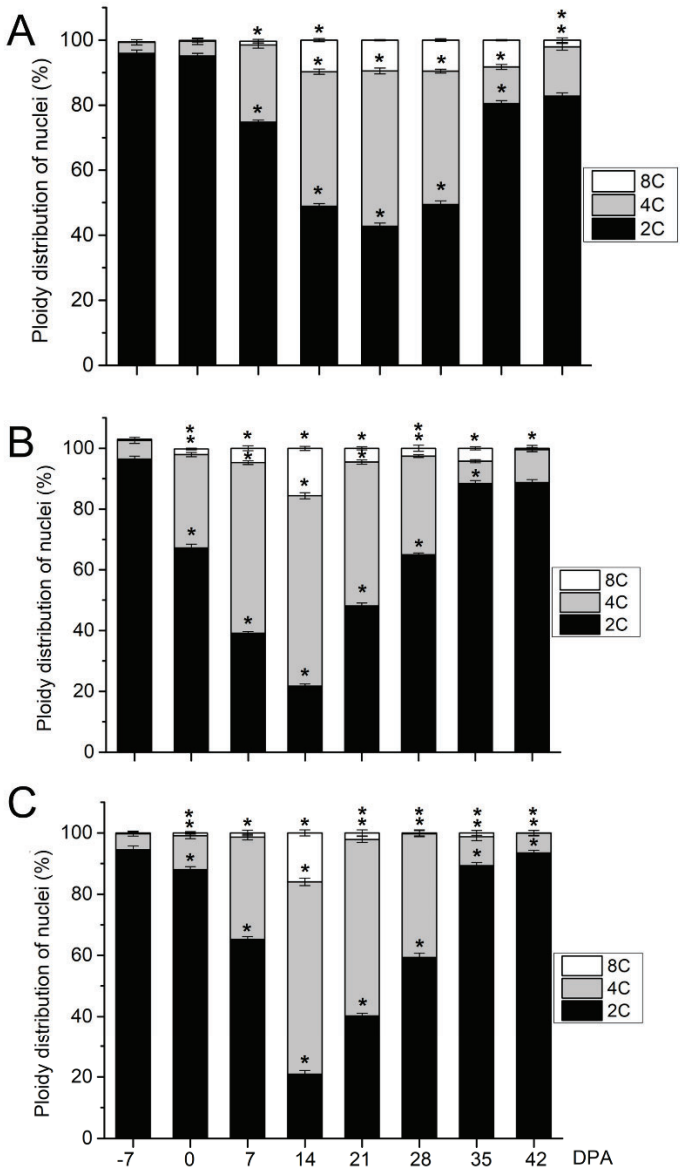

Figure III.6. Nuclear ploidy levels from olive fruits during early development in (A) the 'Arbequina', (B) 'Manzanilla Sevillana' and (C) 'Picual' olive cultivars. The percentage of nuclei in 2C, 4C, and 8C are shown from 0 to 42 DPA in the developing fruits. Each point is the average of four samples. Asterisks denote significant differences based on Tukey's test ($p < 0.05$) from the preceding point and bars are ± SE.

In all cultivars, the maximal proportion of 4C cells was reached at 14 DPA, indicating that intense cell division was activated in the pericarps at this time. The results showed that cell division occurs from 7 to 28 DPA in the fruit pericarps of the three olive cultivars. After 28 DPA, the proportion of 2C cells

increased while the proportion of 4C cells decreased in all pericarps up to 49 DPA (endocarp lignification).

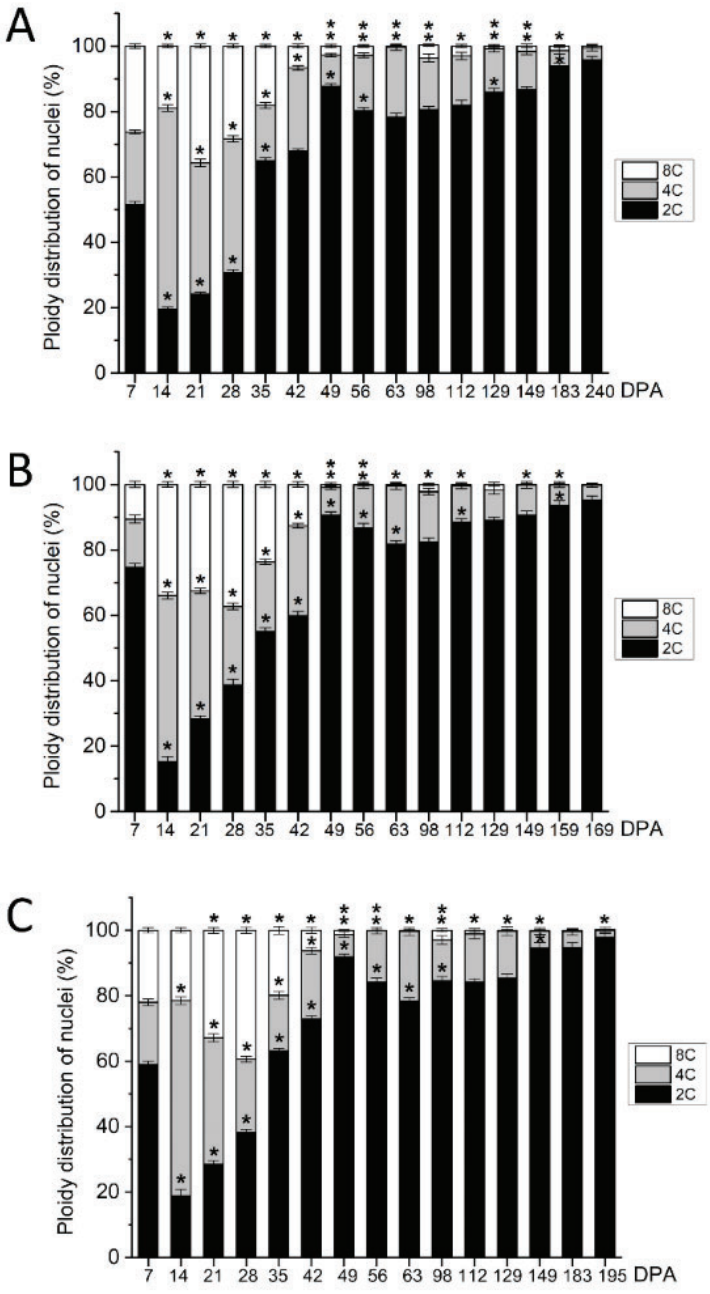

Figure III.7. Nuclear ploidy levels from olive fruit pericarps during growth and ripening in (A) the 'Arbequina', (B) 'Manzanilla Sevillana', and (C) 'Picual' olive cultivars. The percentage of nuclei in 2C, 4C, and 8C are shown in the developing fruit pericarp (epicarp + mesocarp). Each point is the average of four samples. Asterisks denote significant differences based on Tukey's test ($p < 0.05$) from the preceding point and bars are ± SE.

In addition, a similar proportion of endoreduplicated cells of up to 8C (one endocycle) was detected in pericarp cells between olive cultivars during this phase (Fig.III.7). At 98 DPA, endoreduplicated cells increased in pericarp cells of the three cultivars, this occurring in the late phase of olive fruit growth by cell expansion (Figs.III.7).

4. Conclusions

The present study indicates that the basis for fruit size differences between olive cultivars is determined mainly in early fruit growth phase, from anthesis to fruit endocarp lignification. Differences in fruit size between large- and small-fruited cultivars were evident as early as 35 DPA and were compounded as fruit developed. During early fruit growth, the gain of fruit weight rate lasted, on average, 10 days longer in the large-fruited cultivars than in the small-fruited cultivar. Moreover, olive fruit of the large-fruited cultivars enlarged, apparently due to relatively higher cell division and expansion rates during this phase compared with the small-fruited cultivar. The large-fruited cultivars had two-fold more weight than small-fruited cultivar at 42 DPA. Likewise, at this stage, the mesocarp cell area in the small-fruited cultivar was approximately half that of the large-fruited cultivars. On the other hand, the fruit of small-fruited cultivar showed growth by cell division for a shorter duration than did the fruit of large-fruited cultivars. Therefore, it appears that the olive fruit of large-fruited cultivars must have acquired more active cell division and more cell expansion ability, emphasizing the value of early growth events in determining final fruit size in olive.

Conclusiones generales

IV. Conclusiones generales

1. Durante el desarrollo temprano del fruto de olivo, los análisis de citología y de actividad mitótica revelaron la duración y la tasa de las fases de división y expansión celular en la variedad 'Picual'. Estas fases coexistieron durante los primeros 21 días post-antesis en el fruto, mientras que la expansión celular, sin división celular, duró hasta 3 semanas más en el fruto en desarrollo antes de la lignificación del endocarpo.

2. La antesis floral, concomitante con la polinización del ovario y el cuajado del fruto, de olivo se caracteriza por altos niveles de giberelinas (GA_1) y ácido jasmónico, si bien ambos niveles descienden durante el desarrollo temprano del fruto de olivo.

3. En el proceso de fructificación, las primeras señales hormonales que se desencadenaron fueron un aumento de la concentración de auxinas, citoquininas y ácido salicílico en el fruto de olivo. Entre estas, citoquininas (*trans*-Zeatin, *t*Z) y ácido salicílico fueron mayores durante la fase de división celular más intensa, mientras que auxinas, junto a giberelinas (GA_4) y ácido abscísico, tuvieron mayor importancia relativa en la fase en la que el crecimiento del fruto depende principalmente de la expansión celular.

4. El análisis transcriptómico de este trabajo ha sido el primer análisis detallado disponible de una serie de respuestas celulares bajo regulación transcripcional que conducen al desarrollo temprano del fruto de olivo.

5. Mediante el análisis transcriptómico, usando RNA-seq, se demostró la inducción secuencial de genes candidatos que regulan el ciclo celular asociada con cambios de genes implicados en la remodelación de la pared celular y en los flujos de iones, así como en el metabolismo y señalización hormonal durante el desarrollo temprano del fruto de olivo. Esto ocurrió acoplado a la actividad transcripcional de proteínas proteasas similares a las subtilasas y de factores de transcripción implicados en la señalización del crecimiento temprano del fruto de olivo. Este perfil de expresión génica, junto con los contenidos hormonales, contribuye a una mejor comprensión de los procesos que regulan la división y expansión celular y, en última instancia, el rendimiento y el tamaño del fruto de olivo.

6. La caracterización fisiológica del fruto de olivo demostró que el crecimiento del fruto de olivo comprendido entre la lignificación del endocarpo y la maduración del fruto representa el mayor aumento en expansión de las células del mesocarpo (un 60% del tamaño final de la célula del mesocarpo). Este aumento coincidió con una caída de los niveles endógenos de auxinas, citoquininas y ácido jasmónico, y un incremento del nivel de ácido salicílico, mientras que el aumento de los niveles de ácido abscísico, ácido jasmónico y auxinas al inicio de la maduración del fruto de olivo demuestra la participación de estas hormonas en el cambio de color del fruto de olivo.

7. El análisis hormonal parece constatar que el ácido abscísico puede desempeñar un papel central en la regulación de la maduración del fruto de olivo a través de la regulación transcripcional de genes clave de su metabolismo, mientras que los niveles y/o las respuestas de auxinas, citoquininas y giberelinas difieren entre variedades de olivo durante la maduración del fruto.

8. La relativa ausencia o presencia de giberelina GA_1 se correlacionó con diferencias en la morfología y tamaño del fruto, así como en la duración del proceso de maduración del fruto de olivo. Estos resultados constituyen un excelente punto de partida para analizar la implicación de esta hormona en otras variedades de olivo y para el diseño de nuevas estrategias para desarrollar frutos de mayor calidad (tamaño del fruto) y con una duración de maduración más corta en olivo. No obstante, no se puede descartar que otras señales hormonales o fisiológicas, aún no dilucidadas, puedan influir en aspectos del proceso de crecimiento y maduración del fruto de olivo.

9. La diferencia en el contenido de giberelinas del fruto entre las variedades de olivo estudiadas no puede explicarse por diferencias de expresión de la proteína GGPPS (geranilgeranil difosfato sintasa), siendo probablemente el resultado de una regulación metabólica más compleja en la que participan la biosíntesis, el catabolismo y la conjugación.

10. En este trabajo se ha abordado un análisis preliminar sobre la relativa importancia de las fases de división y expansión celular en el tamaño final del fruto examinando el área de la célula del mesocarpo y la actividad mitótica, mediante citometría de flujo, en frutos de olivo de tres variedades durante su desarrollo. Dicho análisis ha permitido concluir que una combinación de una mayor capacidad de división celular y un mayor grado de expansión celular determina el tamaño final del fruto en olivo.

Anexos

V. Anexos

Capítulo I

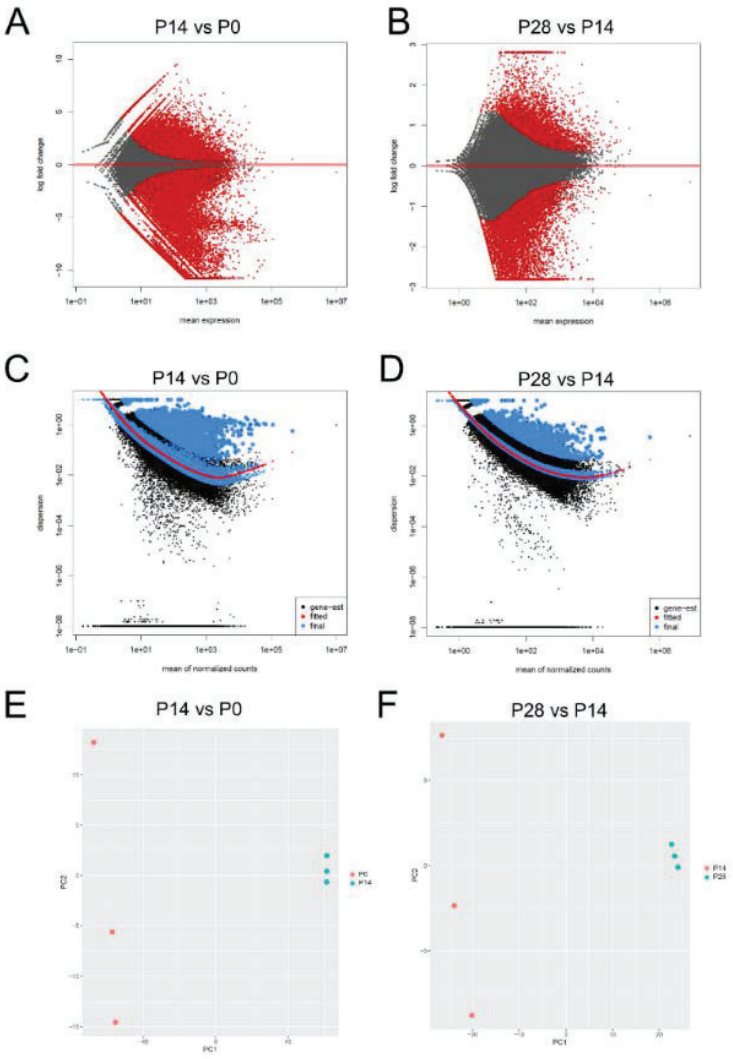

Figure I.S1. Whole transcripts expression during early development in 'Picual' olive. (A) MA plot for differential expression analysis for each gene, the log2 (fold change) (log2(P14/P0) between fruit at 14 DPA and at 0 DPA samples is plotted (A, y axis) against the gene's log2 (average expression) (M, x axis). (B) MA plot for differential expression analysis for each gene, the log2 (fold change) (log2(P28/P14) between fruit at 28 DPA and at 14 DPA samples is plotted (A, y axis) against the gene's log2(average expression) (M, x axis). Transcripts that are identified as significantly differentially expressed are colored in red. (C) Dispersion plot for differential expression analysis between P14 and P0 samples (P14 versus P0). (D) Dispersion plot for differential expression analysis between P28 and P14 samples (P28 versus P14). (E) Principal component analysis of expression data between P14 and P0 samples (P14 versus P0). (F) Principal component analysis of expression data between P28 and P14 samples (P28 versus P14).

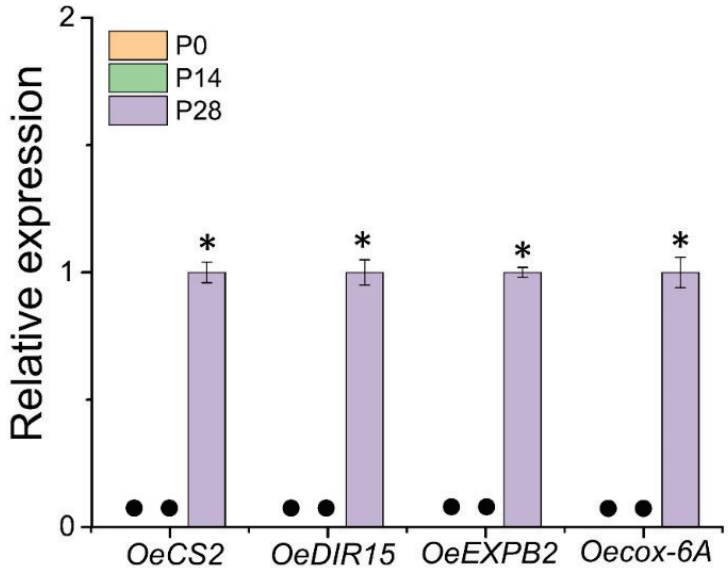

Figure I.S2. Expression of OeCS2, OeDIR15, OeEXPB2 and Oecox-6A during early fruit development in olive. Data are the means ± SD of three biological replicates with three technical repeats each and were determined by qRT-PCR normalized against Olea europaea ubiquitine (Gomez-Jimenez et al., 2010). Statistically significant differences based on unpaired Student's t-test at $p < 0.05$ are denoted by an asterisk. Gene expressions not detected are denoted by a circle.

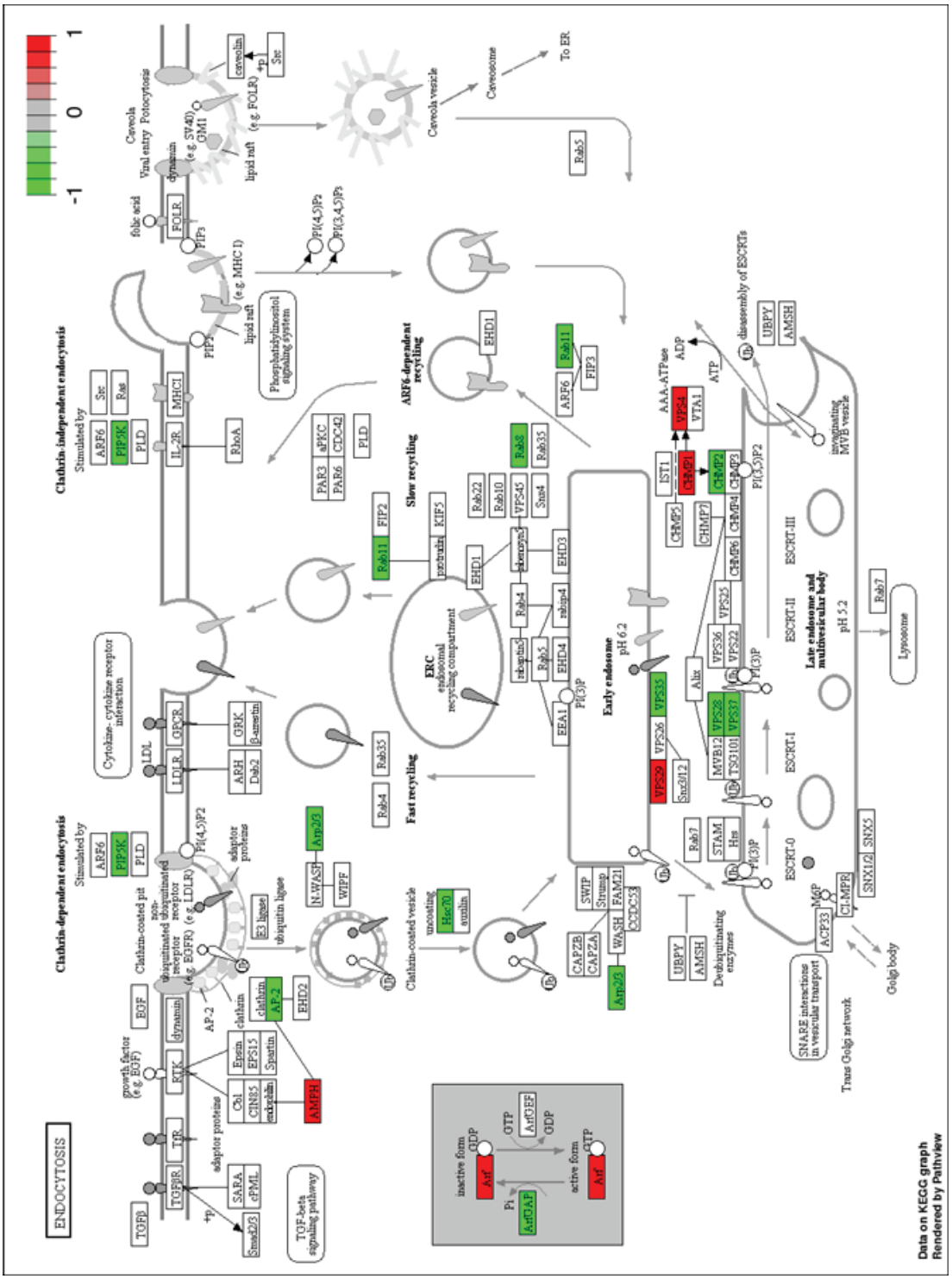

Figure I.S3. Graphic representation of the endocytosis pathway by KEGG. Boxes colored in red or green represent the EC number of the enzymes encoded by up- or down-regulated genes in the P28 versus P14 comparison (fruit at 28 DPA versus fruit at 14 DPA), respectively, generated by this study that are homologous to genes involved in the endocytosis pathway.

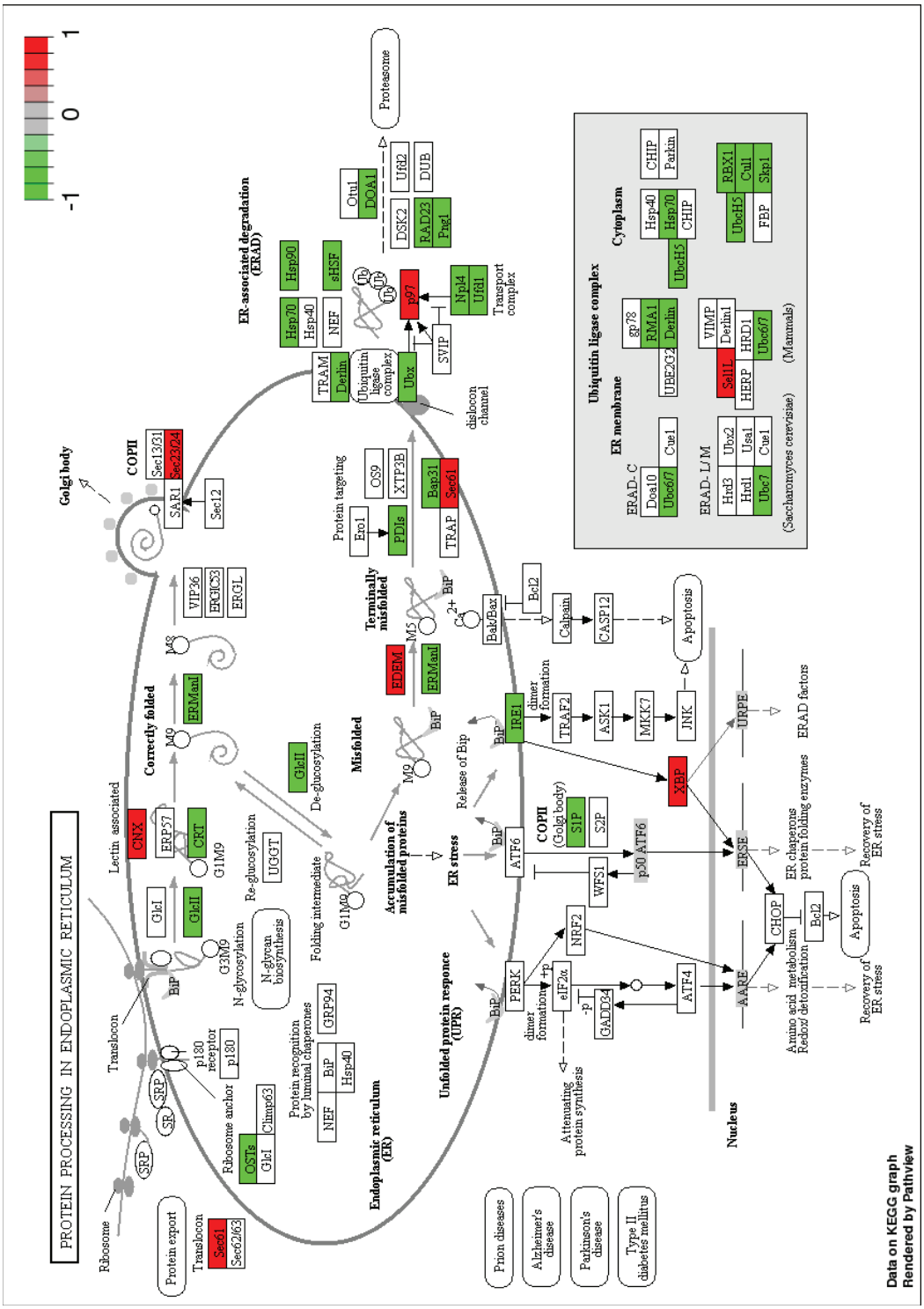

Figure I.S4. Graphic representation of the protein processing in endoplasmic reticulum pathway by KEGG. Boxes colored in red or green represent the EC number of the enzymes encoded by up- or down-regulated genes in the P28 versus P14 comparison (fruit at 28 DPA versus fruit at 14 DPA), respectively, generated by this study that are homologous to genes involved in the protein processing in endoplasmic reticulum pathway.

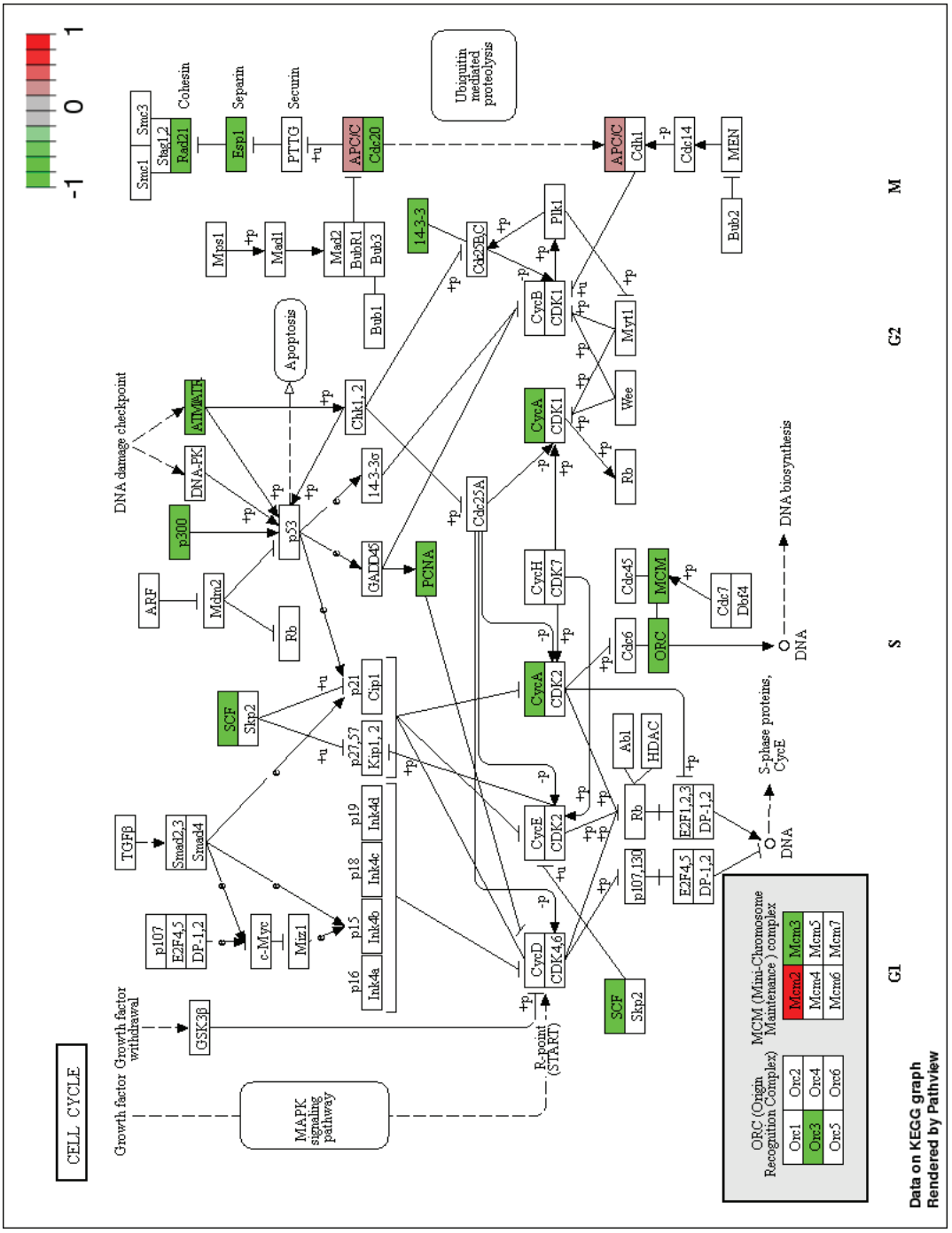

Figure I.S5. Graphic representation of the cell cycle pathway by KEGG. Boxes colored in red or green represent the EC number of the enzymes encoded by up- or down-regulated genes in the P28 versus P14 comparison (fruit at 28 DPA versus fruit at 14 DPA), respectively, generated by this study that are homologous to genes involved in the cell cycle pathway.

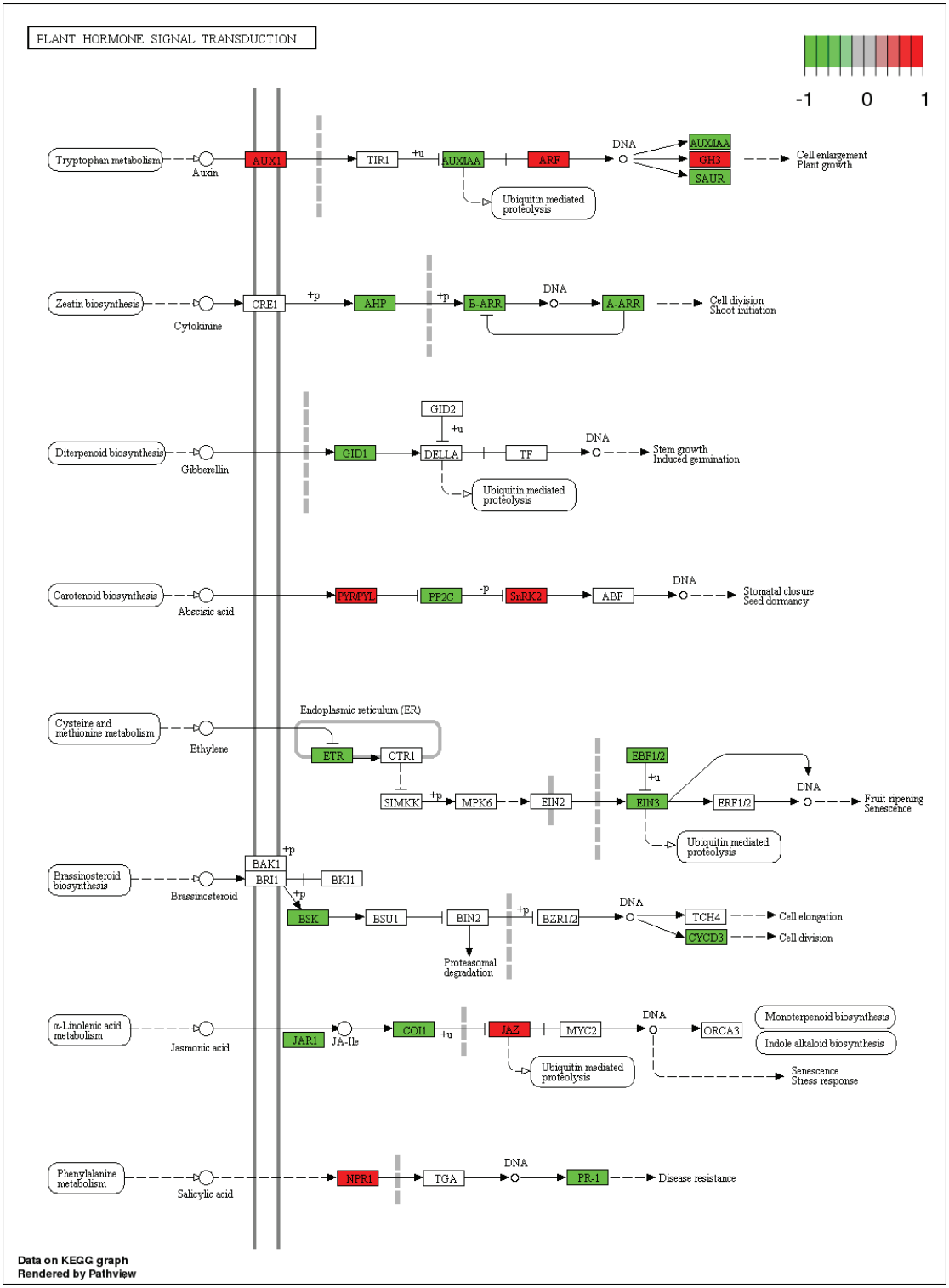

Figure I.S6. Graphic representation of the plant hormone signal transduction pathway by KEGG. Boxes colored in red or green represent the EC number of the enzymes encoded by up- or down-regulated genes in the P28 versus P14 comparison (fruit at 28 DPA versus fruit at 14 DPA), respectively, generated by this study that are homologous to genes involved in the plant hormone signal transduction pathway.

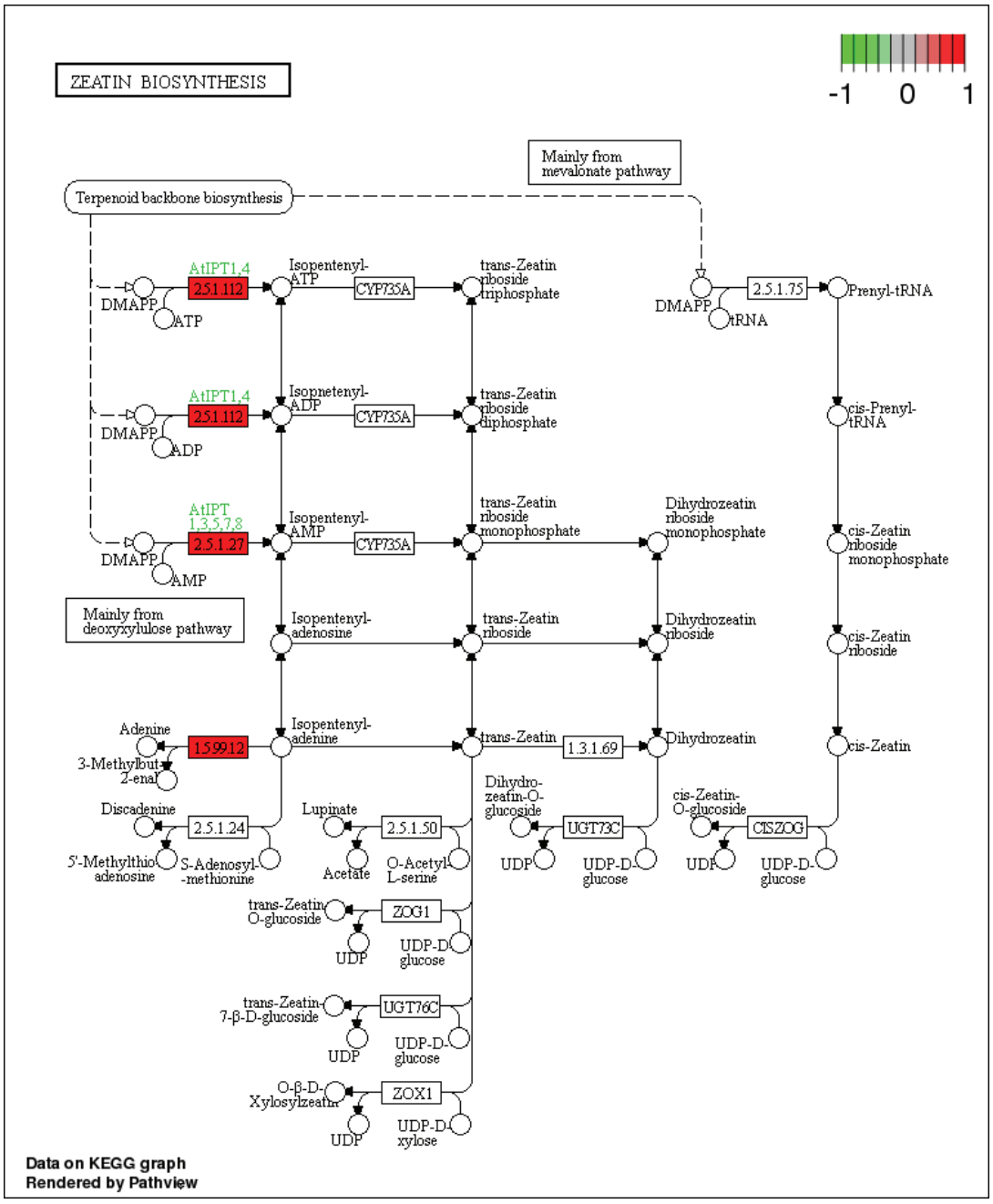

Figure I.S7. Graphic representation of the zeatin biosynthesis pathway by KEGG. Boxes colored in red or green represent the EC number of the enzymes encoded by up- or down-regulated genes in the P28 versus P14 comparison (fruit at 28 DPA versus fruit at 14 DPA), respectively, generated by this study that are homologous to genes involved in the zeatin biosynthesis pathway.

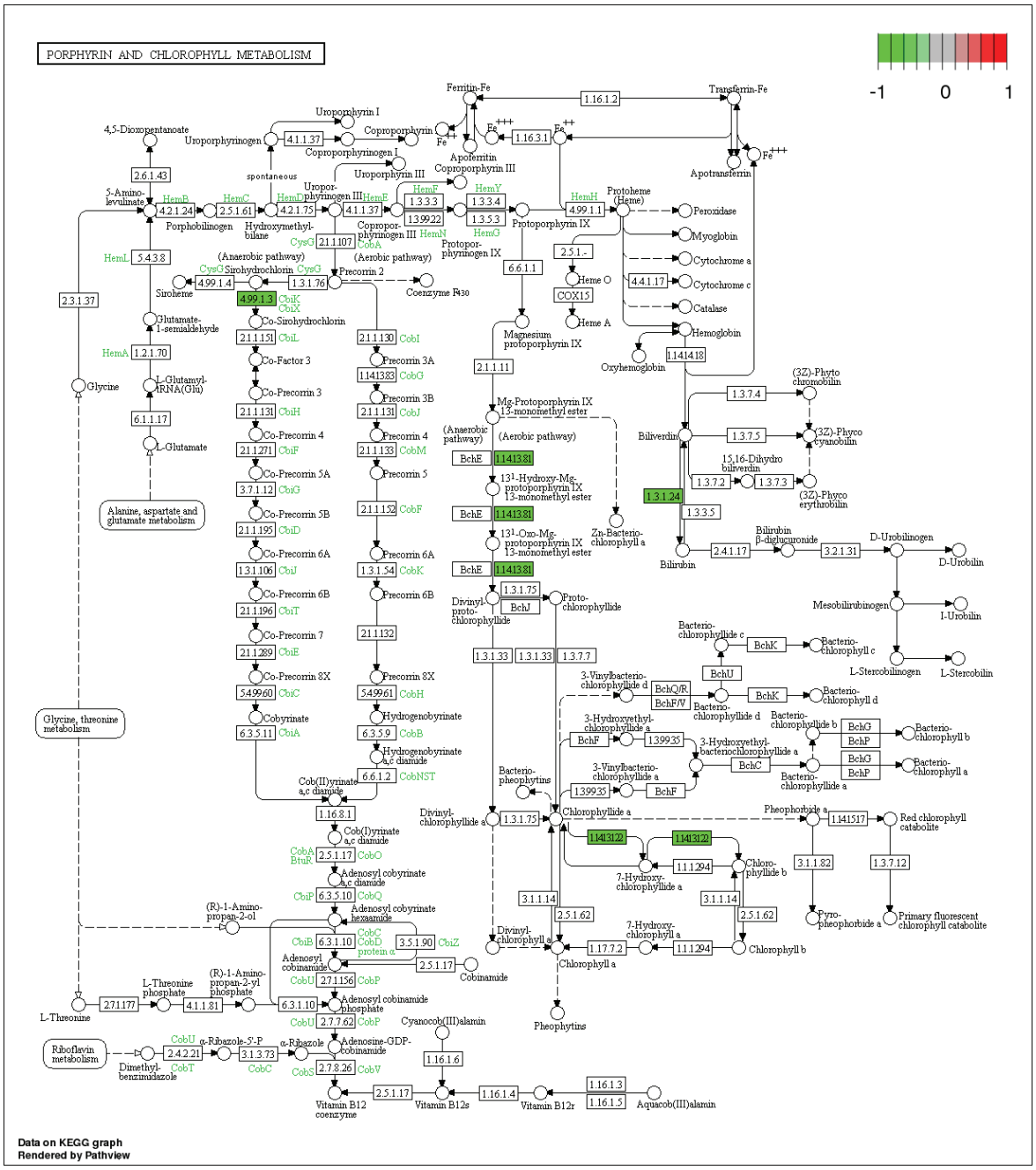

Figure I.S8. Graphic representation of the porphyrin and chlorophyll metabolism pathway by KEGG. Boxes colored in red or green represent the EC number of the enzymes encoded by up- or down-regulated genes in the P28 versus P14 comparison (fruit at 28 DPA versus fruit at 14 DPA), respectively, generated by this study that are homologous to genes involved in the porphyrin and chlorophyll metabolism pathway.

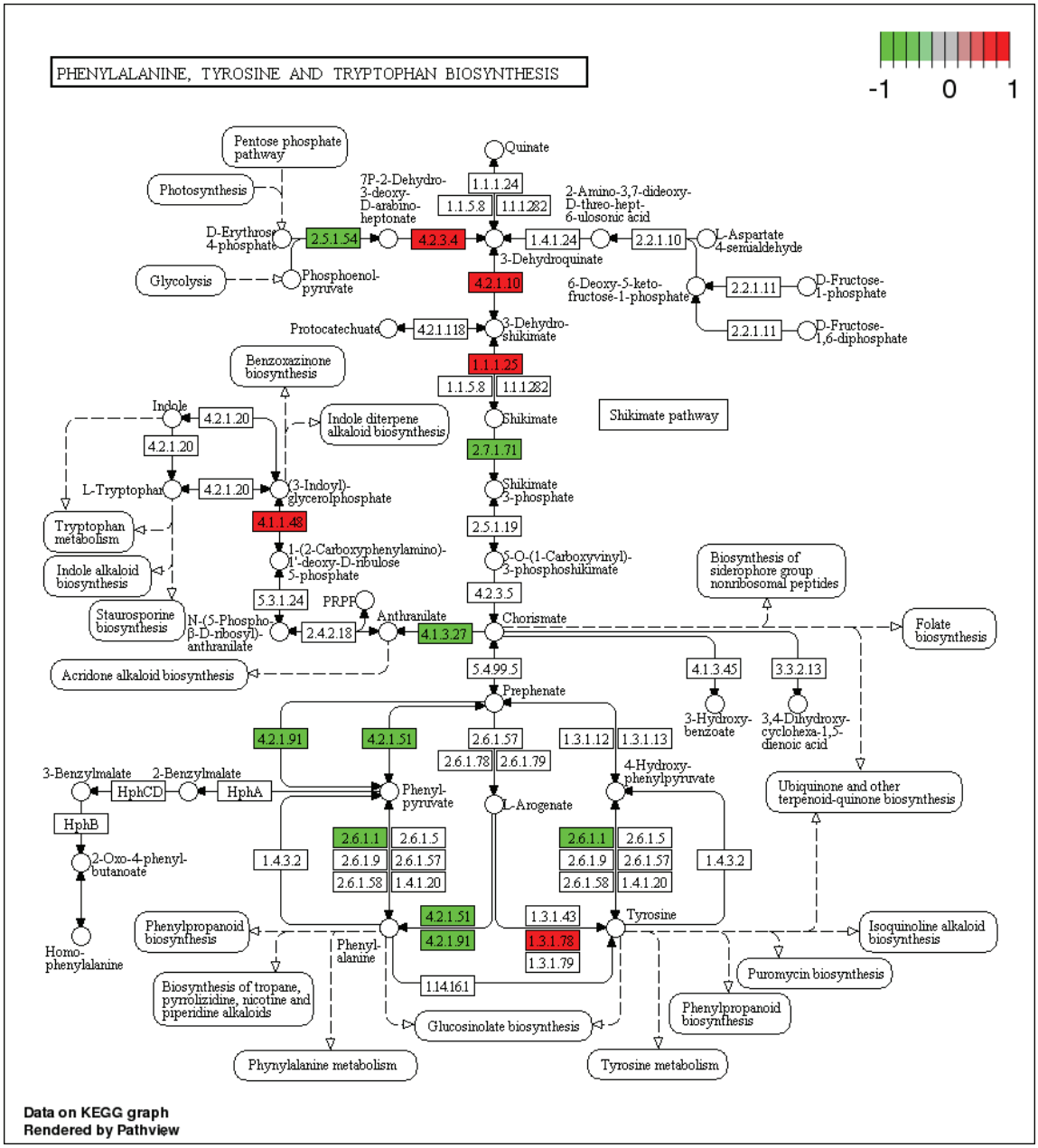

Figure I.S9. Graphic representation of the phenylalanine, tyrosine and tryptophan biosynthesis pathway by KEGG. Boxes colored in red or green represent the EC number of the enzymes encoded by up- or down-regulated genes in the P28 versus P14 comparison (fruit at 28 DPA versus fruit at 14 DPA), respectively, generated by this study that are homologous to genes involved in the phenylalanine, tyrosine and tryptophan biosynthesis pathway.

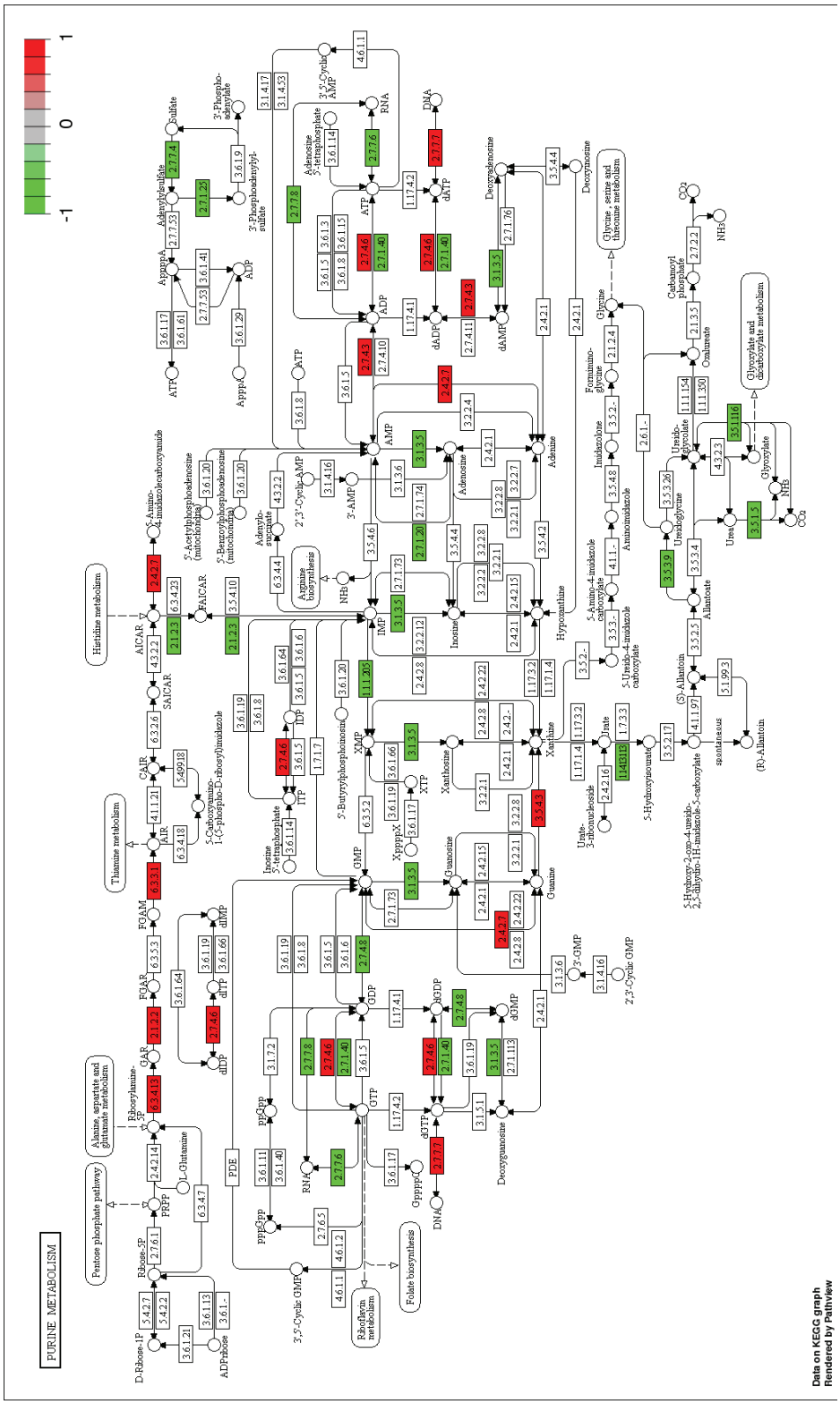

Figure I.S10. Graphic representation of the purine metabolism pathway by KEGG. Boxes colored in red or green represent the EC number of the enzymes encoded by up- or down-regulated genes in the P28 versus P14 comparison (fruit at 28 DPA versus fruit at 14 DPA), respectively, generated by this study that are homologous to genes involved in the purine metabolism pathway.

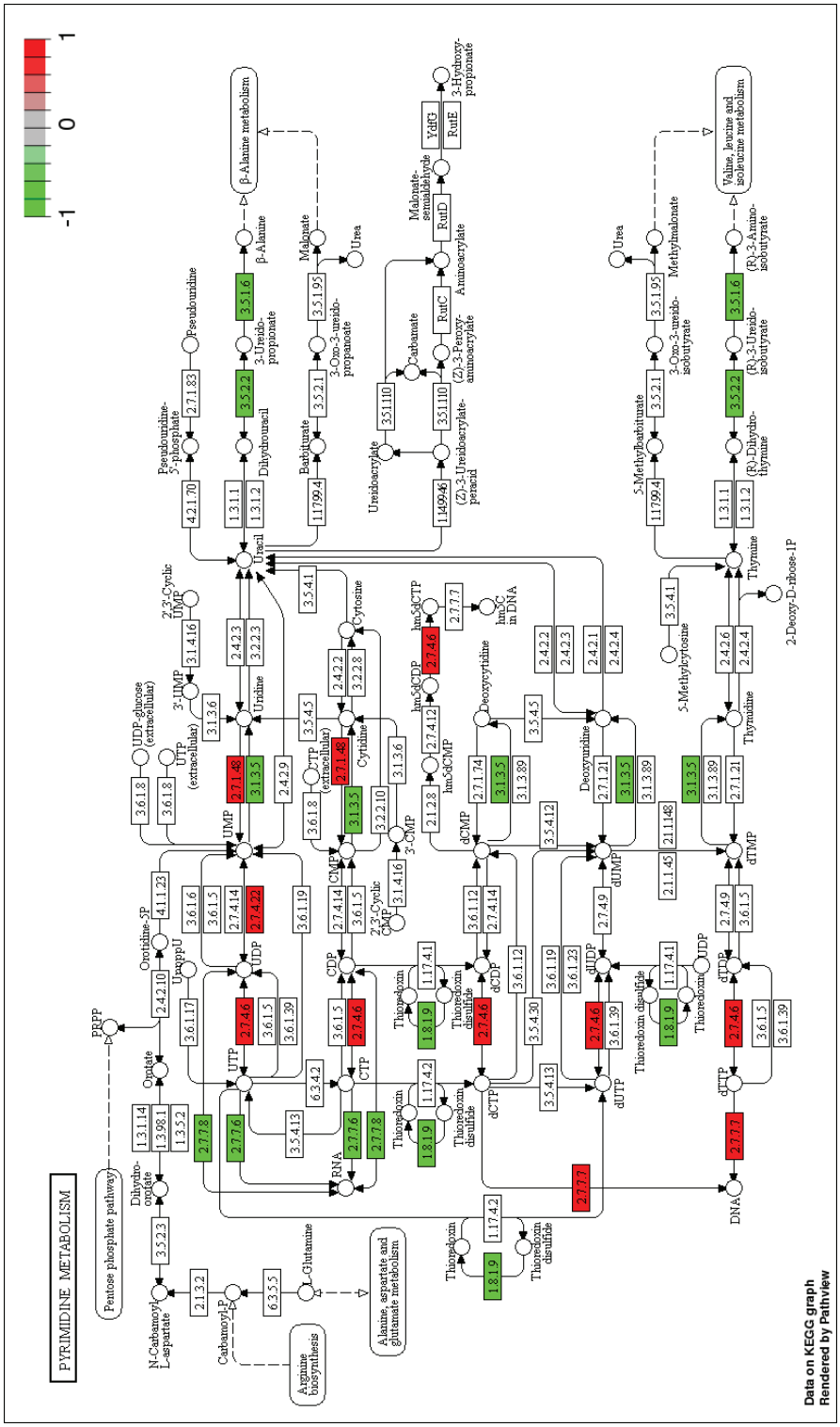

Figure I.S11. Graphic representation of the pyrimidine metabolism pathway by KEGG. Boxes colored in red or green represent the EC number of the enzymes encoded by up- or down-regulated genes in the P28 versus P14 comparison (fruit at 28 DPA versus fruit at 14 DPA), respectively, generated by this study that are homologous to genes involved in the pyrimidine metabolism pathway.

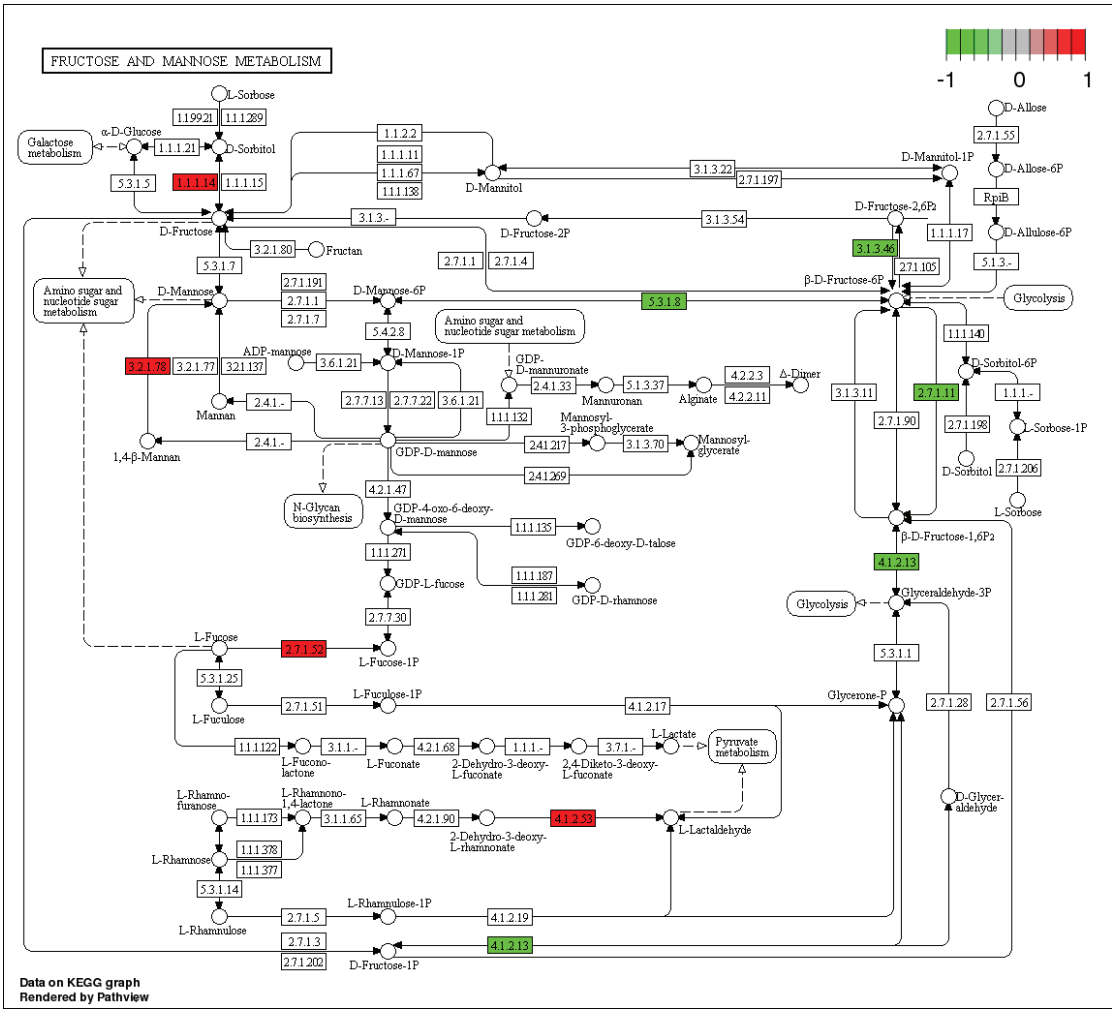

Figure I.S12. Graphic representation of the fructose and mannose metabolism pathway by KEGG. Boxes colored in red or green represent the EC number of the enzymes encoded by up- or down-regulated genes in the P28 versus P14 comparison (fruit at 28 DPA versus fruit at 14 DPA), respectively, generated by this study that are homologous to genes involved in the fructose and mannose metabolism pathway.

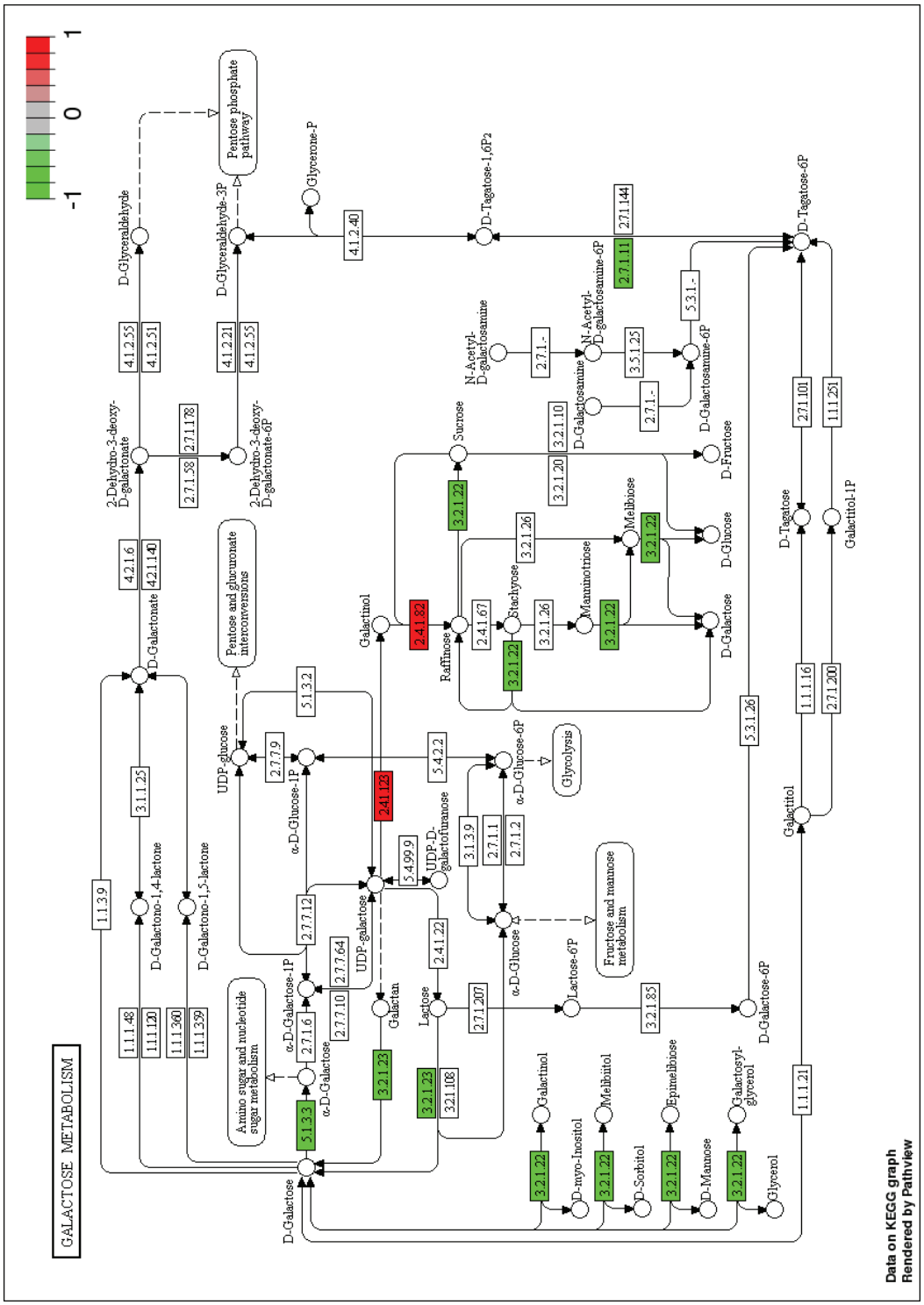

Figure I.S13. Graphic representation of the galactose metabolism pathway by KEGG. Boxes colored in red or green represent the EC number of the enzymes encoded by up- or down-regulated genes in the P28 versus P14 comparison (fruit at 28 DPA versus fruit at 14 DPA), respectively, generated by this study that are homologous to genes involved in the galactose metabolism pathway.

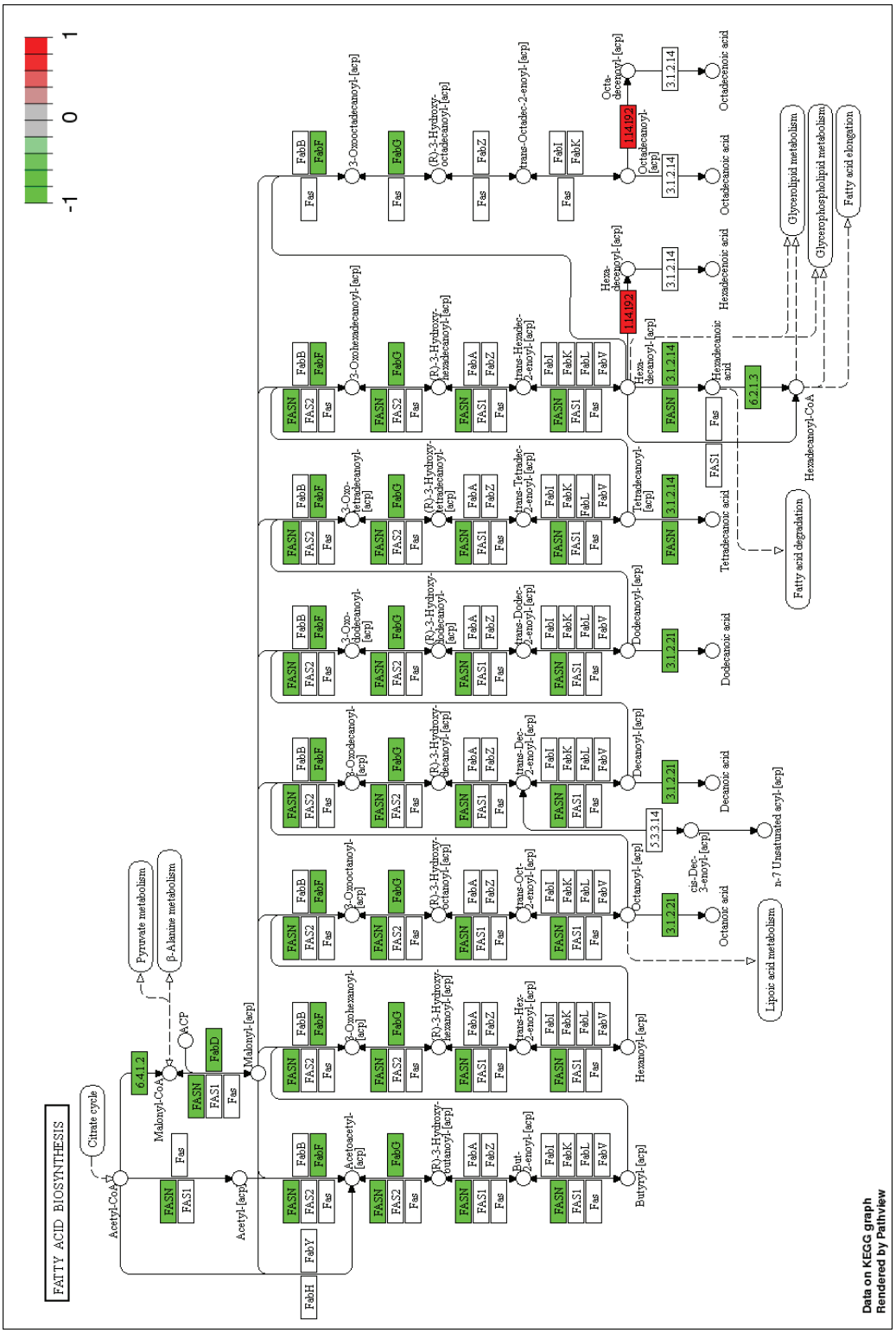

Figure I.S14. Graphic representation of the fatty acid biosynthesis pathway by KEGG. Boxes colored in red or green represent the EC number of the enzymes encoded by up- or down-regulated genes in the P28 versus P14 comparison (fruit at 28 DPA versus fruit at 14 DPA), respectively, generated by this study that are homologous to genes involved in the fatty acid biosynthesis pathway.

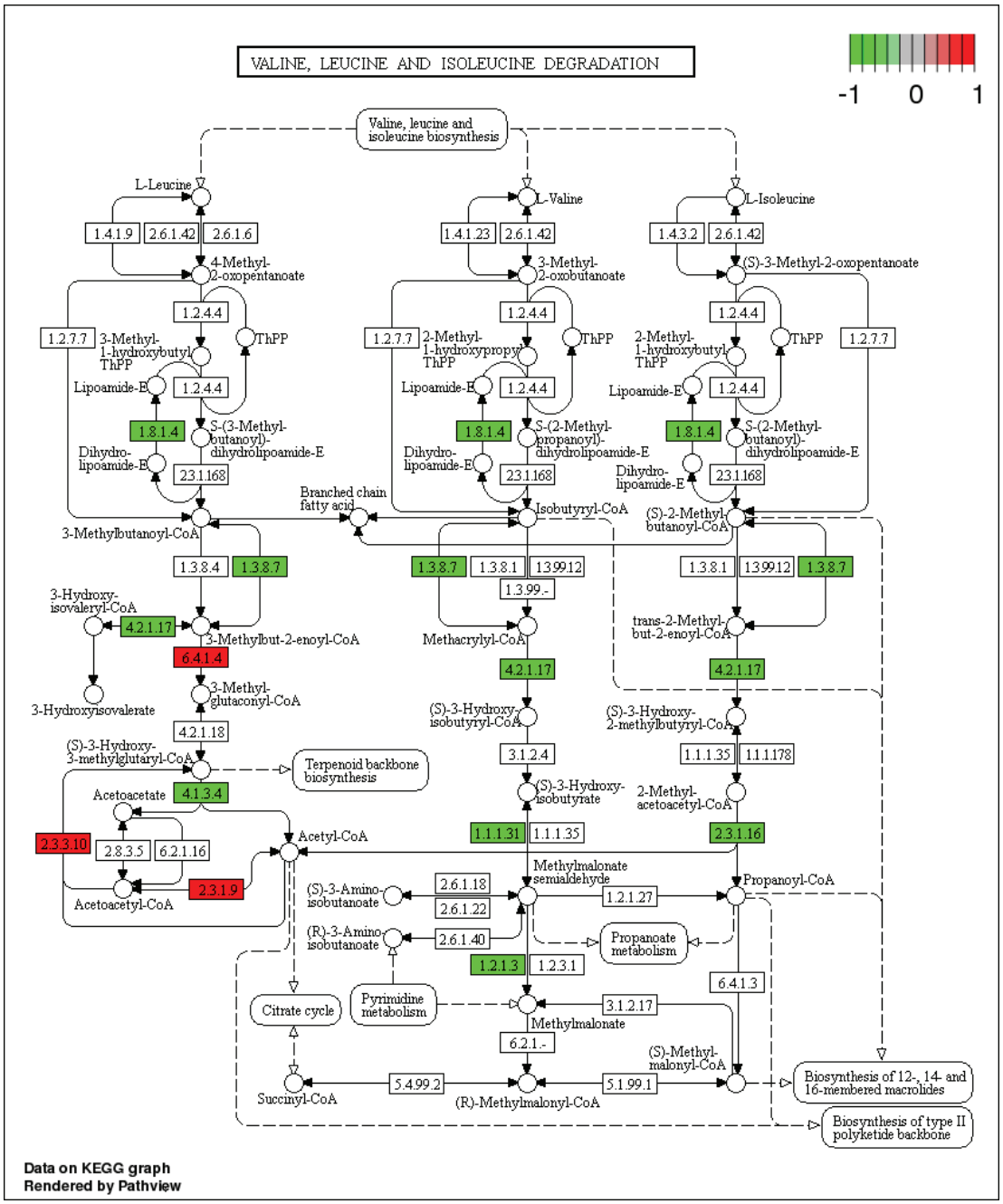

Figure I.S15. Graphic representation of the and valine, leucine and isoleucine degradation pathway by KEGG. Boxes colored in red or green represent the EC number of the enzymes encoded by up- or down-regulated genes in the P28 versus P14 comparison (fruit at 28 DPA versus fruit at 14 DPA), respectively, generated by this study that are homologous to genes involved in the and valine, leucine and isoleucine degradation pathway.

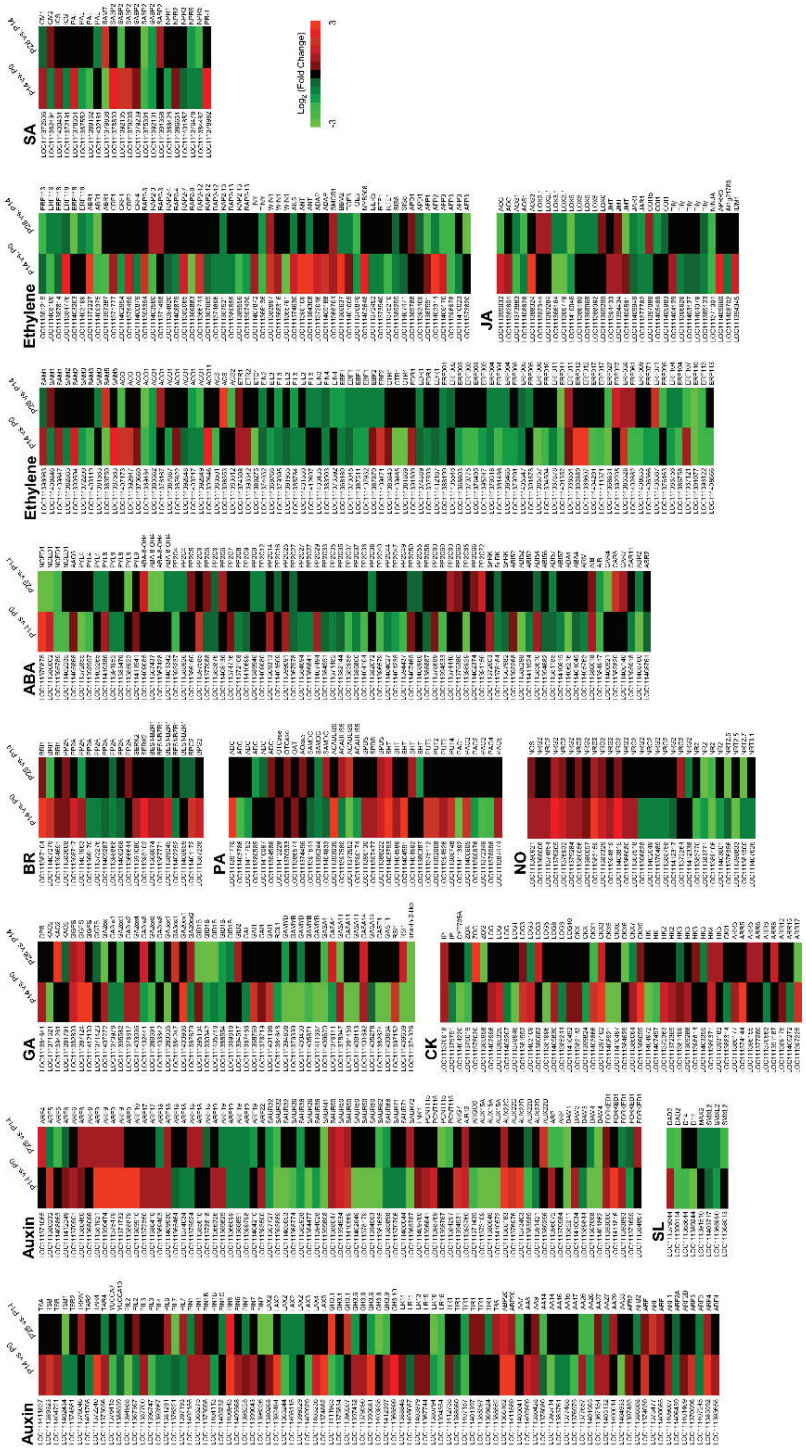

Figure I.S16. Differential gene expression of hormone-related genes during early olive fruit development. Expression values are represented in a heatmap as Log2 Fold Change in both the P14 versus P0 (P14 vs. P0), and the P28 versus P14 (P28 vs. P14) comparisons, and the colour key is indicated at the bottom. Additional information on the hormone-related genes is presented in Table S15.

Table I.S1. PCR-primers used in this study.

Primer	Sequence	Gene_ID
CS2-F	5′-ATGACTGGTTTTCAGGACTAC-3′	*OeCS2*
CS2-R	5′-AAATTCAACTGTAGAGGACGT-3′	(XP_022870513.1)
DIR15-F	5′-AAACCGAGCGAACCGACCCCT-3′	*OeDIR15*
DIR15-R	5′-AACCACCGCCATTTCTCTACC-3′	(XP_022897725.1)
EXPB2-F	5′-GGTTCCAGTGACTACTATTT-3′	*OeEXPB2*
EXPB2-R	5′-CAATGGATTTTCTGAATTGAG-3′	(XP_022856136.1)
COX-6A-F	5′- GGCGGCGCATCTACTCCACGCTCC-3′	*OeCox-6A*
COX-6A-R	5′- ACCCTTGGAAAGGTTAATGACTGC -3′	(XP_027178774.1)
CYCA2;1-F	5′-CCATCATCCTACGATCCATGC-3′	*OeCYCA2;1*
CYCA2;1-R	5′-TGCAGAGGAACTTGCACCAGG-3′	(XP_022881536.1)
CYCA3;1-F	5′-AGCTATGCGT GAGATTCTGGT-3′	*OeCYCA3;1*
CYCA3;1-R	5′-TCCATGTGTATAACGTCTTCT-3′	(XP_022860599.1)
CYCC1;1-F	5′-TGCTGCCACATCCATTTGCC-3′	*OeCYCC1;1*
CYCC1;1-R	5′- ACATTTTGAGCCAATCTTGC-3′	(XP_022874690.1)
CYCB2;4-F	5′-TTGGTAGACTGCCTCATTGT-3′	*OeCYCB2;4*
CYCB2;4-R	5′-GTCGAACTGCTGTTCCATAT-3′	(XP_022881380.1)
CYCB3;1-F	5′-GGAAAACGCTACTCTCTCAAG-3′	*OeCYCB3;1*
CYCB3;1-R	5′-TTGAGCTGATAACTTCCTCG-3′	(XP_022877828.1)
CYCB2;3-F	5′-AAATCGGACATATCCCCTGT-3′	*OeCYCB2;3*
CYCB2;3-R	5′-TTCTCATCTGATCTACGCAT-3′	(XP_022895161.1)
CYCU1;1-F	5′-AACAACACCTAGAGTTCTTACC-3′	*OeCYCU1;1*
CYCU1;1-R	5′-GATACTTATGCACCAACCTGT-3′	(XP_022845538.1)
CYCA1;4-F	5′-TACATAGATAATAATGAAAT-3′	*OeCYCA1;4*
CYCA1;4-R	5′-TCCATGAAGTCAGTAGTAGG-3′	(XP_022875899.1)

CDKC1-F	5′-CATGATTTGACTGGCCTTGCT-3′	*OeCDKC1*
CDKC1-R	5′-GATTAGTAAGATTAGCATTGTG-3′	(XP_022880663.1)
CDKB1-F	5′-CCGTTGCAGGAGGAAGAGAA-3′	*OeCDKB1*
CDKB1-R	5′-TCCATTATTTGATGTGGAT-3′	(XP_022860837.1)
CDKF1-F	5′-CAATCTCATATAAAAGTTGC-3′	*OeCDKF1*
CDKF1-R	5′-CGCTCGTGGA2TTTCGTACTT-3′	(XP_022893380.1)
CKI7-F	5′-TAGAACATCAGCTGCTTTCGA-3′	*OeCKI7*
CKI7-R	5′-TTTAGCTGAACTGTGGACCT-3′	(XP_022844706.1)
SMR6-F	5′-GGTACCCTTCTGTTTAAAAG-3′	*OeSMR6*
SMR6-R	5′-CGAACGGACGTCTTCATCTT-3′	(XP_022865500.1)
SMR9-F	5′-CCTGTAGAAGAAGAACCAGA-3′	*OeSMR9*
SMR9-R	5′-AATACCGTTGGTGTTGGGGT-3′	(XP_022899245.1)
ERFA-F	5′-AATACCGTTGGTGTTGGGGT-3′	*OeERFA*
ERFA-R	5′-TTTGTGACCTTTGACCTGCT-3′	(XP_022841835.1)
MYB3R1-F	5′-TACAGTCCACTTGGCATTCGC-3′	*OeMYB3R1*
MYB3R1-R	5′-ATGATGACAGCATAAGTACT-3′	(XP_022853377.1)
RBR3-F	5′-GCAGTGGGTGAATTATGGTT-3′	*OeRBR3*
RBR3-R	5′-GATTCTATATTCTACTACTC-3′	(XP_022889026.1)
SCL28-F	5′-GAGAAGTGAATCTCATAGTA-3′	*OeSCL28*
SCL28-R	5′-ATGATCATCGGATTCCTTAA-3′	(XP_022846070.1)
SBT1.5-F	5′-TCCTTCAAATTAAATCTCATC-3′	*OeSBT1.5*
SBT1.5-R	5′-ATTAGAGCCCGAATCAGACTC-3′	(XP_022854658.1)
SBT3.5-F	5′-CTCTCTTCAGTCCTGGGAAGT-3′	*OeSBT3.5*
SBT3.5-R	5′-CGATGAATTGAATGGTTCTCC-3′	(XP_022844531.1)
SBT3.6-R	5′-ATTCTTGGAGGCAAAAAGACC-3′	*OeSBT3.6*

SBT3.6-R	5′-AGCACCATATTGACCTCTCAA-3′	(XP_022853451.1)
SBT1.8-F	5′-ATGGAGTCGAGTTCGGCTATT-3′	*OeSBT1.8*
SBT1.8-R	5′-GAAACCATGGTACGCTGTGTC-3′	(XP_022845741.1)
SBT1.1-F	5′-GCAGAAAGAGAAACATATGTG-3′	*OeSBT1.1*
SBT1.1-R	5′AGCATTCCACAGGCCACTACC-3′	(XP_022859421.1)

Table I.S2. Summary of the transcripts assembly.

Assembly name	Total isotigs	TotalBases	Average	N50	N90
FinalAssembly.fasta	244906	293754215	1199.46	1763	664

Table I.S3. Genes up-regulated during early olive fruit development in the first comparison (P14 versus P0). Este anexo es presentado en soporte digital.

Table I.S4. Genes down-regulated during early olive fruit development in the first comparison (P14 versus P0). Este anexo es presentado en soporte digital.

Table I.S5. Genes up-regulated during early olive fruit development in the second comparison (P28 versus P14). Este anexo es presentado en soporte digital.

Table I.S6. Genes down-regulated during early olive fruit development in the second comparison (P28 versus P14). Este anexo es presentado en soporte digital.

Table I.S7. Genes up-regulated during early olive fruit development in both the first (P14 versus P0) and second (P28 versus P14) comparisons. Este anexo es presentado en soporte digital.

Table I.S8. Genes down-regulated during early olive fruit development in both the first (P14 versus P0) and second (P28 versus P14) comparisons. Este anexo es presentado en soporte digital.

Table I.S9. Specific or exclusively expressed genes in olive fruit at selected stage during early fruit development.

DE_Specific_P0				
Genes	**log2FoldChange**	**p value**	**Gene_ID**	**Description**
LOC111370572	-13,17918949	1,20E-29	XP_022848109.1	glycine-rich_cell_wall_structural_protein_1.0-like=Olea europaea var. sylvestris
LOC111374547	-12,01057625	8,86E-54	XP_022852994.1	stress-induced_protein_KIN2-like=Olea europaea var. sylvestris
LOC111368749	-11,68222204	2,51E-33	XP_022845943.1	stem-specific_protein_TSJT1-like=Olea europaea var. sylvestris
LOC111404689	-11,02977962	3,68E-15		uncharacterized_protein=Olea europaea var. sylvestris

LOC111378644	-10,46235309	2,68E-10		uncharacterized_protein=Olea europaea var. sylvestris
LOC111372711	-10,11734126	3,07E-08	XP_022850868.1	major_pollen_allergen_Lig_v_1-like=Olea europaea var. sylvestris
LOC111385879	-9,869034688	1,84E-59	XP_022869103.1	uncharacterized_protein=Olea europaea var. sylvestris
LOC111396530	-9,846419193	8,38E-67	XP_022878712.1	L-ascorbate_oxidase_homolog=Olea europaea var. sylvestris
LOC111383316	-9,833682273	2,07E-12		vicilin-like_seed_storage_protein_At2g28490=Olea europaea var. sylvestris
LOC111401715	-9,808929024	2,34E-21	XP_022885340.1	vignain-like=Olea europaea var. sylvestris
LOC111397691	-9,470658676	2,01E-153	XP_022880457.1	alpha-1,4-glucan-protein_synthase_[UDP-forming]_1-like=Olea europaea var. sylvestris
LOC111376679	-9,452886587	1,90E-10	XP_022855416.1	probable_E3_ubiquitin-protein_ligase_BAH1-like=Olea europaea var. sylvestris
LOC111382436	-9,390080551	5,57E-75	XP_022862182.1	plasma_membrane_ATPase_4-like=Olea europaea var. sylvestris
LOC111412810	-9,375326368	3,73E-36	XP_022899477.1	glucan_endo-1,3-beta-D-glucosidase-like=Olea europaea var. sylvestris
LOC111366861	-9,362785438	2,58E-09		uncharacterized_protein=Olea europaea var. sylvestris
LOC111365434	-9,08755212	6,74E-15	XP_022841745.1	cytochrome_c_oxidase_subunit_6a,_mitochondrial-like=Olea europaea var. sylvestris
LOC111367772	-9,000275348	2,13E-57	XP_022844594.1	COP1-interactive_protein_1-like,_transcript_variant_X2=Olea europaea var. sylvestris
LOC111379532	-8,90443868	4,06E-33	XP_022858692.1	uncharacterized_LOC111379532=Olea europaea var. sylvestris
LOC111383887	-8,87700175	2,23E-75		cellulose_synthase-like_protein_D4=Olea europaea var. sylvestris
LOC111411160	-8,680149185	3,34E-07	XP_022897487.1	WAT1-related_protein_At1g09380-like=Olea europaea var. sylvestris
LOC111410960	-8,55424995	2,02E-69	XP_022897316.1	late_embryogenesis_abundant_protein_47-like=Olea europaea var. sylvestris
LOC111402520	-8,41896109	1,97E-36	XP_022886658.1	ABC_transporter_G_family_member_9=Olea europaea var. sylvestris
LOC111376781	-8,239093534	1,48E-19	XP_022855550.1	guanosine_nucleotide_diphosphate_dissociation_inhibitor_At5g09550=Olea europaea var. sylvestris
LOC111374240	-8,193522163	2,90E-74	XP_022852660.1	LOB_domain-containing_protein_27-like=Olea europaea var. sylvestris
LOC111378423	-8,175857877	3,66E-21		
LOC111367829	-8,148593496	1,01E-20	XP_022844659.1	ABC_transporter_G_family_member_29-like=Olea europaea var. sylvestris
LOC111370525	-8,13711294	1,83E-14		
LOC111380086	-7,953834532	3,04E-09	XP_022859318.1	fatty-acid-binding_protein_2-like=Olea europaea var. sylvestris
LOC111377473	-7,829270879	2,14E-25	XP_022856348.1	uncharacterized_LOC111377473=Olea europaea var. sylvestris
LOC111391121	-7,804390821	1,41E-76	XP_022872037.1	pectin_acetylesterase_8-like,_transcript_variant_X2=Olea europaea var. sylvestris
LOC111383532	-7,573222218	8,33E-13	XP_022863413.1	cation/H(+)_antiporter_15-like=Olea europaea var. sylvestris
LOC111401218	-7,521217859	1,12E-40	XP_022884626.1	microsomal_glutathione_S-transferase_3=Olea europaea var. sylvestris
LOC111375605	-7,460240717	7,14E-30	XP_022854226.1	tetraspanin-8-like=Olea europaea var. sylvestris

LOC111401246	-7,459595927	1,06E-43		
LOC111410528	-7,427147242	2,40E-57	XP_022896682.1	mechanosensitive_ion_channel_protein_6-like=Olea europaea var. sylvestris
LOC111403615	-7,422032239	1,54E-27	XP_022887954.1	transcription_factor_MYB44-like=Olea europaea var. sylvestris
LOC111396414	-7,365796238	3,28E-88	XP_022878619.1	external_alternative_NAD(P)H-ubiquinone_oxidoreductase_B4,_mitochondrial-like=Olea europaea var. sylvestris
LOC111371251	-7,233425813	1,36E-42	XP_022848906.1	cation/H(+)_antiporter_24-like=Olea europaea var. sylvestris
LOC111395252	-7,230282913	4,83E-15		
LOC111379713	-7,215036504	5,40E-21	XP_022858918.1	xyloglucan_endotransglucosylase/hydrolase_protein_2-like=Olea europaea var. sylvestris
LOC111412516	-7,18494582	7,62E-11		transmembrane_emp24_domain-containing_protein_p24delta3-like=Olea europaea var. sylvestris
LOC111383590	-7,179166359	9,22E-31	XP_022863475.1	3-ketoacyl-CoA_synthase_11-like=Olea europaea var. sylvestris
LOC111409675	-7,168078487	1,65E-25	XP_022895460.1	MLO-like_protein_9=Olea europaea var. sylvestris
LOC111371214	-7,157626841	3,51E-16	XP_022848877.1	protein_DMP2-like=Olea europaea var. sylvestris
LOC111382243	-7,111466834	4,01E-57		
LOC111365789	-7,085760686	4,61E-11	XP_022842079.1	mitochondrial_import_inner_membrane_translocase_subunit_TIM17-2-like=Olea europaea var. sylvestris
LOC111377292	-7,079699127	6,58E-11	XP_022856136.1	putative_expansin-B2=Olea europaea var. sylvestris
LOC111389665	-6,979644148	4,93E-18	XP_022870374.1	serine/threonine-protein_kinase_BLUS1-like,_transcript_variant_X3=Olea europaea var. sylvestris
LOC111382780	-6,966578828	2,43E-53	XP_022862585.1	putative_glutamine_amidotransferase_GAT1_2.1=Olea europaea var. sylvestris
LOC111372528	-6,949666325	1,02E-42	XP_022850643.1	glycosyltransferase_family_92_protein_RCOM_0530710-like=Olea europaea var. sylvestris
LOC111395755	-6,94827657	3,69E-49	XP_022877657.1	long-chain-alcohol_O-fatty-acyltransferase-like=Olea europaea var. sylvestris
LOC111374844	-6,903550605	6,18E-15	XP_022853356.1	UDP-glycosyltransferase_83A1-like=Olea europaea var. sylvestris
LOC111370002	-6,844056576	9,65E-22	XP_022847489.1	uncharacterized_LOC111370002=Olea europaea var. sylvestris
LOC111375194	-6,83979972	2,78E-23	XP_022853764.1	beta-D-glucosyl_crocetin_beta-1,6-glucosyltransferase-like=Olea europaea var. sylvestris
LOC111400060	-6,825173308	2,30E-31	XP_022883284.1	BTB/POZ_domain-containing_protein_At5g03250-like=Olea europaea var. sylvestris
LOC111370979	-6,818627575	7,16E-55	XP_022848677.1	type_I_inositol_polyphosphate_5-phosphatase_5-like=Olea europaea var. sylvestris
LOC111382315	-6,766764317	8,43E-47	XP_022862014.1	mechanosensitive_ion_channel_protein_6-like=Olea europaea var. sylvestris
LOC111375880	-6,666459678	7,75E-26	XP_022854560.1	uncharacterized_LOC111375880=Olea europaea var. sylvestris
LOC111401404	-6,656742422	5,24E-45	XP_022884894.1	epoxide_hydrolase_4-like=Olea europaea var. sylvestris
LOC111401095	-6,652557862	4,09E-44	XP_022884418.1	uncharacterized_LOC111401095=Olea europaea var. sylvestris

LOC111410365	-6,640758233	3,32E-27	XP_022896429.1	protein_JINGUBANG-like=Olea europaea var. sylvestris
LOC111388611	-6,640423707	1,88E-82	XP_022869135.1	clathrin_light_chain_1=Olea europaea var. sylvestris
LOC111365505	-6,637067313	1,54E-14	XP_022841829.1	uncharacterized_LOC111365505=Olea europaea var. sylvestris
LOC111385858	-6,591655654	8,04E-59	XP_022866054.1	uncharacterized_LOC111385858=Olea europaea var. sylvestris
LOC111381413	-6,577036355	3,34E-64	XP_022860957.1	cation/H(+)_antiporter_24-like=Olea europaea var. sylvestris
LOC111371040	-6,570770295	3,48E-32	XP_022848729.1	probable_serine/threonine-protein_kinase_PBL26=Olea europaea var. sylvestris
LOC111401681	-6,494100925	1,14E-63	XP_022885306.1	pyruvate_decarboxylase_2-like,_transcript_variant_X2=Olea europaea var. sylvestris
LOC111372855	-6,493164932	7,34E-65	XP_022851036.1	abscisic_acid_receptor_PYL4-like=Olea europaea var. sylvestris
LOC111380122	-6,474966201	2,30E-49		LIM_domain-containing_protein_PLIM2c-like=Olea europaea var. sylvestris
LOC111372493	-6,417183782	1,67E-40	XP_022850611.1	zinc_finger_protein_ZAT5-like=Olea europaea var. sylvestris
LOC111380442	-6,414737417	1,10E-33	XP_022859777.1	uridine_kinase-like_protein_5=Olea europaea var. sylvestris
LOC111389838	-6,404022844	1,32E-48		uncharacterized_LOC111389838=Olea europaea var. sylvestris
LOC111407705	-6,349780379	1,02E-26	XP_022893112.1	putative_respiratory_burst_oxidase_homolog_protein_H=Olea europaea var. sylvestris
LOC111367290	-6,343599464	1,55E-18	XP_022843857.1	transcription_factor_bHLH87,_transcript_variant_X2=Olea europaea var. sylvestris
LOC111378225	-6,324877578	6,29E-58	XP_022857162.1	cysteine-rich_repeat_secretory_protein_12-like=Olea europaea var. sylvestris
LOC111403421	-6,30497908	2,08E-22	XP_022887691.1	1-acyl-sn-glycerol-3-phosphate_acyltransferase_2-like=Olea europaea var. sylvestris
LOC111394906	-6,29793088	6,74E-31	XP_022876724.1	V-type_proton_ATPase_subunit_G-like,_transcript_variant_X2=Olea europaea var. sylvestris
LOC111370251	-6,275439015	1,10E-47	XP_022847702.1	uncharacterized_LOC111370251=Olea europaea var. sylvestris
LOC111404845	-6,273640925	1,20E-21	XP_022889350.1	protein_LURP-one-related_8-like=Olea europaea var. sylvestris
LOC111392832	-6,258820829	2,86E-43	XP_022873993.1	rop_guanine_nucleotide_exchange_factor_9-like=Olea europaea var. sylvestris
LOC111391844	-6,252209376	1,73E-21	XP_022872885.1	ADP-ribosylation_factor_1-like=Olea europaea var. sylvestris
LOC111399437	-6,245334407	1,62E-28		uncharacterized_LOC111399437=Olea europaea var. sylvestris
LOC111380684	-6,223068746	1,52E-24		uncharacterized_LOC111380684,_transcript_variant_X4=Olea europaea var. sylvestris
LOC111408921	-6,213926151	4,36E-17	XP_022894536.1	cytokinin_dehydrogenase_5=Olea europaea var. sylvestris
LOC111408260	-6,167503584	2,21E-29	XP_022893812.1	calcium_uptake_protein,_mitochondrial-like=Olea europaea var. sylvestris
LOC111387557	-6,115625309	6,59E-13		
LOC111411033	-6,086738343	6,13E-14	XP_022897377.1	uncharacterized_LOC111411033,_transcript_variant_X2=Olea europaea var. sylvestris
LOC111388466	-6,050460951	5,98E-17		protein_indeterminate-domain_16-like=Olea europaea var. sylvestris

LOC111404112	-5,956777576	4,03E-36	XP_022888621.1	uncharacterized_LOC111404112=Olea europaea var. sylvestris
LOC111408738	-5,951168785	6,88E-07	XP_022894269.1	putative_glutamine_amidotransferase_GAT1_2.1=Olea europaea var. sylvestris
LOC111374146	-5,917026425	4,14E-29		probable_methyltransferase_PMT15=Olea europaea var. sylvestris
LOC111406910	-5,909790775	3,71E-39	XP_022892040.1	uncharacterized_LOC111406910=Olea europaea var. sylvestris
LOC111375746	-5,879334213	5,03E-43	XP_022854381.1	uncharacterized_LOC111375746=Olea europaea var. sylvestris
LOC111370883	-5,864755757	4,89E-28	XP_022848552.1	eukaryotic_translation_initiation_factor_4E-1-like=Olea europaea var. sylvestris
LOC111406201	-5,828539233	1,18E-44	XP_022891243.1	cell_division_cycle_20.3,_cofactor_of_APC_complex-like,_transcript_variant_X2=Olea europaea var. sylvestris
LOC111412681	-5,827738955	4,54E-31	XP_022899373.1	secoisolariciresinol_dehydrogenase-like=Olea europaea var. sylvestris
LOC111390650	-5,814544749	2,69E-58	XP_022871484.1	probable_alkaline/neutral_invertase_F=Olea europaea var. sylvestris
LOC111379092	-5,758970087	4,70E-18	XP_022858191.1	plant_cysteine_oxidase_2-like,_transcript_variant_X4=Olea europaea var. sylvestris
LOC111408444	-5,732844015	7,82E-26	XP_022893973.1	uncharacterized_LOC111408444=Olea europaea var. sylvestris
LOC111378561	-5,726964617	1,04E-19		
LOC111392725	-5,693356981	2,29E-15		perakine_reductase-like=Olea europaea var. sylvestris
LOC111379322	-5,587636665	2,96E-21	XP_022858446.1	metal_transporter_Nramp2-like=Olea europaea var. sylvestris
LOC111393172	-5,573696858	1,05E-35	XP_022874337.1	IQ_domain-containing_protein_IQM2-like=Olea europaea var. sylvestris
LOC111389474	-5,570220989	0,00050305	XP_022870159.1	uncharacterized_LOC111389474=Olea europaea var. sylvestris
LOC111385050	-5,495458927	1,28E-47		uncharacterized_LOC111385050=Olea europaea var. sylvestris
LOC111406988	-5,479810164	2,07E-43		
LOC111399471	-5,477207587	9,65E-34	XP_022882548.1	serine/threonine-protein_kinase_CBK1-like=Olea europaea var. sylvestris
LOC111374285	-5,467088014	9,06E-43	XP_022852710.1	probable_trehalose-phosphate_phosphatase_F,_transcript_variant_X2=Olea europaea var. sylvestris
LOC111388747	-5,46060374	2,30E-42	XP_022869301.1	uncharacterized_LOC111388747=Olea europaea var. sylvestris
LOC111402164	-5,408953296	1,03E-17		
LOC111388922	-5,393934166	2,17E-26	XP_022869519.1	uncharacterized_LOC111388922=Olea europaea var. sylvestris
LOC111378512	-5,390855704	3,93E-26	XP_022857494.1	calcium-binding_protein_PBP1-like=Olea europaea var. sylvestris
LOC111380076	-5,383426355	0,00254399	XP_022859308.1	guanine_nucleotide-binding_protein_alpha-1_subunit-like=Olea europaea var. sylvestris
LOC111412200	-5,345839912	1,50E-37	XP_022898780.1	ABC_transporter_B_family_member_9-like=Olea europaea var. sylvestris
LOC111404874	-5,314910605	1,49E-18	XP_022889374.1	transcription_repressor_OFP1-like=Olea europaea var. sylvestris
LOC111392872	-5,306533419	1,37E-22	XP_022874040.1	mediator_of_RNA_polymerase_II_transcription_subunit_15a-like=Olea europaea var. sylvestris
LOC111400587	-5,306046834	1,39E-40	XP_022883762.1	probable_acyl-activating_enzyme_1,_peroxisomal=Olea europaea var. sylvestris

LOC111407064	-5,29442253	7,73E-31	XP_022892165.1	transcription_factor_IBH1=Olea europaea var. sylvestris
LOC111372096	-5,29414602	7,86E-19		uncharacterized_LOC111372096=Olea europaea var. sylvestris
LOC111408194	-5,281236539	2,36E-28		
LOC111381330	-5,276037957	5,47E-18	XP_022860882.1	protein_IQ-DOMAIN_1-like,_transcript_variant_X3=Olea europaea var. sylvestris
LOC111386367	-5,269745117	7,69E-38		calcium-dependent_protein_kinase_34-like=Olea europaea var. sylvestris
LOC111396797	-5,239339036	1,72E-24	XP_022879085.1	stearoyl-[acyl-carrier-protein]_9-desaturase_6,_chloroplastic-like=Olea europaea var. sylvestris
LOC111411382	-5,213050701	4,00E-23	XP_022897685.1	zinc_finger_protein_WIP2-like=Olea europaea var. sylvestris
LOC111392776	-5,211772443	4,80E-24	XP_022873940.1	ribonuclease_S-2-like=Olea europaea var. sylvestris
LOC111388145	-5,135394881	2,15E-30	XP_022868591.1	uncharacterized_LOC111388145=Olea europaea var. sylvestris
LOC111377825	-5,12452642	3,33E-30	XP_022856721.1	uncharacterized_LOC111377825=Olea europaea var. sylvestris
LOC111370451	-5,107247546	1,04E-27	XP_022847931.1	probable_phospholipid-transporting_ATPase_5=Olea europaea var. sylvestris
LOC111389550	-5,077354619	7,78E-40	XP_022870246.1	uncharacterized_LOC111389550=Olea europaea var. sylvestris
LOC111380018	-5,069904839	8,16E-38	XP_022859246.1	polyadenylate-binding_protein_7-like=Olea europaea var. sylvestris
LOC111408771	-5,056950195	1,03E-19	XP_022894311.1	polyadenylate-binding_protein_5-like=Olea europaea var. sylvestris
LOC111403851	-5,025280803	5,27E-16	XP_022888252.1	FT-interacting_protein_1-like,_transcript_variant_X2=Olea europaea var. sylvestris
LOC111380840	-5,010249889	1,01E-31		E3_ubiquitin-protein_ligase_MIEL1-like=Olea europaea var. sylvestris
LOC111376103	-4,892122043	1,77E-07	XP_022854799.1	alcohol-forming_fatty_acyl-CoA_reductase-like=Olea europaea var. sylvestris
LOC111401085	-4,871843226	1,87E-20	XP_022884397.1	sodium/hydrogen_exchanger_1-like=Olea europaea var. sylvestris
LOC111402224	-4,827447824	6,76E-33	XP_022886157.1	uncharacterized_LOC111402224=Olea europaea var. sylvestris
LOC111402646	-4,78479798	2,25E-29	XP_022886787.1	auxin-responsive_protein_SAUR50-like=Olea europaea var. sylvestris
LOC111374477	-4,732515833	1,51E-05		uridine_kinase-like_protein_5=Olea europaea var. sylvestris
LOC111391226	-4,731385414	1,20E-18		uncharacterized_LOC111391226=Olea europaea var. sylvestris
LOC111385843	-4,726196495	1,89E-18		putative_clathrin_assembly_protein_At5g57200=Olea europaea var. sylvestris
LOC111399868	-4,703570392	2,00E-15	XP_022883125.1	uncharacterized_LOC111399868=Olea europaea var. sylvestris
LOC111365791	-4,677179649	5,50E-20	XP_022842081.1	ethylene-responsive_transcription_factor_WIN1-like=Olea europaea var. sylvestris
LOC111410697	-4,651162498	8,48E-32	XP_022896938.1	monoacylglycerol_lipase_ABHD6-like,_transcript_variant_X3=Olea europaea var. sylvestris
LOC111376095	-4,649436506	2,00E-22	XP_022854794.1	zinc_finger_protein_ZAT5-like=Olea europaea var. sylvestris
LOC111374096	-4,628874923	2,22E-13	XP_022852497.1	LRR_receptor-like_serine/threonine-protein_kinase_GSO1=Olea europaea var. sylvestris

LOC111375691	-4,600650263	4,20E-17	XP_022854327.1	protein_SENESCENCE-ASSOCIATED_GENE_21,_mitochondrial-like=Olea europaea var. sylvestris
LOC111390990	-4,56487366	1,66E-23	XP_022871894.1	cysteine-rich_and_transmembrane_domain-containing_protein_WIH1-like,_transcript_variant_X2=Olea europaea var. sylvestris
LOC111386702	-4,55650622	5,15E-26	XP_022866935.1	zinc_finger_protein_ZAT5-like=Olea europaea var. sylvestris
LOC111402396	-4,454420864	2,38E-26	XP_022886428.1	subtilisin-like_protease_SBT5.4=Olea europaea var. sylvestris
LOC111400269	-4,412509221	1,13E-13	XP_022883456.1	uncharacterized_LOC111400269=Olea europaea var. sylvestris
LOC111397104	-4,402605827	9,75E-19	XP_022879612.1	uncharacterized_LOC111397104,_transcript_variant_X2=Olea europaea var. sylvestris
LOC111402679	-4,312847703	1,02E-24	XP_022886809.1	uncharacterized_LOC111402679,_transcript_variant_X2=Olea europaea var. sylvestris
LOC111381789	-4,273318672	1,61E-16	XP_022861384.1	S-protein_homolog_29-like=Olea europaea var. sylvestris
LOC111391653	-4,261044339	4,40E-27	XP_022872674.1	putative_invertase_inhibitor=Olea europaea var. sylvestris
LOC111405085	-4,253856125	0,00029983	XP_022889570.1	nuclear_poly(A)_polymerase_4-like,_transcript_variant_X6=Olea europaea var. sylvestris
LOC111385846	-4,048582588	5,56E-18		
LOC111402339	-4,029689031	7,95E-17		
LOC111386638	-3,935127159	5,00E-15	XP_022866872.1	gamma-glutamyl_peptidase_5-like=Olea europaea var. sylvestris
LOC111371872	-3,929609162	7,67E-16	XP_022849798.1	uncharacterized_LOC111371872=Olea europaea var. sylvestris
LOC111381104	-3,826586482	2,00E-14	XP_022860595.1	uncharacterized_LOC111381104,_transcript_variant_X2=Olea europaea var. sylvestris
LOC111398540	-3,693176862	8,20E-17	XP_022881264.1	cytochrome_P450_87A3,_transcript_variant_X2=Olea europaea var. sylvestris
LOC111370065	-3,361739617	3,12E-14	XP_022847543.1	sodium/calcium_exchanger_NCL1-like=Olea europaea var. sylvestris

DE_Specific_P14				
Genes	**log2FoldChange**	**p value**	**Gene_ID**	**Description**
LOC111408989	-8,093494486	1,82E-57	XP_022894638.1	probable_xyloglucan_endotransglucosylase/hydrolase_protein_7=Olea europaea var. sylvestris
LOC111377327	-7,054152299	3,84E-33	XP_022856174.1	BURP_domain-containing_protein_16-like=Olea europaea var. sylvestris
LOC111394967	-6,829794129	1,82E-13	XP_022876772.1	rapid_alkalinization_factor-like=Olea europaea var. sylvestris
LOC111380288	-6,620352403	3,22E-29	XP_022859582.1	uncharacterized_LOC111380288=Olea europaea var. sylvestris
LOC111383563	-6,44528675	1,35E-16	XP_022863446.1	anthocyanidin_3-O-glucosyltransferase_5-like=Olea europaea var. sylvestris
LOC111404076	-6,24582309	6,50E-41	XP_022888574.1	laccase-7-like=Olea europaea var. sylvestris
LOC111411989	-6,132802638	4,21E-36	XP_022898473.1	uncharacterized_LOC111411989=Olea europaea var. sylvestris

LOC111399703	-6,095967231	9,28E-18	XP_022882931.1	subtilisin-like_protease_SBT4.15=Olea europaea var. sylvestris
LOC111407314	-5,894870873	1,52E-13	XP_022892495.1	probable_WRKY_transcription_factor_35=Ole a europaea var. sylvestris
LOC111380888	-5,872059667	5,32E-19	XP_022860316.1	receptor-like_protein_12,_transcript_variant_X2=Olea europaea var. sylvestris
LOC111397229	-5,856053956	4,50E-16	XP_022879818.1	probable_xyloglucan_endotransglucosylase/hydrolase_protein_7=Olea europaea var. sylvestris
LOC111388333	-5,786722824	2,31E-18	XP_022868784.1	transmembrane_protein_45B-like=Olea europaea var. sylvestris
LOC111390983	-5,742528217	3,81E-27	XP_022871882.1	collagen_alpha-2(IV)_chain-like=Olea europaea var. sylvestris
LOC111397047	-5,713448481	3,13E-20	XP_022879532.1	MADS-box_protein_SOC1-like,_transcript_variant_X4=Olea europaea var. sylvestris
LOC111371132	-5,655639496	9,52E-42	XP_022848808.1	uncharacterized_LOC111371132=Olea europaea var. sylvestris
LOC111399011	-5,600641789	1,31E-32	XP_022881974.1	aspartic_proteinase_CDR1-like=Olea europaea var. sylvestris
LOC111391732	-5,535023537	2,47E-22	XP_022872751.1	cation/H(+)_antiporter_20-like=Olea europaea var. sylvestris
LOC111406760	-5,478090662	1,67E-13	XP_022891905.1	uncharacterized_LOC111406760=Olea europaea var. sylvestris
LOC111378770	-5,474511274	1,81E-20	XP_022857775.1	UPF0481_protein_At3g47200-like=Olea europaea var. sylvestris
LOC111381100	-5,427713338	6,57E-30		cysteine-rich_receptor-like_protein_kinase_25=Olea europaea var. sylvestris
LOC111393013	-5,421751451	1,94E-13	XP_022874213.1	MADS-box_protein_AGL42-like,_transcript_variant_X6=Olea europaea var. sylvestris
LOC111396190	-5,421657261	9,82E-44	XP_022878302.1	NAC_transcription_factor_29-like=Olea europaea var. sylvestris
LOC111398321	-5,330195981	1,61E-23		
LOC111384431	-5,270508566	6,47E-27	XP_022864474.1	cysteine-rich_receptor-like_protein_kinase_29=Olea europaea var. sylvestris
LOC111379180	-5,256990531	4,54E-26	XP_022858289.1	probable_polyol_transporter_6=Olea europaea var. sylvestris
LOC111367567	-5,254972752	1,80E-14	XP_022844323.1	MADS-box_protein_JOINTLESS-like,_transcript_variant_X7=Olea europaea var. sylvestris
LOC111397297	-5,112786973	8,40E-17	XP_022879911.1	calcium_uniporter_protein_4,_mitochondrial-like=Olea europaea var. sylvestris
LOC111393511	-5,110344973	1,24E-24	XP_022874843.1	endochitinase_EP3-like=Olea europaea var. sylvestris
LOC111382320	-5,105246433	2,72E-19	XP_022862024.1	ATP-dependent_RNA_helicase_glh-2-like=Olea europaea var. sylvestris
LOC111398706	-5,030385802	1,93E-20	XP_022881517.1	EG45-like_domain_containing_protein=Olea europaea var. sylvestris
LOC111385774	-5,029505775	8,41E-22	XP_022865957.1	endoglucanase-like=Olea europaea var. sylvestris
LOC111390208	-5,019700281	3,92E-21	XP_022870982.1	uncharacterized_LOC111390208=Olea europaea var. sylvestris
LOC111392847	-4,971557789	4,49E-18	XP_022874008.1	protein_LITTLE_ZIPPER_3-like=Olea europaea var. sylvestris
LOC111375723	-4,950497636	1,14E-15	XP_022854358.1	oligopeptide_transporter_7=Olea europaea var. sylvestris
LOC111388132	-4,946720835	1,72E-13	XP_022868576.1	transcription_factor_PRE6-like=Olea europaea var. sylvestris
LOC111371180	-4,933925185	2,12E-23	XP_022848852.1	endoglucanase-like=Olea europaea var. sylvestris

LOC111386881	-4,897873982	2,71E-13	XP_022867140.1	cytochrome_P450_81D11-like=Olea europaea var. sylvestris
LOC111393301	-4,837772085	3,87E-22	XP_022874530.1	protein_CUP-SHAPED_COTYLEDON_3-like=Olea europaea var. sylvestris
LOC111390480	-4,776287221	1,16E-22	XP_022871296.1	transcription_factor_MYB8-like=Olea europaea var. sylvestris
LOC111412367	-4,66959393	2,35E-16	XP_022899035.1	non-specific_lipid-transfer_protein-like_protein_At2g13820=Olea europaea var. sylvestris
LOC111367948	-4,665508786	1,88E-19	XP_022844848.1	GDSL_esterase/lipase_At2g23540-like=Olea europaea var. sylvestris
LOC111382291	-4,635336784	0,00044829	XP_022861978.1	sugar_transport_protein_8-like=Olea europaea var. sylvestris
LOC111376535	-4,616731189	9,87E-15	XP_022855266.1	cytochrome_P450_86B1-like=Olea europaea var. sylvestris
LOC111389453	-4,597753261	4,39E-28	XP_022870138.1	NAC_transcription_factor_56-like=Olea europaea var. sylvestris
LOC111401991	-4,579053028	1,65E-26	XP_022885763.1	cytochrome_P450_81D1-like=Olea europaea var. sylvestris
LOC111403197	-4,536813078	1,29E-16	XP_022887373.1	3-ketoacyl-CoA_synthase_6-like=Olea europaea var. sylvestris
LOC111412115	-4,528017606	1,20E-18	XP_022898658.1	fatty_acyl-CoA_reductase_3-like=Olea europaea var. sylvestris
LOC111410283	-4,526459082	6,14E-16	XP_022896315.1	terpene_synthase_10-like=Olea europaea var. sylvestris
LOC111396650	-4,451124738	5,44E-23	XP_022878859.1	FAM10_family_protein_At4g22670-like,_transcript_variant_X2=Olea europaea var. sylvestris
LOC111391077	-4,430590739	5,18E-13	XP_022871987.1	ethylene-responsive_transcription_factor_ERF110-like=Olea europaea var. sylvestris
LOC111402197	-4,420716465	3,22E-15	XP_022886119.1	AAA-ATPase_At5g57480-like=Olea europaea var. sylvestris
LOC111389639	-4,40436632	2,68E-22	XP_022870341.1	cytochrome_P450_86A1-like=Olea europaea var. sylvestris
LOC111392039	-4,387527548	3,33E-18	XP_022873094.1	cytochrome_P450_94A2-like=Olea europaea var. sylvestris
LOC111377905	-4,349811359	2,57E-17	XP_022856822.1	hexose_carrier_protein_HEX6-like=Olea europaea var. sylvestris
LOC111398732	-4,318211555	5,88E-16	XP_022881560.1	LRR_receptor-like_serine/threonine-protein_kinase_GSO1,_transcript_variant_X5=Olea europaea var. sylvestris
LOC111405457	-4,316314586	1,44E-16	XP_022890118.1	probable_LRR_receptor-like_serine/threonine-protein_kinase_At3g47570=Olea europaea var. sylvestris
LOC111402434	-4,31379445	1,38E-21	XP_022886496.1	tryptophan_synthase_beta_chain_1-like=Olea europaea var. sylvestris
LOC111392612	-4,276476207	4,52E-22	XP_022873739.1	MDIS1-interacting_receptor_like_kinase_2-like=Olea europaea var. sylvestris
LOC111381518	-4,172872016	1,69E-14	XP_022861075.1	uncharacterized_LOC111381518=Olea europaea var. sylvestris
LOC111403309	-4,067430644	2,35E-14	XP_022887526.1	truncated_transcription_factor_CAULIFLOWER_A-like=Olea europaea var. sylvestris
LOC111390670	-4,023940485	4,37E-15	XP_022871502.1	uncharacterized_LOC111390670,_transcript_variant_X2=Olea europaea var. sylvestris
LOC111367123	-4,006790066	1,52E-16	XP_022843615.1	vignain-like=Olea europaea var. sylvestris
LOC111385282	-3,737964334	1,11E-10		beta-galactosidase_14-like=Olea europaea var. sylvestris
LOC111383120	-3,731713412	6,66E-13	XP_022862962.1	putative_methylesterase_11,_chloroplastic=Olea europaea var. sylvestris

LOC111390577	-3,672178201	1,84E-13	XP_022871406.1	uncharacterized_LOC111390577=Olea europaea var. sylvestris
LOC111384954	-3,655885618	1,03E-13	XP_022865070.1	WRKY_transcription_factor_6-like,_transcript_variant_X2=Olea europaea var. sylvestris
LOC111366093	-3,629430686	1,80E-12	XP_022842515.1	protein_LURP-one-related_6=Olea europaea var. sylvestris

DE_Specific_P28				
Genes	**log2FoldChange**	**p value**	**Gene_ID**	**Description**
LOC111389777	4,983370401	8,52E-20	XP_022870513.1	chorismate_synthase_2,_chloroplastic-like=Olea europaea var. sylvestris
LOC111411422	5,256814581	1,37E-11	XP_022897725.1	dirigent_protein_15-like=Olea europaea var. sylvestris
LOC111377292	7,369813116	1,50E-11	XP_022856136.1	putative_expansin-B2=Olea europaea var. sylvestris
LOC111365434	7,406973296	0,01207031	XP_022841745.1	cytochrome_c_oxidase_subunit_6a,_mitochondrial-like=Olea europaea var. sylvestris

Table I.S10. The enrichment analysis of GO terms based on up-regulated DEGs in the dividing fruits at 14 (P14) versus the flowers at anthesis stage (P0) during early olive fruit development. Este anexo es presentado en soporte digital.

Table I.S11. The enrichment analysis of GO terms based on down-regulated DEGs in the dividing fruits at 14 (P14) versus the flowers at anthesis stage (P0) during early olive fruit development. Este anexo es presentado en soporte digital.

Table I.S12. The enrichment analysis of GO terms based on up-regulated DEGs in the expanding fruits at 28 (P28) DPA versus the dividing fruits at 14 (P14) during early olive fruit development. Este anexo es presentado en soporte digital.

Table I.S13. The enrichment analysis of GO terms based on down-regulated DEGs in the expanding fruits at 28 (P28) DPA versus the dividing fruits at 14 (P14) during early olive fruit development. Este anexo es presentado en soporte digital.

Table I.S14. Cell-cycle-related genes induced or repressed in the dividing fruits at 14 (P14) versus the flowers at anthesis stage (P0), and the expanding fruits at 28 (P28) DPA versus the dividing fruits at 14 (P14) during early olive fruit development.

P14 vs. P0_UP				
Genes	**log2FoldChange**	**p value**	**Gene_ID**	**Description**
LOC111374859	6,048370903	8,86E-26	XP_022853377.1	MYB3R-1 transcription factor MYB3R-1-like=Olea europaea var. sylvestris
LOC111409023	5,772578862	4,34E-154	XP_022894685.1	CYCD3;1cyclin-D3-1-like=Olea europaea var. sylvestris
LOC111372156	4,479241534	1,22E-17	XP_022850120.1	CYCD6;1 cyclin-D6-1, transcript variant X2=Olea europaea var. sylvestris
LOC111413007	3,443969868	5,55E-15	XP_022899656.1	cyclin S13-7 G2/mitotic-specific cyclin S13-7-like=Olea europaea var. sylvestris
LOC111379297	3,407744116	5,19E-23	XP_022858425.1	cyclin-2 G2/mitotic-specific cyclin-2-like, transcript variant X3=Olea europaea var. sylvestris

LOC111398716	3,324755017	6,21E-27	XP_022881536.1	CYCA2;1 cyclin-A2-1-like=Olea europaea var. sylvestris
LOC111378817	3,205300595	1,46E-38	XP_022857856.1	CYCD3;1 cyclin-D3-1-like=Olea europaea var. sylvestris
LOC111383417	3,184731222	1,98E-24	XP_022863293.1	cyclin-2 G2/mitotic-specific cyclin-2-like=Olea europaea var. sylvestris
LOC111409342	2,94117809	9,25E-20	XP_022895161.1	CYCB2;3 cyclin-B2-3-like, transcript variant X2=Olea europaea var. sylvestris
LOC111385349	2,799197118	5,44E-10	XP_022865500.1	SMR6 cyclin-dependent protein kinase inhibitor SMR6-like=Olea europaea var. sylvestris
LOC111380900	2,762181223	1,20E-55	XP_022860331.1	SCL6 scarecrow-like protein 6, transcript variant X2=Olea europaea var. sylvestris
LOC111382893	2,756563302	3,53E-09	XP_022862696.1	SMR6 cyclin-dependent protein kinase inhibitor SMR6-like=Olea europaea var. sylvestris
LOC111389737	2,712907531	2,50E-13	XP_022870456.1	CYCD6;1 cyclin-D6-1=Olea europaea var. sylvestris
LOC111368834	2,672078255	1,12E-42	XP_022846070.1	SCL28 scarecrow-like protein 28=Olea europaea var. sylvestris
LOC111381523	2,640545589	8,98E-12	XP_022861077.1	MYB3R-4 transcription factor MYB3R-4-like=Olea europaea var. sylvestris
LOC111394360	2,569857686	9,64E-33	XP_022875899.1	CYCA1;4 cyclin-A1-4-like=Olea europaea var. sylvestris
LOC111396137	2,490060923	2,13E-12	XP_022878218.1	CYCD1;1 cyclin-D1-1-like=Olea europaea var. sylvestris
LOC111387421	2,456983299	2,87E-27	XP_022867743.1	cyclin-1 G2/mitotic-specific cyclin-1-like=Olea europaea var. sylvestris
LOC111388187	2,447707518	8,61E-16	XP_022868640.1	CYCD3;1 cyclin-D3-1-like=Olea europaea var. sylvestris
LOC111400590	2,439044524	6,14E-37	XP_022883766.1	cyclin S13-7 G2/mitotic-specific cyclin S13-7-like=Olea europaea var. sylvestris
LOC111407526	2,317497071	1,78E-19	XP_022892830.1	SCL28 scarecrow-like protein 28=Olea europaea var. sylvestris
LOC111401639	2,181243408	1,19E-17	XP_022885233.1	E2FE transcription factor-like E2FE=Olea europaea var. sylvestris
LOC111381105	2,114887123	1,41E-06	XP_022860599.1	CYCA3;1 cyclin-A3-1-like=Olea europaea var. sylvestris
LOC111375324	2,108574482	7,31E-29	XP_022853898.1	cyclin S13-7 G2/mitotic-specific cyclin S13-7-like, transcript variant X2=Olea europaea var. sylvestris
LOC111368142	2,106587242	2,83E-12	XP_022845140.1	E2FE transcription factor-like E2FE=Olea europaea var. sylvestris
LOC111397535	2,057311298	3,84E-16	XP_022880286.1	CYCB2;3 cyclin-B2-3-like=Olea europaea var. sylvestris
LOC111387967	1,975443835	1,65E-31	XP_022868378.1	SCL6 scarecrow-like protein 6=Olea europaea var. sylvestris
LOC111365450	1,945885339	6,26E-16	XP_022841766.1	SCL4 scarecrow-like protein 4=Olea europaea var. sylvestris
LOC111374856	1,889014404	9,16E-16	XP_022853374.1	MYB3R-1 transcription factor MYB3R-1-like, transcript variant X4=Olea europaea var. sylvestris
LOC111387106	1,831746945	8,22E-18	XP_022867393.1	CYCA1;4 cyclin-A1-4-like=Olea europaea var. sylvestris

LOC111381297	1,821715277	2,59E-22	XP_022860837.1	CDKB;1 cyclin-dependent kinase B1-1=Olea europaea var. sylvestris
LOC111390525	1,76696065	6,46E-11	XP_022871347.1	CYCD4;2 cyclin-D4-2-like=Olea europaea var. sylvestris
LOC111398618	1,754866053	2,24E-16	XP_022881380.1	CYCB2;4 cyclin-B2-4-like, transcript variant X4=Olea europaea var. sylvestris
LOC111401995	1,688886307	2,82E-14	XP_022885770.1	CYCD3;3 cyclin-D3-3-like, transcript variant X2=Olea europaea var. sylvestris
LOC111380714	1,657235848	3,51E-12	XP_022860117.1	CYCD5;1 cyclin-D5-1-like=Olea europaea var. sylvestris
LOC111395860	1,61184221	7,72E-09	XP_022877828.1	CYCB3;1 cyclin-B3-1=Olea europaea var. sylvestris
LOC111376836	1,590638086	5,95E-07	XP_022855600.1	CYCD5;1 cyclin-D5-1-like=Olea europaea var. sylvestris
LOC111373586	1,564672109	7,03E-05	XP_022851907.1	CKI3 cyclin-dependent kinase inhibitor 3-like=Olea europaea var. sylvestris
LOC111397931	1,236906364	9,88E-09	XP_022880663.1	CDKC;1 cyclin-dependent kinase C-1-like=Olea europaea var. sylvestris
LOC111368503	1,186869029	1,62E-05	XP_022845538.1	CYCU1;1 cyclin-U1-1-like=Olea europaea var. sylvestris
LOC111376211	1,17103027	1,08E-11	XP_022854929.1	MYB3R-1 transcription factor MYB3R-1-like, transcript variant X2=Olea europaea var. sylvestris
LOC111365512	1,117259864	3,63E-04	XP_022841835.1	E2FA transcription factor E2FA-like=Olea europaea var. sylvestris
LOC111411897	1,111711568	2,23E-06	XP_022898321.1	SCL3 scarecrow-like protein 3=Olea europaea var. sylvestris
LOC111404452	1,101166533	1,62E-10	XP_022889026.1	RBR3-like cell wall protein RBR3-like=Olea europaea var. sylvestris
LOC111378780	1,073620464	5,24E-04	XP_022857787.1	E2FA transcription factor E2FA-like, transcript variant X5=Olea europaea var. sylvestris
LOC111392136	0,979411028	4,30E-06	XP_022873165.1	CYCA3;1 cyclin-A3-1=Olea europaea var. sylvestris
LOC111381566	0,646816395	2,27E-02	XP_022861127.1	CYCD6;1 cyclin-D6-1=Olea europaea var. sylvestris
LOC111391530	0,615749967	6,23E-04	XP_022872530.1	SCL21 scarecrow-like protein 21, transcript variant X3=Olea europaea var. sylvestris
LOC111381677	0,599358063	1,84E-04	XP_022861258.1	CYCL1;1 cyclin-L1-1-like, transcript variant X9=Olea europaea var. sylvestris
LOC111373799	0,592906372	1,66E-05	XP_022852131.1	SCL22 scarecrow-like protein 22, transcript variant X2=Olea europaea var. sylvestris
LOC111410139	0,590042033	2,29E-02	XP_022896126.1	CYCD3;1 cyclin-D3-1-like=Olea europaea var. sylvestris
LOC111370390	0,562921965	4,15E-04	XP_022847840.1	SCL23 scarecrow-like protein 23=Olea europaea var. sylvestris
LOC111367209	0,541832216	2,00E-03	XP_022843732.1	CYCD3;3 cyclin-D3-3-like=Olea europaea var. sylvestris
LOC111389206	0,420317011	2,10E-02	XP_022869865.1	SCL4 scarecrow-like protein 4=Olea europaea var. sylvestris
LOC111412542	4,869840689	2,18E-16	XP_022899245.1	SMR9 cyclin-dependent protein kinase inhibitor SMR9-like=Olea europaea var. sylvestris

P14 vs. P0_DOWN				
Genes	**log2FoldChange**	**p value**	**Gene_ID**	**Description**
LOC111383345	-5,422611328	5,42E-57	XP_022863230.1	CYCU4;1 cyclin-U4-1-like, transcript variant X3=Olea europaea var. sylvestris
LOC111393529	-4,603600926	2,31E-69	XP_022874865.1	SCL14 scarecrow-like protein 14=Olea europaea var. sylvestris
LOC111411586	-4,176908917	6,73E-17	XP_022897859.1	CKI7 X2 cyclin-dependent kinase inhibitor 7-like, transcript variant X2=Olea europaea var. sylvestris
LOC111410601	-3,673397747	1,41E-34	XP_022896795.1	CKI7 X2 cyclin-dependent kinase inhibitor 7-like, transcript variant X2=Olea europaea var. sylvestris
LOC111410267	-3,518631522	4,26E-22	XP_022896307.1	CYCU4;1 cyclin-U4-1-like=Olea europaea var. sylvestris
LOC111381245	-2,377495205	1,43E-28	XP_022860768.1	SCL3 scarecrow-like protein 3, transcript variant X2=Olea europaea var. sylvestris
LOC111390501	-2,14179076	1,92E-34	XP_022871314.1	CYCT1;3 cyclin-T1-3-like=Olea europaea var. sylvestris
LOC111409888	-1,957369315	2,07E-52	XP_022895752.1	SCL6 scarecrow-like protein 6, transcript variant X2=Olea europaea var. sylvestris
LOC111391983	-1,939326733	1,04E-06	XP_022873042.1	SCL3 scarecrow-like protein 3, transcript variant X2=Olea europaea var. sylvestris
LOC111393263	-1,894471683	6,39E-60	XP_022874491.1	SCL8 scarecrow-like protein 8, transcript variant X2=Olea europaea var. sylvestris
LOC111403941	-1,879723572	1,10E-10	XP_022888392.1	SCL21 scarecrow-like protein 21=Olea europaea var. sylvestris
LOC111378462	-1,609352525	6,13E-15	XP_022857427.1	CYCU4;1 cyclin-U4-1-like=Olea europaea var. sylvestris
LOC111408955	-1,60385405	1,68E-18	XP_022894579.1	CYCT1;3 cyclin-T1-3-like, transcript variant X3=Olea europaea var. sylvestris
LOC111374402	-1,585473297	3,67E-21	XP_022852839.1	CKI4 cyclin-dependent kinase inhibitor 4-like=Olea europaea var. sylvestris
LOC111395674	-1,521911682	7,16E-39	XP_022877549.1	SCL21 scarecrow-like protein 21=Olea europaea var. sylvestris
LOC111367864	-1,449793002	6,06E-22	XP_022844706.1	CKI7 cyclin-dependent kinase inhibitor 7-like=Olea europaea var. sylvestris
LOC111407903	-1,410337655	1,86E-24	XP_022893380.1	CDKF;1 cyclin-dependent kinase F-1=Olea europaea var. sylvestris
LOC111395898	-1,294776019	1,74E-30	XP_022877882.1	SCL13 scarecrow-like protein 13, transcript variant X2=Olea europaea var. sylvestris
LOC111377566	-1,208991673	7,55E-11	XP_022856462.1	SCL3 scarecrow-like protein 3=Olea europaea var. sylvestris
LOC111401867	-1,150121807	2,75E-24	XP_022885594.1	CDKG;2 X3 cyclin-dependent kinase G-2-like, transcript variant X3=Olea europaea var. sylvestris
LOC111387356	-1,097540086	1,77E-08	XP_022867679.1	CDKF;4 cyclin-dependent kinase F-4=Olea europaea var. sylvestris
LOC111376230	-1,06246955	2,84E-06	XP_022854951.1	CYCD1;1 cyclin-D1-1-like=Olea europaea var. sylvestris
LOC111380541	-0,963753099	7,22E-07	XP_022859897.1	CYCL1;1 cyclin-L1-1-like, transcript variant X5=Olea europaea var. sylvestris

LOC111410342	-0,926340834	1,75E-06	XP_022896390.1	CKI7 X2 cyclin-dependent kinase inhibitor 7-like, transcript variant X2=Olea europaea var. sylvestris
LOC111385820	-0,778537174	1,90E-03	XP_022866013.1	CYCU4;1 cyclin-U4-1-like=Olea europaea var. sylvestris
LOC111369301	-0,777662554	5,54E-07	XP_022846530.1	CDKG;2 X3 cyclin-dependent kinase G-2-like, transcript variant X3=Olea europaea var. sylvestris
LOC111409194	-0,757087702	2,48E-06	XP_022894949.1	CYCB1;2 cyclin-B1-2-like=Olea europaea var. sylvestris
LOC111379178	-0,740875274	3,05E-06	XP_022858287.1	SCL15 scarecrow-like protein 15=Olea europaea var. sylvestris
LOC111401071	-0,708221558	4,33E-05	XP_022884381.1	SCL15 scarecrow-like protein 15=Olea europaea var. sylvestris
LOC111403429	-0,682859215	7,49E-06	XP_022887697.1	CDKC;2 cyclin-dependent kinase C-2-like=Olea europaea var. sylvestris
LOC111408509	-0,654623784	2,43E-03	XP_022894024.1	CYCL1;1 cyclin-L1-1-like=Olea europaea var. sylvestris
LOC111406285	-0,638949076	1,83E-08	XP_022891400.1	CDKG;2 X8 cyclin-dependent kinase G-2-like, transcript variant X8=Olea europaea var. sylvestris
LOC111399724	-0,629241081	7,58E-03	XP_022882955.1	MYB3R-5 transcription factor MYB3R-5-like transcript variant X2=Olea europaea var. sylvestris
LOC111374749	-0,626186843	3,26E-04	XP_022853254.1	MYB3R-5 transcription factor MYB3R-5-like=Olea europaea var. sylvestris
LOC111389861	-0,608924559	4,16E-05	XP_022870605.1	SCL15 scarecrow-like protein 15=Olea europaea var. sylvestris
LOC111402001	-0,599670341	1,62E-04	XP_022885787.1	CYCP3;1 cyclin-P3-1-like=Olea europaea var. sylvestris
LOC111385852	-0,576506075	3,83E-06	XP_022866049.1	CYCT1;5 cyclin-T1-5-like=Olea europaea var. sylvestris
LOC111396796	-0,550518591	3,01E-04	XP_022879084.1	SCL1 scarecrow-like protein 1, transcript variant X4=Olea europaea var. sylvestris
LOC111367616	-0,548019141	1,01E-03	XP_022844355.1	SCL4 scarecrow-like protein 4=Olea europaea var. sylvestris
LOC111371348	-0,524325919	6,71E-03	XP_022849040.1	CKI3 X2 cyclin-dependent kinase inhibitor 3-like, transcript variant X2=Olea europaea var. sylvestris
LOC111412051	-0,516225129	5,91E-04	XP_022898562.1	PAT1 scarecrow-like transcription factor PAT1, transcript variant X3=Olea europaea var. sylvestris
LOC111388925	-0,501020752	7,52E-03	XP_022869522.1	MYB3R-3 transcription factor MYB3R-3-like=Olea europaea var. sylvestris
LOC111408732	-0,500615137	5,77E-06	XP_022894259.1	SCL1 scarecrow-like protein 1=Olea europaea var. sylvestris
LOC111393407	-0,492379314	2,23E-03	XP_022874693.1	CYCC1;2 cyclin-C1-2-like, transcript variant X2=Olea europaea var. sylvestris
LOC111407544	-0,356826565	1,03E-03	XP_022892874.1	SCL14 scarecrow-like protein 14, transcript variant X3=Olea europaea var. sylvestris
LOC111369670	-0,324513848	0,01565139	XP_022847042.1	SCL30 scarecrow-like protein 30=Olea europaea var. sylvestris

P28 vs. P14_UP				
Genes	**log2FoldChange**	**p value**	**Gene_ID**	**Description**
LOC111410601	2,887622581	2,70E-18	XP_022896795.1	CKI7 X2 cyclin-dependent kinase inhibitor 7-like, transcript variant X2=Olea europaea var. sylvestris
LOC111372156	1,417023888	2,25E-09	XP_022850120.1	CYCD6;1 cyclin-D6-1, transcript variant X2=Olea europaea var. sylvestris
LOC111378814	1,378016239	4,39E-08	XP_022857853.1	CYCD3;1 cyclin-D3-1-like=Olea europaea var. sylvestris
LOC111393406	1,16472348	1,11E-03	XP_022874690.1	CYCC1;1 cyclin-C1-1-like=Olea europaea var. sylvestris
LOC111375947	1,088510569	1,28E-03	XP_022854637.1	SCL9 scarecrow-like protein 9=Olea europaea var. sylvestris
LOC111389627	0,995668403	0,00121378	XP_022870326.1	CYCU2;1 cyclin-U2-1-like=Olea europaea var. sylvestris
LOC111387106	0,970237897	2,81E-07	XP_022867393.1	CYCA1;4 cyclin-A1-4-like=Olea europaea var. sylvestris
LOC111393407	0,955666692	2,98E-08	XP_022874693.1	CYCC1;2 cyclin-C1-2-like, transcript variant X2=Olea europaea var. sylvestris
LOC111374859	0,913615003	6,32E-05	XP_022853377.1	MYB3R-1 transcription factor MYB3R-1-like=Olea europaea var. sylvestris
LOC111397535	0,886454866	1,27E-03	XP_022880286.1	CYCB2;3 cyclin-B2-3-like=Olea europaea var. sylvestris
LOC111367504	0,881738064	4,62E-03	XP_022844184.1	CYCD4;1 cyclin-D4-1-like=Olea europaea var. sylvestris
LOC111394360	0,853772145	1,74E-05	XP_022875899.1	CYCA1;4 cyclin-A1-4-like=Olea europaea var. sylvestris
LOC111412542	0,847495762	1,81E-03	XP_022899245.1	SMR9 cyclin-dependent protein kinase inhibitor SMR9-like=Olea europaea var. sylvestris
LOC111398618	0,812512157	5,97E-08	XP_022881380.1	CYCB2;4 cyclin-B2-4-like, transcript variant X4=Olea europaea var. sylvestris
LOC111389737	0,758528917	4,87E-04	XP_022870456.1	CYCD6;1 cyclin-D6-1=Olea europaea var. sylvestris
LOC111409342	0,687669227	5,93E-04	XP_022895161.1	CYCB2;3 cyclin-B2-3-like, transcript variant X2=Olea europaea var. sylvestris
LOC111383417	0,678755993	6,08E-04	XP_022863293.1	cyclin-2 G2/mitotic-specific cyclin-2-like=Olea europaea var. sylvestris
LOC111381297	0,658374434	2,26E-04	XP_022860837.1	CDKB;1 cyclin-dependent kinase B1-1=Olea europaea var. sylvestris
LOC111378817	0,656596321	5,05E-03	XP_022857856.1	CYCD3;1 cyclin-D3-1-like=Olea europaea var. sylvestris
LOC111401639	0,648748361	2,68E-04	XP_022885233.1	E2FE transcription factor-like E2FE=Olea europaea var. sylvestris
LOC111365450	0,625352309	5,27E-04	XP_022841766.1	SCL4 scarecrow-like protein 4=Olea europaea var. sylvestris
LOC111368850	0,609255465	2,26E-03	XP_022846093.1	CYCD3;3 cyclin-D3-3-like=Olea europaea var. sylvestris
LOC111380714	0,592264316	3,23E-03	XP_022860117.1	CYCD5;1 cyclin-D5-1-like=Olea europaea var. sylvestris
LOC111381566	0,557740394	3,36E-03	XP_022861127.1	CYCD6;1 cyclin-D6-1=Olea europaea var. sylvestris

LOC111379297	0,533282873	8,91E-03	XP_022858425.1	cyclin-2 G2/mitotic-specific cyclin-2-like, transcript variant X3=Olea europaea var. sylvestris
LOC111396137	0,506660067	7,46E-03	XP_022878218.1	CYCD1;1 cyclin-D1-1-like=Olea europaea var. sylvestris
LOC111380541	0,498809345	4,35E-03	XP_022859897.1	CYCL1;1 cyclin-L1-1-like, transcript variant X5=Olea europaea var. sylvestris
LOC111368834	0,469944872	8,36E-04	XP_022846070.1	SCL28 scarecrow-like protein 28=Olea europaea var. sylvestris
LOC111385600	0,464907413	9,12E-03	XP_022865775.1	RBRA probable E3 ubiquitin-protein ligase rbrA=Olea europaea var. sylvestris

P28 vs. P14_DOWN				
Genes	**log2FoldChange**	**p value**	**Gene_ID**	**Description**
LOC111401071	-2,363905275	1,88E-25	XP_022884381.1	SCL15 scarecrow-like protein 15=Olea europaea var. sylvestris
LOC111379178	-2,127492511	3,86E-21	XP_022858287.1	SCL15 scarecrow-like protein 15=Olea europaea var. sylvestris
LOC111381245	-2,00352672	7,70E-07	XP_022860768.1	SCL3 scarecrow-like protein 3, transcript_variant X2=Olea europaea var. sylvestris
LOC111411897	-1,803240763	1,58E-14	XP_022898321.1	SCL3 scarecrow-like protein 3=Olea europaea var. sylvestris
LOC111365512	-1,537454168	1,29E-07	XP_022841835.1	E2FA transcription factor E2FA-like=Olea europaea var. sylvestris
LOC111410139	-1,506282208	1,65E-07	XP_022896126.1	CYCD3;1 cyclin-D3-1-like=Olea europaea var. sylvestris
LOC111393263	-1,298794247	3,82E-13	XP_022874491.1	SCL8 scarecrow-like protein 8, transcript variant X2=Olea europaea var. sylvestris
LOC111412051	-1,284546077	3,49E-15	XP_022898562.1	PAT1 scarecrow-like transcription factor PAT1, transcript variant X3=Olea europaea var. sylvestris
LOC111369660	-0,930676307	3,30E-10	XP_022847027.1	SCL33 scarecrow-like protein 33=Olea europaea var. sylvestris
LOC111369670	-0,894883244	2,99E-08	XP_022847042.1	SCL30 scarecrow-like protein 30=Olea europaea var. sylvestris
LOC111409888	-0,847477725	1,71E-03	XP_022895752.1	SCL6 scarecrow-like protein 6, transcript variant X2=Olea europaea var. sylvestris
LOC111397931	-0,812623772	1,65E-04	XP_022880663.1	CDKC;1 cyclin-dependent kinase C-1-like=Olea europaea var. sylvestris
LOC111410841	-0,746918853	1,89E-03	XP_022897183.1	SCL6 scarecrow-like protein 6=Olea europaea var. sylvestris
LOC111385124	-0,739124808	1,99E-03	XP_022865268.1	SCL9 scarecrow-like protein 9, transcript variant X4=Olea europaea var. sylvestris
LOC111396796	-0,736733867	6,45E-07	XP_022879084.1	SCL1 scarecrow-like protein 1, transcript variant X4=Olea europaea var. sylvestris
LOC111367864	-0,725241012	0,00015756	XP_022844706.1	CKI7 cyclin-dependent kinase inhibitor 7-like=Olea europaea var. sylvestris
LOC111387241	-0,677696731	4,51E-03	XP_022867562.1	SCL27 scarecrow-like protein 27, transcript variant X2=Olea europaea var. sylvestris

LOC111406004	-0,669314748	1,35E-04	XP_022890935.1	SCL14 scarecrow-like protein 14, transcript variant X3=Olea europaea var. sylvestris
LOC111371348	-0,665207009	1,74E-03	XP_022849040.1	CKI3 X2 cyclin-dependent kinase inhibitor 3-like, transcript variant X2=Olea europaea var. sylvestris
LOC111374402	-0,649098296	7,09E-04	XP_022852839.1	CKI4 cyclin-dependent kinase inhibitor 4-like=Olea europaea var. sylvestris
LOC111408732	-0,589869012	1,04E-05	XP_022894259.1	SCL1 scarecrow-like protein 1=Olea europaea var. sylvestris
LOC111373799	-0,540584543	9,73E-04	XP_022852131.1	SCL22 scarecrow-like protein 22, transcript_variant X2=Olea europaea var. sylvestris
LOC111389861	-0,495137622	1,09E-02	XP_022870605.1	SCL15 scarecrow-like protein 15=Olea europaea var. sylvestris
LOC111395674	-0,489730414	0,00124431	XP_022877549.1	SCL21 scarecrow-like protein 21=Olea europaea var. sylvestris
LOC111407544	-0,410513136	0,00229879	XP_022892874.1	SCL14 scarecrow-like protein 14, transcript variant X3=Olea europaea var. sylvestris

Table I.S15. Hormone-related genes induced or repressed in the dividing fruits at 14 (P14) versus the flowers at anthesis stage (P0), and the expanding fruits at 28 (P28) DPA versus the dividing fruits at 14 (P14) during early olive fruit development. Este anexo es presentado en soporte digital.

Table I.S16. Peptide-signaling-related and subtilisin-like proteases genes induced or repressed in the dividing fruits at 14 (P14) versus the flowers at anthesis stage (P0), and the expanding fruits at 28 (P28) DPA versus the dividing fruits at 14 (P14) during early olive fruit development.

P14 vs. P0_UP				
Genes	**log2FoldChange**	**p value**	**Gene_ID**	**Description**
LOC111380164	4,174073072	1,24E-28	XP_022859421.1	subtilisin-like protease SBT1.1=*Olea europaea var. sylvestris*
LOC111403579	2,789542363	2,27E-131	XP_022887944.1	subtilisin-like protease SBT1.5 =*Olea europaea var. sylvestris*
LOC111368699	2,508289231	2,38E-69	XP_022845874.1	subtilisin-like protease SBT2.2 =*Olea europaea var. sylvestris*
LOC111397017	2,103790964	1,45E-52	XP_022879447.1	subtilisin-like protease SBT1.7 =*Olea europaea var. sylvestris*
LOC111408800	2,090020103	5,96E-31	XP_022894339.1	subtilisin-like protease SBT1.9 =*Olea europaea var. sylvestris*
LOC111403829	2,017718685	2,00E-10	XP_022888224.1	subtilisin-like protease SBT2.5 =*Olea europaea var. sylvestris*
LOC111367731	1,519047726	3,47E-22	XP_022844531.1	subtilisin-like protease SBT3.5=*Olea europaea var. sylvestris*
LOC111403831	1,423968802	9,86E-06	XP_022888225.1	subtilisin-like protease SBT2.5 =*Olea europaea var. sylvestris*
LOC111403915	1,39428887	2,31E-36	XP_022888348.1	subtilisin-like protease SBT1.3 =*Olea europaea var. sylvestris*
LOC111411447	1,318622856	1,18E-31	XP_022897749.1	subtilisin-like protease SBT1.8 =*Olea europaea var. sylvestris*
LOC111410115	1,20771549	3,00E-23	XP_022896089.1	subtilisin-like protease SBT1.6=*Olea europaea var. sylvestris*
LOC111397286	1,146180093	3,91E-17	XP_022879899.1	subtilisin-like protease SBT1.9 =*Olea europaea var. sylvestris*
LOC111366809	1,134659606	4,40E-10	XP_022843272.1	subtilisin-like protease SBT1.7 =*Olea europaea var. sylvestris*

LOC111372582	0,950431752	4,19E-06	XP_022850724.1	subtilisin-like protease SBT1.6 =*Olea europaea var. sylvestris*
LOC111407513	0,846751132	0,000302303	XP_022892810.1	subtilisin-like protease SBT1.2 =*Olea europaea var. sylvestris*
LOC111397287	0,835802988	0,000385703	XP_022879901.1	subtilisin-like protease SBT1.9 =*Olea europaea var. sylvestris*
LOC111383057	0,774161071	0,019628173	XP_022862886.1	subtilisin-like protease SBT5.3 =*Olea europaea var. sylvestris*
LOC111374885	0,619672196	4,79E-09	XP_022853412.1	subtilisin-like protease SBT1.6 =*Olea europaea var. sylvestris*
LOC111368621	0,296464244	0,003014546	XP_022845741.1	subtilisin-like protease SBT1.8 =*Olea europaea var. sylvestris*
LOC111377909	3,218060212	1,48E-44	XP_022856830.1	leucine-rich repeat receptor-like protein kinase TDR =*Olea europaea var. sylvestris*
LOC111412020	1,958363422	1,18E-24	XP_022898524.1	putative phytosulfokines 6 (PSK6)=*Olea europaea var. sylvestris*
LOC111391687	1,726866922	1,92E-16	XP_022872700.1	leucine-rich repeat receptor-like serine/threonine-protein kinase BAM1 =*Olea europaea var. sylvestris*
LOC111383022	1,560508957	5,86E-20	XP_022862844.1	leucine-rich repeat receptor-like protein kinase TDR =*Olea europaea var. sylvestris*
LOC111410856	1,517903553	4,44E-41	XP_022897200.1	leucine-rich repeat receptor-like serine/threonine-protein kinase BAM1 =*Olea europaea var. sylvestris*
LOC111396050	1,49803329	2,75E-06	XP_022878088.1	receptor-like protein kinase HSL1=*Olea europaea var. sylvestris*
LOC111375576	1,461693005	4,58E-10	XP_022854181.1	leucine-rich repeat receptor-like protein CLAVATA2 (CLV2) =*Olea europaea var. sylvestris*
LOC111381865	1,390308656	2,55E-18	XP_022861481.1	leucine-richrepeat receptor-like serine/threonine-protein kinase BAM3 =*Olea europaea var. sylvestris*
LOC111388919	1,37383983	2,69E-14	XP_022869517.1	receptor-like protein kinase HAIKU2 =*Olea europaea var. sylvestris*
LOC111405568	1,328047472	6,66E-13	XP_022890282.1	LRR receptor-like serine/threonine-protein kinase GSO2 =*Olea europaea var. sylvestris*
LOC111370593	1,291219042	9,60E-21	XP_022848151.1	receptor-like protein kinase HSL1=*Olea europaea var. sylvestris*
LOC111390627	1,24437704	5,57E-11	XP_022871479.1	leucine-rich repeat receptor-like protein kinase TDR =*Olea europaea var. sylvestris*
LOC111404195	1,208772568	1,84E-05	XP_022888732.1	leucine-rich repeat receptor-like protein kinase TDR =*Olea europaea var. sylvestris*
LOC111382819	0,999161232	1,28E-15	XP_022862628.1	leucine-rich repeat receptor-like serine/threonine-protein kinase BAM1 =*Olea europaea var. sylvestris*
LOC111384807	0,980414742	0,003306415	XP_022864902.1	leucine-rich repeat receptor-like serine/threonine-protein kinase At1g17230 =*Olea europaea var. sylvestris*
LOC111398732	0,904704723	0,010399241	XP_022881560.1	LRR receptor-like serine/threonine-protein kinase GSO1 =*Olea europaea var. sylvestris*
LOC111409824	0,900640288	0,004542522	XP_022895664.1	leucine-rich repeat receptor-like serine/threonine-protein kinase BAM3 =*Olea europaea var. sylvestris*
LOC111386822	0,82477381	1,76E-05	XP_022867066.1	leucine-rich repeat receptor-like protein kinase TDR =*Olea europaea var. sylvestris*
LOC111401029	0,594639642	0,013758584	XP_022884330.1	LRR receptor-like serine/threonine-protein kinase HSL2 =*Olea europaea var. sylvestris*
LOC111375618	0,337972876	0,011179295	XP_022854237.1	leucine-rich repeat receptor-like serine/threonine-protein kinase BAM3 =*Olea europaea var. sylvestris*
LOC111381100	3,596914056	1,95E-20	XP_022860590.1	cysteine-rich receptor-like protein kinase 25 (CRK25)=*Olea europaea var. sylvestris*

LOC111386022	3,465773762	5,23E-14	XP_022866219.1	cysteine-rich receptor-like protein kinase 15 (CRK15) =*Olea europaea var. sylvestris*
LOC111386021	3,460752857	1,09E-13	XP_022866217.1	cysteine-rich receptor-like protein kinase 26 (CRK26) =*Olea europaea var. sylvestris*
LOC111403389	1,015983778	1,24E-09	XP_022887649.1	cysteine-rich receptor-like protein kinase 2 (CRK2) =*Olea europaea var. sylvestris*
LOC111402144	0,997992301	1,89E-16	XP_022886051.1	cysteine-rich receptor-like protein kinase 2 (CRK2) =*Olea europaea var. sylvestris*
LOC111368691	0,972423478	2,14E-08	XP_022845861.1	cysteine-rich receptor-like protein kinase 25 (CRK25) =*Olea europaea var. sylvestris*
LOC111390863	0,860924537	2,31E-06	XP_022871762.1	protein RALF-like 24 (RALF24)=*Olea europaea var. sylvestris*
LOC111392780	0,78574319	7,78E-05	XP_022873944.1	cysteine-rich receptor-like protein kinase 25 (CRK25) =*Olea europaea var. sylvestris*
LOC111403386	0,528702503	0,004027556	XP_022887646.1	cysteine-rich receptor-like protein kinase 2 (CRK2) =*Olea europaea var. sylvestris*
LOC111372640	0,282512547	0,027400284	XP_022850792.1	receptor-like protein kinase FERONIA =*Olea europaea var. sylvestris*
LOC111386717	4,700541848	4,51E-19	XP_022866950.1	leucine-rich repeat receptor protein kinase EMS1 =*Olea europaea var. sylvestris*
LOC111384431	4,351782202	7,93E-20	XP_022864474.1	cysteine-rich receptor-like protein kinase 29 (CRK29) =*Olea europaea var. sylvestris*

P14 vs. P0_DOWN				
Genes	**log2FoldChange**	**p value**	**Gene_ID**	**Description**
LOC111399703	-4,611454166	4,21E-163	XP_022882931.1	subtilisin-like protease SBT4.15 =*Olea europaea var. sylvestris*
LOC111409644	-2,095239509	1,49E-86	XP_022895442.1	subtilisin-like protease SBT1.7 =*Olea europaea var. sylvestris*
LOC111372971	-1,146070933	6,48E-09	XP_022851182.1	subtilisin-like protease SBT1.2=*Olea europaea var. sylvestris*
LOC111402276	-1,046594975	7,54E-24	XP_022886218.1	subtilisin-like protease SBT1.4 =*Olea europaea var. sylvestris*
LOC111389318	-0,849858974	1,19E-16	XP_022870004.1	subtilisin-like protease SBT1.7 =*Olea europaea var. sylvestris*
LOC111401229	-0,512521652	4,52E-06	XP_022884642.1	subtilisin-like protease SBT3.5 =*Olea europaea var. sylvestris*
LOC111387773	-0,391084996	0,000235017	XP_022868130.1	subtilisin-like protease SBT1.4 =*Olea europaea var. sylvestris*
LOC111410688	-4,862065719	1,08E-140	XP_022896919.1	phytosulfokines-like (PSK) =*Olea europaea var. sylvestris*
LOC111372920	-2,196698581	3,72E-11	XP_022851116.1	putative phytosulfokines 6 (PSK6) =*Olea europaea var. sylvestris*
LOC111380730	-2,006436553	1,85E-56	XP_022860131.1	probable leucine-rich repeat receptor-like protein kinase At2g33170 =*Olea europaea var. sylvestris*
LOC111375443	-1,477837859	8,19E-28	XP_022854039.1	leucine-rich repeat receptor-like serine/threonine-protein kinase At1g17230 =*Olea europaea var. sylvestris*
LOC111369898	-1,21629477	1,62E-18	XP_022847381.1	LRR receptor-like serine/threonine-protein kinase GSO1 =*Olea europaea var. sylvestris*
LOC111367605	-1,181882023	1,46E-10	XP_022844336.1	receptor protein-tyrosine kinase CEPR1-like =*Olea europaea var. sylvestris*
LOC111397375	-1,076412639	6,96E-07	XP_022880041.1	receptor protein kinase CLAVATA1-like (CLV1) =*Olea europaea var. sylvestris*
LOC111401367	-1,008390479	3,05E-07	XP_022884838.1	receptor protein-tyrosine kinase CEPR1-like =*Olea europaea var. sylvestris*
LOC111373583	-0,929555448	8,55E-05	XP_022851902.1	CLAVATA3/ESR (CLE)-related protein TDIF-like (TDIF) =*Olea europaea var. sylvestris*
LOC111393632	-0,911844337	2,60E-05	XP_022875035.1	probable leucine-rich repeat receptor-like protein kinase At2g33170 =*Olea europaea var. sylvestris*

LOC111401824	-0,833854642	0,000398327	XP_022885515.1	LRR receptor-like serine/threonine-protein kinase GSO1 =*Olea europaea var. sylvestris*
LOC111369439	-0,716008314	0,000320734	XP_022846722.1	putative phytosulfokines 6 (PSK6) =*Olea europaea var. sylvestris*
LOC111372588	-0,702040836	0,013711328	XP_022850728.1	LRR receptor-like serine/threonine-protein kinase GSO2 = *Olea europaea var. sylvestris*
LOC111401022	-0,61713423	0,005410748	XP_022884320.1	phytosulfokines 3-like (PSK3) =*Olea europaea var. sylvestris*
LOC111366328	-6,070461494	1,15E-223	XP_022842839.1	pollen receptor-like kinase 1 (PRK1) =*Olea europaea var. sylvestris*
LOC111396460	-5,977847773	2,39E-176	XP_022878660.1	protein RALF-like 19 (RALFL19) =*Olea europaea var. sylvestris*
LOC111396463	-5,717834794	3,04E-229	XP_022878663.1	protein RALF-like 19 (RALFL19) =*Olea europaea var. sylvestris*
LOC111402717	-5,643145455	1,62E-209	XP_022886831.1	pollen receptor-like kinase 1 (PRK1) =*Olea europaea var. sylvestris*
LOC111369803	-5,268983923	4,32E-122	XP_022847235.1	pollen receptor-like kinase 4 (PRK4) =*Olea europaea var. sylvestris*
LOC111409662	-5,238003148	1,67E-142	XP_022895452.1	pollen receptor-like kinase 3 (PRK3) =*Olea europaea var. sylvestris*
LOC111372561	-4,862343021	2,05E-154	XP_022850696.1	pollen receptor-like kinase 3 (PRK3) =*Olea europaea var. sylvestris*
LOC111394967	-4,695224502	9,70E-26	XP_022876772.1	rapid alkalinization factor-like (RALF) =*Olea europaea var. sylvestris*
LOC111394269	-4,214208078	1,28E-60	XP_022875794.1	protein RALF-like 19 (RALF19) =*Olea europaea var. sylvestris*
LOC111382577	-2,549051426	7,85E-52	XP_022862364.1	rapid alkalinization factor-like (RALF) =*Olea europaea var. sylvestris*
LOC111389588	-2,237443793	6,27E-78	XP_022870287.1	rapid alkalinization factor (RALF) =*Olea europaea var. sylvestris*
LOC111403022	-2,033149746	3,91E-25	XP_022887135.1	receptor-like protein kinase FERONIA=*Olea europaea var. sylvestris*
LOC111368310	-1,722139179	6,46E-17	XP_022845311.1	cysteine-rich receptor-like protein kinase 25 (CRK25)=*Olea europaea var. sylvestris*
LOC111372642	-1,395277568	5,76E-05	XP_022850793.1	receptor-like protein kinase FERONIA =*Olea europaea var. sylvestris*
LOC111368721	-1,208671821	2,41E-13	XP_022845902.1	cysteine-rich receptor-like protein kinase 29 (CRK29) =*Olea europaea var. sylvestris*
LOC111374777	-0,832982736	1,06E-14	XP_022853283.1	receptor-like protein kinase FERONIA =*Olea europaea var. sylvestris*
LOC111380312	-0,576233759	6,21E-08	XP_022859605.1	cysteine-rich receptor-like protein kinase 10 (CRK10) =*Olea europaea var. sylvestris*
LOC111367074	-0,468430931	0,000741685	XP_022843543.1	cysteine-rich receptor-like protein kinase 42 (CRK42) =*Olea europaea var. sylvestris*
LOC111374096	-4,628874923	2,22E-13	XP_022852497.1	LRR receptor-like serine/threonine-protein kinase GSO1 =*Olea europaea var. sylvestris*
LOC111402396	-4,454420864	2,38E-26	XP_022886428.1	subtilisin-like protease SBT5.4 =*Olea europaea var. sylvestris*

P28 vs. P14_UP				
Genes	**log2FoldChange**	**p value**	**Gene_ID**	**Description**
LOC111375971	2,387006197	2,04E-10	XP_022854658.1	subtilisin-like protease SBT1.5 =*Olea europaea var. sylvestris*
LOC111374920	1,867939315	1,43E-25	XP_022853451.1	subtilisin-like protease SBT3.6 =*Olea europaea var. sylvestris*
LOC111380164	1,485013623	4,92E-14	XP_022859421.1	subtilisin-like protease SBT1.1 =*Olea europaea var. sylvestris*
LOC111366809	1,303179783	1,41E-18	XP_022843272.1	subtilisin-like protease SBT1.7 =*Olea europaea var. sylvestris*
LOC111374885	0,896727088	9,04E-13	XP_022853412.1	subtilisin-like protease SBT1.6 =*Olea europaea var. sylvestris*
LOC111397286	0,869600766	7,97E-08	XP_022879899.1	subtilisin-like protease SBT1.9 =*Olea europaea var. sylvestris*

LOC111411447	0,829209995	1,69E-11	XP_022897749.1	subtilisin-like protease SBT1.8 =*Olea europaea var. sylvestris*
LOC111403579	0,70741021	9,99E-09	XP_022887944.1	subtilisin-like protease SBT1.5 =*Olea europaea var. sylvestris*
LOC111408800	0,679475199	0,002450008	XP_022894339.1	subtilisin-like protease SBT1.9=*Olea europaea var. sylvestris*
LOC111368621	0,557628704	2,78E-05	XP_022845741.1	subtilisin-like protease SBT1.8 =*Olea europaea var. sylvestris*
LOC111403915	0,532131254	2,41E-05	XP_022888348.1	subtilisin-like protease SBT1.3=*Olea europaea var. sylvestris*
LOC111410115	0,479232147	0,000144385	XP_022896089.1	subtilisin-like protease SBT1.6 =*Olea europaea var. sylvestris*
LOC111366066	0,454948033	0,008557753	XP_022842485.1	subtilisin-like protease SBT2.5 =*Olea europaea var. sylvestris*
LOC111412020	1,448652259	1,97E-10	XP_022898524.1	putative phytosulfokines 6 (PSK6) =*Olea europaea var. sylvestris*
LOC111377909	1,022404561	1,39E-08	XP_022856830.1	leucine-rich repeat receptor-like protein kinase TDR =*Olea europaea var. sylvestris*
LOC111383022	0,592658841	0,002050769	XP_022862844.1	leucine-rich repeat receptor-like protein kinase TDR =*Olea europaea var. sylvestris*
LOC111398260	1,562848483	0,000310333	XP_022880957.1	receptor-like protein kinase FERONIA =*Olea europaea var. sylvestris*
LOC111404922	1,146466846	3,05E-05	XP_022889413.1	rapid alkalinization factor-like (RALF) =*Olea europaea var. sylvestris*

P28 vs. P14_DOWN				
Genes	**log2FoldChange**	**p value**	**Gene_ID**	**Description**
LOC111409395	-2,92567104	2,62E-58	XP_022895215.1	subtilisin-like protease SBT1.9 =*Olea europaea var. sylvestris*
LOC111367731	-2,675881497	9,78E-50	XP_022844531.1	subtilisin-like protease SBT3.5 =*Olea europaea var. sylvestris*
LOC111373695	-0,910030989	3,16E-06	XP_022852030.1	subtilisin-like protease SBT5.6 =*Olea europaea var. sylvestris*
LOC111389318	-0,82003298	1,49E-09	XP_022870004.1	subtilisin-like protease SBT1.7 =*Olea europaea var. sylvestris*
LOC111387773	-0,511756637	6,81E-05	XP_022868130.1	subtilisin-like protease SBT1.4 =*Olea europaea var. sylvestris*
LOC111401229	-0,436364272	0,002959688	XP_022884642.1	subtilisin-like protease SBT3.5 =*Olea europaea var. sylvestris*
LOC111409644	-0,373596275	0,011253229	XP_022895442.1	subtilisin-like protease SBT1.7=*Olea europaea var. sylvestris*
LOC111369439	-3,653072275	7,68E-32	XP_022846722.1	putative phytosulfokines 6 (PSK6) =*Olea europaea var. sylvestris*
LOC111397375	-2,816943852	8,36E-12	XP_022880041.1	receptor protein kinase CLAVATA1-like (CLV1) =*Olea europaea var. sylvestris*
LOC111369479	-2,810627634	1,78E-27	XP_022846765.1	receptor-like protein kinase HAIKU2 =*Olea europaea var. sylvestris*
LOC111401367	-2,351069288	4,27E-16	XP_022884838.1	receptor protein-tyrosine kinase CEPR1-like =*Olea europaea var. sylvestris*
LOC111367605	-2,060053144	2,18E-13	XP_022844336.1	receptor protein-tyrosine kinase CEPR1-like =*Olea europaea var. sylvestris*
LOC111367262	-2,027629635	5,07E-06	XP_022843802.1	phytosulfokines-like (PSK) =*Olea europaea var. sylvestris*
LOC111410688	-1,905494985	1,62E-09	XP_022896919.1	phytosulfokines-like (PSK) =*Olea europaea var. sylvestris*
LOC111401824	-1,839763621	2,89E-07	XP_022885515.1	LRR receptor-like serine/threonine-protein kinase GSO1 =*Olea europaea var. sylvestris*
LOC111373583	-1,770467261	5,62E-07	XP_022851902.1	CLAVATA3/ESR (CLE)-related protein TDIF-like (TDIF) =*Olea europaea var. sylvestris*
LOC111401368	-1,728582337	4,45E-29	XP_022884839.1	receptor-like protein kinase HAIKU2 =*Olea europaea var. sylvestris*
LOC111388919	-1,532023359	1,97E-08	XP_022869517.1	receptor-like protein kinase HAIKU2 =*Olea europaea var. sylvestris*

LOC111375443	-1,47368505	1,22E-11	XP_022854039.1	leucine-rich repeat receptor-like serine/threonine-protein kinase At1g17230 =*Olea europaea var. sylvestris*
LOC111396050	-1,343676453	5,68E-05	XP_022878088.1	receptor-like protein kinase HSL1 =*Olea europaea var. sylvestris*
LOC111401823	-1,202944561	5,15E-05	XP_022885512.1	LRR receptor-like serine/threonine-protein kinase GSO1 =*Olea europaea var. sylvestris*
LOC111398674	-1,146363651	1,05E-16	XP_022881465.1	receptor-like protein kinase HSL1 =*Olea europaea var. sylvestris*
LOC111370841	-1,113780989	6,15E-09	XP_022848503.1	receptor-like protein kinase HSL1 =*Olea europaea var. sylvestris*
LOC111384807	-1,018682043	0,001276607	XP_022864902.1	leucine-rich repeat receptor-like serine/threonine-protein kinase At1g17230 =*Olea europaea var. sylvestris*
LOC111405568	-0,991597902	4,62E-08	XP_022890282.1	LRR receptor-like serine/threonine-protein kinase GSO2 =*Olea europaea var. sylvestris*
LOC111392161	-0,904774981	3,83E-05	XP_022873195.1	receptor protein kinase CLAVATA1-like (CLV1) =*Olea europaea var. sylvestris*
LOC111386822	-0,649047619	0,000192421	XP_022867066.1	leucine-rich repeat receptor-like protein kinase TDR =*Olea europaea var. sylvestris*
LOC111380730	-0,53479095	0,001650266	XP_022860131.1	probable leucine-rich repeat receptor-like protein kinase At2g33170 =*Olea europaea var. sylvestris*
LOC111369898	-0,508145254	0,000250973	XP_022847381.1	LRR receptor-like serine/threonine-protein kinase GSO1 =*Olea europaea var. sylvestris*
LOC111381865	-0,492515109	0,001806123	XP_022861481.1	leucine-rich repeat receptor-like serine/threonine-protein kinase BAM3 =*Olea europaea var. sylvestris*
LOC111394269	-6,275903728	4,13E-81	XP_022875794.1	protein RALF-like 19 (RALF19) =*Olea europaea var. sylvestris*
LOC111386022	-4,102580292	1,35E-19	XP_022866219.1	cysteine-rich receptor-like protein kinase 15 (CRK15) =*Olea europaea var. sylvestris*
LOC111396463	-3,24768388	2,30E-31	XP_022878663.1	protein RALF-like 19 (RALF19) =*Olea europaea var. sylvestris*
LOC111402717	-3,108094813	1,85E-15	XP_022886831.1	pollen receptor-like kinase 1 (PRK1) =*Olea europaea var. sylvestris*
LOC111369803	-2,47171847	1,15E-09	XP_022847235.1	pollen receptor-like kinase 4 (PRK4) =*Olea europaea var. sylvestris*
LOC111403387	-2,165245245	1,94E-10	XP_022887648.1	cysteine-rich receptor-like protein kinase 2 (CRK2) =*Olea europaea var. sylvestris*
LOC111366328	-2,040312585	8,40E-10	XP_022842839.1	pollen receptor-like kinase 1 (PRK1) =*Olea europaea var. sylvestris*
LOC111368309	-1,939803711	6,14E-09	XP_022845310.1	cysteine-rich receptor-like protein kinase 25 (CRK25) =*Olea europaea var. sylvestris*
LOC111368721	-1,91623939	6,50E-10	XP_022845902.1	cysteine-rich receptor-like protein kinase 29 (CRK29) =*Olea europaea var. sylvestris*
LOC111380312	-1,479269714	3,86E-26	XP_022859605.1	cysteine-rich receptor-like protein kinase 10 (CRK10) =*Olea europaea var. sylvestris*
LOC111372640	-1,289518173	1,61E-16	XP_022850792.1	receptor-like protein kinase FERONIA =*Olea europaea var. sylvestris*
LOC111368310	-1,228561902	0,000330049	XP_022845311.1	cysteine-rich receptor-like protein kinase 25 (CRK25) =*Olea europaea var. sylvestris*
LOC111392780	-1,117979164	3,30E-08	XP_022873944.1	cysteine-rich receptor-like protein kinase 25 (CRK25) =*Olea europaea var. sylvestris*
LOC111372561	-1,001219484	0,002032707	XP_022850696.1	pollen receptor-like kinase 3 (PRK3) =*Olea europaea var. sylvestris*
LOC111402144	-0,362165216	0,007086939	XP_022886051.1	cysteine-rich receptor-like protein kinase 2 (CRK2)=*Olea europaea var. sylvestris*
LOC111394967	-6,829794129	1,82E-13	XP_022876772.1	rapid alkalinization factor-like (RALF) =*Olea europaea var. sylvestris*
LOC111399703	-6,095967231	9,28E-18	XP_022882931.1	subtilisin-like protease SBT4.15 =*Olea europaea var. sylvestris*

LOC111381100	-5,427713338	6,57E-30	XP_022860590.1	cysteine-rich receptor-like protein kinase 25 (CRK25) =*Olea europaea var. sylvestris*
LOC111384431	-5,270508566	6,47E-27	XP_022864474.1	cysteine-rich receptor-like protein kinase 29 (CRK29) =*Olea europaea var. sylvestris*
LOC111398732	-4,318211555	5,88E-16	XP_022881560.1	LRR receptor-like serine/threonine-protein kinase GSO1 =*Olea europaea var. sylvestris*

Table I.S17. Proteases genes induced or repressed in the dividing fruits at 14 (P14) versus the flowers at anthesis stage (P0), and the expanding fruits at 28 (P28) DPA versus the dividing fruits at 14 (P14) during early olive fruit development. Este anexo es presentado en soporte digital.

Table I.S18. Cell-wall-related genes induced or repressed in the dividing fruits at 14 (P14) versus the flowers at anthesis stage (P0), and the expanding fruits at 28 (P28) DPA versus the dividing fruits at 14 (P14) during early olive fruit development. Este anexo es presentado en soporte digital.

Table I.S19. Transport-related and vesicle-trafficking-related genes repressed or induced in the dividing fruits at 14 (P14) versus the flowers at anthesis stage (P0), and the expanding fruits at 28 (P28) DPA versus the dividing fruits at 14 (P14) during early olive fruit development.

Table I.S20. Transcription factors (TF) genes repressed or induced in the dividing fruits at 14 (P14) versus the flowers at anthesis stage (P0), and the expanding fruits at 28 (P28) DPA versus the dividing fruits at 14 (P14) during early olive fruit development. Este anexo es presentado en soporte digital.

Capítulo II

Table II. S1. PCR-primers used in this study.

Primer	Sequence	Gene
GID1B-F	5′-AGATTGGTTCCACTTAATACCTGG-3′	*OeGID1B*
GID1B-R	5′-ATGAGTAAAGCTTCCCCCGTGGAA-3′	
GGPPS-F	5′-GAAGGACTAGTGGCTGGACAGGTA-3′	*OeGGPPS*
GGPPS-R	5′-AAACAAGAGCCCAATACACCTAGC-3′	
PAL-F	5′-GATATATTGAAGCTCATGTCGTCT-3′	*OePAL*
PAL-R	5′-AAGAACTTGCCTCAATTTTTGCAT-3′	
CKX-F	5′-AAATGGATCAGAGTGCTTTACTCA-3′	*OeCKX*
CKX-R	5′-TGGGTGTGGAAGATCCCACAATCC -3′	
JAR1-F	5′-GATTTGCAGCTGGCTGTAGAAGCA-3′	*OeJAR1*
JAR1-R	5′-TTTGAATTGGCTAACAGCAGCTCC-3′	
ABA-8OH-F	5′-ATGCCATTTGGCAGTGGAGTACAT-3′	*OeABA-8OH*
ABA-8OH-R	5′-GGTTGGTTCTTGTTTCCAAAATAT-3′	
AOS-F	5′-TCCCAACATGCTTAAATGGGTTGGT-3′	*OeAOS*
AOS-R	5′-GGATTCAATCACGAAGTCGCGTTT-3′	
LOX2-F	5′-GGCCATGCAGACAAGAAGGATGA-3′	*OeLOX2*
LOX2-R	5′-CCCGAGATACTCCTCGTCGGGCGA-3′	

NCED5-F	5′-AACCTAGAAGCCGGTATGGTTAAC-3′	*OeNCED5*
NCED5-R	5′-CCCGTGGAACCCGTATGGGACTCT-3′	
ARF2-F	5′-ATGCCGCCTGGTCATTCAAGAGAA-3′	*OeARF2*
ARF2-R	5′- CTTGGCAAGATCAACAGACCTGCC-3′	
SAUR-F	5′-CAAACAGCAGTTTTGAAGCAAATT-3′	*OeSAUR*
SAUR-R	5′-TCGAAGCATTGACGTTAGAGATCG-3′	
TIR1-F	5′-CCAATGGATGAAGGCTTTGGA-3′	*OeTIR1*
TIR1-R	5′-GTCACCAGCAAAAGCAACTGACA -3′	
IAA1-F	5′-GGATGGCCTCCAGTGAGATCATAC-3′	*OeIAA1*
IAA1-R	5′- AGGGACATCTCCAACTAACATCCA -3′	

Bibliografía

VI. Bibliografía

Abel S., Savchenko T., Levy M. (2005). Genome-wide comparative analysis of the IQD gene families in Arabidopsis thaliana and Oryza sativa. BMC Evol. Biol. 5, 72

Acebedo M. M., Cañete M.L., Cuevas J. (2000). Processes affecting fruit distribution and its quality in the canopy of olive tree. Advances in Horticultural Science, Vol. 14, No. 4, 169-175

Alagna F., Cirilli M., Galla G., Carbone F., Daddiego L., Facella P., Lopez L., Colao C., Mariotti R., Cultrera N., Rossi M., Barcaccia G., Baldoni L., Muleo R., Perrotta G. (2016). Transcript Analysis and Regulative Events during Flower Development in Olive (Olea europaea L.). PLoS One. 11(4): e0152943.

Alagna F., D'Agostino N., Torchia L., Servili M., Rao R., Pietrella M., Giuliano G., Chiusano ML., Baldoni L., Perrotta G. (2009). Comparative 454 pyrosequencing of transcripts from two olive genotypes during fruit development. BMC Genomics 10:399.

Alagna F., Mariotti R., Panara F., Caporali S., Urbani S., Veneziani G., Esposto S., Taticchi A., Rosati A., Rao R., Perrotta G., Servili M., Baldoni L. (2012). Olive phenolic compounds: Metabolic and transcriptional profiling during fruit development. BMC Plant Biol. 12, 162. https://doi.org/10.1186/1471-2229-12-162

Alferez F., de Carvalho D. U., Boakye D. (2021). Interplay between abscisic acid and gibberellins, as related to ethylene and sugars, in regulating maturation of non-climacteric fruit. Int. J. Mol. Sci. 22, 669. https://doi.org/10.3390/ijms22020669

Alonge M., Wang X., Benoit M., Soyk S., Pereira L., Zhang L., Suresh H., Ramakrishnan S., Maumus F., Ciren D., Levy Y., Harel T. H., Shalev-Schlosser G., Amsellem Z., Razifard H., Caicedo A. L., Tieman D. M., Klee H., Kirsche M., Aganezov S., Ranallo-Benavidez T. R., Lemmon Z. H., Kim J., Robitaille G., Kramer M., Goodwin S., McCombie W. R., Hutton S., Van Eck J., Gillis J., Eshed Y., Sedlazeck F. J., van der Knaap E., Schatz M. C., Lippman Z. B. (2020). Major impacts of widespread structural variation on gene expression and crop improvement in tomato. Cell 182, 145–161

Alpert K.B., Tanksley S.D. (1996). High-resolution mapping and isolation of a yeast artificial chromosome contig containing fw2.2: a major fruit weight quantitative trait locus in tomato. Proc. Natl. Acad. Sci. U. S. A. 93, 15503–15507

Ambawat S., Sharma P., Yadav N.R., Yadav R.C. (2013). MYB transcription factor genes as regulators for plant responses: an overview. Physiol. Mol. Biol. Plants. 19, 307-321. doi: 10.1007/s12298-013-0179-1

Amini F., Ramin A.A. (2015). Effect of 1-methylcyclopropane in combination with calcium chloride on postharvest storage and quality of green olives. Prog. Biol. Sci. 5, 121-131

Amiot M. J., Fleuriet A., Macheix J. J. (1986). Importance and evolution of phenolic compounds in olive during growth and maturation. Journal of Agriculture and Food Chemistry, 34, 823–826.

Amiot M. J., Fleuriet A., Macheix J. J. (1989). Accumulation of oleuropein derivatives during olive maturation. Phytochemistry. 28: 67-69.

An J. P., Wang X. F., Li Y. Y., Song L. Q., Zhao L. L., You C. X., Hao Y. J. (2018). EIN3-LIKE1, MYB1, and ETHYLENE RESPONSE FACTOR3 Act in a Regulatory Loop That Synergistically Modulates Ethylene Biosynthesis and Anthocyanin Accumulation1[OPEN]. Plant Physiol. 178, 808–823

An J., Almasaud R.A., Bouzayen M., Zouine M., Chervin C. (2020). Auxin and ethylene regulation of fruit set. Plant Sci. (Oxford), 292, 110381.

Anastasiou E., Kenz S., Gerstung M., MacLean D., Timmer J., Fleck C., Lenhard M. (2007). Control of plant organ size by KLUH/CYP78A5-dependent intercellular signaling. Dev. Cell 13, 843–856

Ando K., Carr K.M., Grumet R. (2012). Transcriptome analyses of early cucumber fruit growth identifies distinct gene modules associated with phases of development. BMC Genom. 13:518. doi:10.1186/1471-2164-13-518

Anuario de estadística 2021. Ministerio de Agricultura, Pesca y Alimentación

Arambarri A. (1992). La oleicultura antigua. Editorial Agrícola Española, Madrid

Ardila T., Redondo-Cuadrado M.J., Gallardo M., Sanchez-Calle I.M., Gomez-Jimenez M.C. (2012). The interaction between ethylene and polyamines during ripening of olive fruit. Acta Hortic. 949, 147-153. https://doi.org/10.17660/ActaHortic.2012.949.20

Arslan D., Özcan M.M. (2011). Influence of growing area and harvest date on the organic acid composition of olive fruits from Gemlik variety. Sci. Hort. 130, 634–641.

Arteca R. N. (1996). Plant Growth Substances: Principles and Applications. Chapman and Hall Press, New York, USA, p. 332.

Atta-Aly M.A., Riad G.S., Lacheene Z.E.S., El-Beltagy A.S. (1999). Early ethrel applications extend tomato fruit cell division and increase fruit size and yield with ripening delay. J. Plant. Growth Regul. 18, 15-24.

Ayub R., Guis M., Amor M.B., Gillot L., Roustan J.P., Latche A., Bouza- yen M., Pech J.C. (1996). Expression of ACC oxidase antisense gene inhibits ripening of cantaloupe melon fruits. Nat. Biotechnol. 14, 862–866.

Badad O., Lakhssassi N., Zaid N., El Baze A., Zaid Y., Meksem J., Lightfoot D.A., Tombuloglu H., Zaid E.H., Unver T., Meksem K. (2021). Genome wide medip-seq profiling of wild and cultivated olives trees suggests DNA methylation fingerprint on the sensory quality of olive oil. Plants, 10 (7), art. no. 1405

Baghel M., Nagaraja A., Srivastav M., Meena N.K., Senthil Kumar M., Kumar A., Sharma R.R. (2019). Pleiotropic influences of brassinosteroids on fruit crops: a review. Plant Growth Regul. 87, 375–388.

Bai Q., Huang Y., Shen Y. (2021). The physiological and molecular mechanism of abscisic acid in regulation of fleshy fruit ripening. Front. Plant Sci. 11, 619953. https://doi.org/10.3389/fpls.2020.619953.

Baldoni L., Belaj A. (2009). Olive. In: Vollmann J, Rajean I (eds) Oil crops. Handbook of plant breeding, vol 4. Springer Science + Business Media, New York, pp 397–421. doi 10.1007/978-0-387-77594-4_13

Banilas G., Karampelias M., Makariti I., Kourti A., Hatzopoulos P. (2011). The olive DGAT2 gene is developmentally regulated and shares overlapping but distinct expression patterns with DGAT1. J. Exp. Bot. 62, 521-532

Banilas G., Moressis A., Nikoloudakes N., Hatzopoulos P. (2005). Spatial and temporal expressions of two distinct oleate desaturases from olive (Olea europaea L.). Plant Sci. 168, 547–555

Banilas G., Nikiforiadis A., Makariti I., Moressis A., Hatzopoulos P. (2007). Discrete roles of a microsomal linoleate desaturase gene in olive identified by spatiotemporal transcriptional analysis. Tree Physiol. 27, 481–490.

Barranco D. (1999). Variedades y patrones. In 'El cultivo del olivo'. (Eds D Barranco, R Fernández Escobar, L Rallo) pp. 63–89. (Mundi-Prensa: Madrid, Spain)

Barranco D., Caballero J.M., Martín A., Rallo L., Del Río C., Tous J., Trujillo I. (2005). Variedades de olivo en España, Mundi prensa, Madrid, Spain.

Barranco D., Fernandez-Escobar R., Rallo L. (2017). El cultivo del olivo 7ª edición, Mundi-prensa, Madrid

Bartolini G. (2018). Olive germplasm (Olea europaea L.). Available online: http://www.oleadb.it/olivodb.html (accessed on 21 January 2021)

Bartolini S., Leccese A., Andreini L. (2014). Influence of canopy fruit location on morphological, histochemical and biochemical changes in two oil olive cultivars. Plant Biosyst. 148, 1221-1230.

Bassa C., Audran-Delalande C., Mila I., Bouzayen M. (2012). Phenotypes Associated with Down-Regulation of Sl-IAA27 Support Functional Diversity Among Aux/IAA Family Members in Tomato. Plant Cell Physiol. 53, 1583–1595.

Bastías A., Lopez-Climent M., Valcarcel M., Rosello S., Gomez-Cadenas A., Casaretto J.A. (2011). Modulation of organic acids and sugar content in tomato fruits by an abscisic acid-regulated transcription factor. Physiol. Plant. 141, 215–226.

Bastías A., Yañez M., Osorio S., Arbona V., Gómez-Cadenas A., Fernie A.R., Casaretto J.A. (2014). The transcription factor AREB1 regulates primary metabolic pathways in tomato fruits. J. Exp. Bot. 65, 2351–2363.

Batista-Silva W., Nascimento V.L., Medeiros D.B., Nunes-Nesi A., Ribeiro D.M., Zsogon A., Araujo W.L. (2018). Modifications in organic acid profiles during fruit development and ripening: correlation or causation? Front. Plant Sci. 9, 1689.

Baxter C.E.L., Costa M. M. R., Coen E.S. (2007). Diversification and co-option of RAD-like genes in the evolution of floral asymmetry. Plant J. 52, 105–113

Bazakos C., Alexiou KG., Ramos-Onsins S., Koubouris G., Tourvas N., Xanthopoulou A., Mellidou I., Moysiadis T., Vourlaki I. T., Metzidakis I., Sergentani C., Manolikaki I., Michailidis M., Pistikoudi A., Polidoros A., Kostelenos G., Aravanopoulos F., Molassiotis A., Ganopoulos I. (2023). Whole genome scanning of a Mediterranean basin hotspot collection provides new insights into olive tree biodiversity and biology. Plant J. doi: 10.1111/tpj.16270. Epub ahead of print. PMID: 37164361.

Bazakos C., Manioudaki M. E., Sarropoulou E., Spano T1., Kalaitzis P. (2015). 454 Pyrosequencing of Olive (Olea europaea L.) Transcriptome in Response to Salinity. PLoS One. 10(11): e0143000.

Beauchet A., Gévaudant F., Gonzalez N., Chevalier C. (2021). In search of the still unknown function of FW2. 2/CELL NUMBER REGULATOR, a major regulator of fruit size in tomato. J. Exp. Bot. https://doi.org/10.1093/jxb/erab207

Belaj A., de la Rosa R., León L., Gabaldón-Leal C., Santos C., Porras R., de la Cruz-Blanco M., Lorite I. J. (2020). Phenological diversity in a World Olive Germplasm Bank: Potential use for breeding programs and climate change studies. https://doi.org/10.5424/sjar/2020181-15017.

Belaj A., de la Rosa R., León L., Gabaldón-Leal C., Santos C., Porras R., de la Cruz-Blanco M., LoriteI J. (2020). Phenological diversity in a World Olive Germplasm Bank: Potential use for breeding programs and climate change studies. Spanish Journal of Agricultural Research, 18(1), e0701. https://doi.org/10.5424/sjar/2020181-15017

Belaj A., Dominguez-Garcia M. C., Atienza S. G., Martin-Urdiroz N., De la Rosa R., Satovic Z., Martín A., Kilian A., Trujillo I., Valpuesta V., Del Río C. (2012). Developing a core collection of olive (Olea europaea L.) based on molecular markers (DArTs, SSRs, SNPs) and agronomic traits. Tree Genet. Genomes 8, 365–378.

Belaj A., Rallo L., Trujillo I., Baldoni L. (2004). Use of RAPD and AFLP markers to distinguish individuals obtained by clonal selection of the olive cultivars Arbequina and Manzanilla de Sevilla. HortScience 39, 1566–1570

Belaj A., Veral M.G., Sikaoui H., Moukhli A., Khadari B., Mariotti R., Baldoni L. (2016). Olive Genetic Resources. In The Olive Tree Genome. Compendium of Plant Genomes; Rugini, E., Baldoni, L., Muleo, R., Sebastiani, L., Eds.; Springer: Cham, Switzerland, pp. 27–54, doi:10.1007/978-3-319-48887-5_3

Bellini E., Giordani E., Parlati M.V., Pandolfi S. (2002). Olive genetic improvement: Thirty years of research. Acta Hortic. 586, 105–108, doi:10.17660/ActaHortic.2002.586.13

Beltrán G., del Río C., Sánchez S., Martínez L. (2004). Seasonal changes in olive fruit characteristics and oil accumulation during ripening process. J. Sci. Food Agric. 84, 1783-1790.

Beltrán G., Jiménez A., del Rio C., Sánchez S., Martínez L., Uceda M., Aguilera M.P. (2010). Variability of vitamin E in virgin olive oil by agronomical and genetic factors. J. Food Compos. Anal. 23, 633-639. https://doi.org/10.1016/j.jfca.2010.03.003.

Beltrán G., Bejaoui M.A., Jimenez A., Sanchez-Ortiz A. (2015). Ethanol in Olive Fruit. Changes during Ripening. J. Agric. Food Chem. 63, 5309–5312, doi: 10.1021/acs.jafc.5b01453.

Benjamini Y., Hochberg Y. (1995). Controlling the false discovery rate: a practical and powerful approach to multiple testing. J. R. Stat. Soc. 57, 289-300.

Bergervoet J.H.W., Verhoeven H.A., Gilissen L.J.W., Bino R.J. (1996). High amounts of nuclear DNA in tomato (Lycopersicon esculentum Mill.) pericarp. Plant Sci. 116: 141-145.

Bergh O. (1985). Effect of the previous crop on cortical cell number of Malus Domestica cv. 'Starking Delicious' apple flower primordia, flowers and fruit. S. Afr. J. Plant Soil 2, 191–196

Bergougnoux V. (2014). The history of tomato: from domestication to biopharming. Biotechnol. Adv. 32, 170–189

Bertin N. (2005). Analysis of the tomato fruit growth response to temperature and plant fruit load in relation to cell division, cell expansion and DNA endoreduplication. Ann. Bot. 295, 439-447.

Bertin N., Borel C., Brunel B., Cheniclet C., Causse M. (2003). Do genetic make-up and growth manipulation affect tomato fruit size by cell number, or cell size and DNA endoreduplication. Ann. Bot. 92, 415–424

Besnard G., García-Verdugo C., De Casas R., Treier U.A., Galland N., Vargas P. (2008). Polyploidy in the olive complex (Olea europaea): Evidence from flow cytometry and nuclear microsatellite analyses. Ann. Bot. 101, 25-30.

Bianco L., Alagna F., Baldoni L., Finnie C., Svensson B., Perrotta G. (2013). Proteome regulation during Olea europaea fruit development. PLoS ONE 10.1371/journal.pone.0053563.

Bianco L., Perrotta G. (2016). Fruit development and ripening: Proteomic as an approach to study Olea europaea and other non-model organisms. In Agricultural Proteomics Volume 1: Crops, Horticulture, Farm Animals, Food, Insect and Microorganisms; Springer, Cham. pp. 53–65, ISBN 9783319432755.

Biton I., Doron-Faigenboim A., Jamwal M., Mani Y., Eshed R., Rosen A., Sherman A., Ophir R., Lavee S., Avidan B. (2015). Development of a large set of SNP markers for assessing phylogenetic relationships between the olive cultivars composing the Israeli olive germplasm collection. Mol. Breed. 35, doi:10.1007/s11032-015-0304-7.

Blanch G. P., Flores G., Gómez-Jiménez M. C., Castillo M. L. R. D. (2018a). Abscisic acid sprayed on olive tree (Olea europaea L.) affects the phenolic composition of olive fruit cultivars. J. Agric. Sci. 10, 37. https://doi.org/10.5539/jas.v10n4p37.

Blanch G. P., Flores G., Gómez-Jiménez M. C., Castillo M. L. R. D. (2018b). Effect of the treatment of the olive tree (Olea europaea L.) on the phenolic content and antioxidant properties in olive fruits. J. Food Nutr. Res. 6, 49-55. https://doi.org/10.12691/jfnr-6-1-8.

Blanch G. P., Gómez-Jiménez M. C., Ruiz Del Castillo M. L. (2020b). Variations in fatty acid composition and antioxidant content in olive fruits as a result of the application of phytoregulators to the olive tree (Olea europaea L.). CYTA J Food, 18, 76-83.

Blanch G.P., Gómez-Jiménez M.C., Ruiz del Castillo M.L. (2020a). Enrichment of Olive Fruits in Antioxidant Content by Pre-Harvest Salicylic Acid Treatment. Foods 9, 1513.

Bodanapu R., Gupta S.K., Basha P.O., Sakthivel K., Sadhana S., Sreelakshmi Y., Sharma R. (2016). Nitric oxide overproduction in tomato shr mutant shifts metabolic profiles and suppresses fruit growth and ripening. Front. Plant Sci. 7, 1714.

Bodoira R., Torres M., Pierantozzi P., Taticchi A., Servili M., Maestri D. (2015). Oil biogenesis and antioxidant compounds from "Arauco" olive (Olea europaea L.) cultivar during fruit development and ripening. Eur. J. Lipid Sci. Technol. 117, 377–388. doi: 10.1002/ejlt.201400234

Bollier N., Sicard A., Leblond J., Latrasse D., Gonzalez N., Gévaudant F., Benhamed M., Raynaud C., Lenhard M., Chevalier C., Hernould M., Delmas F. (2018). At-MINI ZINC FINGER2 and Sl-INHIBI-TOR OF MERISTEM ACTIVITY, a conserved missing link in the regulation of floral meristem termination in arabidopsis and tomato. Plant Cell 30, 83–100

Borbolla y Alcala, J.M.R., Fernandez Diez M.J., Gonzalez Pelliso F. (1955). Cambios en la composición de la aceituna durante su desarrollo. Grasas Aceites (Sevilla), 6: 5-22.

Boudolf V., Lammens T., Boruc J., Van Leene J., Van Den Daele H., Maes S., Van Isterdael G., Russinova E., Kondorosi E., Witters E., De Jaeger G., Inzé D., De Veylder L. (2009). CDKB1;1 forms a functional complex with CYCA2;3 to suppress endocycle onset. Plant Physiol. 150, 1482-1493. doi: 10.1104/pp.109.140269.

Bourdon M., Frangne N., Mathieu-Rivet E., Nafati M., Cheniclet C., Renaudin J.P., Chevalier C. (2010). Endoreduplication and growth of fleshy fruits. Progress in Botany 71, 101-132.

Breton C., Bervillé A. (2013). From the olive flower to the drupe: flower types, pollination, self and inter-compatibility and fruit set. In: Sladonja, B. (Ed.), The Mediterranean Genetic Code-Grapevine and Olive, InTech, doi:10.5772/55312

Briegas B., Corbacho J., Parra-Lobato M.C., Paredes M.A., Labrador J., Gallardo M., Gomez-Jimenez M.C. (2020). Transcriptome and hormone analyses revealed insights into hormonal and vesicle trafficking regulation among Olea europaea fruit tissues in late development. Int. J. Mol. Sci. 21:4819. doi:10.3390/ijms21144819

Brummell D.A. (2006). Cell wall disassembly in ripening fruit. Funct. Plant Biol. 33,103–119.

Bruno L., Chiappetta A., Muzzalupo I., Gagliardi C., Iaria D., Bruno A., Greco M., Giannino D., Perri E., Bitonti M. B. (2009). Role of geranylgeranyl reductase gene in organ development and stress response in olive (Olea europaea) plants. Funct. Plant Biol. 36, 370–381. doi: 10.1071/FP08219

Bruno L., Picardi E., Pacenza M., Chiappetta A., Muto A., Gagliardi O., Muzzalupo I., Pesole G., Bitonti M.B. (2019). Changes in gene expression and metabolic profile of drupes of Olea europaea L. cv Carolea in relation to maturation stage and cultivation area. BMC Plant. Biol. 19: 428. doi:10.1186/s12870-019-1969-6

Bulankova P., Akimcheva S., Fellner N., Riha K. (2013). Identification of Arabidopsis Meiotic Cyclins Reveals Functional Diversification among Plant Cyclin Genes. PLoS Genet. 9: e1003508. doi: 10.1371/journal.pgen.1003508

Bustan A., Avni A., Lavee S., Zipori I., Yeselson Y., Schaffer A.A., Riov J., Dag A. (2011). Role of carbohydrate reserves in yield production of intensively cultivated oil olive (Olea europaea L.) trees. Tree Physiology, 31 (5), pp. 519-530.

Bustan A., Avni A., Yermiyahu U., Ben-Gal A., Riov J., Erel R., Zipori I., Dag A. (2013). Interactions between fruit load and macroelement concentrations in fertigated olive (Olea europaea L.) trees under arid saline conditions. Scientia Horticulturae, 152, pp. 44-55.

Camarero M.C., Briegas B., Corbacho J., Labrador J., Gallardo M., Gomez-Jimenez M.C. (2023). Characterization of Transcriptome Dynamics during Early Fruit Development in Olive (Olea europaea L.). Int. J. Mol. Sci. 24, 961.

Camposeo S., Vivaldi G. A., Gattullo C. E. (2013). Ripening indices and harvesting times of different olive cultivars for continuous harvest. Sci. Hortic. 151, 1-10. https://doi.org/10.1016/j.scienta.2012.12.019.

Cantu D., Vicente A.R., Labavitch J.M., Bennett A.B., Powell A.L.T. (2008). Strangers in the matrix: plant cell walls and pathogen susceptibility. Trends Plant Sci. 13, 610–617.

Cao D., Wang J., Ju Z., Liu Q., Li S., Tian H., Fu D., Zhu H., Luo Y., Zhu B. (2016). Regulations on growth and development in tomato cotyledon, flower and fruit via destruction of miR396 with short tandem target mimic. Plant Sci. 247, 1-12.

Caponio F., Gomes T., Pasqualone A. (2001). Phenolic compounds in virgin olive oils: influence of the degree of olive ripeness on organoleptic characteristics and shelf-life. Eur. Food Res. Technol. 212, 329–333.

Carbone F., Bruno L., Perrotta G., Bitonti M.B., Muzzalupo I., Chiappetta A. (2019). Identification of miRNAs involved in fruit ripening by deep sequencing of Olea europaea L. transcriptome. PLOS ONE 14: e0223354. doi:10.1371/journal.pone.0221460

Carpita N.C., Gibeaut D.M. (1993). Structural models of primary cell walls in flowering plants: consistency of molecular structure with the physical properties of the walls during growth. Plant J. 3, 1–30.

Carrari F., Fernie A.R. (2006). Metabolic regulation underlying tomato fruit development. J. Exp. Bot. 57, 1883–1897.

Carrión Y., Ntinou M., Badal E. (2010). Olea europaea L. in the North Mediterranean Basin during the Pleniglacial and the Early-Middle Holocene. Quat Sci Rev 29: 952-968

Catalá C., Rose J.K., Bennett A.B. (2000). Auxin-regulated genes encoding cell wall-modifying proteins are expressed during early tomato fruit growth. Plant Physiol. 122, 527-534.

Cecchi L., Migliorini M., Cherubini C., Giusti M., Zanoni B., Innocenti M., Mulinacci N. (2013). Phenolic profiles, oil amount and sugar content during olive ripening of three typical Tuscan cultivars to detect the best harvesting time for oil production. Food Res. Int. 54, 1876–1884, doi: 10.1016/j.foodres.2013.04.033.

Chai L., Wang Z., Chai P., Chen S., Ma H. (2017). Transcriptome analysis of San Pedro-type fig (Ficus carica L.) parthenocarpic breba and non parthenocarpic main crop reveals divergent phytohormone-related gene expression. Tree Genet. Genomes, 13, 83.

Chai Y., Zhang Q., Tian L., Li C.L., Xing Y., Qin L., Shen Y. Y. (2013). Brassinosteroid is involved in strawberry fruit ripening. Plant Growth Regul. 69,63–69.

Chakrabarti M., Zhanga N., Sauvage C., Muños S., Blanca J., Cañizares J., Diez M. J., Schneidera R., Mazoureke M., McCleada J., Causse M., van der Knaap E. (2013). A cytochrome P450 regulates a domestication trait in cultivated tomato. Proc. Natl. Acad. Sci. U. S. A. 110, 17125–17130

Chen P., Takatsuka H., Takahashi N., Kurata R., Fukao Y., Kobayashi K., Ito M., Umeda M. (2017). Arabidopsis R1R2R3-Myb proteins are essential for inhibiting cell division in response to DNA damage. Nat. Commun. 8:635. doi:10.1038/s41467-017-00676-4

Chen S., Wang X. J., Tan G. F., Zhou W. Q., Wang G. L. (2020). Gibberellin and the plant growth retardant Paclobutrazol altered fruit shape and ripening in tomato. Protoplasma 257, 853-861.

Cheng G.W., Breen P.J. (1992). Cell count and cell size in relation to fruit size among strawberry cultivars. J. Amer. Soc. Hort. Sci. 117:946-950.

Cheniclet C., Rong W.Y., Causse M., Frangne N., Bolling L., Carde J.P., Renaudin J.P. (2005). Cell expansion and endoreduplication show a large genetic variability in pericarp and contribute strongly to tomato fruit growth. Plant Physiol. 139, 1984-1994.

Chevalier C., Bourdon M., Pirrello J., Cheniclet C., Gévaudant F., Frangne N. (2014). Endoreduplication and fruit growth in tomato: evidence in favour of the karyoplasmic ratio theory. J. Exp. Bot. 65, 2731-2746.

Chevalier C., Nafati M., Mathieu-Rivet E., Bourdon M., Frangne N., Cheniclet C., Renaudin J.P., Gvaudant F., Hernould M. (2011). Elucidating the functional role of endoreduplication in tomato fruit development. Ann. Bot. 107. 1159-1169.

Chu Y.H., Jang J.C., Huang Z., Van der Knaap E. (2019). Tomato locule number and fruit size controlled by natural alleles of lc and fas. Plant Direct 3, e00142

Chun J., Lee J., Ye L., Exler J., Eitenmiller R. R. (2006). Tocopherol and tocotrienol contents of raw and processed fruits and vegetables in the United States diet. J. Food Comp. Anal. 19, 196–204. doi: 10.1016/j.jfca.2005.08.001

Chung M.Y., Vrebalov J., Alba R., Lee J., McQuinn R., Chung J.D., Klein P., Giovannoni J. (2010). A tomato (Solanum lycopersicum) APETALA2/ERF gene, SlAP2a, is a negative regulator of fruit ripening. Plant J. 64, 936–947.

Cirilli M., Caruso G., Gennai C., Urbani S., Frioni E., Ruzzi M., Servili M., Gucci R., Poerio E., Muleo R. (2017). The role of polyphenoloxidase, peroxidase, and β-glucosidase in phenolics accumulation in Olea europaea L. Fruits under different water regimes Frontiers in Plant Science, 8, art. no. 717.

Clark S.E., Running M. P., Meyerowitz E. M. (1995). CLAVATA3 is a specific regulator of shoot and floral meristem development affecting the same processes as CLAVATA. Development 121, 2057-2067

Coelho J., Almeida-Trapp M., Pimentel D., Soares F., Reis P., Rego C., Mithöfer A., Fortes A. M. (2019). The study of hormonal metabolism of Trincadeira and Syrah cultivars indicates new roles of salicylic acid, jasmonates, ABA and IAA during grape ripening and upon infection with Botrytis cinerea. Plant Science 283, 266-277.

Coimbra M.A., Waldron K.W., Delgadillo I., Selvendran R.R. (1996). Effect of processing on cell wall polysaccharides of green table olives. J. Agric. Food Chem. 44, 2394–2401.

Concha C. M., Figueroa N. E., Poblete L. A., Oñate F. A., Schwab W., Figueroa C. R. (2013). Methyl jasmonate treatment induces changes in fruit ripening by modifying the expression of several ripening genes in Fragaria chiloensis fruit. Plant Physiol. Biochem. 70, 433-444. https://doi.org/10.3389/fpls.2020.00538.

Conde C., Delrot S., Gero H. (2008). Physiological, biochemical and molecular changes occurring during olive development and ripening. J. Plant Physiol. 165, 1545-1562. doi: 10.1016/j.jplph.2008.04.018

Cong B., Liu J., Tanksley S. D. (2002). Natural alleles at a tomato fruit size quantitative trait locus differ by heterochronic regulatory mutations. Proc. Natl. Acad. Sci. U. S. A. 99, 13606–13611

Cong B., Tanksley S.D. (2006). FW2. 2 and cell cycle control in developing tomato fruit: a possible example of gene co-option in the evolution of a novel organ. Plant Mol. Biol. 62, 867-880

Cong L., Yue R., Wang H., Liu J., Zhai R., Yang J., Wu M., Si M., Zhang H., Yang C., Xu L., Wang Z. (2019). 2,4-D-induced parthenocarpy in pear is mediated by enhancement of GA (4) biosynthesis. Physiol. Plant. 166, 812–820.

Connor DJ., Fereres E. (2005). The physiology of adaptation and yield expression in olive. Hortic Rev. 31: 155-229

Contreras C., Mariotti R., Mousavi S., Baldoni L., Guerrero C., Roka L., Cultrera N., Pierantozzi P., Maestri D., Gentili L., Tivani M., Torres M. (2020). Characterization and validation of olive FAD and SAD gene families: Expression analysis in different tissues and during fruit development. Mol. Biol. Rep. 47, 4345–4355.

Corbacho J., Inês C., Paredes M.A., Labrador J., Cordeiro A.M., Gallardo M., Gomez-Jimenez M.C. (2018). Modulation of sphingolipid long-chain base composition and gene expression during early olive-fruit development, and putative role of brassinosteroid. J Plant Physiol. 231, 383-392.

Corley S.B., Carpenter R., Copsey L., Coen E. (2005). Floral asymmetry involves an interplay between TCP and MYB transcription factors in Antirrhinum. Proc. Natl. Acad. Sci. U. S. A. 102, 5068–5073

Costagli G., Gucci R., Rapoport H. F. (2003). Growth and development of olive fruits (cv. 'Frantoio') under irrigated and rainfed conditions. J. Hortic. Sci. Biotechnol. 78, 119–124.

Crane J.C. (1964). Growth Substances in Fruit Setting and Development. Annu. Rev. Plant. Physiol. 15, 303–326

Crisosto C.H., Kader A.A. (2005). Olive postharvest quality maintenance guidelines. Univ. Calif. Fresh Prod. Factsheet 1, 1-6.

Cruz F., Julca I., Gómez-Garrido J., Loska D., Marcet Houben M., Cano E., Galán B., Frias L., Ribeca P., Derdak S., Sánchez-Fernández M., García J. L., Gut I. G., Vargas P., Alioto T. S., Gabaldón T. (2016). Genome sequence of the olive tree, Olea europaea. Gigascience 5, 29, doi:10.1186/s13742-016-0134-5.

Cruz-Castillo JG., Lawes GS., Woolley DJ. (1991). The influence of the time of anthesis, seed factors, and the application of a growth regulator mixture on the growth of kiwifruit. Acta Horticulturae 297, 475–480. doi:10.17660/ActaHortic.1992.297.62

Csukasi F., Donaire L., Casañal A., Martínez-Priego L., Botella M. A., Medina-Escobar N., Llave C., Valpuesta V. (2012). Two strawberry miR159 family members display developmental-specific expression patterns in the fruit receptacle and cooperatively regulate Fa-GAMYB. New Phytologist. 195, 47-57. https://doi.org/10.1111/j.1469-8137.2012.04134.x.

Csukasi F., Osorio S., Gutierrez J.R., Kitamura J., Giavalisco P., Nakajima M., Fernie A. R., Rathjen J. P., Botella M. A., Valpuesta V., Medina-Escobar N. (2011). Gibberellin biosynthesis and signalling during development of the strawberry receptacle. New Phytol. 191, 376–390.

Cunha S.C., Ferreira I.M.P.L.V.O., Fernandes J.O., Faria M.A., Beatriz M., Oliveira P.P., Ferreira M.A. (2001). Determination of lactic, acetic, succinic, and citric acids in table olives by HPLC/UV. J. Liq. Chrom. Relat. Tech. 24 (7), 1029–1038.

Czerednik A., Busscher M., Bielen B. A. M., Wolters-Arts M., De Maagd R. A., Angenent G. C. (2012). Regulation of tomato fruit pericarp development by an interplay between CDKB and CDKA1 cell cycle genes. J. Exp. Bot. 63, 2605–2617

Dag A., Kerem Z., Yogev N., Zipori I., Lavee S., Ben-David E. (2011). Influence of time of harvest and maturity index on olive oil yield and quality. Sci. Hortic. 127, 358–366

Dağdelen A., Tümen G., Özcan M.M., Dündar E. (2013). Phenolics profiles of olive fruits (Olea europaea L.) and oils from Ayvalik, Domat and Gemlik varieties at different ripening stages. Food Chem. 136, 41–45.

De Jong M., Mariani C., Vriezen W. H. (2009). The role of auxin and gibberellin in tomato fruit set. J. Exp. Bot. 60, 1523–1532

De Jong M., Wolters-Arts M., Feron R., Mariani C., Vriezen W.H. (2009). The Solanum lycopersicum auxin response factor 7 (SlARF7) regulates auxin signaling during tomato fruit set and development. Plant J. 57, 160-170.

De Jong M., Wolters-Arts M., Schimmel B. C. J., Stultiens C. L. M., De Groot P. F. M., Powers S. J., Tikunov Y. M., Bovy A. G., Mariani C., Vriezen W. H., Rieu I. (2015). Solanum lycopersicum AUXIN RESPONSE FACTOR 9 regulates cell division activity during early tomato fruit development. J. Exp. Bot. 66, 3405–3416

De la Rosa R., Angiolillo A., Rallo L., Guerrero C., Pellegrini M., Besnard G., Bervillé A., Martin A., Baldoni L. (2003). A first genetic linkage map of olive (Olea europaea L.) cultivars using RAPD and AFLP markers. Theor. Appl. Genet. 106, 1273–1282

De la Rosa R., Lorenzo L., Moreno I., Barranco D., Rallo L. (2008). Ripening time and fruit characteristics of advanced olive selections for oil production. Australian Journal of Agricultural Research 59, 46-51.

De la Rosa R., Talhaoui N., Rouis H., Velasco L., León L. (2013). Fruit characteristics and fatty acid composition in advanced olive breeding selections along the ripening period. Food Res. Int. 54, 1890-1896. https://doi. org/10.1016/j.foodres.2013.08.039.

De Veylder L., Beeckman T., Inzé D. (2007). The ins and outs of the plant cell cycle. Nat. Rev. Mol. Cell Biol. 8, 655–665

De Veylder L., Larkin J.C., Schnittger A. (2011). Molecular control and function of endoreplication in development and physiology. Trends Plant. Sci. 16, 624-634. doi: 10.1016/j.tplants.2011.07.001.

Deborde C., Moing A., Roch L., Jacob D., Rolin D., Giraudeau P. (2017). Plant metabolism as studied by NMR spectroscopy. Prog. Nucl. Mag n. Reson. Spectrosc.102–103, 61–97.

Denne M. P. (1960). The growth of apple fruitlets, and the effect of early thinning on fruit development. Ann. Bot. 24, 397–406

Devoghalaere F., Doucen T., Guitton B., Keeling J., Payne W., Ling T. J., Ross J. J., Hallett I. C., Gunaseelan K., Dayatilake GA., Diak R., Breen K. C., Tustin D. S., Costes E., Chagné D., Schaffer J., David K. M. (2012). A genomics approach to understanding the role of auxin in apple (Malus x domestica) fruit size control. BMC Plant Biol. 12,7.

Di Donna L., Mazzotti F., Naccarato A., Salerno R., Tagarelli A., Taverna D., Sindona G. (2010). Secondary metabolites of Olea europaea leaves as markers for the discrimination of cultivars and cultivation zones by multivariate analysis. Food Chem.121, 492–496, doi: 10.1016/j.foodchem.2009.12.070.

Dolan L., Davies J. (2004). Cell expansion in roots. Curr Opin Plant Biol 7: 33–39

Dolezel J., Greilhuber J., Suda J. (2007). Estimation of nuclear DNA content in plants using flow cytometry. Nature Protocols 2, 2233-2244.

Donaire J.P., Sanchez-Raya A.J., Lopez-Gorge J., Recalde, L. (1977). Etudes physiologiques et biochimiques de olive. I. Variation de la concentration de divers metabolites pendant son cycle evoluti£ Agrochimica, 21: 311-321.

Donaire J.P., Sanchez-Raya A.J., Lopez-Gorge J., Recalde, L., (1975). Metabolic changes in fruit and leaf during ripening in the olive. Phytochemistry, 14:1167-1169.

Dreyer I., Uozumi N. (2011). Potassium channels in plant cells. FEBS J. 278, 4293-4303. doi:10.1111/j.1742-4658.2011. 08371.x

Dubravka Škevin., Desanka Rade., Dubravka Štrucelj., Željko Mokrovšak., Sandra Neđeral., Đani Benčić. (2003). The influence of variety and harvest time on the bitterness and phenolic compounds of olive oil. European Journal of Lipid Science and Techonology 105, 536-541

Ebrahimzadeh H., Motamed N., Rastgar-Jazt F., Montasser-Kouhsai S., Shokrap E. H. (2003). Oxidative enzyme activities and soluble protein content in leaves and fruits of olives during ripening. J. Food Biochem. 27, 181–196

Edgar BA., Orr-Weaver T.L. (2001). Endoreplication cell cycles. Cell 105, 297-306. doi: 10.1016/S0092-8674(01)00334-8.

El-Sharkawy I., El Kayal W., Prasath D., Fernández H., Bouzayen M., Svircev A.M., Jayasankar S. (2012). Identification and genetic characterization of a gibberellin 2-oxidase gene that controls tree stature and reproductive growth in plum. J. Exp. Bot. 63, 1225-1239. https://doi.org/10.1093/jxb/err345.

El-Sharkawy I., Kim W.S., Jayasankar S., Svircev A.M., Brown D.C.W. (2008). Differential regulation of four members of the ACC synthase gene family in plum. J. Exp. Bot. 59, 2009–2027.

El-Sharkawy I., Sherif S., Abdulla M., Jayasankar S. (2017). Plum fruit development occurs via gibberellin-sensitive and-insensitive DELLA repressors. PLoS One, 12, e0169440.

El-Sharkawy I., Sherif S., El Kayal W., Mahboob A., Abubaker K., Ravindran P., Jyothi-Prakash P.A., Kumar P.P., Jayasankar S. (2014). Characterization of gibberellin-signalling elements during plum fruit ontogeny defines the essentiality of gibberellin in fruit development. Plant Mol. Biol. 84, 399-413.

Encuesta de Superficies y Rendimientos de cultivos (ESYRCE 2019). Ministerio de Agricultura, Pesca y Alimentación

Ergönül P.G., Nergiz C. (2010). Determination of organic acids in olive fruit by HPLC. Czech. J. Food Sci. 28 (3), 202–205.

Esteve C., Cañas B., Moreno-Gordaliza E., Del Río C., García M.C., Marina M.L. (2011). Identification of olive (Olea europaea) pulp proteins by matrix-assisted laser desorption/ionization time-of-flight mass spectrometry and nano-liquid chromatography tandem mass spectrometry. J. Agric. Food Chem. 59, 12093–12101, doi:10.1021/jf203363q.

Esti M., Cinquanta L., Notte E. L. (1998). Phenolic compounds in different olive varieties. Journal of Agricultural and Food Chemistry. 46: 32–35.

Ezer D., Shepherd S.J.K., Brestovitsky A., Dickinson P., Cortijo S., Charoensawan V., Box M.S., Biswas S., Jaeger K.E., Wigge P.A. (2017). The G-Box transcriptional regulatory code in Arabidopsis. Plant Physiology 175, 628-640. doi:10.1104/pp.17.01086.

Fabbri A., Bartolini G., Lambardi M., Kailis S. G. (2004). Olive Propagation Manual. Landlinks, Collingwood, Vic

Fan D., Wang W., Hao Q., Jia W. (2022). Do non-climacteric fruits share a common ripening mechanism of hormonal regulation. Front. Plant Sci. 13, 923484. https://doi.org/10.3389/fpls.2022.923484.

FAO (2023). Dirección de Estadística

Farinati S., Forestan C., Canton M., Galla G., Bonghi C., Varotto S. (2021). Regulation of fruit growth in a peach slow ripening phenotype. Genes. 12: 482. doi: 10.3390/genes12040482

Farmer E.E., Goossens A. (2019). Jasmonates: What ALLENE OXIDE SYNTHASE does for plants. J. Exp. Bot. 70, 3373-3378.

Fenn M. A., Giovannoni J. J. (2021). Phytohormones in fruit development and maturation. Plant J. 105, 446-458.

Fernandez A.I., Viron N., Alhagdow M., Karimi M., Jones M., Amsellem Z., Sicard A., Czerednik A., Angenent G., Grierson D., May S., Seymour G., Eshed Y., Lemaire-Chamley M., Rothan C., Hilson P. (2009). Flexible tools for gene expression and silencing in tomato. Plant Physiol. 151, 1729–1740

Fernandez-Bolanos J., Fernandez Diez M.J., Rivas Moreno M., Gil Serrano A. (1982). Azúcares y polioles en aceitunas verdes. II. Identification y determinación cuantitativa por cromatografía sobre papel. Grasas Aceites (Sevilla), 4: 208-211.

Fernandez-Bolanos J., Fernandez Diez M.J., Rivas Moreno M., Gil Serrano A., Perez Romero T. (1983). Azucares y polioles en aceitunas verdes. III. Determinacion cuantitativa por cromatografia gas líquido. Grasas Aceites (Seville), 3: 168-171.

Fernández-Cuesta A., León L., Velasco L., De la Rosa R. (2013). Changes in squalene and sterols associated with olive maturation. Food Res. Int. 54, 1885–1889, doi: 10.1016/j.foodres.2013.07.049.

Fernández-Escobar R., De la Rosa R., León L., Gómez J.A., Testi F., Orgaz F., Gil-Ribes J.A., Quesada-Moraga E., Trapero A., Msallmen M. (2012). Sistemas de Producción en Olivicultura. Olivae 118; pp. 55-68

Fletcher J.C. (1999). Signaling of cell fate decisions by CLAVATA3 in Arabidopsis shoot meristems. Science 283, 1911–1914

Fontanazza G. (1993). Mechanised Intensive Olive Growing. Calderini, Bologna, Italy, pp 1È312.

Fontanesi F., Soto I.C., Barrientos A. (2008). Cytochrome c oxidase biogenesis: new levels of regulation. IUBMB Life 60, 557-568.

Forlani S., Masiero S., Mizzotti C. (2019). Fruit ripening: the role of hormones, cell wall modifications, and their relationship with pathogens. J. Exp. Bot. 70, 2993–3006.

Fos M., Proaño K., Nuez F., García-Martínez J.L. (2001). Role of gibberellins in parthenocarpic fruit development induced by the genetic system pat-3/pat-4 in tomato. Physiol. Plant. 111, 545-550

Franken P., Schrell S., Peterson P.A., Saedler H., Wienand U. (1989). Molecular analysis of protein domain function encoded by the myb homologous maize genes C1, Zm1 and Zm38. Plant J. 6, 21-30.

Frary A. (2000). fw2.2: a quantitative trait locus key to the evolution of tomato fruit size. Science 289, 85–88

Fu F.Q., Mao W.H., Shi K., Zhou Y.H., Asami T., Yu J.Q. (2008). A role of brassinosteroids in early fruit development in cucumber. J. Exp. Bot. 59, 2299-2308.

Fu L., Niu B., Zhu Z., Wu S., Li W. (2012). CD-HIT: accelerated for clustering the next generation sequencing data. Bioinformatics, 28, 3150-3152. doi:10.1093/bioinformatics/bts565.

Fuentes L., Figueroa C.R., Valdenegro M. (2019). Recent advances in hormonal regulation and cross-talk during non-climacteric fruit development and ripening. Horticulturae 5(2):45.

Furuya T., Saito M., Uchimura H., Satake A., Nosaki S., Miyakawa T., Shimadzu S., Yamori W., Tanokura M., Fukuda H., Kondo Y. (2021). Gene co-expression network analysis identifies BEH3 as a stabilizer of secondary vascular development in Arabidopsis. The Plant Cell 33, 2618-2636. doi: 10.1093/plcell/koab151.

Gahan P. B. (1984). Plant Histochemistry and Cytochemistry. Academic Press: London. UK.

Galanakis C.M. (2011). Olive fruit dietary fiber: components, recovery and applications. Trends Food Sci. Technol. 22, 175–184.

Galla G., Barcaccia G., Ramina A., Collani S., Alagna F., Baldoni L., Cultrera N. G., Martinelli F., Sebastiani L., Tonutti P. (2009). Computational annotation of genes differentially expressed along olive fruit development. BMC Plant Biol 9:128.

Gao J., Zhang Y., Li Z., Liu M. (2020). Role of ethylene response factors (ERFs) in fruit ripening. Food Qual. Saf. 4,15–20.

Garcia J.M., Yousfi K. (2005). Non-destructive and objective methods for the evaluation of the maturation level of olive fruit. Eur. Food Res. Technol. 221, 538–541.

García P., Brenes M., Romero C., Garrido A. (1995). Respiration and physicochemical changes in harvested olive fruits. J. Hortic. Sci. 70, 925-933. https://doi.org/10.1080/14620316.1995.11515368.

García-Hurtado N., Carrera E., Ruiz-Rivero O., López-Gresa M. P., Hedden P., Gong F., García-Martínez J. L. (2012). The characterization of transgenic tomato overexpressing gibberellin 20-oxidase reveals induction of parthenocarpic fruit growth, higher yield, and alteration of the gibberellin biosynthetic pathway. J. Exp. Bot. 63, 5803-5813.

Garrido-Bigotes A., Figueroa C.R., Figueroa P.M. (2018). Jasmonate metabolism and its relationship with abscisic acid during strawberry fruit development and ripening. J. Plant Growth Regul. 37, 101–113.

Génard M., Reich M., Lobit R. P., Besset J. (1999). Correlations between sugar and acid content and peach growth. J. Hortic. Sci. Biotechnol. 74, 772–776.

Georgiadou E. C., Ntourou T., Goulas V., Manganaris G. A., Kalaitzis P., Fotopoulos V. (2015). Temporal analysis reveals a key role for VTE5 in vitamin E biosynthesis in olive fruit during on-tree development. Front. Plant Sci. 6:871. doi: 10.3389/fpls.2015.00871

Georgiadou E.C., Goulas V., Ntourou T., Manganaris G.A., Kalaitzis P., Fotopoulos V. (2016). Regulation of on-tree vitamin E biosynthesis in olive fruit during successive growing years: The impact of fruit development and environmental cues. Frontiers in Plant Science, 7 (NOVEMBER2016), art. no. 1656.

Ghorbani S., Fernandez A., Hilson P., Beeckman T. (2014). Signaling peptides in plants. Cell Dev. Biol. 3: 141.

Ghorbani S., Hoogewijs K., Pečenková T., Fernandez A., Inzé A., Eeckhout D., Kawa D., De Jaeger G., Beeckman T., Madder A., Van Breusegem F., Hilson P. (2016). The SBT6.1 subtilase processes the GOLVEN1 peptide controlling cell elongation. J. Exp. Bot. 67, 4877-4887.

Gil-Amado J. A., Gomez-Jimenez M.C. (2013). Transcriptome analysis of mature fruit abscission control in olive. Plant Cell Physiol 54(2):244–269.

Gillaspy G., Ben-David H., Gruissem W. (1993). Fruits: a developmental perspective. Plant Cell 5, 1439–1451

Giovannoni J. J. (2004). Genetic regulation of fruit development and ripening. Plant Cell 16: 170–180.

Giovannoni J., Nguyen C., Ampofo B., Zhong S., Fei Z. (2017). The epigenome and transcriptional dynamics of fruit ripening. Annu. Rev. Plant Biol. 68,61–84.

Gómez M.D., Vera-Sirera F., Pérez- Amador M. A. (2013). Molecular programme of senescence in dry and fleshy fruits. Journal of Experimental Botany, 65, 4515–4526

Gómez-Caravaca A. M., Bendini A., Cerretani L., Carretero A. S., Fernandez-Gutierrez A., Compagnone D., Del Carlo M., Cichelli A. (2008). Effects of fly attack (Bactrocera oleae) on the phenolic profile and selected chemical parameters of olive oil, J. Agric. Food Chem., 56, 4577–4583

Gómez-González S., Ruiz-Jiménez J., Luque De Castro M.D. (2011). Oil Content and Fatty Acid Profile of Spanish Cultivars During Olive Fruit Ripening. J. Am. Oil Chem. Soc., 88, 1737–1745, doi:10.1007/s11746-011-1840-x.

Gómez-Jimenez M. C., Paredes M. A., Gallardo M., Sanchez-Calle I.M. (2010). Mature fruit abscission is associated with up-regulation of polyamine metabolism in the olive abscission zone. J Plant Physiol 167(17):1432–1441.

Gómez-Jimenez M.C., Paredes M.A., Gallardo M., Fernandez-Garcia N., Olmos E., Sanchez-Calle I.M. (2010). Tissue-specific expression of olive S-adenosyl methionine decarboxylase and spermidine synthase genes and polyamine metabolism during flower opening and early fruit development. Planta 232, 629-647.

Gómez-Rico A., Salvador M. D., Moriana A., Pérez D., Olmedilla N., Ribas F., Fregapane G. (2007). Influence of different irrigation strategies in a traditional Cornicabra cv. olive orchard on virgin olive oil composition and quality. Food Chemistry 100: 568–578.

Gouthu S., Deluc L. G. (2015). Timing of ripening initiation in grape berries and its relationship to seed content and pericarp auxin levels. BMC Plant Biol. 15, 1-16. https://doi.org/10.1186/s12870-015-0440-6.

Grandillo S., Ku H.M., Tanksley S.D. (1999). Identifying the loci responsible for natural variation in fruit size and shape in tomato. Theor. Appl. Genet. 99, 978–987

Green P.S. (2002). A revision of Olea L. (Oleaceae). Kew Bulletin, 57: 91-140

Groot S.P.C., Bruinsma J., Karssen C. M. (1987). The role of endogenous gibberellin in seed and fruit development of tomato: studies with a gibberellin-deficient mutant. Physiol. Plant. 71, 184–190

Gucci R., Caruso G., Sebastiani L. (2010). Seasonal changes in leaf nitrogen of olive trees grown under different irrigation regimes and crop level. Journal of Plant Nutrition, 33 (12), pp. 1849-1859.

Gucci R., Lodolini E. M., Rapoport, H. F. (2009). Water deficit-induced changes in mesocarp cellular processes and the relationship between mesocarp and endocarp during olive fruit development. Tree Physiol. 29, 1575–1585.

Gucci R., Lodolini E., Rapoport H. F. (2007). Productivity of olive trees with different water status and crop load. Journal of Horticultural Science and Biotechnology 82: 648–656

Guo M., Rupe M. A., Dieter J. A., Zou J., Spielbauer D., Duncan K. E., Howard R. J., Hou Z., Simmons C. R. (2010). Cell Number Regulator1 affects plant and organ size in maize: implications for crop yield enhancement and heterosis. Plant Cell 22, 1057–1073

Gupta K., Wani S. H., Razzaq A., Skalicky M., Samantara K., Gupta S., Pandita D., Goel S., Grewal S., Hejnak V., Shiv A., El-Sabrout A.M., Elansary H.O., Alaklabi A., Brestic M. (2022). Abscisic acid: Role in fruit development and ripening. Front. Plant Sci. 13, 856. https://doi.org/10.3389/fpls.2022.817500.

Gustafson F.G. (1936). Inducement of fruit development by growth-promoting chemicals. Proc. Natl. Acad. Sci. U. S. A. 22, 628–636

Gutiérrez F., Jimenez B., Ruiz A., Albi M. A. (1999). Effect of olive ripeness on the oxidative stability of virgin olive oil extracted from the varieties Picual and Hojiblanca and on the different components involved. Journal of Agricultural and Food Chemistry. 47: 121–127.

Gómez-Rico A., Fregapane G., Salvador M.D. (2008). Effect of cultivar and ripening on minor components in Spanish olive fruits and their corresponding virgin olive oils. Food Res. Int., 41 433-440. https://doi.org/10.1016/j.foodres.2008.02.003.

Hackbusch J., Richter K., Muller J., Salamini F., Uhrig J. F. (2005). A central role of Arabidopsis thaliana ovate family proteins in networking and subcellular localization of 3-aa loop extension homeodomain proteins. Proc. Natl. Acad. Sci. U. S. A. 102, 4908–4912

Hamada K., Hasegawa K., Kitajima A., Ogata T. (2008). The relationship between fruit size and cell division and enlargement in cultivated and wild persimmons. Journal of Horticultural Science & Biotechnology 83, 218–222. doi:10.1080/14620316.2008.11512372

Hammami S. B. M., Costagli G., Rapoport H. F. (2013). Cell and tissue dynamics of olive endocarp sclerification vary according to water availability. Physiol Plant 149:571–582

Hammami S. B. M., Manrique T., Rapoport H. F. (2011). Cultivar-based fruit size in olive depends on different tissue and cellular processes throughout growth. Scientia Horticulturae, 130:445-451

Hammami S. B. M., Rapoport H. F. (2012). Quantitative analysis of cell organization in the external region of the olive fruit. International Journal of Plant Sciences, 173: 993-1004

Hamze L.M., Trentacoste E.R., Searles P.S., Rousseaux C. (2022). Spring reproductive and vegetative phenology of olive (Olea europaea L.) cultivars at different air temperatures along a latitudinal-altitudinal gradient in Argentina. Sci. Hortic. 304, 111327 https://doi.org/10.1016/j.scienta.2022.111327.

Han Y. C., Kuang J. F., Chen J. Y., Liu X. C., Xiao Y. Y., Fu C. C., Wang J. N., Wu K. Q., Lu W. J. (2016). Banana transcription factor MaERF11 recruits histone deacetylase MaHDA1 and represses the expression of MaACO1 and expansins during fruit ripening. Plant Physiol. 171, 1070–1084.

Han Y., Chen C., Yan Z., Li J., Wang Y. (2019). The methyl jasmonate accelerates the strawberry fruits ripening process. Sci. Hortic. 249, 250-256. https://doi.org/10.1016/j.scienta.2019.01.061.

Hao Y., Oh E., Choi G., Liang Z., Wang Z. Y. (2012). Interactions between HLH and bHLH fac- tors modulate light-regulated plant development. Mol. Plant 5, 688–697

Harada T., Kurahashi W., Yanai M., Wakasa Y., Satoh T. (2005). Involvement of Cell Proliferation and Cell Enlargement in Increasing the Fruit Size of Malus Species. Sci. Hortic. 105, 447–456. [CrossRef]

Haralampidis K., Milioni D., Sanchez J., Baltrusch M., Heinz E., Hatzopoulos P. (1998). Temporal and transient expression of stearoyl-ACP carrier protein desaturase gene during olive fruit development. J. Exp. Bot. 49, 1661-1669.

Hassapidou M. N., Manoukas A. G. (1993). Tocopherol and tocotrienol compositions of raw table olive fruit. J. Sci. Food Agric. 61, 277–280. doi: 10.1002/jsfa.2740610223

Hatzopoulos P. (2015). A defence-related Olea europaea b-glucosidase hydrolyses and activates oleuropein into a potent protein cross-linking agent. J. Exp. Bot. 66, 2093–2106

Hatzopoulos P., Banilas G., Giannoulia K., Gazis F., Nikoloudakis N., Milioni D., Haralampidis K. (2002). Breeding, molecular markers and molecular biology of the olive tree. Eur. J. Lipid Sci. Technol. 104, 574-586.

Hernández L., Sicardo M.D., Arjona M. P.M., Martínez-Rivas J.M. (2019). Specialized Functions of Olive FAD2 Gene Family Members Related to Fruit Development and the Abiotic Stress Response. Plant Cell Physiol. 61, 427-441.

Hernández M. L., Mancha M., Martínez-Rivas J. M. (2005). Molecular cloning and characterization of genes encoding two microsomal oleate desaturases (FAD2) from olive. Phytochemistry 66, 1417–1426

Hernández M. L., Padilla M. N., Mancha M., Martínez-Rivas J. M. (2009). Expression analysis identifies FAD2-2 as the olive oleate desaturase gene mainly responsible for the linoleic acid content in virgin olive oil. J. Agric. Food Chem. 57, 6199–6206.

Hernández M. L., Padilla M. N., Sicardo M. D., Mancha M., Martínez-Rivas J. M. (2011). Effect of different environmental stresses on the expression of oleate desaturase genes and fatty acid composition in olive fruit. Phytochemistry 72, 178–187

Hernández M. L., Sicardo M. D., Arjona P. M., Martínez-Rivas, J. M. (2020). Specialized functions of olive FAD2 gene family members related to fruit development and the abiotic stress response. Plant Cell Physiol. 61, 427–441.

Hernández M. L., Sicardo M. D., Martínez-Rivas J. M. (2016). Differential contribution of endoplasmic reticulum and chloroplast &-3 fatty acid desaturase genes to the linolenic acid content of olive (Olea europaea) fruit. Plant Cell Physiol. 57, 138–151.

Hernández M.L., Sicardo M.D., Belaj A., Martínez-Rivas J.M. (2021). The oleic/linoleic acid ratio in olive (Olea europaea L.) fruit mesocarp is mainly controlled by OeFAD2-2 and OeFAD2-5 genes together with the different specificity of extraplastidial acyltransferase enzymes. Front Plant Sci. 12, 653997. https://doi.org/10.3389/fpls.2021.653997.

Hernández-Santana V., Perez-Arcoiza A., Gomez-Jimenez M.C., Diaz-Espejo A. (2021). Disentangling the link between leaf photosynthesis and turgor in fruit growth. Plant J. 107, 1788-1801. doi: 10.1111/tpj.15418

Hewezi T., Maier T.R., Nettleton D., Baum T.J. (2012). The Arabidopsis microRNA396-GRF1/GRF3 regulatory module acts as a developmental regulator in the reprogramming of root cells during cyst nematode infection. Plant Physiol. 159, 321-335. doi: 10.1104/pp.112.193649.

Heywood H.U. (1978). Flowering Plants of the World. Oxford University Press, London. 335 pp

Horiguchi G., Kim G. T., Tsukaya H. (2005). The transcription factor AtGRF5 and the transcription coactivator AN3 regulate cell proliferation in leaf primordia of Arabidopsis thaliana: control of leaf shape and size by AtGRF5 and AN3. Plant J. 43, 68–78

Hu J., Israeli A., Ori N., Sun T. (2018). The interaction between DELLA and ARF/IAA mediates crosstalk between gibberellin and auxin signaling to control fruit initiation in tomato. Plant Cell, 30, 1710–1728.

Hu Z., Lan S., Zhao N., Su N., Xue Q., Liu J., Deng Q., Yang J., Zhang M. (2019). Soft-X-irradiated pollens induce parthenocarpy in watermelon via rapid changes of hormone-signalings and hormonal regulation. Scientia Horticulturae (Amsterdam), 250, 317–328.

Huang H., Liu B., Liu L., Song S. (2017). Jasmonate action in plant growth and development. J. Exp. Bot. 68, 1349-1359.

Huang W., Peng S., Xian Z., Lin D., Hu G., Yang L., Ren M., Li Z. (2017). Overexpression of a tomato miR171 target gene SlGRAS24 impacts multiple agronomical traits via regulating gibberellin and auxin homeostasis. Plant Biotechnol. J. 15, 472–488

Hussain Q., Shi J., Scheben, A., Zhang J., Wang X., Liu G., Yan G., King G. J., Edwards D., Wang H. (2020). Genetic and signalling pathways of dry fruit size: targets for genome editing-based crop improvement. Plant Biotechnol. J. 18, 1124–1140.

Iaria D. L., Chiappetta A., Muzzalupo I. (2016). A de novo transcriptomic approach to identify flavonoids and anthocyanins "switch-off" in olive (Olea europaea L.) drupes at different stages of maturation. Front Plant Sci. 6, 1246.

Iaria D., Chiappetta A., Muzzalupo I. (2016). De Novo Transcriptome Sequencing of Olea europaea L. to Identify Genes Involved in the Development of the Pollen Tube. Scientific World Journal. doi: 10.1155/2016/4305252.

Inês C., Corbacho J., Paredes M.A., Labrador J., Cordeiro A.M., Gomez-Jimenez M.C. (2019). Regulation of sterol content and biosynthetic gene expression during flower opening and early fruit development in olive. Physiol. Plant. 167, 526-539.

Inês C., Parra-Lobato M.C., Paredes M.A., Labrador J., Gallardo M., Saucedo-García M., Gavilanes-Ruiz M., Gomez-Jimenez M.C. (2018). Sphingolipid distribution, content and gene expression during olive-fruit development and ripening. Front. Plant Sci. 9:28. doi:10.3389/fpls.2018.00028

Inglese P., Gullo G., Pace L.S., Ronzello G. (1999). Fruit growth, oil accumulation and ripening of the olive cultivar "Carolea" in relation to fruit density. – Acta Horticult. 474: 265-268.

Iqbal M.A., Khan M.A., Azam M., Bhatti M.I.N., Feroze M.A., Zulfiqar B., Umar H., Asif M. (2022). Seasonal Fluctuations of N, P and K in Leaves Influenced Nutrient Requirement During Fruit Development Stages in Different Olive Genotypes. Brazilian Archives of Biology and Technology, 65, art. no. e22210347.

Iqbal N., Khan N.A., Ferrante A., Trivellini A., Francini A., Khan M.I.R. (2017). Ethylene role in plant growth, development and senescence: interaction with other phytohormones. Front. Plant Sci. 8, 475.

Ito M., Araki S., Matsunaga S., Itoh T., Nishihama R., Machida Y., Doonan J.H., Watanabe A. (2001). G2/M-phase-specific transcription during the plant cell cycle is mediated by c-Myb-like transcription factors. Plant Cell 13, 1891-905. doi: 10.1105/tpc.010102.

Jia H., Xie Z., Wang C., Shangguan L., Qian N., Cui M., Liu Z., Zheng T., Wang M., Fang J. (2017). Abscisic acid, sucrose, and auxin coordinately regulate berry ripening process of the Fujiminori grape. Funct. Integr. Genom. 17, 441-457.

Jiang N., Gao D., Xiao H., Van der Knaap E. (2009). Genome organization of the tomato sun locus and characterization of the unusual retrotransposon Rider. Plant J. 60, 181–193

Jiménez-Ruiz J., Ramírez-Tejero J.A., Fernández-Pozo N., De la O Leyva-Pérez M., Yan H., De la Rosa R, Belaj A., Montes E., Rodríguez-Ariza M.O., Navarro F., Bautista Barroso J., Beuzón C. R., Valpuesta V., Bombarely A., Luque F. (2020). Transposon activation is a major driver in the genome evolution of cultivated olive trees (Olea europaea L.). Plant Genome 13, 1–19, doi:10.1002/tpg2.20010.

Joubès J., Phan T. H., Just D., Rothan C., Bergounioux C., Raymond P., Chevalier C. (1999). Molecular and biochemical characterization of the involvement of cyclin-dependent kinase CDKA during the early development of tomato fruit. Plant Physiol. 121, 857-869.

Joubès J., Walsh D., Raymond P., Chevalier C. (2000). Molecular characterization of the expression of distinct classes of cyclins during the early development of tomato fruit. Planta 211, 430-439.

Kafkaletou M., Fasseas C., Tsantili E. (2019). Increased firmness and modified cell wall composition by ethylene were reversed by the ethylene inhibitor 1-methylcyclopropene (1-MCP) in the non-climacteric olives harvested at dark green stage - Possible implementation of ethylene for olive quality. J. Plant Physiol. 238, 63-71. https://doi.org/10.1016/j.jplph.2019.05.006.

Kafkaletou M., Ouzounidou G., Tsantili E. (2021). Fruit ripening, antioxidants and oil composition in koroneiki olives (Olea europea l.) at different maturity indices Agronomy, 11 (1), art. no. 122.

Kanaoka M.M., Pillitteri L.J., Fujii H., Yoshida Y., Bogenschutz N.L., Takabayashi J., Zhu J.K., Torii K.U. (2008). SCREAM/ICE1 and SCREAM2 specify three cell-state transitional steps leading to Arabidopsis stomatal differentiation. Plant Cell 20, 1775-1785. doi: 10.1105/tpc.108.060848.

Kang C.Y., Darwish O., Geretz A., Shahan R., Alkharouf N., Liu, Z.C. (2013). Genome-scale transcriptomic insights into early-stage fruit development in woodland strawberry Fragaria vesca. Plant Cell 25, 1960-1978.

Kaniewski K., Van Campo E., Boiy T., Terral J.F., Khadari B., Besnard G. (2012). Primary domestication and early uses of the emblematic olive tree: palaeobotanical, historical and molecular evidence from the Middle East. Biol Rev 87: 885-899

Karagiannis E., Tanou G., Samiotaki M., Michailidis M., Diamantidis G., Minas I.S., Molassiotis A. (2016). Comparative Physiological and Proteomic Analysis Reveal Distinct Regulation of Peach Skin Quality Traits by Altitude. Front. Plant Sci. 7, 1689

Kende H., Bradford K.J., Brummell D.A., Cho H.T., Cosgrove D.J., Fleming A.J., Gehring C., Lee Y., McQueen-Mason S., Rose J.K.C., Laurentius A.C.J., Voesenek L.A.J. (2004). Nomenclature for members of the expansin superfamily of genes and proteins. Plant Mol. Biol. 55, 311-314.

Khew C. Y., Mori I. C., Matsuura T., Hirayama T., Harikrishna J. A., Lau E. T., Mercer Z.J.A., Hwang S. S. (2020). Hormonal and transcriptional analyses of fruit development and ripening in different varieties of black pepper (Piper nigrum). J. Plant Res. 133, 73-94. https://doi.org/10.1007/s10265-019-01156-0.

Khosravi A., Zucchini M., Giorgi V., Mancini A., Neri D. (2021). Continuous monitoring of olive fruit growth by automatic extensimeter in response to vapor pressure deficit from pit hardening to harvest Horticulturae, 7 (10), art. no. 349

Kim J., Lee J.G., Hong Y., Lee E.J. (2019). Analysis of eight phytohormone concentrations, expression levels of ABA biosynthesis genes, and ripening-related transcription factors during fruit development in strawberry. J. Plant Physiol. 239,52–60.

Kim J.H., Choi D., Kende H. (2003). The AtGRF family of putative transcription factors is involved in leaf and cotyledon growth in Arabidopsis. Plant J. 36, 94–104

Kim J.H., Tsukaya H. (2015). Regulation of plant growth and development by the GROWTH-REGULATING FACTOR and GRF-INTERACTING FACTOR duo. J. Exp. Bot. 66, 6093-6107.

King J.R. (1938). Morphological development of the fruit of the olive. Hilgardia, 11: 437- 458

Klee H.J., Giovannoni J.J. (2011). Genetics and Control of Tomato Fruit Ripening and Quality Attributes. In (Bassler, B.L., Lichten, M. and Schupbach, G., eds) Annual Review of Genetics, vol 45. Palo Alto: Annual Reviews, pp. 41–59.

Komaki S., Sugimoto K. (2012). Control of the plant cell cycle by developmental and environmental cues. Plant Cell Physiol. 53, 953-564. doi: 10.1093/pcp/pcs070.

Kondo S., Fukuda K. (2001). Changes of jasmonates in grape berries and their possible roles in fruit development. Sci. Hortic. 91, 275-288. https://doi.org/10.1016/S0304-4238(01)00271-0.

Kondo S., Yamada H., Setha S. (2007). Effect of jasmonates differed at fruit ripening stages on 1-aminocyclopropane-1-carboxylate (ACC) synthase and ACC oxidase gene expression in pears. J. Am. Soc. Hortic. Sci. 132, 120-125. https://doi.org/10.21273/JASHS.132.1.120.

Kou X., Feng Y., Yuan S., Zhao X., Wu C., Wang C., Xue Z. (2021). Different regulatory mechanisms of plant hormones in the ripening of climacteric and non-climacteric fruits: a review. Plant Mol. Biol. 1-21. https://doi.org/10.1007/s11103-021-01199-9.

Kovaleva L.V., Zakharova E.V., Voronkov A.S., Timofeeva G.V., Andreev, I.M. (2017). Role of abscisic acid and ethylene in the control of water transport-driving forces in germinating petunia male gametophyte. Russ. J. Plant Physiol. 64, 782–793.

Ku H.M., Grandillo S., Tanksley S. D. (2000). fs8.1, a major QTL, sets the pattern of tomato carpel shape well before anthesis. Theor. Appl. Genet. 101, 873–878

Kumar R., Khurana A., Sharma A.K. (2014). Role of plant hormones and their interplay in development and ripening of fleshy fruits. J. Exp. Bot. 65, 4561–4575.

Lamprecht M.R., Sabatini D.M., Carpenter A.E. (2007). CellProfiler: free, versatile software for automated biological image analysis. Biotechniques 42, 71-75.

Langmead B., Salzberg S.L. (2012). Fast gapped-read alignment with Bowtie 2. Nat. Methods 9, 357-359. doi: 10.1038/nmeth.1923.

Laux T., Mayer K. F., Berger J., Jurgens G. (1996). The WUSCHEL gene is required for shoot and floral meristem integrity in Arabidopsis. Development 122, 87–96

Lavee S. (1978). 'Kadesh' table olive. HortScience, 13: 62-63.

Lavee S. (1990). Aims, methods, and advances in breeding of new olive cultivars. Acta Hortic. 286, 23–36, doi:10.17660/ActaHortic.1990.286.1

Lavee S. (1996). Biology and physiology of the olive. In: World olive encyclopaedia. Madrid: IOOC

Lavee S., Hanoch E., Wodner M., Abramowitch H. (2007). The effect of predetermined deficit irrigation on the performance of cv. Muhasan olives (Olea europaea L.) in the eastern coastal plain of Israel. Scientia Horticulturae 112: 156–163

Lee G. B., Lee J. E., Lee J. H., Lee Y. J., Park Y. H., Choi Y. W., Son B. G., Kang N.J., Je I. l., Kang J. S. (2020). Phytohormone profiles of 'Seolhyang' and 'Maehyang' strawberry fruits during ripening. Hortic. Environ. Biotechnol. 61, 229-239. https://doi.org/10.1007/s13580-019-00213-w.

Lee S., Lee S., Yang K. Y., Kim Y. M., Park S. Y., Kim S. Y., Soh M. S. (2006). Overexpression of PRE1 and its homologous genes activates gibberellin-dependent responses in Arabidopsis thaliana. Plant Cell Physiol. 47, 591–600

Lemaire-Chamley M., Petit J., Garcia V., Just D., Baldet P., Germain V., Fagard M., Mouassite M., Cheniclet C., Rothan C. (2005). Changes in transcriptional profiles are associated with early fruit tissue specialization in tomato. Plant Physiol. 139, 750-769. doi:10.1104/pp.105.063719

Leng P., Yuan B., Guo Y. (2014). The role of abscisic acid in fruit ripening and responses to abiotic stress. J. Exp. Bot. 65, 4577–4588.

León L., De la Rosa R., Barranco D., Rallo, L. (2004). Ten years of olive breeding in Córdoba (Spain). Acta Hort. 663, 747–750

Li H., Handsaker B., Wysoker A., Fennell T., Ruan J., Homer N., Marth G., Abecasis G., Durbin R., 1000 Genome Project Data Processing Subgroup. (2009). The Sequence Alignment/Map format and SAM tools. Bioinform. 25, 2078-2079. doi: 10.1093/bioinformatics/btp352.

Li H., Wu H., Qi Q., Li H., Li Z., Chen S., Ding Q., Wang Q., Yan Z., Gai Y., Jiang X., Ding J., Gu T., Hou X., Richard M., Zhao Y., Li Y. (2019). Gibberellins play a role in regulating tomato fruit ripening. Plant Cell Physiol. 60, 1619-1629.

Li J., Wu Z., Cui L., Zhang T., Guo Q., Xu J., Jia L., Lou Q., Huang S., Li Z., Chen J. (2014). Transcriptome comparison of global distinctive features between pollination and parthenocarpic fruit set reveals transcriptional phytohormone cross-talk in cucumber (Cucumis sativus L.). Plant Cell Physiol. 55, 1325–1342.

Li M., Wang X., Li C., Li H., Zhang J., Ye Z. (2018). Silencing GRAS2 reduces fruit weight in tomato: GRAS2 is involved in fruit development. J. Integr. Plant Biol. 60, 498–513

Li M., Yu G., Cao C., Liu P. (2021a). Metabolism, signaling, and transport of jasmonates. Plant Commun. 2:100231.

Li Q., Luo S., Zhang L., Feng Q., Song L., Sapkota M., Xuan S., Wang Y., Zhao J., Van der knaap E., Chen X., Shen S. (2023). Molecular and genetic regulations of fleshy fruit shape and lessons from Arabidopsis and rice. Hortic. Res. 10,108.

Li S., Chen K., Grierson D. (2019). A critical evaluation of the role of ethylene and MADS transcription factors in the network controlling fleshy fruit ripening. New Phytol. 221, 1724–1741

Li S., Chen K., Grierson D. (2021). Molecular and hormonal mechanisms regulating fleshy fruit ripening. Cells 10, 1136.

Li S.B., Xie Z.Z., Hu C.G., Zhang J. Z. (2016a). A review of auxin response factors (ARFs) in plants. Front. Plant Sci. 7, 47.

Li T., Jiang Z., Zhang L., Tan D., Wei Y., Yuan H., Li T., Wang A. (2016b). Apple (Malus domestica) MdERF2 negatively affects ethylene biosynthesis during fruit ripening by suppressing MdACS1 transcription. Plant J. 88, 735–748.

Li Y.J., Yu Y., Liu X., Zhang X.S., Su Y.H. (2021b). The Arabidopsis MATERNAL EFFECT EMBRYO ARREST45 protein modulates maternal auxin biosynthesis and controls seed size by inducing AINTEGUMENTA. Plant Cell 33, 1907-1926.

Liao X., Li M., Liu B., Yan M., Yu X., Zi H., Liu R., Yamamuro C. (2018). Interlinked regulatory loops of ABA catabolism and biosynthesis coordinate fruit growth and ripening in woodland strawberry. Proc. Natl Acad. Sci. USA, 115, E11542–E11550.

Liljegren S.J., Roeder A.H., Kempin S.A., Gremski K., Østergaard L., Guimil S., Reyes D.K., Yanofsky M.F. (2004). Control of fruit patterning in Arabidopsis by INDEHISCENT. Cell 116, 843-853.

Liu J., Van Eck J., Cong B., Tanksley S. D. (2002). A new class of regulatory genes underlying the cause of pear-shaped tomato fruit. Proc. Natl. Acad. Sci. U. S. A. 99, 13302–13306

Liu K., Yuan C., Feng S., Zhong S., Li H., Zhong J., Shen C., Liu J. (2017). Genome-wide analysis and characterization of Aux/IAA family genes related to fruit ripening in papaya (Carica papaya L.). BMC Genom. 18, 351.

Liu L., Shao Z., Zhang M., Wang Q. (2015). Regulation of carotenoid metabolism in tomato. Mol. Plant. 8,28–39.

Liu S., Zhang Y., Feng Q., Quin L., Pan C., Tumbeh Lamin-Samu A., Lu G. (2018). Tomato AUXIN RESPONSE FACTOR 5 regulates fruit set and development via the mediation of auxin and gibberellin signaling. Sci. Rep. 8, 2971

Liu X., Guo L., Zhang J., Xue L., Luo Y., Rao G. (2021). Integrated analysis of fatty acid metabolism and transcriptome involved in olive fruit development to improve oil composition. Forests 12:1773. doi:10.3390/f12121773

Liu X., Kim Y. J., Muller R., Yumul R. E., Liu C., Pan Y., Cao X., Goodrich J., Chen X. (2011). AGAMOUS terminates floral stem cell maintenance in Arabidopsis by directly repressing WUSCHEL through recruitment of polycomb group proteins. Plant Cell 23, 3654–3670

Liu X., Xu T., Dong X., Liu Y., Liu Z., Shi Z., Wang Y., Qi M., Li T. (2016). The role of gibberellins and auxin on the tomato cell layers in pericarp via the expression of ARFs regulated by miRNAs in fruit set. Acta Physiol. Plant. 38.

Llop-Tous I., Barry C.S., Grierson D. (2000). Regulation of ethylene biosynthesis in response to pollination in tomato flowers. Plant Physiol. 123, 971–978.

López-García E., Benítez-Cabello A., Rodríguez-Gómez F., Martín-Arranz V., Garrido-Fernández A., Arroyo-López F.N. (2022). Influence of 1-Methylcyclopropene (1-MCP) on the Processing and Microbial Communities of Spanish-Style and Directly Brined Green Table Olive Fermentations. Fermentation. 8, 441.

Loureiro J. (2009). Flow cytometric approaches to study plant genomes. Ecosistemas 18, 103-108.

Loureiro J., Rodriguez E., Costa A., Santos C. (2007). Nuclear DNA content estimations in wild olive (Olea europaea L. ssp. europaea var. sylvestris Brot.) and Portuguese cultivars of O. europaea using flow cytometry. Genet. Resour. Crop. Evol. 54, 21-25.

Love M.I., Huber W., Anders S. (2014). Moderated estimation of fold change and dispersion for RNA-seq data with DESeq2. Genome Biol. 15, 550. doi: 10.1186/s13059-014-0550-8.

Lu W., Mao L., Chen J., Han X., Ren X., Ying T., Luo Z. (2018). Interaction of abscisic acid and auxin on gene expression involved in banana ripening. Acta Physiol. Plant. 40, 46.

Luo J., Zhou J.J., Zhang J.Z. (2018). Aux/IAA gene family in plants: molecular structure, regulation, and function. Int. J. Mol. Sci. 19,1

Luo W., Li Y., Sun Y., Lu L., Zhao Z., Zhou J., Li X. (2021). Comparative RNA-seq analysis reveals candidate genes associated with fruit set in pumpkin. Sci. Hortic. 288:110255. doi: 10.1016/j.scienta.2021.110255

Ma C., Li B., Wang L., Xu M., Lizhu E., Jin H., Wang Z., Ye J. (2019). Characterization of phytohormone and transcriptome reprogramming profiles during maize early kernel development. BMC Plant Biol. 19, 197.

MacAlister C.A., Ortiz-Ramírez C., Becker J. D., Feijó J. A., Lippman Z. B. (2016). Hydroxyproline O-arabinosyltransferase mutants oppositely alter tip growth in Arabidopsis thaliana and Physcomitrella patens. Plant J. 85, 193–208

Machado M., Felizardo C., Fernandes-Silva A.A., Nunes F.M., Barros A. (2013). Polyphenolic compounds, antioxidant activity and l-phenylalanine ammonia-lyase activity during ripening of olive cv. "Cobrançosa" under different irrigation regimes. Food Res. Int. 51, 412–421, doi: 10.1016/j.foodres.2012.12.056.

Machemer K., Shaiman O., Salts Y., Shabtai S., Sobolev I., Belausov E., Grotewold E., Barg R. (2011). Interplay of MYB factors in differential cell expansion, and consequences for tomato fruit development: FSM1, FSB1 and MYBI interactions control cell size. Plant J. 68, 337–350

Macheroux P., Schmid J., Amrhein N., Schaller A. (1999). A unique reaction in a common pathway: mechanism and function of chorismate synthase in the shikimate pathway. Planta 207, 325-334.

Magyar Z., Horváth B., Khan S., Mohammed B., Henriques R., De Veylder L., Bakó L., Scheres B., Bögre L. (2012). Arabidopsis E2FA stimulates proliferation and endocycle separately through RBR-bound and RBR-free complexes. EMBO J. 31:1480-93. doi: 10.1038/emboj.2012.13.

Mara C.D., Huang T., Irish V.F. (2010). The Arabidopsis floral homeotic proteins APETALA3 and PISTILLATA negatively regulate the BANQUO genes implicated in light signaling. Plant Cell 22, 690-702. doi: 10.1105/tpc.109.065946.

Mariotti L., Picciarelli P., Lombardi L., Ceccarelli N. (2011). Fruit-set and early fruit growth in tomato are associated with increases in indoleacetic acid, cytokinin, and bioactive gibberellin contents. J. Plant Growth Regul. 30, 405–415

Mariotti R., Cultrera N.G.M., Munoz-Diez C., Baldoni L., Rubini A. (2010). Identification of new polymorphic regions and differentiation of cultivated olives (Olea europaea L.) through platome sequence comparison. BMC Plant Biol 10:211.

Martin G. C., Ferguson L., Sibbett G. S. (2005). 'Flowering, pollination, fruiting, alternate bearing, and abscission', p. 49-54. In: Sibbett, G.S., Ferguson, L., Coviello, J.L., and Lindstrand, M. (Eds.). Olive Production Manual. University of California, Agriculture and Natural Resources, Oakland, California

Martinelli F., Basile B., Morelli G., d'Andria R., Tonutti P. (2012). Effects of irrigation on fruit ripening behavior and metabolic changes in olive. Sci. Hortic. 144, 201-207.

Martinelli F., Remorini D., Saia S., Massai R., Tonutti P. (2013). Metabolic profiling of ripe olive fruit in response to moderate water stress. Sci. Hortic. 159, 52–58, doi: 10.1016/j.scienta.2013.04.039.

Martinelli F., Tonutti P. (2012). Flavonoid metabolism and gene expression in developing olive (Olea europaea L.) fruit. Plant Biosyst. 146, 164-170. doi: 10.1080/11263504.2012.681320.

Martsinkovskaya A.I., Poghosyan Z.P., Haralampidis K., Murphy D.J., Hatzopoulos P. (1999). Temporal and spatial gene expression of cytochrome B5 during flower and fruit development in olives. Plant Mol. Biol. 40, 79-90

Mathieu-Rivet E., Gévaudant F., Sicard A., Salar S., Do P. T., Mouras A., Fernie A. R., Gibon Y., Rothan C., Chevalier C., Hernould M. (2010). Functional analysis of the anaphase promoting complex activator CCS52A highlights the crucial role of endo-reduplication for fruit growth in tomato: endo-reduplication and fruit growth in tomato. Plant J. 62, 727–741

Matthew A.F., Giovannoni J.J. (2021). Phytohormones in fruit development and maturation. The Plant Journal 105, 446–458

Mauxion J.P., Chevalier C., Gonzalez N. (2021). Complex cellular and molecular events determining fruit size. Trends Plant Sci. 26, 1023-1038. doi: 10.1016/j.tplants.2021.05.008

Maxie E. C., Catlin P. B., Hartmann H. T. (1960). Respiration and ripening of olive fruits. Proceedings Am. Soc. Hortic. Sci. 75, 275-91.

Mazzoni-Putman S. M., Brumos J., Zhao C., Alonso J. M., Stepanova A. N. (2021). Auxin interactions with other hormones in plant development. Cold Spring Harb. Perspect. Biol. 13, a039990.

McAtee P., Karim S., Schaffer R., David K. (2013). A dynamic interplay between phytohormones is required for fruit development, maturation, and ripening. Front. Plant Sci. 4, 79.

McGarry R., Ozga J.A., Reinecke D.M. (2001). Differences in fruit development among large- and small-fruited cultivars of saskatoon (Amelanchier alnifolia Nutt.). Journal of the American Society for Horticultural Science 126, 381–385. doi:10.21273/JASHS.126.4.381

McQuinn R.P., Gapper N.E., Gray A.G., Zhong S., Tohge T., Fei Z., Fernie A.R., Giovannoni J.J. (2020). Manipulation of ZDS in tomato exposes carotenoid- and ABA-specific effects on fruit development and ripening. Plant Biotechnol. J. 18, 2210–2224

Medjkouh L., Abderezak T., Alves R. C., Araújo M., Beatriz M., Oliveira P. P. (2016). Effect of Bactrocera oleae on phenolic compounds and antioxidant and antibacterial activities of two Algerian olive cultivars, Food Funct., 7, 4372–4378.

Medjkouh L., Tamendjari A., Alves R.C., Laribi R., Oliveira M.B.P.P. (2018). Phenolic profiles of eight olive cultivars from Algeria: Effect of: Bactrocera oleae attack Food and Function, 9 (2), pp. 890-897.

Michailidis M., Karagiannis E., Tanou G., Karamanoli K., Lazaridou A., Matsi T., Molassiotis A. (2017). Metabolomic and physicochemical approach unravel dynamic regulation of calcium in sweet cherry fruit physiology. Plant Physiol. Biochem., 116, 68–79

Montealegre C.; Esteve C.; García M.C.; García Ruiz C.; Marina M.L. (2014). Proteins in Olive Fruit and Oil. Crit. Rev. Food Sci. Nutr. 54, 611–624, doi:10.1080/10408398.2011.598639.

Moret M., Ramírez-Tejero J. A., Serrano A., Ramírez-Yera E., Cueva-López M. D., Belaj A., Luque F. (2023). Identification of genetic markers and genes putatively involved in determining olive fruit weight. Plants, 12(1), 155.

Morgan M., Shepherd L. (2019). AnnotationHub: Client to access Annotation- Hub resources. R package version 3.2.2. https://bioconductor.org/packages/release/bioc/html/AnnotationHub.html.

Moriana A., Orgaz F., Pastor M., Fereres E. (2003). Yield responses of a mature olive orchard to water deficits. Journal of the American Society for Horticultural Science 128: 425–431

Mougiou N., Trikka F., Trantas E., Ververidis F., Makris A., Argiriou A., Vlachonasios K.E. (2018). Expression of hydroxytyrosol and oleuropein biosynthetic genes are correlated with metabolite accumulation during fruit development in olive, Olea europaea, cv. Koroneiki. Plant Physiol. Biochem. 128, 41-49.

Mounet F., Moing A., Garcia V., Petit J., Maucourt M., Deborde C., Bernillon S., Le Gall G., Colquhoun I., Defernez M., Giraudel J.L., Rolin D., Rothan C., Lemaire-Chamley M. (2009). Gene and metabolite regulatory network analysis of early developing fruit tissues highlights new candidate genes for the control of tomato fruit composition and development. Plant Physiol. 149, 1505-1528.

Mousavi S., De la Rosa R., Moukhli A., El Riachy M., Mariotti R., Torres M., Pierantozzi P., Stanzione V., Mastio V., Zaher H., El Antari A., Ayoub S., Dandachi F., Youssef H., Aggelou N., Contreras C., Maestri D., Belaj A., Bufacchi M., Baldoni L., León L. (2019). Plasticity of fruit and oil traits in olive among different environments. Sci Rep 9, 16968. https://doi.org/10.1038/s41598-019-53169-3.

Mraicha F., Ksantini M., Zouch O., Ayadi M., Bouaziz M., Sayadi S. S. (2010). Effect of olive fruit fly infestation on the quality of olive oil from Chemlali, cultivar during ripening, Food Chem. Toxicol.,48, 3235–3241.

Mu Q., Huang Z., Chakrabarti M., Illa-Berenguer E., Liu X., Wang Y., Ramos A., Van der knaap E. (2017). Fruit weight is controlled by Cell Size Regulator encoding a novel protein that is expressed in maturing tomato fruits. PLoS Genet. 13, e1006930

Muños S., Ranc N., Botton E., Bérard A., Rolland S., Duffe P., Carretero Y., Le Paslier M. C., Delalande C., Bouzayen M., Brunel D., Causse M. (2011). Increase in tomato locule number is controlled by two single-nucleotide polymorphisms located near WUSCHEL. Plant Physiol. 156, 2244–2254

Muñoz-Mérida A., González-Plaza J.J., Cañada A., Blanco A.M., Del García-López M.C., Rodríguez J.M., Pedrola L., Sicardo M.D., Hernández M.L., De la Rosa R., Belaj A., Gil-Borja M., Luque F., Martínez-Rivas J.M., Pisano D.G., Trelles O., Valpuesta V., Beuzón C.R. (2013). De novo assembly and functional annotation of the olive (olea europaea) transcriptome. DNA Res 20(1):93–108.

Musseau C., Jorly J., Gadin S., Sorensen I., Deborde C., Bernillon S., Mauxion J. P., Atienza I., Moing A., Lemaire-Chamley M., Rose J. K. C., Chevalier C., Rothan C., Fernandez-Lochu L., Gévaudant F. (2020). The tomato guanylate-binding protein SlGBP1 enables fruit tissue differentiation by maintaining endopolyploid cells in a non-proliferative state. Plant Cell 32, 3188–3205

Muzzalupo I., Stefanizzi F., Perri E., Chiappetta A.A. (2011). Transcript Levels of CHL P Gene, Antioxidants and Chlorophylls Contents in Olive (Olea europaea L.) Pericarps: A Comparative Study on Eleven Olive Cultivars Harvested in Two Ripening Stages. Plant Foods Hum. Nutr. 66, 1–10

Nanos G.D., Agtsidou E., Sfakiotakis E. (2002). Temperature and propylene effects on ripening of green and black Conservolea olives. Hort Sci. 37, 1079-1081.

Nardozza S., Cooney J., Boldingh H.L., Hewitt K.G., Trower T., Jones D., Thrimawithana A.H., Allan A.C., Richardson A.C. (2020). Phytohormone and transcriptomic analysis reveals endogenous cytokinins affect kiwifruit growth under restricted carbon supply. Metabolites, 10, 23.

Nergiz C., Engez Y. (2000). Compositional variation of olive fruit during ripening. Food Chem. 69, 55–59.

Nergiz C., Ergönül P.G. (2009). Organic acid content and composition of the olive fruits during ripening and its relationship with oil and sugar. Sci. Hortic. 122, 216–220.

Niu E., Gao S., Hu W., Zhang C., Liu D., Shen G., Zhu S. (2022). Genome-Wide Identification and Functional Differentiation of Fatty Acid Desaturase Genes in Olea europaea L. Plants, 11 (11), art. no. 1415.

Niwa T., Suzuki T., Takebayashi Y., Ishiguro R., Higashiyama T., Sakakibara H., Ishiguro S. (2018). Jasmonic acid facilitates flower opening and floral organ development through the upregulated expression of SlMYB21 transcription factor in tomato. Biosci. Biotechnol. Biochem. 82, 292–303.

Nomoto Y., Takatsuka H., Yamada K., Nomoto Y., Takatsuka H., Yamada K., Suzuki T., Suzuki T., Huang Y., Latrasse D., An J., Gombos M., Breuer C., Ishida T., Maeo K., Imamura M., Yamashino T., Sugimoto K., Magyar Z., Bögre L., Raynaud C., Benhamed M., Ito M. (2022). A hierarchical transcriptional network activates specific CDK inhibitors that regulate G2 to control cell size and number in Arabidopsis. Nat. Commun. 13:1660. doi:10.1038/s41467-022-29316-2

Ofori P.A., Di Donato M., Geisler M., Matsumoto S., Otagaki S., Pengchao H., Shiratake K. (2018). Tomato ATP-binding cassette transporter SlABCB4 is involved in auxin transport in the developing fruit. Plants, 7, 65.

Ohyama K., Shinohara H., Ogawa-Ohnishi M., Matsubayashi Y. (2009). A glycopeptide regulating stem cell fate in Arabidopsis thaliana. Nat. Chem. Biol. 5, 578–580

Olmstead J.W., Iezzoni A.F., Whiting M.D. (2007). Genotypic Differences in Sweet Cherry Fruit Size Are Primarily a Function of Cell Number. J. Am. Soc. Hortic. Sci. 132, 697–703. [CrossRef]

Ozga J.A., Brenner M.L., Reinecke D.M. (1992). Seed effects on gibberellin metabolism in pea pericarp. Plant Physiol. 100,88–94

Pabón-Mora N., Litt A. (2011). Comparative anatomical and developmental analysis of dry and fleshy fruits of Solanaceae. Am. J. Bot. 98, 1415–1436

Pál M., Szalai G., Gondor O.K., Janda T. (2021). Unfinished story of polyamines: Role of conjugation, transport and light-related regulation in the polyamine metabolism in plants. Plant Sci. 308:110923. doi: 10.1016/j.plantsci.2021.110923.

Palma J.M., Freschi L., Rodriguez-Ruiz M., Gonzalez-Gordo S., Cor pas, F.J. (2019). Nitric oxide in the physiology and quality of fleshy fruits. J. Exp. Bot. 70, 4405–4417.

Palomo-Ríos E., Narváez I., Pliego-Alfaro F., Mercado J.A. (2021). Olive (Olea europaea L.) Genetic Transformation: Current Status and Future Prospects. Genes 12, 386

Pan Y., Liang X., Gao M., Liu H., Meng H., Weng Y., Cheng Z. (2017). Round fruit shape in WI7239 cucumber is controlled by two interacting quantitative trait loci with one putatively encoding a tomato SUN homolog. Theor. Appl. Genet. 130, 573–586

Pandolfini T., Molesini B., Spena A. (2007). Molecular dissection of the role of auxin in fruit initiation. Trends Plant Sci. 12, 327-329.

Paniagua C., Pačínková A., Jackson P., Dabravolski S., Riber W., Didi V., Houser J., Gigli-Bisceglia N., Wimmerová M., Budinská E., Hamann T., Hejatko J. (2017). Dirigent proteins in plants: modulating cell wall metabolism during abiotic and biotic stress exposure. J. Exp. Bot. 68, 3287-3301.

Panizzi L.; Scarpati M. L.; Oriente G. (1960). Gazzetta chimica Italiana. 90: 1149.

Parra R., Gomez-Jimenez M.C. (2020). Spatio-temporal immunolocalization of extensin protein and hemicellulose polysaccharides during olive fruit abscission. Planta 252, 32. https://doi.org/10.1007/s00425-020-03439-6.

Parra R., Paredes M.A., Labrador J., Nunes C., Coimbra M.A., Fernandez-Garcia N., Olmos E., Gallardo M., Gomez-Jimenez M.C. (2020). Cell wall composition and ultrastructural immunolocalization of pectin and arabinogalactan protein during Olea europaea L. fruit abscission. Plant. Cell Physiol. 61, 814-825.

Parra R., Paredes M.A., Sanchez-Calle I.M., Gomez-Jimenez M.C. (2013). Comparative transcriptional profiling analysis of olive ripe fruit pericarp and abscission zone tissues shows expression differences and distinct patterns of transcriptional regulation. BMC Genom. 9:866. doi: 10.1186/1471-2164-14-866

Parra-Lobato M.C., Delgado-Martínez F.J., Gomez-Jimenez M.C. (2012). Morphological traits and RAPD markers for characterization and identification of minor Spanish olive cultivars from the Extremadura region. Genet. Mol. Res. 11, 2401-2411

Parra-Lobato M.C., Gomez-Jimenez M.C. (2011). Polyamine-induced modulation of genes involved in ethylene biosynthesis and signalling pathways and nitric oxide production during olive mature fruit abscission. J Exp Bot 62(13):4447–4465.

Parra-Lobato M.C., Paredes M.A., Labrador J., Saucedo-García M., Gavilanes-Ruiz M., Gomez-Jimenez M.C. (2017). Localization of sphingolipid enriched plasma membrane regions and long-chain base composition during mature-fruit abscission in olive. Front. Plant Sci. 8, 1138.

Parvini F., Sicardo M. D., Hosseini-Mazinani M., Martínez-Rivas J. M., Hernández M. L. (2016). Transcriptional analysis of stearoyl-acyl carrier protein desaturase genes from olive (Olea europaea) in relation to the oleic acid content of the virgin olive oil. J. Agric. Food Chem. 64, 7770–7781.

Parvini F., Zeinanloo A.A., Ebrahimie E., Tahmasebi-Enferadi S., Hosseini-Mazinani M. (2015). Differential expression of fatty acid desaturases in Mari and Shengeh olive cultivars during fruit development and ripening. Eur. J. Lipid Sci. Technol. 117, 523-531.

Pattison R.J., Catalá C. (2012). Evaluating auxin distribution in tomato (Solanum lycopersicum) through an analysis of the PIN and AUX/LAX gene families. Plant J. 70, 585–598.

Pattison R.J., Csukasi F., Catalá C. (2014). Mechanisms regulating auxin action during fruit development. Physiol. Plant. 151:62-72. doi: 10.1111/ppl.12142.

Pattison R.J., Csukasi F., Zheng Y., Fei Z., Van der Knaap E., Catalá C. (2015). Comprehensive tissue-specific transcriptome analysis reveals distinct regulatory programs during early tomato fruit development. Plant Physiol. 168, 1684–1701.

Patumi M., Fontanazza G., Baldoni L., Brambilla I. (1990). Determination of some precursors of lipid biosynthesis in olive fruits during ripening. Acta Hortic. 286, 199–202.

Pećinar I., Quarrie S.P., Bertin N., Rančić D., Savić S., Jovanović Z., Stikić R. (2021). Tomato fruit development in response to different irrigation practices: developmental study of pericarp cell layers. Biol. Life Sci. Forum. 4:105. doi: 10.3390/IECPS2020-08855

Peragón J. (2013). Time course of pentacyclic triterpenoids from fruits and leaves of olive tree (Olea europaea L.) cv. Picual and cv. Cornezuelo during ripening. J. Agric. Food Chem. 61, 6671–6678

Perotti M. F., Posé D., Martín-Pizarro C. (2023). Non-climacteric fruit development and ripening regulation. The Phytohormones Show. J. Exp. Bot. erad271. https://doi.org/10.1093/jxb/erad271.

Phukan U.J., Jeena G.S., Tripathi V., Shukla R.K. (2017). Regulation of Apetala2/Ethylene response factors in plants. Front. Plant Sci. 8, 150.

Piga A., Del Caro A., Pinna I., Agabbio M. (2005). Anthocyanin and colour evolution in naturally black table olives during anaerobic processing. LWT - Food Science and Technology 38, 425-429.

Pirrello J., Deluche C., Frangne N., Gevaudant F., Maza E., Djari A., Bourge M., Renaudin J.P., Brown S., Bowler C., Zouine M., Chevalier C., Gonzalez N. (2018). Transcriptome profiling of sorted endoreduplicated nuclei from tomato fruits: how the global shift in expression ascribed to DNA ploidy influences RNA-Seq data normalization and interpretation. Plant J. 93,387-398. doi: 10.1111/tpj.13783

Poghosyan Z. P., Haralampidis K., Martsinkowskaya A. I., Murphy D. J., Hatzopoulos P. (1999). Developmental regulation and spatial expression of a plastidial fatty acid desaturase from Olea europaea. Plant Physiol. Biochem. 37, 109–119.

Ponce C., Kuhn N., Arellano M., Time A., Multari S., Martens S., Carrera E., Sagredo B., Donoso J.M., Meisel L.A. (2021). Differential phenolic compounds and hormone accumulation patterns between early- and mid-maturing sweet cherry (Prunus avium L.) cultivars during fruit development and ripening. J. Agric. Food Chem. 69, 8850-8860.

Proietti P. (2000). Effect of fruiting on leaf gas exchange in olive (Olea europaea L.). Photosynthetica 38: 397-402.

Proietti P., Famiani F., Tombesi A. (1999). Gas exchange in olive fruit. Photosynthetica, 36, 423-432.

Proietti P., Nasini L., Famiani F. (2006). Effect of different leaf-to-fruit ratios on photosynthesis and fruit growth in olive (Olea europaea L.). PHOTOSYNTHETICA 44 (2): 275-285

Puertas C.M., Trentacoste E.R., Morábito J.A., Perez Peña J. (2011). Effects of regulated deficit irrigation during stage III of fruit development on yield and oil quality of olive trees (Olea europaea L. 'Arbequina') Acta Horticulturae, 889, pp. 303-310.

Quinet M., Angosto T., Yuste-Lisbona F.J., Blanchard-Gros R., Bigot, S., Martinez J.P., Lutts S. (2019). Tomato fruit development and metabolism. Front. Plant Sci. 10:1554. doi:10.3389/fpls.2019.01554.

Rallo L., Barranco D., De la Rosa R., León L. (2008). 'Chiquitita' olive. HortScience 43, 529–531

Rallo L., Díez C.M., Morales-Sillero A., Mihoa H., Priego-Capote F., Rallo P. (2018). Quality of olives: A focus on agricultural preharvest factors. Sci. Hortic. 233, 491-509.

Rallo P., Rapoport H. (2001). Early growth and development of the olive fruit mesocarp. J. Hort. Sci. Biotechnol.76, 408-412.

Ramezani S., Shekafandeh A. (2009). Roles of gibberellic acid and zinc sulphate in increasing size and weight of olive fruit. African Journal of Biotechnology, 8 (24), pp. 6791-6794.

Ramin A.A. (2007). Effects of storage temperatures and 1-MCP treatment on postharvest quality of green olives. Fruits 62, 383-390. https://doi.org/10.1051/fruits:2007036.

Ramírez-Parra E., Gutierrez C. (2007). E2F regulates FASCIATA1, a chromatin assembly gene whose loss switches on the endocycle and activates gene expression by changing the epigenetic status. Plant Physiol. 144, 105-120. doi: 10.1104/pp.106.094979.

Ranalli A.; Tombesi A.; Ferrante M.L.; De Mattia G. (1998). Respiratory rate of olive drupes during their ripening cycle and quality of oil extracted. J. Sci. Food Agric. 77, 359–367.

Randall R.S., Miyashima S., Blomster T., Zhang J., Elo A., Karlberg A., Immanen J., Nieminen K., Lee J.Y., Kakimoto T., Blajecka K., Melnyk C.W., Alcasabas A., Forzani C., Matsumoto-Kitano M., Mähönen A.P., Bhalerao R., Dewitte W., Helariutta Y., Murray J.A.H. (2015). AINTEGUMENTA and the D-type cyclin CYCD3;1 regulate root secondary growth and respond to cytokinins. Biol. Open 4, 1229-1236. doi:10.1242/bio.013128

Rangel B., Platt K.A., Thomson W.W. (1997). Ultrastructural aspects of the cytoplasmic origin and accumulation of oil in olive fruit (Olea europaea). Physiologia Plantarum, 101: 109-114

Rao G., Sui J., Zhang J. (2016). Metabolomics reveals significant variations in metabolites and correlations regarding the maturation of walnuts (Juglans regia L.). Biol. Open 5, 829–836, doi:10.1242/bio.017863

Rao G., Zhang J., Liu X., Li X., Wang C. (2021). Combined metabolome and transcriptome profiling reveal optimal harvest strategy model based on different production purposes in olive. Foods 10, 360. https://doi.org/10.3390/foods10020360.

Rao G., Zhang J., Liu X., Lin C., Xin H., Xue L., Wang C. (2021). De novo assembly of a new Olea europaea genome accession using nanopore sequencing. Hortic. Res. 8, doi:10.1038/s41438-021-00498-y.

Rapoport H. F., Fabbri A., Sebastiani L. (2016). Olive Biology. The Olive Tree Genome book. DOI 10.1007/978-3-319-48887-5_2

Rapoport H. F., Perez-Lopez D., Hammami S. B. M. (2013). Fruit pit hardening: physical measurement during olive fruit growth. Ann Appl Biol 163:200–208

Rapoport H., Costagli G., Gucci R. (2004). The effect of water deficit during early fruit development on olive fruit morphogenesis. J. Amer. Soc. Hort. Sci. 129: (in press).

Reale L., Nasini L., Cerri M., Regni L., Ferranti F., Proietti P. (2019). The influence of light on olive (Olea europaea l.) fruit development is cultivar dependent. Frontiers in Plant Science, 10, art. no. 385.

Renaudin J. P., Cheniclet C., Rouyère V., Chevalier C., Frangne N. (2023). The cell pattern of tomato fruit pericarp is quantitatively and differentially regulated by the level of gibberellin in four cultivars. J. Plant Growth Regul. https://doi.org/10.1007/s00344-023-10978-1.

Renaudin J.P., Deluche C., Cheniclet C., Chevalier C., Frangne N. (2017). Cell layer-specific patterns of cell division and cell expansion during fruit set and fruit growth in tomato pericarp. J Exp Bot 68:1613–1623. https://doi.org/10.1093/jxb/erx058

Renau-Morata B., Carrillo L., Cebolla-Cornejo J., Molina R. V., Martí R., Domínguez-Figueroa J., Vicente-Carbajosa J., Medina J., Nebauer S. G., (2020). The targeted overexpression of SlCDF4 in the fruit enhances tomato size and yield involving gibberellin signalling. Sci. Rep. 10, 10645

Renau-Morata B., Molina R. V., Carrillo L., Cebolla-Cornejo J., Sánchez - Perales M., Pollmann S., Domínguez-Figueroa J., Corrales A. R., Flexas J., Vicente-Carbajosa J., Medina J., Nebauer S. G. (2017). Ectopic expression of CDF3 genes in tomato enhances biomass production and yield under salinity stress conditions. Front. Plant Sci. 8, 660

Richter J., Watson J.M., Stasnik P., Borowska M., Neuhold J., Berger M., Stolt-Bergner P., Schoft V., Hauser M.T. (2018). Multiplex mutagenesis of four clustered CrRLK1L with CRISPR/Cas9 exposes their growth regulatory roles in response to metal ions. Sci Rep. 8:12182. doi: 10.1038/s41598-018-30711-3.

Robinson D.O., Coate J.E., Singh A., Hong L., Bush M., Doyle J.J., Roeder A.H.K. (2018). Ploidy and Size at Multiple Scales in the Arabidopsis Sepal. Plant Cell 30, 2308-2329.

Rodrigues M.A., Ferreira I.Q., Claro A.M., Arrobas M. (2012). Fertilizer recommendations for olive based upon nutrients removed in crop and pruning. Sci. Hortic. 142: 205-11.

Rodríguez G.R., Muños S., Anderson C., Sim S. C., Michel A., Causse M., McSpadden Gardener B. B., Francis D., Van der Knaap E. (2011). Distribution of SUN, OVATE, LC, and FAS in the tomato germplasm and the relationship to fruit shape diversity. Plant Physiol. 156, 275–285

Romero-Segura C., García-Rodríguez R., Sánchez-Ortiz A., Sanz C., Pérez A.G. (2012). The role of olive β-glucosidase in shaping the profile of virgin olive oil. Food Research International 45(1): 191-196

Rosati A., Caporali S., Hammami S.B.M., Moreno-Alías I., Paoletti A., Rapoport H.F. (2011). Differences in ovary size among olive (Olea europaea L.) cultivars are mainly related to cell number, not to cell size. Scientia Horticulturae, 130:185-190

Rosati A., Caporali S., Hammami S.B.M., Moreno-Alías I., Rapoport H. (2020). Fruit growth and sink strength in olive (Olea europaea) are related to cell number, not to tissue size. Functional Plant Biology, 2020, 47, 1098–1104. https://doi.org/10.1071/FP20076

Rosati R., Caporali S., Hammami S., Moreno-Alías I., Paoletti A., Rapoport H.F. (2012). Tissue size and cell number in the olive (Olea europaea) ovary determine tissue growth and partitioning in the fruit. Functional Plant Biology 39(7):580-587. doi: 10.1071/FP12114

Rose J.K.C., Bennett A.B. (1999). Cooperative disassembly of the cellulose-xyloglucan network of plant cell walls: parallels between cell expansion and fruit ripening. Trends Plant Sci. 4, 176–183.

Rothan C., Diouf I., Causse M. (2019). Trait discovery and editing in tomato. Plant J. 97, 73–90

Rotondi A., Bendini A., Cerretani L., Mari M., Lercker G., Toschi T.G. (2004). Effect of Olive Ripening Degree on the Oxidative Stability and Organoleptic Properties of Cv. Nostrana di Brisighella Extra Virgin Olive Oil. J. Agric. Food Chem. 52, 3649–3654

Rugini E., Baldoni L., Silvestri C., Mariotti R., Narvaez I., Cultrera N., Cristofori V., Bashir M., Mousavi S., Palomo-Rios E. (2020). Olea europaea olive. In Litz, R.E., Pliego-Alfaro, F., Hormaza, J.I. (Eds.), Biotechnology of Fruit and Nut Crops, CAB International: Wallingford, UK.

Rugini E., Bongi G., Fontanazza G. (1982). Effects of Ethephon on Olive Ripening. J. Am. Soc. Hortic. Sci. 107, 835-838.

Rugini E., De Pace C., Gutiérrez-Pesce P., Muleo R. (2011). Olea. De: Kole, C. (editor). Wild crop relatives: genomic and breeding resources, temperate fruits. Springer-Verlag, Berlín, Heidelberg, pp. 79-117

Rugini E., Pannelli G., Ceccarelli M., Muganu M. (1996). Isolation of triploid and tetraploid olive (Olea europaea L.) plants from mixoploid cv. 'Frantoio' and 'Leccino' mutants by in vivo and in vitro selection. Plant. Breed. 115, 23-27.

Rugini E., Pezza A., Muganu M., Caricato G. (1995). Somatic embryogenesis in olive (Olea europaea L.). In Biotechnology in Agriculture and Forestry, Bajaj, Y.P.S., Ed.; Springer, Berlin, Volume 30, Somatic embryogenesis and synthetic seed I, pp. 404–414, doi:10.1007/978-3-662-03091-2_2

Sagar M., Chervin C., Mila I., Hao Y., Roustan J. P., Benichou M., Gibon Y., Biais B., Maury P., Latché A., Pech J.C., Bouzayen M., Zouine M. (2013). SlARF4, an auxin response factor involved in the control of sugar metabolism during tomato fruit development. Plant Physiol. (Rockville), 161, 1362–1374.

Salvador M. D., Aranda F., Fregapane G. (2001). Influence of fruit ripening on ''Cornicabra'' virgin olive oil quality. A study of four successive crop seasons. Food Chemistry. 73: 45–53.

Samuel D., Liu Y.J., Cheng C.S., Lyu P.C. (2002). Solution Structure of Plant Nonspecific Lipid Transfer Protein-2 from Rice (Oryza sativa). J. Biol. Chem. 277, 35267-35273. DOI 10.1074/jbc.M203113200.

Sánchez J. (1994). Lipid photosynthesis in olive fruit. Progr. Lipid Res. 33: 97-104.

Sánchez J., Harwood J.L. (2002). Biosynthesis of triacylglycerols and volatiles in olives. Eur J Lipid Sci Technol 2002; 104:564–73.

Sarri V., Baldoni L., Porceddu A., Cultrera N.G.M., Contento A., Frediani M., Belaj A., Trujillo I., Cionini P.G. (2006). Microsatellite markers are powerful tools for discriminating among olive cultivars and assigning them to geographically defined populations. Genome 49, 1606–1615

Sarrwy S.M.A., Mohamed E.A., Hassan H.A.S. (2010). Effect of foliar sprays with potassium nitrate and mono-potassium phosphate on leaf mineral contents, fruit set, yield and fruit quality of picual olive trees grown under sandy soil conditions. Am.-Eurasian J. of Agric. and Environ. Sci. 8(4): 420-30.

Scalisi A., Marino G., Marra F.P., Caruso T., Lo Bianco R. (2020). A Cultivar-Sensitive Approach for the Continuous Monitoring of Olive (Olea europaea L.) Tree Water Status by Fruit and Leaf Sensing. Frontiers in Plant Science, 11, art. no. 340.

Schneider C. (2005). Chemistry and biology of vitamin E. Mol. Nutr. Food Res. 49,7–30. doi: 10.1002/mnfr.200400049

Schoof H., Lenhard M., Haecker A., Mayer K.F., Jurgens G., Laux T. (2000). The stem cell population of Arabidopsis shoot meristems is maintained by a regulatory loop between the CLAVATA and WUSCHEL genes. Cell 100, 635–644

Scorzal R., May L.G., Purnell B., Upchurch B. (1991). Differences in number and area of mesocarp cells between small-and-large-fruited peach cultivars. Journal of the American Society for Horticultural Science 116, 861–864. doi:10.21273/JASHS.116.5.861

Seifi E., Guerin J., Kaiser B., Sedgley M. (2015). 'Flowering and fruit set in olive: a review'. Iranian Journal of Plant Physiology 5 (2), 1263-1272

Sen C. K., Khanna S., Roy S. (2007). Tocotrienols in health and disease: the other half of the natural vitamin E family. Mol. Aspects Med. 28, 692–728. doi: 10.1016/j.mam.2007.03.001

Serrani J.C., Sanjuán R., Ruiz-Rivero O., Fos M., García-Martínez, J.L. (2007). Gibberellin regulation of fruit set and growth in tomato. Plant Physiol. 145, 246-257. https://doi.org/10.1104/pp.107.098335.

Servili M., Esposto S., Lodolini E., Selvaggini R., Taticchi A., Urbani S., Montedoro G., Serravalle M., Gucci R. (2007). Irrigation effects on quality, phenolic composition, and selected volatiles of virgin olive oils cv. Leccino. Journal of Agricultural and Food Chemistry 55: 6609–6618.

Servili M., Sordini B., Esposto S., Taticchi A., Urbani S., Sebastiani L. (2016). Metabolomics of Olive Fruit: A Focus on the Secondary Metabolites. In The Olive Tree Genome; Springer: Cham. pp. 123–139

Seymour G. B., Chapman N. H., Chew B. L., Rose J. K. (2013). Regulation of ripening and opportunities for control in tomato and other fruits. Plant Biotechnology Journal, 11(3), 269-278.

Sezer F., Taşkin K.M. (2017). Molecular characterization of tocopherol biosynthesis genes from Olea europaea (L.) cv. Ayvalık Turkish Journal of Botany, 41 (6), pp. 559-568.

Shi M., Hu X., Wei Y., Hou X., Yuan X., Liu J., Liu Y. (2017). Genome wide profiling of small RNAs and degradome revealed conserved regulations of miRNAs on auxin-responsive genes during fruit enlargement in peaches. Int. J. Mol. Sci. 18, 2599

Shin J.H., Mila I., Liu M., Rodrigues M.A., Vernoux T., Pirrello J., Bouzayen M. (2019). The RIN-regulated Small Auxin-Up RNA SAUR69 is involved in the unripe-to-ripe phase transition of tomato fruit via enhancement of the sensitivity to ethylene. New Phytol. 222, 820–836.

Shin S., Lee J., Rudell D., Evans K., Zhu Y. (2016). Transcriptional regulation of auxin metabolism and ethylene biosynthesis activation during apple (Malus× domestica) fruit maturation. J. Plant Growth Regul. 35, 655-666. https://doi.org/10.1007/s00344-015-9568-8.

Shinozaki Y., Hao S., Kojima, M., Sakakibara H., Ozeki-Lida Y., Zheng Y., Fei Z., Zhong S., Giovannoni J. J., Rose J. K. C., Okabe Y., Heta Y., Ezura H., Ariizumi T. (2015). Ethylene suppresses tomato (Solanum lycopersicum) fruit set through modification of gibberellin metabolism. Plant J. 83, 237–251.

Shinozaki Y., Nicolas P., Fernandez-Pozo N., Ma Q., Evanich D. J., Shi Y., Xu Y., Zheng Y., Snyder S. I., Martin L. B. B., Ruiz-May E., Thannhauser T. W., Chen K., Domozych D. S., Catalá C., Fei Z., Mueller L. A., Giovannoni J. J., Rose J. K. C. (2018). High-resolution spatiotemporal transcriptome mapping of tomato fruit development and ripening. Nat. Commun. 9, 364.

Shu-e Y., Fang L., Xian-bi L., Qi-bin H., Yun-lan Z., Ming-yu H., Ting W., Sha-Sha D., Yan P., Ming L. (2015). Over-expression of GhDWF4 gene improved tomato fruit quality and accelerated fruit ripening. J. Integrat Agriculture, 14, 1980–1991.

Shulman Y., Erez A., Lavee S. (1974). Delay in the ripening of picked olives due to ethylene treatments. Scientia Hortic. 2, 21-27.

Shulman Y., Lavee S. (1976). Endogenous cytokinins in maturing Manzanillo olive fruits. Plant Physiol. 57, 490-492.

Shulman Y., Lavee S. (1980). Gibberellin-like substances during ripening of olive fruit. Sci. Hortic. 12, 169-175. https://doi.org/10.1016/0304-4238(80)90124-7.

Shulman Y., Lavee S.Y. (1979). Fruit development and maturation of olives as affected by treatments with auxins. Riv. Orto-florofrutt. ital. 63: 31-39.

Sicard A., Petit J., Mouras A., Chevalier C., Hernould M. (2008). Meristem activity during flower and ovule development in tomato is controlled by the mini zinc finger gene INHIBITOR OF MERISTEM ACTIVITY. Plant J. 55, 415–427

Skodra C., Titeli V.S., Michailidis M., Bazakos C., Ganopoulos I., Molassiotis A., Tanou G. (2021). Olive Fruit Development and Ripening: Break on through to the "-Omics" Side. Int. J. Mol. Sci 22, 5806.

Solinas M., Angerosa F., Marsilio V. (1988). Research on some flavour components of virgin olive oil in relation to olive variety. Riv Ital Sost Grasse 65 361-368.

Solinas M., Di Giovacchino L., Cucurachi A. (1975). Variations of some polyphenols of olive oil during the ripening cycle of olives. Note 1. Ann Ist Sper Elaiot 5 105-126.

Sotelo-Silveira M., Marsch-Martínez N., De Folter S. (2014). Unraveling the signal scenario of fruit set. Planta, 239, 1147-1158.

Stintzi A., Schaller A. (2022). Biogenesis of post-translationally modified peptide signals for plant reproductive development. Curr. Opin. Plant Biol. 102274. doi: 10.1016/j.pbi.2022.102274

Stiti N., Triki S., Hartmann M.A. (2007). Formation of triterpenoids throughout Olea europaea fruit ontogeny. Lipids 42:55–67.

Su L., Audran C., Bouzayen M., Roustan J. P., Chervin C. (2015). The Aux/IAA, Sl-IAA17 regulates quality parameters over tomato fruit development. Plant Signal. Behav. 10, e1071001

Su L., Bassa C., Audran C., Mila I., Cheniclet C., Chevalier C., Bouzayen M., Roustan J. P., Chervin C. (2014). The auxin Sl-IAA17 transcriptional repressor controls fruit size via the regulation of endoreduplication-related cell expansion. Plant Cell Physiol. 55, 1969–1976

Suehiro Y., Mochida K., Tsuma M., Yasuda Y., Itamura H., Esumi T. (2019). Effects of Abscisic Acid/Ethephon treatments on berry development and maturation in the yellow-green skinned "Shine Muscat" Grape. Horticulture J. 88, 189–201.

Sun L., Rodríguez G. R., Clevenger J. P., Illa-Berenguer E., Lin J., Blakeslee J. J., Liu W., Fei Z., Wijeratne A., Meulia T., Van der Knaap E. (2015). Candidate gene selection and detailed morphological evaluations of fs8.1, a quantitative trait locus controlling tomato fruit shape. J. Exp. Bot. 66, 6471–6482

Sun X., Cahill J., Hautegem T. V., Feys K., Whipple C., Novák O., Delbare S., Versteele C., Demuynck K., De Block J., Storme V., Claeys H., Van Lijsebettens M., Coussens G., Ljung K., De Vliegher A., Muszynski M., Inze D., Nelissen H. (2017). Altered expression of maize PLASTOCHRON1 enhances biomass and seed yield by extending cell division duration. Nat. Commun. 8, 14752

Swietlik D. (2002). Zinc Nutrition of Fruit Trees by Foliar Sprays. (International Symposium on Foliar Nutrition of Perennial Fruit Plants). Acta Hortic. 594.

Tadayon M.S., Hosseini S.M. (2022). Effect of Irrigation Regimes and Foliar Nutrition on Flower Development and Water Productivity of Olive (Olea europaea L. cv. 'Shengeh'). Journal of Plant Growth Regulation

Tadayon M.S., Hosseini S.M. (2022). Effect of Irrigation Regimes and Foliar Nutrition on Flower Development and Water Productivity of Olive (Olea europaea L. cv. 'Shengeh'). Journal of Plant Growth Regulation.

Tamendjari A., Angerosa F., Mettouchi S., Bellal M. M. (2009). The effect of fly attack (Bactrocera oleae) on the quality and phenolic content of Chemlal olive oil, Grasas Aceites 60, 507–513

Tani E., Tsaballa A., Stedel C., Kalloniati C., Papaefthimiou D., Polidoros A., Darzentas N., Ganopoulos I., Flemetakis E., Katinakis P., Tsaftaris A. (2011). The study of a SPATULA-like bHLH transcription factor expressed during peach (Prunus persica) fruit development. Plant Physiol. Biochem. 49:654-663.

Tanksley S. D. (2004). The genetic, developmental, and molecular bases of fruit size and shape variation in tomato. The plant cell, 16(suppl_1), S181-S189.

Tao X., Wu Q., Li J., Wang D., Nassarawa S. S., Ying T. (2021). Ethylene biosynthesis and signal transduction are enhanced during accelerated ripening of postharvest tomato treated with exogenous methyl jasmonate. Sci. Hortic. 281, 109965.

Tenhaken R. (2015). Cell wall remodeling under abiotic stress. Front. Plant Sci. 5 (771), 1–9.

Tenorio-Berrío R., Pérez-Alonso M.M., Vicente-Carbajosa J., Martín-Torres L., Dreyer I., Pollmann S. (2018). Identification of two auxin-regulated potassium transporters involved in seed maturation. Int. J. Mol. Sci. 19, 2132. doi:10.3390/ijms19072132

The H. F., Neoh B. K., Wong Y. C., Kwong Q. B., Ooi T. E. K., Ng T. L. M., Tiong S.H., Low J.Y.S., Danial A.D., Ersad M.A., Kulaveerasingam H., Appleton D. R. (2014). Hormones, polyamines, and cell wall metabolism during oil palm fruit mesocarp development and ripening. J. Agric. Food Chem. 62, 8143-8152.

Thompson J., Higgins D., Gibson T. (1994). CLUSTAL W: improving the sensitivy of progressive multiple sequence through sequence weighting, position-specific gap penalties and weight matrix choice. Nucl. Acids Res. 22, 4673-4680

Tieman D., Zeigler M., Schmelz E., Taylor M.G., Rushing S., Jones J.B., Klee H.J. (2010). Functional analysis of a tomato salicylic acid methyl transferase and its role in synthesis of the flavor volatile methyl salicylate. Plant J. 62, 113–123.

Tindall H.D. (2002). Classification, origin, diffusion and history of the olive. Food & Agriculture Org., Rome, Italy

Tombesi A., Pilli M., Boco M., Proietti P. (1994). Evolution of olive fruit respiration, photosynthesis and oil composition during ripening. Acta Hortic. 356, 278-283.

Trentacoste E. R., Gómex-del-Campo M., Rapoport H. F. (2016). Olive fruit growth, tissue development and composition as affected by irradiance received in different hedgerow positions and orientations. Sci. Hortic. 198, 284–293.

Trentacoste E., Puertas C., Sadras V.O. (2012). Modelling the intraspecific variation in the dynamics of fruit growth, oil and water concentration in olive (Olea europaea L.). Eur. J. Agron. 38, 83-93.

Tsantili E., Pontikis C. (2004). Response to ethylene and its interactive effect with N6-benzyladine (BA) in harvested green olives during ripening. Post. Biol. Technol. 33, 153-162.

Tsukaya H. (2019). Re-examination of the role of endoreduplication on cell-size control in leaves. J. Plant Res. 132, 571-580. doi:10.1007/s10265-019-01125-7

Tuck K.L., Hayball P.J. (2002). Major phenolic compounds in olive oil: Metabolism and health effects. J. Nutr. Biochem. 13, 636–644.

Uceda M., Frias L. (1975). Evolution of the fruit oil content, oil composition and oil quality. In Proceedings of the International Olive Oil Council, Cordoba, Spain, 6–17 October; pp. 125–130.

Unver T., Wu Z., Sterck L., Turktas M., Lohaus R., Li Z., Yang M., He L., Deng T., Escalante F.J. (2017). Genome of wild olive and the evolution of oil biosynthesis. Proc. Natl. Acad. Sci. USA 114, E9413 E9422, doi:10.1073/pnas.1708621114.

Valitova J. N., Sulkarnayeva A. G., Minibayeva F. V. (2016). Plant sterols: diversity, biosynthesis, and physiological functions. Biochem. 81, 819-834. doi:10.1134/S0006297916080046

Van der Knaap E., Chakrabarti M., Chu Y. H., Clevenger J. P., Illa-Berenguer E., Huang Z., Keyhaninejad N., Mu Q., Sun L., Wang Y., Wu S. (2014). What lies beyond the eye: the molecular mechanisms regulating tomato fruit weight and shape. Front. Plant Sci. 5, 227

Van der Knaap E., Lippman Z. B., Tanksley S. D. (2002). Extremely elongated tomato fruit controlled by four quantitative trait loci with epistatic interactions. Theor. Appl. Genet. 104, 241–247

Vanhaeren H., Nam Y.J., De Milde L., Chae E., Storme, V., Weigel D., Gonzalez N., Inzé D. (2017). Forever Young: The role of ubiquitin receptor DA1 and E3 Ligase BIG BROTHER in controlling leaf growth and development. Plant Physiol. 173, 269-1282. doi: 10.1104/pp.16.01410

Vásquez A., Graciani E., Maestro R. (1974). Grasas Aceites 25: 269.

Vercruysse J., Van Bel M., Osuna-Cruz C., Kulkarni S. R., Storme V., Nelissen H., Gonzalez N., Inzé D., Vandepoele K. (2020). Comparative transcriptomics enables the identification of functional orthologous genes involved in early leaf growth. Plant Biotechnol. J. 18, 553–567

Vicente A.R., Saladié M., Rose J.K.C., Labavitch J.M. (2007). The linkage between cell wall metabolism and fruit softening: looking to the future. J. Sci. Food Agric. 87, 1435–1448.

Vilanova L., Vall-Llaura N., Torres R., Usall J., Teixidó N., Larrigaudière C., Giné-Bordonaba J. (2017). Penicillium expansum (compatible) and Penicillium digitatum (non-host) pathogen infection differentially alter ethylene biosynthesis in apple fruit. Plant Physiol. Biochem. 120, 132–143.

Villarreal N.M., Nardi C.F., Civello P.M., Martínez G.A. (2016). Novel insights of ethylene role in strawberry cell wall metabolism. Plant Sci. 252, 1–11.

Vinha A.F., Ferreres F., Silva B.M., Valentão P., Gonçalves A., Pereira J.A., Oliveira M.B., Seabra R.M., Andrade P.B. (2005). Phenolic profiles of Portuguese olive fruits (Olea europaea L.): Influences of cultivar and geographical origin. Food Chem. 89, 561–568.

Vlahov G. (1976). Organic acids of olives: malic acid/citric acid ratio as a maturation index. Ann Ist Sper Elaiot 6, 93-110.

Wahl V., Brand L. H., Guo Y. L., Schmid M. (2010). The FANTASTIC FOUR proteins influence shoot meristem size in Arabidopsis thaliana. BMC Plant Biol. 10, 285

Wang H., Gong J., Su X., Li L., Pang X., Zhang Z. (2017a). MaCDPK7, a calcium-dependent protein kinase gene from banana is involved in fruit ripening and temperature stress responses. J Horticult. Sci. Biotechnol. 92, 240–250.

Wang H., Jones B., Li Z., Frasse P., Delalande C., Regad F., Chaabouni S., Latché A., Pech J. C., Bouzayen M. (2005). The Tomato Aux/IAA transcription factor IAA9 is involved in fruit development and leaf morphogenesis. Plant Cell, 17, 2676–2692.

Wang H., Schauer N., Usadel B., Frasse P., Zouine M., Hernould M., Latché A., Pech J.J., Fernie A.R., Bouzayen M. (2021). Regulatory features underlying pollination-dependent and -independent tomato fruit set revealed by transcript and primary metabolite profiling. Plant Cell 21, 1428-1452.

Wang L., Tang W., Hu Y., Zhang Y., Sun J., Guo X., Lu H., Yang Y., Fang C., Niu X., Yue J., Fei Z., Liu Y. (2019b). A MYB/bHLH complex regulates tissue-specific anthocyanin biosynthesis in the inner pericarp of red-centered kiwifruit Actinidia chinensis cv. Hongyang. Plant J. 99, 359-378. doi: 10.1111/tpj.14330

Wang P., Lu S., Zhang X., Hyden B., Qin L., Liu L., Bai Y., Han Y., Wen Z., Xu J., Cao H., Chen H. (2021). Double NCED isozymes control ABA biosynthesis for ripening and senescent regulation in peach fruits. Plant Sci. 304, 110739.

Wang R., Tavano E.C.D.R., Lammers M., Martinelli A.P., Angenent G.C., De Maagd R.A. (2019). Re-evaluation of transcription factor function in tomato fruit development and ripening with CRISPR/Cas9-mutagenesis. Sci. Rep. 9, 1696.

Wang W., Scali M., Vignani R., Spadafora A., Sensi E., Mazzuca S., Cresti M. (2003). Protein extraction for two-dimensional electrophoresis from olive leaf, a plant tissue containing high levels of interfering compounds. Electrophoresis 24, 2369–2375

Wang W., Tai F., Hu X. (2010). Current Initiatives in Proteomics of the Olive Tree. In Olives and Olive Oil in Health and Disease Prevention; Academic Press, pp. 25–32

Wang W., Vignani R., Scali M., Sensi E., Tiberi P., Cresti M. (2004). Removal of lipid contaminants by organic solvents from oilseed protein extract prior to electrophoresis. Anal. Biochem. 329, 139–141

Wang W., De-Dios-Alché J., Castro A.J., Rodríguez-García M.I. (2001). Characterization of seed storage proteins and their synthesis during seed development in Olea europaea. Int. J. Dev. Biol. 45, 63–64.

Wang X., Aguirre L., Rodríguez-Leal D., Hendelman A., Benoit M., Lippmann Z.B. (2021). Dissecting cis-regulatory control of quantitative trait variation in a plant stem cell circuit. Nat. Plants 7, 419–427

Wang X., Ding Y., Wang Y., Pan L., Niu L., Lu Z., Cui G., Zeng W., Wang, Z. (2017b). Genes involved in ethylene signal transduction in peach (Prunus persica) and their expression profiles during fruit maturation. Sci. Hortic. 224, 306–316.

Wang X., Yin W., Wu J., Chai L., Yi H. (2016). Effects of exogenous abscisic acid on the expression of citrus fruit ripening-related genes and fruit ripening. Sci. Hortic. 201, 175-183.

Wang Y., Clevenger J.P., Illa-Berenguer E., Meulia T., Van der Knaap E., Sun L. (2019a). A comparison of sun, ovate, fs8.1 and auxin application on tomato fruit shape and gene expression. Plant Cell Physiol. 60, 1067-1081.

Wang Y., Ding G., Gu T., Ding J., Li Y. (2017). Bioinformatic and expression analyses on carotenoid dioxygenase genes in fruit development and abiotic stress responses in Fragaria vesca. Mol. Genet. Genomics 292, 895-907. https://doi.org/10.1007/s00438-017-1321-5.

Wei J., Wen X., Tang L. (2017). Effect of methyl jasmonic acid on peach fruit ripening progress. Sci. Hortic. 220, 206-213.

Weijers D., Benkova E., Jager K. E., Schlereth A., Hamann T., Kientz M., Wilmoth J. C., Reed J.W., Jurgens G. (2005). Developmental specificity of auxin response by pairs of ARF and Aux/IAA transcriptional regulators. EMBO J. 24, 1874–1885

Weimer A.K., Biedermann S., Harashima H., Roodbarkelari F., Takahashi N., Foreman J., Guan Y., Pochon G., Heese M., Van Damme D., Sugimoto K., Koncz C., Doerner P., Umeda M., Schnittger A. (2016). The plant-specific CDKB1-CYCB1 complex mediates homologous recombination repair in Arabidopsis. EMBO J. 35, 2068-2086.

Whale S., Singh Z., Janes J. (2004). Ethylene biosynthesis and fruit color development in 'Pink Lady' apples during growth and maturation. HortScience, 39, 762C–762.

Wittwer S.H., Bukovac M. J., Sell H. M., Weller L. E. (1957). Some effects of gibberellin on flowering and fruit setting. Plant Physiol. 32, 39–41

Wodner M., Lavee S., Epstain E., (1987). Identification and seasonal changes of glucose, fructose and mannitol in relation to oil accumulation during development in Olea europaea (L.). Sci. Hortic. 36, 45–54

Wodner M., Lavee S., Epstein E. (1988). Identification and seasonal changes of glucose, fructose and mannitol in relation to oil accumulation during fruit development in Olea europaea (L.). Sci. Hort. 36, 47–54.

Wong D. C. J., Lopez Gutierrez R., Dimopoulos N., Gambetta G. A., Castellarin S. D. (2016). Combined physiological, transcriptome, and cis-regulatory element analyses indicate that key aspects of ripening, metabolism, and transcriptional program in grapes (Vitis vinifera L.) are differentially modulated accordingly to fruit size. BMC genomics 17, 416. https://doi.org/10.1186/s12864-016-2660-z.

Wu S. C., Zhang Y. (2011). Cyclin-dependent kinase 1 (CDK1)-mediated phosphorylation of Enhancer of Zeste 2 (Ezh2) regulates its stability. J. Biol. Chem. 286, 28511-28519.

Wu S., Clevenger J. P., Sun L., Visa S., Kamiya Y., Jikumaru Y., Blakeslee J., Van der Knaap E. (2015). The control of tomato fruit elongation orchestrated by sun, ovate and fs8.1 in a wild relative of tomato. Plant Sci. 238, 95–104

Wu S., Xiao H., Cabrera A., Meulia T., Van der Knaap E. (2011). SUN regulates vegetative and reproductive organ shape by changing cell division patterns. Plant Physiol. 157, 1175–1186

Wu S.B., Collins G., Sedgley M. (2004). A molecular linkage map of olive (Olea europaea L.) based on RAPD, microsatellite and SCAR markers. Genome 47, 26–35

Xiao H., Jiang N., Schaffner E., Stockinger E. J., Van der Knaap E. (2008). A retrotransposon-mediated gene duplication underlies morphological variation of tomato fruit. Science 319, 1527–1530

Xiao H., Radovich C., Welty N., Hsu J., Li D., Meulia T., Van der Knaap E. (2009). Integration of tomato reproductive developmental landmarks and expression profiles, and the effect of SUN on fruit shape. BMC Plant Biol. 9, 49

Xiaoxia L., Jianguo Z., Ying L., Guodong R. (2020). Metabolome and transcriptome analyses reveal tissue-specific variations in gene expression and metabolites of olive. J. Plant Biol. 63, 73-82.

Xiong L., Zhu, J.K. (2003). Regulation of abscisic acid biosynthesis. Plant Physiol. 133,29–36.

Xu C., Liberatore K. L., MacAlister C. A., Huang Z., Chu Y. H., Jiang K., Brooks C., Ogawa-Ohnishi M., Xiong G., Pauly M., Van Eck J., Matsubayashi Y., Van der Knaap E., Lippmann Z. B. (2015). A cascade of arabinosyltransferases controls shoot meristem size in tomato. Nat. Genet. 47, 784–792

Xu Y.Y., Wang X. M., Li J., Li J. H., Wu J. S., Walker J. C., Xu Z. H., Chong K. (2005). Activation of the WUS gene induces ectopic initiation of floral meristems on mature stem surface in Arabidopsis thaliana. Plant Mol. Biol. 57, 773–784

Ya-cong C., Zheng-hai Z., Li-hao W., Xiao-lei S., Zhen-xian Z., Bao-xi Z. (2016). Cloning and characterization of CaGID1s and CaGAI in capsicum annuum L. J. Integrat. Agricult. 15, 775–784

Yamaguchi M., Haji T., Miyake M., Yaegaki H. (2002). Varietal Differences in Cell Division and Enlargement Periods during Peach (Prunus persica Batsch) Fruit Development. J. Jpn. Soc. Hortic. Sci. 71, 155–163.

Yu G., Wang L.G., Han Y., He Q.Y. (2012). clusterProfler: an R package for com- paring biological themes among gene clusters. Omics J Integr Biol.16, 284–287.

Yuste-Lisbona F.J., Fernández-Lozano A., Pineda B., Bretones S., Ortíz-Atienza A., García-Sogo B., Müller N. A., Angosto T., Capel J., Moreno V., Jiménez-Gómez J. M., Lozano R. (2020). ENO regulates tomato fruit size through the floral meristem development network. Proc. Natl. Acad. Sci. U. S. A. 117, 8187–8195

Zamora R., Alaiz M., Hidalgo F.J. (2001). Influence of cultivar and fruit ripening on olive (Olea europaea) fruit protein content, composition, and antioxidant activity. J. Agric. Food Chem 49, 4267–4270

Zeng W., Pan L., Liu H., Niu L., Zhenhua L.u., Cui G., Wang Z. (2015). Characterization of 1-aminocyclopropane-1-carboxylic acid synthase (ACS) genes during nectarine fruit development and ripening. Tree Genet. Genomes, 11,18–18.

Zhang B., Liu J., Yang Z.E., Chen E.Y., Zhang C.J., Zhang X.Y., Li F.G. (2018a). Genome-wide analysis of GRAS transcription factor gene family in Gossypium hirsutum L. BMC Genom. 19, 348.

Zhang H., Tan J., Zhang M., Huang S., Chen X. (2020a). Comparative transcriptomic analysis of two bottle gourd accessions differing in fruit size. Genes, 11, 359.

Zhang L.Y., Bai M.Y., Wu J.Y., Zhu J.Y., Wang H., Zhang Z., Wang W., Sun Y., Zhao J., Sun X., Yang H., Xu Y., Kim S.H., Fujioka S., Lin W.H., Chong K., Lu T., Wang Z.Y. (2009). Antagonistic HLH/bHLH transcription factors mediate brassinosteroid regulation of cell elongation and plant development in rice and Arabidopsis. Plant Cell 21, 3767-3780.

Zhang Y., Li Z., Yun T.u., Cheng W., Yang Y. (2018b). Tomato (Solanum lycopersicum) SlIPT4, encoding an isopentenyltransferase, is involved in leaf senescence and lycopene biosynthesis during fruit ripening. BMC Plant Biol. 18, 107–107.

Zhang Z., Wang B., Wang S., Lin T., Yang L., Zhao Z., Zhang Z., Huang S., Yang X. (2020b). Genome-wide target mapping shows histone deacetylase complex1 regulates cell proliferation in cucumber fruit. Plant Physiol. 182, 167–184.

Zheng K., Wang Y., Zhang N., Jia Q., Wang X., Hou C., Chen J.C., Wang S. (2017). Involvement of PACLOBUTRAZOL RESISTANCE6/KIDARI, an atypical bHLH transcription factor, in auxin responses in arabidopsis. Front. Plant Sci. 8:1813. doi: 10.3389/fpls.2017.01813

Zhu Z., Chen G., Guo X., Yin W., Yu X., Hu J., Hu Z. (2017). Overexpression of SlPRE2, an atypical bHLH transcription factor, affects plant morphology and fruit pigment accumulation in tomato. Sci. Rep. 7, 5786

Zhu Z., Liang H., Chen G., Li F., Wang Y., Liao C., Hu Z. (2019). The bHLH transcription factor SlPRE2 regulates tomato fruit development and modulates plant response to gibberellin. Plant Cell Rep. 38, 1053-1064.

Zouine M., Fu Y., Chateigner-Boutin A. L., Mila I., Frasse P., Wang H., Audran C., Roustan J. P., Bouzayen M. (2014). Characterization of the tomato ARF gene family uncovers a multi-levels post-transcriptional regulation including alternative splicing. PLoS One 9, e84203

Zouine M., Maza E., Djari A., Lauvernier M., Frasse P., Smouni A., Pirrello J., Bouzayen M. (2017). TomExpress, a unified tomato RNASeq platform for visualization of expression data, clustering and correlation networks. Plant J. 92, 727–735.